



University
of Glasgow

Hernandez-Martinez, Juan-Manuel (2015) *Role of kynurenines and oxidative stress in the differentiation of SH-SY5Y cells*. PhD thesis.

<http://theses.gla.ac.uk/6133/>

Copyright and moral rights for this thesis are retained by the author

A copy can be downloaded for personal non-commercial research or study, without prior permission or charge

This thesis cannot be reproduced or quoted extensively from without first obtaining permission in writing from the Author

The content must not be changed in any way or sold commercially in any format or medium without the formal permission of the Author

When referring to this work, full bibliographic details including the author, title, awarding institution and date of the thesis must be given

**Role of Kynurenines and Oxidative Stress in the
Differentiation of SH-SY5Y Cells**

**Juan-Manuel Hernandez-Martinez
B.Sc. (UNAM)**

**A thesis submitted in fulfilment of the
requirements for the Degree of PhD**

**Institute of Neuroscience and Psychology
College of Medical, Veterinary and Life Sciences
University of Glasgow**

September 2014

Abstract

Neuroblastoma is the most common solid extracranial tumour in children. The neuroblastoma SH-SY5Y cell line is a third successive subclone established from a metastatic bone tumour biopsy. It can be induced to differentiate (regress) into a neuronal phenotype when treated with any of several molecules including retinoic acid (RA). This characteristic has been exploited in several studies that use the SH-SY5Y cell line as a neuronal model. These studies have had far-reaching implications in shaping our understanding of certain key aspects of neurotoxicity and neurodevelopment yet their genuine relevance becomes evident when approached from an oncological point of view, as they provide information about the process underlying tumour regression which in turn can lead to the development of better therapies for the clinical management of this malignancy.

It has been shown both *in vitro* and *in vivo* that several tumours constitutively catabolize the essential amino acid tryptophan (Trp) promoting cancer-associated inflammation, immune response suppression, immune escape and tumour outgrowth. The main degradation pathway of Trp is the kynurenine pathway: it involves its transformation into several bioactive compounds such as kynurenic acid (KA) and quinolinic acid (QA). QA has been implicated in several neurodegenerative diseases where it is believed to induce excitotoxic neuronal death through the activation of the N-methyl-D-aspartate (NMDA) receptor, a type of ionotropic glutamate receptor, as well as by causing oxidative stress and energy metabolism disruption. Conversely, KA acts as an NMDA receptor antagonist and exerts neuroprotection.

Similarly, glutamate signaling and its dysregulation has been implicated in the development and progression of cancer. Furthermore, several glutamate receptor antagonists, including kynurenic acid, have been shown to inhibit the proliferation and migration of neoplastic cells. Conversely, it has recently been reported that QA increases the proliferation of SK-N-SH cells and protects gliomas against oxidative stress by acting as a precursor of NAD⁺.

In view of all that has been mentioned thus far, the SH-SY5Y cell line was used as a model to investigate the effect of certain Trp metabolites such as QA, KA

and 3-hydroxyanthranilic acid (3-HAA) on cellular morphology, viability and neurite extension. An important part of this study was to determine whether the available methods could reliably be employed to investigate these parameters in the SH-SY5Y cell line. It was confirmed that the acquired SH-SY5Y cell line retains its ability to differentiate and to die, and that both processes can be accurately quantified. Additionally, the optimal culturing conditions for the SH-SY5Y cell line were determined.

Treatment with RA (10 μM) was used as a positive control of differentiated SH-SY5Y cells. Overall, the morphology adopted by cells after QA (50 μM) treatment was similar to the one that follows RA-induced differentiation. It was demonstrated that QA caused an increase in the neurite/soma ratio in SH-SY5Y cells, which was confirmed by Western blot analysis as evidenced by an increase in the total cellular content of β 3-tubulin. These results were also confirmed by a neurite outgrowth assay that selectively quantified the neuritic mass present in cultures. However, unlike RA, QA did not decrease the levels of the neuronal proliferation marker doublecortin; the term neuritogenesis is therefore more appropriately used to refer to the series of morphological and molecular changes induced by QA in SH-SY5Y cells.

The morphological changes induced by QA were not reproduced by application of NMDA, nor were they inhibited by blockade of the NMDA receptor with MK-801. Furthermore, SH-SY5Y cells were not susceptible to NMDA excitotoxic death. In view of this, the expression of GluN1 protein was determined by Western blot. GluN1 could not be detected in either undifferentiated or differentiated SH-SY5Y cells, confirming that QA-induced neuritogenesis occurs through a mechanism independent of NMDAR activation. The results herein contained suggest that the SH-SY5Y cell line does not have functional NMDARs, nonetheless it is recognized that a more exhaustive study would be necessary to fully establish which glutamate receptor subtypes are found in the SH-SY5Y cell line.

The effect of QA on the production of reactive oxygen species (ROS) was also investigated. QA caused an increase in the intracellular levels of ROS as evidenced by an increase in the fluorescence of oxidised ethidium. Additionally QA-treatment caused an increase in the expression of NRF2, a transcription

factor that responds to oxidative stress and which has been implicated in ROS-induced differentiation in SH-SY5Y cells.

In contrast, superoxide dismutase (SOD; 300 U/ml) significantly reduced the levels of ROS induced by QA treatment, which in turn caused an increase in cell proliferation and a reduction in the number of neurites. Similarly, diphenylene iodonium (DPI; an inhibitor of NADPH oxidase) also inhibited QA-induced neuritogenesis. These results suggest that the action mechanism of QA is mainly via the production of ROS, most likely superoxide ($O_2^{\cdot-}$) through NADPH-oxidase.

Interestingly, nicotinamide (1 nM-1mM; another precursor of NAD^+) caused a dose dependent increase in the number of neurites and in the expression of β 3-tubulin, which suggests that the action mechanism of QA may be mediated by metabolites of the nicotinate and Nam pathway, including NAD^+ either before or after the induction of ROS.

Cells were treated with 3-hydroxyanthranilic acid (3-HAA) in order to ascertain whether other pro-oxidant molecules could induce neuritogenesis as well. Single and repeated application of 3-HAA (100 μ M) induced cell death in SH-SY5Y cells. Furthermore, when 3-HAA was delivered in combination with SOD, there was a shift in the IC_{50} values indicating that toxicity was potentiated by SOD. Catalase (CAT; 100 U/ml) afforded complete protection from the exacerbated damage induced by the single co-application of 3-HAA + SOD. However, when repeated treatments were performed, CAT no longer afforded any protection. Interestingly, the serum concentration in the medium did not affect the IC_{50} of 3-HAA but it did modulate the response to CAT, indicating that the specific ROS produced after 3-HAA treatment depend on the medium in which 3-HAA is delivered. At sublethal doses, 3-HAA interfered with the expression of NeuN (neuronal marker) through a mechanism that involves high production of ROS. The ability of some kynurenines to induce differentiation and cell death in SH-SY5Y cells may open new and exciting avenues of research. If these results can be confirmed *in vivo* they could impact the way in which certain neuroblastomas are treated.

Table of Contents

Abstract.....	2
List of Tables.....	9
List of Figures.....	10
Acknowledgements.....	11
Author's Declaration.....	13
Definitions/Abbreviations.....	14
Chapter 1 - INTRODUCTION.....	19
1.1 Neuroblastoma.....	20
1.1.1 The Neuroblastoma cell line SH-SY5Y.....	23
1.2 Glutamatergic transmission - a general overview.....	28
1.2.1 NMDARs.....	30
1.2.2 GluN1 splice variants.....	33
1.2.3 Neurotrophic Effect of Glutamate.....	35
1.2.4 Glutamate Signaling and Cancer.....	36
1.3 The kynurenine pathway: a general overview.....	40
1.3.1 Principal Metabolites and enzymes of the Kynurenine Pathway.....	42
1.3.2 Kynurenic Acid.....	43
1.3.2.1 KA derivatives.....	46
1.3.3 3-Anthranilic Acid (AA), Hydroxykynurenine (3-HK) and 3-Hydroxyanthranilic acid (3-HAA).....	47
1.3.3.1 Role of 3-HK and 3-HAA in pathological events.....	49
1.3.3.2 Autoxidation of 3-HAA.....	51
1.3.3.3 Protection by 3-HAA.....	53
1.3.4 Quinolinic Acid (QA).....	55
1.3.5 Regulating the metabolism of Trp metabolites.....	57
1.3.6 The Kynurenine pathway in cancer pathogenesis.....	58
1.4 Nicotinamide metabolism.....	67
1.4.1 Role of NAD ⁺ in cancer.....	72
1.5 Reactive Oxygen Species (ROS) and Oxidative Stress.....	75
1.5.1 Reactive Oxygen species.....	75
1.5.2 Superoxide Anion.....	76
1.5.2.1 Xanthine Oxidoreductases.....	76
1.5.2.2 NADPH-oxidase (NOX).....	77
1.5.3 Hydrogen Peroxide.....	78
1.5.4 Hydroxyl radical.....	78
1.5.5 Nitric oxide.....	79
1.5.6 Peroxynitrite.....	80

1.6	Antioxidant Defences	80
1.6.1	Superoxide dismutase (SOD).....	80
1.6.2	Catalase	81
1.6.3	Glutathione Peroxidase (GPx)	82
1.6.4	A-tocopherol	82
1.7	Oxidative stress	83
1.7.1	Lipid Peroxidation.....	84
1.7.2	Protein Oxidative Modifications.....	85
1.7.3	DNA Oxidative Damage	85
1.8	ROS in Cancer	87
1.8.1	NF- κ B	90
1.8.2	NRF-2	92
1.8.3	HIF-1	93
1.8.4	AP-1	94
1.9	Rationale of Study	96
1.9.1	Reasons for Study	96
1.9.2	Reasons for the use of SH-SY5Y cells.....	96
1.9.3	General Aims.....	96
Chapter 2 - MATERIALS AND METHODS		98
2.1	SH-SY5Y culture procedures	98
2.1.1	Materials.....	98
2.1.2	Chemicals	99
2.1.3	Medium preparation	100
2.1.4	Overview	101
2.1.5	Cell line Resuscitation.....	101
2.1.6	Cell harvesting.....	101
2.1.7	Culture plating	102
2.1.8	Poly-D-Lysine coating.....	102
2.2	Probes for Cell viability/proliferation	103
2.2.1	Fluorescein diacetate (FDA)	103
2.2.2	AlamarBlue®.....	103
2.3	Neurite Extension.....	106
2.3.1	Morphology of SH-SY5Y cells.....	106
2.3.2	Neurite Outgrowth assay	106
2.4	DHE ROS quantification.....	107
2.5	Immunocytochemistry	108
2.5.1	Materials.....	108

2.5.2	Antibodies.....	108
2.5.3	Immunocytochemistry protocol.....	109
2.6	Microscopy photography.....	109
2.7	Protein sample preparation and quantification.....	110
2.7.1	Materials.....	110
2.7.2	Protein preparation.....	110
2.7.3	Protein quantification.....	111
2.8	Western Blotting.....	112
2.8.1	Materials.....	112
2.8.2	Chemicals.....	112
2.8.3	Antibodies.....	113
2.8.4	Gel running procedure.....	114
2.8.5	Protein transfer procedure.....	114
2.8.6	Ponceau staining.....	115
2.8.7	Antibody incubation.....	116
2.8.8	Enhanced Chemiluminescence.....	116
2.9	Statistical analysis.....	117
2.10	Treatments.....	119
2.10.1	Chemicals.....	119
2.11	Methods (carried out by others).....	121
2.11.1	High performance liquid chromatography (HPLC).....	121
2.11.1.1	Sample's origin.....	121
Chapter 3 - OPTIMISING CULTURE CONDITIONS AND ASSESSING THE OVERALL STATE OF SH-SY5Y CELLS.....		122
3.1	Introduction.....	122
3.2	Aims and objectives.....	124
3.3	Results.....	125
3.3.1	SH-SY5Y cells show different growing profiles depending on the batch of foetal bovine serum (FBS).....	125
3.3.2	RA and NGF induce differentiation in SH-SY5Y cells.....	127
3.3.2.1	Qualitative assessment of the morphology.....	127
3.3.3	Hydrogen peroxide is a potent inducer of cell death in SH-SY5Y cells.....	131
3.4	Discussion.....	133
3.5	Conclusion.....	135
Chapter 4 - CONTRASTING EFFECTS OF QUINOLINIC AND 3-HYDROXYANTHRANILIC ACID.....		136
4.1	Introduction.....	136
4.2	Aims and objectives.....	137

4.3	Results	139
4.3.1	QA effect on SH-SY5Y survival and neuritogenesis	139
4.3.1.1	QA does not negatively affect the survival of SH-SY5Y cells	139
4.3.1.2	SOD treatment increases the number of cells in culture.	140
4.3.1.3	SOD reduces QA and RA-induced neuritogenesis.	142
4.3.1.4	QA causes an early and transient increase in the level of ROS	146
4.3.1.5	NMDA does not affect the survival or neuritogenesis of SH-SY5Y cells. 148	
4.3.1.6	Kynurenic acid (KA) does not affect cell survival	150
4.3.1.7	GluN1 expression was not detected in SH-SY5Y cells.....	151
4.3.1.8	Nam increases the number of neurites in a dose-dependent manner	152
4.3.1.9	Neurite Outgrowth assay and DPI inhibition of neuritogenesis.....	154
4.3.1.10	QA increases NRF2 expression	155
4.3.2	Effect of 3-HAA on SH-SY5Y survival and neuritogenesis	157
4.3.2.1	3-HAA induces cell death in SH-SY5Y cells	157
4.3.2.2	SOD increases the levels of ROS in cells treated with 3-HAA.....	160
4.3.2.3	Catalase prevents the death of SH-SY5Y induced by 3-HAA+SOD	161
4.3.2.4	3-HAA affects RA-induced differentiation in SH-SY5Y cells.....	163
4.3.2.5	SH-SY5Y cells recover from a single 3-HAA treatment	165
4.3.2.6	HPLC quantification of 3-HAA in medium of cultures and cell-free preparation (Samples were processed by Dr. Alexandra Ferguson).....	168
4.3.2.7	SH-SY5Y cell viability after daily 3-HAA treatment for 72 h.....	169
4.4	Discussion.....	174
4.5	Future Avenues	189
Chapter 5 - GENERAL DISCUSSION.....		191
Appendix.....		194
List of References		200

List of Tables

Table 1 Ploidy level of some neuroblastoma tumours and neuroblastoma-derived cell lines.	22
Table 2 Overview of the molecular families of glutamate receptors.	29
Table 3 Radical and non-radical reactive species.	76
Table 4. SOD causes a shift in the IC ₅₀ values for 3-HAA treatment.	158
Table 5. Half-life values for 3-HAA in cell-free preparations and in cell cultures.	169
Table 6. Daily treatments cause a shift in the IC ₅₀ values for 3-HAA.	170
Table 7 Preparation of standard solutions for calibrations curves of 3-HAA.	195
Table 8 Clinical trials targeting the kynurenine pathway enzyme Indolamine 2,3-dioxygenase.	198

List of Figures

Figure 1. Tryptophan metabolism Kynurenine pathway and Methoxyindole pathway.	40
Figure 2 Three-step reaction for the complete oxidation of 3-HAA.	51
Figure 3- Intracellular NAD ⁺ metabolism.	71
Figure 4 Transcription factors activated by ROS.	92
Figure 5- The reduction of non-fluorescent resazurin.	104
Figure 6. Foetal bovine serum affects the growth rate of SH-SY5Y cells.	126
Figure 7. RA and NGF alter the morphology of SH-SY5Y cells.	128
Figure 8. RA and NGF increase the expression of neuronal markers in SH-SY5Y cells.	129
Figure 9. Catalase protects SH-SY5Y cells against H ₂ O ₂ -induced toxicity.	132
Figure 10. QA does not promote cell death in SH-SY5Y cells.	139
Figure 11- SOD increases the number of cells after 72 h treatment with QA plus RA.	140
Figure 12 Inhibitory effect of SOD on QA and RA-induced neuritogenesis.	143
Figure 13 QA increases the levels of B3-tubulin without decreasing those of doublecortin.	145
Figure 14- QA promotes the early formation of ROS in SH-SY5Y cells.	147
Figure 15- NMDA does not induce cell death in SH-SY5Y cells.	149
Figure 16 Lack of effect of KA on the survival of SH-SY5Y cells.	150
Figure 17. Western blotting showing the lack of GluN 1 expression in SH-SY5Y cells.	151
Figure 18. Nicotinamide increases the number of neurites and the expression of B3-tubulin in SH-SY5Y cells.	152
Figure 19. Inhibitory effect of DPI (but not MK-801) on QA-induced neuritogenesis.	154
Figure 20 QA increases the expression of NRF2 in SH-SY5Y cells.	156
Figure 21. Cellular death is induced by 3-HAA in SH-SY5Y cells.	157
Figure 22 The IC ₅₀ of 3-HAA is reduced when co-applied with SOD.	159
Figure 23. SOD exacerbates the production of ROS induced by single 3-HAA treatment.	160
Figure 24. SOD exacerbates the production of ROS induced by single 3-HAA treatment.	161
Figure 25. Catalase protects against the exacerbated toxicity of combined treatment with 3-HAA and SOD.	163
Figure 26. Effect of a single 3-HAA treatment delivered in 1% FBS medium on the expression of NeuN 72 h after treatment.	164
Figure 27- Effect of a single 3-HAA treatment delivered in 10% FBS medium on the expression of NeuN, 72 h after treatment.	165
Figure 28- Viability recovery from single 3-HAA treatment.	166
Figure 29- Concentration of 3-HAA in cultures and cell-free preparation determined by HPLC.	168
Figure 30. Catalase protects against the exacerbated toxicity of 2 daily 3-HAA treatments.	172
Figure 31. Catalase protects against the exacerbated toxicity of 3 daily 3-HAA treatments.	173

Acknowledgements

Immeasurable appreciation and deep gratitude to the following persons who, in one way or another, contributed in making this dissertation possible.

First, I would like to thank my three supervisors for their guidance. Warm thanks to Professor Trevor Stone for accepting me as a PhD student to conduct my research under his supervision. I am grateful for his constructive comments and for encouraging me to always remain critical about my own work. I am also very grateful to Professor Robert Smith for his unreserved support and advice, his constructive criticism and for all his time and dedication to this project, even after his retirement. Finally, I would like to express my deepest gratitude to Dr. Caroline Forrest, not only for her invaluable moral support during the hard times, but also for her vast technical, methodological and scientific knowledge which she never hesitated to share with me. It truly would not have been possible to carry out this project without her help.

I would also like to extend my most sincere gratitude to my examiners: Professor Giles Hardingham and Professor Stuart Cobb, for their additional and invaluable feedback, which not only injected me with new energy and enthusiasm, but also led me to see my research in a completely different light.

I would like to thank all the members of the laboratory who, in one way or another, have positively contributed to the development of my research. In particular, I thank Dr. Alexandra Ferguson who carried out the HPLC analysis for me. I would also like to thank the Mexican government for funding my studies through its main body for scientific and technological development, CONACyT.

I would like to thank all my family members, present and departed, for believing in me at all times. Especially my parents, without whose emotional and financial support, the completion of this project would have been most difficult. I would like to thank my father for fostering and encouraging my scientific curiosity from an early age; my mum, Jola, for her genuine interest into my research and for her corrections of the different versions of this manuscript. I would like to acknowledge my brother, for paving the way and being a true inspiration, both professionally and personally. I would not have been able to successfully

conclude my thesis without the unwavering support of Andrew Barr, who has been there for me every step of the way. This thesis also benefitted immensely from the input of my dear friend, Blanca Estela Paramo-Sanchez MSc., who spent long hours helping me with various aspects of this thesis.

“Nothing in Cancer Biology Makes Sense Except in the Light of Evolution”
(Seyfried, 2012)

Author's Declaration

I, Juan Manuel Hernandez Martinez, declare that all the work in this thesis was performed and composed by me except where referenced. No part of this work has been submitted for consideration as part of any other degree or award

Definitions/Abbreviations

3-HAA = 3-Hydroxyanthranilic acid

3-HAO = 3-Hydroxyanthranilic acid 3,4-dioxygenase

3-HK = 3-Hydroxykynurenine

5-HT = 5-Hydroxytryptamine, Serotonin

8-OHDG = 8-Hydroxy-deoxyguanosine

AA = Anthranilic acid

ADP = Adenosine diphosphate

AIDS = Acquired immunodeficiency syndrome

AMPA = α -amino-3-hydroxy-5-methyl-4-isoxazole propionate

ANOVA = Analysis of variance

ATP = Adenosine triphosphate

BBB = Blood brain barrier

BDNF = Brain-derived neurotrophic factor

CNS = Central Nervous System

CSF = Cerebrospinal fluid

Cu-Zn-SOD = Copper, zinc-dependent superoxide dismutase

DC = Dendritic cell

DHE = Dihydroethidium

DNA = Deoxyribonucleic acid

DPI = Diphenylene iodonium chloride

DTPA = Diethylenetriaminepentaacetic acid

EDTA = Ethylenediaminetetraacetate

FBS= Foetal bovine serum; previously known as foetal calf serum

FDA= Fluorescein diacetate

GABA = γ -aminobutyric acid

Glu = Glutamate

H₂O₂ = Hydrogen peroxide

HD = Huntington's disease

HMGB1 = High-mobility group box protein 1

HNP1-3 = Human neutrophil peptide 1-3

HPLC = High performance liquid chromatography

HSP = Heat shock protein

IDO = Indoleamine 2,3-dioxygenase

IFN- γ = Interferon- γ

IL = Interleukin

IL-2 = Interleukin-2

iNOS = Inducible nitric oxide synthase

IPA = Indole-3-pyruvic acid

KA = Kynurenic acid

KAT = Kynurenine aminotransferase

KH = Kynurenine 3-hydrolase

KMO = Kynurenine 3-monooxygenase

KYN = Kynurenine

KYNU = Kynureninase

Mn-SOD= Manganese-dependent superoxide dismutase

NaAD: Nicotinic acid adenine dinucleotide

NaADP: Nicotinic acid adenine dinucleotide phosphate

NAD⁺ =Nicotinamide adenine dinucleotide

NADH: Nicotinamide adenine dinucleotide reduced

NADP⁺: β-Nicotinamide adenine dinucleotide phosphate

NADPH: Nicotinamide adenine dinucleotide phosphate reduced

Nadsyn1: Glutamine-dependent NAD⁺ synthetase

Nam: Nicotinamide

NaMN: Nicotinic acid mononucleotide

NF-κB = Nuclear factor kappa-light-chain-enhancer of activated B cells

NGF = Nerve growth factor

Nicotinic acid: 3-Carboxypyridine, 3-Pyridylcarboxylic acid.

NK cells = Natural killer cells

NMDA = N-methyl-D-aspartate

NMDAR = N-methyl-D-aspartate receptor

Nmnat = Nicotinamide-nucleotide adenylyltransferase 2

nNOS = Neuronal nitric oxide synthase

NOS = Nitric oxide synthase

NOX = Nicotinamide adenine dinucleotide phosphate-oxidase/ NADPH-oxidase

O₂^{•-} = Superoxide anion

OGD = Oxygen glucose deprivation

PARP = Poly (ADP-ribose) polymerase

PBS = Phosphate buffered saline

PCA = Perchloric acid

PD = Parkinson's disease

PET = Positron emission tomography

PMNs = Polymorphonuclear cells Interferon

QA = Quinolinic Acid

Qprt = Quinolate phosphoribosyl transferase

RA = Retinoic acid

ROS = Reactive oxygen species

SD = Standard deviation

SEM = Standard error of the mean

SOD = Superoxide dismutase

S-PBN = *N*-tert-butyl- α -(2-sulphophenyl)-nitron

SPE = solid phase extraction

TDO = Tryptophan 2,3-dioxygenase

TGF- β = Transforming growth factor- β

TMPO = 3,3,5,5-tetramethylpyrroline *N*-oxide

TNF- α = Tumour necrosis factor- α

T_{reg} = Regulatory T cells

Trp = Tryptophan

α 7-nACh = α 7-Nicotinic acetylcholine

Chapter 1 – INTRODUCTION

This study of the role of kynurenines and oxidative stress in the differentiation of SH-SY5Y cells consists of six chapters, including this introductory section. The first section of the introduction (1.1) deals with some key aspects of neuroblastoma biology and those of the neuroblastoma-derived cell line used in the present study (SH-SY5Y).

In the second section (1.2), glutamatergic transmission and its role as a trophic factor involved in cancer pathogenesis is explored, with special emphasis on the NMDA ionotropic glutamate receptor on which KA and QA (both members of the kynurenine pathway) act as an antagonist and an agonist, respectively.

The third section of the introduction (1.3) describes the kynurenine pathway and the formation of KA, 3-hydroxyanthranilic acid (3-HAA) and QA. It also provides evidence for how the kynurenine pathway is involved in preventing effective immune responses which in turn contributes to the initiation and progression of transformant cells.

Given that QA is a precursor of NAD^+ , section 1.4 then describes a possible mechanism by which both molecules may also contribute to cancer pathogenesis. Oxygen metabolism and the production of reactive oxygen species is also discussed in section 1.5, 1.6, and 1.7 of the introduction, as the oxidant and antioxidant nature of some kynurenine metabolites has been shown to underlie their mechanism of action. Finally, the rationale of the study is presented in which the general aims are presented as well as the reason why the SH-SY5Y was chosen. This then concludes the introductory chapter.

1.1 Neuroblastoma

Neuroblastoma (NB) is a paediatric solid malignant tumour with broad clinical characteristics and patient outcome. The disease was originally described by Virchow in 1863 when he clinically characterised an abdominal tumour which he designated as a “glioma” (Virchow, 1863). However, the term neuroblastoma was coined in 1910 by Wright when he demonstrated that the origin of the tumour was from embryonic neuroblasts of the sympathetic peripheral nervous system (Wright, 1910). Since then, an immense amount of research has been performed to try to understand neuroblastomas.

Neuroblastoma is almost exclusively a paediatric disease since there are only a few occasional cases diagnosed after the age of five. Neuroblastoma is the third most common cancer in children after leukaemia and CNS tumours. It is therefore the most prevalent solid extracranial tumour of neuroendocrine origin in children (Young *et al.*, 1986). More than 600 cases are diagnosed in the United States each year, accounting for approximately 15 percent of all paediatric cancer fatalities (Goodman *et al.*, 1999).

It is estimated that in the United Kingdom NB affects approximately 100 children each year. This is approximately 8% of the total number of paediatric cancers (Stiller and Parkin, 1992). These statistics stress the relevance of NB research, and that of the cell lines derived from it, not only as part of a quest to accumulate scientific knowledge but also to discover reliable treatment for those who suffer it.

There are five clinically recognised stages for neuroblastomas according to localization and age of diagnosis. Stage 1-3 neuroblastomas are unilocular and generally appear within the first 1.5 years of age. Patients can be treated by surgical methods and have a favourable prognosis (30% survival). Some stage 1-3 tumours may sporadically turn into benign ganglioneuromas, the survival rate for this maturative subtype is at 100%. Stage 4 neuroblastomas are characterised by extensive dissemination, patients then have to undergo extensive chemotherapy and radiation with a 20% survival rate. Some cases fall into an intriguing 4s stage in which spontaneous regression occurs and for which the survival rate is 80-85% (Berthold and Simon, 2005; Edsjo *et al.*, 2007).

Chapter 1

One signature characteristic of neuroblastomas is their clinical heterogeneity, understood as the variability in the populations studied (patient age at diagnosis, location of the tumour and its clinical stage), the interventions involved, and the outcomes measured or prognosis (Lohr *et al.*, 2010). The advent of molecular cytogenetics and the successful establishment of tumour-derived cell lines uncovered that the clinical heterogeneity observed in neuroblastoma correlates with their molecular constitution (Maris and Matthay, 1999).

Murray and Stout in 1947 discovered that neuroblastomas could be kept *in vitro* from explants of tumours grown in plasma-clot cultures. They also noticed that, *in vitro*, neuroblastoma cells exhibit an immature neuronal phenotype (flat cell bodies and few neuritic processes). They noticed that once in culture, neuroblastoma readily projected elongated structures similar to axons (Murray and Stout, 1947).

Certain characteristics of neuroblastomas made them ideal cell lines for research. Firstly, neuroblastomas can be kept in long-term culture and secondly, they can undergo differentiation associated with the appearance of easily recognizable properties. Therefore, during the seventies, the isolation and characterization of human neuroblastoma cell lines and its subclones was performed by several research groups (Goldstein, 1968; Biedler *et al.*, 1973; Seeger *et al.*, 1977; Biedler *et al.*, 1978).

One of the earliest karyotyping studies of neuroblastoma cell lines reported numerical chromosome abnormalities in SK-N-SH and SK-N-MC, the ploidy level found for each line was 47 and 46 respectively (Biedler *et al.*, 1973).

Several other groups confirmed the occurrence of numerical chromosome abnormalities in these and other neuroblastoma-derived cell lines, as well as in explants of primary neuroblastoma tumours (Biedler and Spengler, 1976; Balaban-Malenbaum and Gilbert, 1977; Brodeur *et al.*, 1977; Seeger *et al.*, 1977).

A meta-analysis of 24 karyotypes of human neuroblastomas, from both tumours and cell lines, revealed that in addition to numerical chromosome abnormalities (see Table 1), neuroblastomas also have structural chromosome abnormalities

Chapter 1

corresponding to the loss of the distal part of the short arm of chromosome 1 (Brodeur *et al.*, 1981).

	Ploidy (Mode)	Type	Origin	Reference
SH-SY5Y	47	Cell line	Bone Marrow	(Yusuf <i>et al.</i> , 2013)
SK-N-SH	47	Cell line	Bone Marrow	(Biedler <i>et al.</i> , 1973; Brodeur <i>et al.</i> , 1977; Seeger <i>et al.</i> , 1977)
SK-N-MC	47-45	Cell line	Bone Marrow	(Biedler <i>et al.</i> , 1973; Brodeur <i>et al.</i> , 1977; Seeger <i>et al.</i> , 1977)
LA-N-1	87	Explant	Bone Marrow	(Seeger <i>et al.</i> , 1977)
LA-N-2	73	Explant	Metastasis	(Seeger <i>et al.</i> , 1977)
IMR-32	47	Cell line	Abdominal	(Brodeur <i>et al.</i> , 1977; Seeger <i>et al.</i> , 1977)
NGP	47	Cell line	Metastasis	(Brodeur <i>et al.</i> , 1977)
NMB	89	Cell line	Bone Marrow	(Brodeur <i>et al.</i> , 1977)

Table 1 Ploidy level of some neuroblastoma tumours and neuroblastoma-derived cell lines.

There is a striking correlation between the level of ploidy, tumour malignancy and prognosis. The majority of stage 1, 2, and 4S tumours are near triploid and show excellent outcome, whereas most stage 4 tumours are diploid or tetraploid and have very poor clinical outcomes (Kaneko *et al.*, 1987).

The differentiation, or regression of some neuroblastomas in stage 4s is a very interesting biologic occurrence that is relevant to several branches of biology. For instance, in the field of neuroscience, neuroblastoma cell lines have been used as a model of neurodevelopment to study some of the occurrences that take place during neuronal differentiation such as: reduction in cell proliferation, changes in morphology, increases in the expression of neuronal cytoskeletal proteins and membrane antigens and finally, the acquisition of molecular machinery necessary for the synthesis and storage of monoamines and neuropeptides). Once differentiated, neuroblastoma cells are used as neuronal model to study the neurotoxic effects of several compounds.

On the other hand, cancer research on the SH-SY5Y cell line has mainly focused on the mechanisms by which immortalised cells regain the ability to halt

Chapter 1

proliferation and/or to die after treatment with any of several compounds. The acquisition of a neuronal phenotype is incidental and not necessarily the research focus. The clinical relevance of neuroblastoma differentiation is highlighted by cancer research, as is its applicability in the management of this malignancy.

1.1.1 The Neuroblastoma cell line SH-SY5Y

The SH-SY5Y cell line is a third successive subclone of the parental cell line SK-N-SH. The SK-N-SH cell line was first subcloned to SH-SY, then to SH-SY5 and finally to SH-SY5Y (Biedler *et al.*, 1973).

Originally, the SK-N-SH cell line was established from a metastatic bone marrow biopsy of a four year-old girl. The SK-N-SH cell line contains three morphologically and biochemically different cell types: a neuroblastic (N-type), a substrate adherent non-neuronal form (S-type), and an intermediate type (I-type). The N-type cells correspond to sympathoadrenal neuroblasts, which grow as poorly attached aggregates of small, rounded cells with short neuritic processes. The S-type cells have large, flat soma and resemble non-neuronal precursor cells. They are substrate adherent and cell growth is inhibited at high confluence. The I-type cells tend to clump together in culture, they are small, flattened and moderately adherent and sometimes present small neuritic elongations (Ross *et al.*, 1995).

There is evidence suggesting that the SH-SY5Y cell line is comprised of more than two morphologically distinct phenotypes. For instance, in a normal SH-SY5Y culture there are adherent and floating cells, both of which are viable. The molecular differences between adherent and floating cells have not yet been determined since floating cells are discarded during media changes and their interference should be minimal.

Of more biological relevance is the presence of two additional adherent subpopulations, within the SH-SY5Y cell line, with different molecular profiles; one neuroblastic and the other epithelial-like (Encinas *et al.*, 2000). The presence of these two cell types can cause the underestimation of several quantifiable parameters. For example, cells presenting the neuroblastic

Chapter 1

phenotype express tyrosine hydroxylase and dopamine- β -hydroxylase (Ross *et al.*, 1983) and respond to NGF (Oe *et al.*, 2005), whereas the epithelial-like population does not.

The origin of both phenotypes remains a matter of debate; they could correspond to the N and S types earlier described for the SK-N-SH cell line. An initial hypothesis, based on the presence of shared chromosome markers (Ross *et al.*, 1983), is that interconversion or trans-differentiation can spontaneously occur. However, G-banding, spectral karyotyping (SKY) and fluorescence *in situ* hybridization (FISH) of these population subtypes showed that they have different DNA copy number variations (CNVs) which makes clonal expansion of one cell type over the other a more likely hypothesis, instead of the interconversion model (Cohen *et al.*, 2003). The clonal expansion hypothesis can only be true if contamination with other cell types took place during the subcloning process. This would be extremely unlikely, particularly in a thrice-subcloned cell line as is the case of the SH-SY5Y cell line.

Bacterial artificial chromosome (BAC) microarray-based comparative genomic hybridization (CGH) has been used for the analysis of genome-wide chromosomal aberrations in SH-SY5Y cells (Do *et al.*, 2007) and SH-EP cells (Do *et al.*, 2011). In these studies, unbalanced chromosomal changes (gains and losses) were identified at a high resolution (1 Mb), confirming that the neuroblastic and epithelial-like cell types have different genomic identities further discrediting the interconversion model. CNVs related to tumorigenicity were more frequently amplified in SH-SY5Y cells but those related to cell homeostasis were more frequently amplified in SH-EP cells. The authors propose that the cancer stem cell theory may explain the coexistence and origin of neuroblastic and epithelial-like cells in culture (Do *et al.*, 2011).

The cancer stem-like cell (CSC) theory suggests that, in many tumours, CSCs are responsible for cancer initiation, progression and relapse. Since CSCs are capable of regenerating themselves, they can produce an unlimited progeny that will differentiate (albeit aberrantly) and will not respond adequately to homeostatic controls (Aktipis *et al.*, 2013; Beck and Blanpain, 2013).

Chapter 1

It has been conclusively shown that there are several cell types within most neuroblastoma tumours, particularly reactive Schwann cells, perineurial cells, satellite cells and even melanocytes (George *et al.*, 2001; Shimada *et al.*, 2001; Fisher and Tweddle, 2012). The evidence presented thus far shows that this diversity is also maintained in cell lines derived from these tumours. Whereas some of this diversity may arise from the increased mutation rate and genetic instability of cancerous cells (Lengauer *et al.*, 1998; Shen, 2011), some may also result from the differentiation of cancer stem-like cells which have also been found in both tumours and in the cell lines derived from them (Hirschmann-Jax *et al.*, 2004; Hansford *et al.*, 2007).

In a study that set out to determine the effect of hypoxia in SH-SY5Y cells, it was found that the hypoxic stimulus enables the purging of the neuroblastoma stem cell compartment (Marzi *et al.*, 2007). Furthermore, CD133 (a cell surface marker commonly used to identify stem-like cells) is expressed by 8-10% of cells in SK-N-SH cultures and by at least 0.5% of cells in SH-SY5Y cultures (Vangipuram *et al.*, 2010). A decrease in the number of cells expressing CD133 in each subclone is consistent with what would occur during a successive selection of the N-type phenotype. Du and collaborators (2008) demonstrated that neuroblastoma cells induce the differentiation of bone marrow stromal cells and mesenchymal stem cells into glial cells *in vitro* (Du *et al.*, 2008). Whereas, these studies may explain the presence of different cell types in SH-SY5Y cultures and why they were not detected during the establishment of this cell line, they do not successfully determine the specific origin of these cell types.

Molecular studies show that N-type, S-type and I-type cells resemble sympathoadrenal precursor cells, glial/melanoblastic cells and stem cells, respectively (Walton *et al.*, 2004). This has been considered to be an indicator of a shared common origin. Such conclusions are unsatisfactory because they are based on the premise that similarity reflects evolutionary relationships, which is not always the case. Surprisingly, there are no molecular phylogenetic studies to unquestionably establish the relationship and origin of the different cell types found in neuroblastomas.

The fact that there are no studies of this kind is partly due to the lack of analytical tools necessary to establish evolutionary inferences that are specific

Chapter 1

to tumour cells. Recently a new Minimum Event Distance for Intra-tumour Copy-number Comparisons (MEDICC) algorithm has been developed which can be used to quantify tumour heterogeneity as well as to reconstruct phylogenetic relationships (Schwarz *et al.*, 2014). Until fairly recently, quantitative and high-throughput technologies that allow automated and rapid screening of the whole genome, transcriptome and proteome had not been applied to neuroblastomas and their derived cell lines. Kryh and collaborators (2011) published the first high-density single-nucleotide polymorphism (SNP) array study for the SH-SY5Y cell line (Kryh *et al.*, 2011). Taken together, these recent developments could be used to definitively establish the origin of the different cell types found in neuroblastoma tumours, as well as of those types found in cultures.

Perhaps the most interesting characteristic of the SH-SY5Y cell line is that it is able to differentiate into a functional and morphological neuronal phenotype after treatment with an array of natural or synthetic chemicals, and with several biological factors such as; retinoic acid (RA) (Nicolini *et al.*, 1998), neurotrophic factors, or phorbol esters (Pahlman *et al.*, 1995; Kim *et al.*, 1997; Encinas *et al.*, 1999; Olsson *et al.*, 2000). Therefore, this cell line is one of the most widely used models for the study of neuronal differentiation.

When SH-SY5Y cells undergo differentiation, there is an increase in the number of processes as well as an increased accumulation of norepinephrine, neuron specific enolase (Aanerud *et al.*, 2012) and other neuronal specific markers (Encinas *et al.*, 2000). This cell line exhibits neuronal marker enzyme activity (tyrosine as well as dopamine- β -hydroxylases), specific norepinephrine uptake, and expresses neurofilament proteins. The SH-SY5Y cell line also expresses opioid, muscarinic, and nerve growth factor receptors. There are a number of neuroblastoma differentiation protocols available, most of them employing treatment of the cells with retinoids and growth factors such as nerve growth factor (NGF) alone or in combination. This process was initially discovered to be caused by retinoids *in vitro*, which resulted in the introduction of 13-cis-retinoic acid (isotretinoin) as the standard of care for high-risk neuroblastoma (Ferrari-Toninelli *et al.*, 2010; Gardner *et al.*, 2012; Veal *et al.*, 2013). Indeed, the greatest positive clinical impact in the treatment of neuroblastomas has been achieved with the use of retinoids as differentiation/regression inducers. The

Chapter 1

exact mechanism of action of retinoids is not yet fully understood (Reynolds *et al.*, 2003a; Reynolds *et al.*, 2003b).

1.2 Glutamatergic transmission - a general overview

Glutamate (Glu), besides being an amino acid, is the most abundant excitatory neurotransmitter in the central nervous system (CNS) of mammals. It plays an important role in a myriad of neurological processes such as the regulation of sensory information pathways, motor coordination, emotions, neuronal plasticity, and long-term potentiation, among others (Salt and Herrling, 1991; Hassel and Dingledine, 2012). The synaptic transmission regulated by Glu is known as glutamatergic transmission. A large number of various types of neuronal populations use Glu as a neurotransmitter. It has been suggested that approximately 80-90% of all excitatory synapses are glutamatergic (Garey, 1999). A considerable amount of energy is required to restore the membrane potential of depolarised glutamatergic neuron and a great amount of the overall glucose and O₂ intake is used within the brain in order to sustain glutamatergic transmission (Attwell and Laughlin, 2001). Depending on the downstream cascade of events that follows their activation, glutamate receptors (GluR) are divided into two classes: ionotropic (iGlu) and metabotropic (mGlu). iGlus are ionic channels that after Glu activation suffer conformational changes, enabling specific ions to enter the cell. On the other hand, mGlus do not permit the flux of ions; they are ligand-binding G protein coupled receptors (GPCRs) that activate signal transduction pathways and second messengers upon Glu binding (Kim *et al.*, 2008; Hassel and Dingledine, 2012).

iGlus were originally classified into two groups, NMDA receptors (NMDARs) and non-NMDARs, depending on their responsiveness to N-methyl-D-Aspartate (NMDA). Non-NMDARs can be further organised into two categories (AMPA receptors and kainate receptors) depending on whether they are activated by α -amino-3-(3-hydroxy-5-methyl-isoxazol-4-yl)propanoic acid (AMPA) or by kainate (Lodge, 1997).

Chapter 1

Glutamate Receptors					
Ionotropic receptors (iGlu)			Metabotropic Receptors (mGlu)		
NMDA	AMPA	KAINATE	Class I	Class II	Class III
GluN1	GluA1	GluK1	mGlu ₁	mGlu ₂	mGlu ₄
GluN2A	GluA2	GluK2	mGlu ₅	mGlu ₃	mGlu ₆
GluN2B	GluA3	GluK3			mGlu ₇
GluN2C	GluA4	GluK4			mGlu ₈
GluN2D		GluK5			
GluN3A					
GluN3B					

Table 2 Overview of the molecular families of glutamate receptors. Illustrating both the ionotropic (iGlu) and metabotropic (mGlu) glutamate receptors as well as their known subunits. Modified from (Kew and Kemp, 2005) and updated with the current iGlu nomenclature accepted by the International Union of Basic and Applied Pharmacology (IUPHAR) in 2009 (Collingridge *et al.*, 2009) as well as the mGlu nomenclature as accepted by NC-IUPHAR Subcommittee on Metabotropic Glutamate Receptors (Alexander *et al.*, 2011).

Since the cloning of the first kainate receptor, GluK1, in 1989 (Hollmann *et al.*, 1989), a total of sixteen mammalian genes encoding for functional iGlus have been discovered as well as eight mGlus (Watkins and Jane, 2006). These molecular advancements, in conjunction with the analysis of ligand-binding selectivity, have led to an accurate classification of GluRs and its subunits which reflects their genetic relationship and homology (Kew and Kemp, 2005).

Each of the two main GluR divisions (iGlu and mGlu) comprise three functionally defined groups of receptors. These are made up of several subunits, each encoded by a different gene (Table 2). There is a fourth iGlu gene family that includes GluD1 and GluD2, however neither seems to form a channel that responds to Glu or glycine and therefore their exact role in synaptic transmission remains to be elucidated.

The most recent subunit nomenclature proposed by the International Union of Basic and Applied Pharmacology (IUPHAR) in 2009 reflects the genetic relationships of the different iGlu subunits with the exception of GluK1-3 and GluK4-5, which are encoded by distinct gene families, previously named GluR5-7 and KA1-2 respectively. All iGlus are formed by the assembly of a particular set of subunits (Table 2). AMPA receptors are polymers formed by the assembly of GluA1-4, kainate receptors are formed by assembly of the GluK1-5 subunits, and

Chapter 1

NMDARs by the assembly of GluN1 with GluN2A-D and GluN3A-B (Collingridge *et al.*, 2009).

To date, eight G-protein-coupled mGluRs have been discovered (mGlu1-8) as well as several splice variants. With the exception of mGluR6, which is confined to the retina, all mGluRs are expressed in the CNS. They are subdivided into three classes based on pharmacological properties, second messenger associations and sequence homology (Alexander *et al.*, 2011).

Class I receptors (mGlu1 and mGlu5) are expressed primarily at postsynaptic sites and couple via $G_{\alpha q/11}$ leading to phospholipase C activation which in turn cleaves phospholipid phosphatidylinositol 4,5-bisphosphate (PIP₂) into diacylglycerol (DAG) and inositol 1,4,5-trisphosphate (IP₃), (Kew and Kemp, 2005).

Both Class II (mGlu2 and mGlu3) and Class III (mGlu4, mGlu6, mGlu7, mGlu8) mGluRs couple via $G_{\alpha i/o}$, which inhibits adenylyl cyclase activity, resulting in a decrease in the intracellular concentration of cAMP. However, class III mGluRs are expressed predominantly at presynaptic sites regulating neurotransmitter release whereas class II mGluRs are expressed both pre- and postsynaptically (Kim *et al.*, 2008).

Other intracellular signaling cascades can be set into motion by all three classes of mGluRs through coupling to their respective G_{α} subunit. For instance, Ca²⁺ channels can be regulated by all three classes of mGluRs, K⁺ channels can be regulated by both class I and class II mGluRs and finally, adenylyl cyclase can be activated by class I mGluRs (Watkins and Jane, 2006).

1.2.1 NMDARs

During the early stages of NMDARs research, binding and patch-clamp studies provided evidence suggesting that not all NMDARs behave the same way (Cull-Candy *et al.*, 1988) Subsequent cloning of the NMDAR subunits yielded more information about the specific properties of each individual NMDAR according to its subunit composition (Moriyoshi *et al.*, 1991; Cull-Candy and Leszkiewicz, 2004).

Chapter 1

NMDA receptors (NMDARs) mediate several important functions in the CNS, yet very little is known about the exact stoichiometry of these receptors. The stoichiometry of the receptor remains dubious due to contradicting reports (Behe *et al.*, 1995; Premkumar *et al.*, 1997). Consequently, there is still uncertainty as regards to the exact function, pharmacology and biochemistry of the distinct NMDARs subtypes found in the brain tissue.

Functional NMDARs are made up of monomeric complexes associating in different combinations from the subunits GluN1, GluN2 and GluN3. For each one of these subunits there are various isoforms with distinct regional distribution and electrophysiological properties, thus further increasing the functional diversity of NMDARs within the CNS.

NMDARs are coupled to high conductance cationic channels, which are permeable to Ca^{2+} , Na^+ and K^+ . Upon activation of the NMDAR, the ionotropic channel will open causing the influx of Ca^{2+} and Na^+ and the efflux of K^+ . Though the current and membrane potential is affected by the added effect of individual ions, it has been shown that K^+ efflux is regulated by a different mechanism than Ca^{2+} and Na^+ influx (Ichinose *et al.*, 2003).

The first GluRs discovered were the NMDARs. Their characterisation was possible due to the ready availability of NMDA and to the existence of relatively specific agonists and antagonists.

The NMDAR is one of the most tightly regulated neurotransmitter receptors; it has at least six binding sites for endogenous ligands, which affect the probability of finding the channel in its open conformation. For instance, a typical NMDAR has a binding site for Glu (found in the GluN2 subunit), glycine, polyamines, as well as recognition sites for Mg^{2+} , Zn^{2+} and H^+ which will inhibit ionic flux in receptors with bound agonist (Nowak *et al.*, 1984; Hassel and Dingledine, 2012).

NMDARs are positively modulated by glycine and the channel to which the receptor is coupled is blocked in a use- and voltage-dependent manner by Mg^{2+} (Danysz and Parsons, 1998). The site of glycine modulation is found in the GluN1 subunit. Therefore, the NMDAR can only be activated after a depolarization of the postsynaptic membrane releases the Mg^{2+} ion from the

Chapter 1

channel's pore. This mechanism of Mg^{2+} regulation is responsible for the NMDARs contribution to the slow component of the current (Lodge, 1997). It is also the reason why NMDAR exhibit a late response to Glu when compared to non-NMDARs even though its EC_{50} is four hundred per cent lower than that of AMPA (Dingledine *et al.*, 1999).

The redox state of the receptor also affects its response. For instance, one of the three pairs of cysteine has to be reduced (which increases the currents mediated by the receptor) or oxidised, forming disulphide bonds (which reduces the currents) (Bough *et al.*, 2006; Karakas *et al.*, 2011).

The NMDAR is unique in that it needs the simultaneous stimulation of two agonists (Glu and glycine) for its activation. The binding site for glycine in the NMDAR is different to the one found in the glycine receptor in that it cannot be blocked by strychnine nor can it be activated by β -alanine (Karakas *et al.*, 2011).

Even though glycine and Glu are necessary for NMDAR activation, the receptor's overall electric response will ultimately be regulated by Mg^{2+} , which binds to the extracellular region of the pore when the channel is in its open state. Several uncompetitive NMDAR antagonists act in a similar way to Mg^{2+} , such as ketamine, phencyclidine, dextromethorphan, memantine, and dizocilpine maleate (MK-801). However, the specific blocking kinetics as well as the voltage dependence of each one of these antagonists varies greatly (Rogawski, 1993; Parsons *et al.*, 1995; Lodge *et al.*, 1996; Danysz and Parsons, 1998).

The GluN3 subunit forms a channel that is activated by glycine when it binds with the GluN1 subunit. The GluN3 subunit has a dominant-negative effect on channel behaviour when it is coexpressed with the GluN1 and GluN2 subunits. This is possibly due to the fact that the GluN3 subunit decreases the magnitude of GluN1/GluN2 receptor-mediated currents by a novel mechanism that involves the formation of a narrow constriction in the outer vestibule of the channel, making the channel impermeable to sulfhydryl-specific agents (Wada *et al.*, 2006).

Another endogenous allosteric inhibitor of the NMDAR acting on the GluN2B subunit is H^+ , as protons reduce the frequency with which the channel opens its

Chapter 1

pore. For instance, at a pH of 6, the activation of the channel is completely suppressed (Traynelis *et al.*, 1995).

Aside from the regulation mechanisms mentioned above, the NMDAR is also inhibited in a calcium dependent manner through activation of various calcium-dependent proteins, including calmodulin, calcineurin, protein kinase C, and α -actinin-2. It has been shown that an intracellular increase of Ca^{2+} can activate calmodulin, which in turn interacts with the GluN1 subunit leading to a reduction in the duration of native NMDAR single-channel openings from 3.5 ± 0.6 msec to 1.71 ± 0.2 msec (Ehlers *et al.*, 1996). Phosphatase 1 and 2a have been shown to regulate the calcium-calmodulin complex through the phosphorylation of calcium-calmodulin kinases suggesting yet another regulatory mechanism for the activation of NMDAR (Ehlers *et al.*, 1996; Rycroft and Gibb, 2002, 2004).

The NMDARs electrophysiological properties mentioned above (permeability, modulatory sites, voltage dependence) along with their ability to differentially respond to a given stimulus, are some of the underlying mechanisms that cooperate to achieve synaptic plasticity.

Most high affinity glycine B antagonists tested *in vitro* show very poor blood-brain barrier permeability and become inactive after systemic administration (Danysz and Parsons, 1998). Therein lies the importance of some kynurenine pathway members, such as kynurenic acid (KA) and some of its derivatives, which act as endogenous antagonists of the NMDAR.

1.2.2 GluN1 splice variants

The effect of NMDRs varies significantly depending on their specific subunit combination (homooligomeric, heterodimeric and tri-heteromeric), which confers them with distinct pharmacological properties that result in the activation/inhibition of a large number of signaling pathways.

The configurational and functional complexity of the NMDARs is further increased as GluN1 subunits are prone to post-transcriptional events (RNA editing and alternative splicing), which may result in distinct isoforms (eight for

Chapter 1

the GluN1 subunit) caused by the presence of independent sites of alternative splicing. According to this, there are at least a dozen functionally distinct NMDARs subtypes though, it has been suggested there could be a considerably higher number of these subtypes, especially since receptor subunits might undergo further posttranslational and epigenetic modifications (such as phosphorylation, glycosylation, and palmitoylation). Each of these modifications determines the specific properties of each NMDAR such as its channel functions which result in an even more intricate complexity and diversity of signal transductions (Paoletti, 2011; Paoletti *et al.*, 2013).

1.2.3 Neurotrophic Effect of Glutamate.

Growth factors (also known as trophic factors) bind to cell-surface receptors to initiate signaling pathways that result in the survival, growth and differentiation of numerous cell types by promoting the synthesis of various macromolecules or by inhibiting their degradation.

Apoptosis in the developing brain is a naturally occurring process that determines adult brain functioning. The inability of cells to undergo apoptosis during brain development leads to adult malformations as well as cognitive and behavioural deficits (Sastry and Rao, 2000). The signaling mechanism by which some cells survive and others are removed involves the competition of innervating terminals for trophic factors. The neurotrophic hypothesis states that during critical periods of brain development, migrating cells compete for limited amounts of trophic factors: those that fail to establish functional synapses with their target cells die by apoptosis (Aloe *et al.*, 2012; Serrano-Castro and Garcia-Torrecillas, 2012).

Whereas this was initially proved to be true for Nerve Growth Factor (NGF), Ciliary Neurotrophic Factor (CNTF) and Glial Derived Neurotrophic Factor (GDNF), it is now evident that the trophic effect of Glu receptor activation (acting via mGluR or iGluR) is developmental stage dependent and regulates a variety of aspects of neurodevelopment such as proliferation, migration, differentiation as well as the survival of neurons that managed to establish proper connections (Lujan *et al.*, 2005; Jansson and Akerman, 2014). It has been shown that selectively blocking GluRs during this critical developmental period causes the widespread loss of neurons. Conversely, interfering with the physiological removal of redundant cells causes brain malformations. In addition to synaptic transmission, the physiological stimulation of GluRs can act as a trophic stimulus in the adult brain and is also involved in neuronal plasticity (Balazs, 2006).

For example, Glu acts as a chemoattractant molecule (enhancing migration) on neurons in the developing cortex through the activation of the NMDAR (Behar *et al.*, 1999). Another example comes from cultured somatosensory relay neurons, where NMDAR blockade promotes cell death through the activation of BAX

Chapter 1

(apoptosis regulator bcl-2-like protein 4) which temporally coincides with a peak in cell death and synaptogenesis during development *in vivo* (de Rivero Vaccari *et al.*, 2006).

Similarly, primary cultures of cerebellar granule neurons undergo apoptosis when grown in low potassium (5mM) medium. Under the same conditions, apoptosis is prevented by the addition of NMDA (Balazs *et al.*, 1988) or by other depolarizing stimuli (Yan *et al.*, 1994). It has been hypothesised that this depolarization mimics the *in vivo* neurotrophic effect that pontocerebellar mossy fibres exert on ectopic CGNs or those in the granular layer (Hamori and Somogyi, 1983; Berciano and Lafarga, 1988). Conversely, blockade of NMDAR during late foetal or early neonatal life causes apoptosis in the rat brain (Ikonomidou *et al.*, 1999).

Following NMDAR activation, there is an increase in the intracellular concentration of Ca^{2+} , which activates protein kinases of the canonical pathway Ras-MAPK/ERK, and PI3-K-Akt. These protein kinases will in turn activate transcription factors such as CREB, SRF, MEF, NF- κ B and Arc ultimately regulating the expression of genes involved in survival and synaptic plasticity (Zheng *et al.*, 2009).

It has been suggested that several cancers recapitulate the same underlying biology (regarding the trophic effect of Glu) that occurs during the early developmental stages of the CNS, where Glu receptor activation acts as a trophic factor promoting neuronal migration and survival (Sontheimer, 2008).

1.2.4 Glutamate Signaling and Cancer

Although cancer and the loss of tissue homeostasis arise from oncogenic mutations rather than by the sole effect of growth factors, the latter play a crucial role in the subsequent steps of tumour progression (clonal expansion, migration, angiogenesis and colonization). Oncogenic mutations that affect signaling pathways activated by growth factors enable tumours to proliferate in the absence of growth factors. The ability of uncontrollable propagation and migration through deregulation of growth factor receptor activity is common in several tumours (Witsch *et al.*, 2010).

Chapter 1

Due to the overlap between the signaling pathways that follow NMDAR and growth factor receptor activation in cancer (in particular the PI 3-K and MAPK pathway activated by EGF and FGF) it is not surprising that glutamate was suggested as a potential growth factor in tumour development (Li and Hanahan, 2013).

A long-standing paradigm suggested that Glu signaling is limited to the central nervous system. However this notion has been revised due to several studies that have unequivocally proved the existence of GluRs in peripheral organs (Hinoi *et al.*, 2004) and neoplastic cells (Kalariti *et al.*, 2005). The widespread expression of GluRs in different tissues highlights the importance of studying the role that Glu signaling may play in the development of cancer especially in view of the fact that cancer stem cells share several characteristics, such as proliferation, migration and Glu responsiveness, with neuronal embryonic cells. This was recently proven by the differential expression of functional calcium-permeable AMPA receptors in glioblastoma brain tumour initiating cells in contrast to tumour cultures consisting of non-stem cells (Oh *et al.*, 2012).

Perhaps the most compelling evidence linking Glu signaling and cancer comes from studies showing that excessive Glu release promotes tumour growth through the activation of iGluR and mGluR (Ye and Sontheimer, 1999; Rothstein and Brem, 2001; Takano *et al.*, 2001; Haas *et al.*, 2005; Kalariti *et al.*, 2005; Ishiuchi *et al.*, 2007) . Conversely, it has been shown both *in vitro* and *in vivo* that Glu antagonists effectively inhibit cancer growth, cell division and migration while enabling different human tumour cells (including those of nervous system origin) to regain the ability to die (Cavalheiro and Olney, 2001; Rzeski *et al.*, 2001; Takano *et al.*, 2001; Rzeski *et al.*, 2005; Stepulak *et al.*, 2005; Wang *et al.*, 2006; Haas *et al.*, 2007; Namkoong *et al.*, 2007).

It has been suggested that Glu promotes tumour growth via at least three mechanisms: a) the trophic effect leading to cell division and the activation of survival pathways such as PI3K and AKT; b) the induction of excitotoxic death in surrounding cells; c) the cysteine/glutamate exchanger system and GSH production. (Sontheimer, 2008; Herner *et al.*, 2011; Haas *et al.*, 2013; Li and Hanahan, 2013; D'Mello S *et al.*, 2014; Stepulak *et al.*, 2014).

Chapter 1

In a glutamate transport study comparing glioma cells and normal astrocytes, it was shown for the first time that gliomas produce high amounts of Glu (100 μM within hours) which causes the excitotoxic death of surrounding cells. The NMDAR antagonist MK-801 effectively protected surrounding cells from undergoing excitotoxic death and phenylglycine derivatives acting on mGluR completely inhibited the release of Glu in glioma cells (Ye and Sontheimer, 1999).

The release of Glu by gliomas and the subsequent excitotoxic death of surrounding neurons may explain the incidence of tumour-associated seizures in patients with glioma. Furthermore, it may represent an essential mechanism that enables tumoural growth *in vivo* where the skull limits space as, unless normal brain cells are destroyed, tumours cannot expand. Indeed, the NMDAR antagonists MK-801 and memantine slow the growth of Glu-secreting tumours *in situ* (Rothstein and Brem, 2001; Takano *et al.*, 2001).

It has been shown that Glu production in gliomas fuels the cysteine/glutamate exchanger system (xCT) by enabling the release of copious amounts of Glu and import of the cysteine necessary for the synthesis of glutathione (GSH), a major cellular antioxidant that protects tumour cells from endogenously produced reactive oxygen and nitrogen species. Pre-clinical data demonstrates that inhibition of xCT leads to GSH depletion, which in turn slows tumour growth. Conversely, GSH levels positively correlate with tumour resistance to radiation and chemotherapy (Sontheimer, 2008).

Although the majority of paediatric solid tumours of the CNS (including glioma) do not express functional NMDAR (Sontheimer, 2008; Brocke *et al.*, 2010), high GluN2B expression levels correlated with high vGluT2 (vesicular glutamate transporter) expression. Furthermore, the survival of patients with glioblastoma is significantly shorter when the expression of GluN2B/vGLUT2 is elevated (Li and Hanahan, 2013). Activated NMDARs increase the proliferation of both U87MG and U251MG glioma. Conversely, blockade of the NMDAR by MK-801 decreases their proliferation (Ramaswamy *et al.*, 2014). Similarly, silencing the GluN2A subunit-targeted gene inhibits the proliferation of gastric cancer cells with an arrest on the G1-phase of the cell cycle (Watanabe *et al.*, 2008). Analogously,

Chapter 1

GluN1 knockdown TE671 and A549 cells (lung cancer) exhibit reduced survival as opposed to their wild-type counterparts (Luksch *et al.*, 2011).

A few reports have demonstrated that tumour size, the presence of lymph node metastases and the cancer stage correlate to high GluN1 expression in patients with oral squamous cell carcinoma (Choi *et al.* 2004). Additionally, it has been shown that the occurrence of somatic mutation in GRIN1 and GRIN2A is a common feature in melanomas with the latter being the most prevalent target (Wei *et al.*, 2011). It has been reported that the methylation rates of the promoter CpG islands of GRIN2B are increased in samples from *in situ* ductal carcinoma (not yet invasive or metastatic) when compared against pre-invasive lesions which suggests that methylation of GRIN2B is an early event in mammary cancer progression (Park *et al.*, 2011). Taken together, these results suggest that hijacking the signaling pathways controlled by NMDARs provides cancer cells with a selective advantage that enables them to proliferate.

Although NMDAR antagonists (such as norketamine 72, memantine and MK-801) have little effect on glioma growth *in vitro* (due to the lack of NMDAR in gliomas), preclinical studies have shown that NMDAR antagonist have been shown to have antiproliferative and anti-excitotoxic effects *in vivo*. These results have subsequently led to the entering of memantine in a Phase II clinical trial to determine its safety/efficacy for patients with glioma (<http://Clinicaltrials.gov/#NCT01260467>); the study has been completed but results are not yet available.

The evidence presented in this section opens up the possibility that other endogenous ligands of the Glu receptor such as QA (QA; agonist) and kynurenic acid (KA; antagonist), which are both members of the kynurenine pathway, could also be involved in the regulation of tumoural development. *in vitro* studies have shown that QA restores cell proliferation in two cell lines derived from human colorectal carcinomas (Thaker *et al.*, 2013) and conversely KA inhibits growth, DNA synthesis and migration of several cancer cell lines such as colon adenocarcinoma (Walczak *et al.*, 2011) and renal cancer cells (Walczak *et al.*, 2012).

1.3 The kynurenine pathway: a general overview

The kynurenine pathway is the main catabolic pathway of the essential amino acid L-Tryptophan (Trp). Approximately 95% of bioavailable Trp goes through this metabolic pathway, and it owes its name to the fact that almost all of its metabolites are derived directly or indirectly from L-kynurenine (Figure 1), which in turn is the major degradation product of this pathway (Stone and Darlington, 2002).

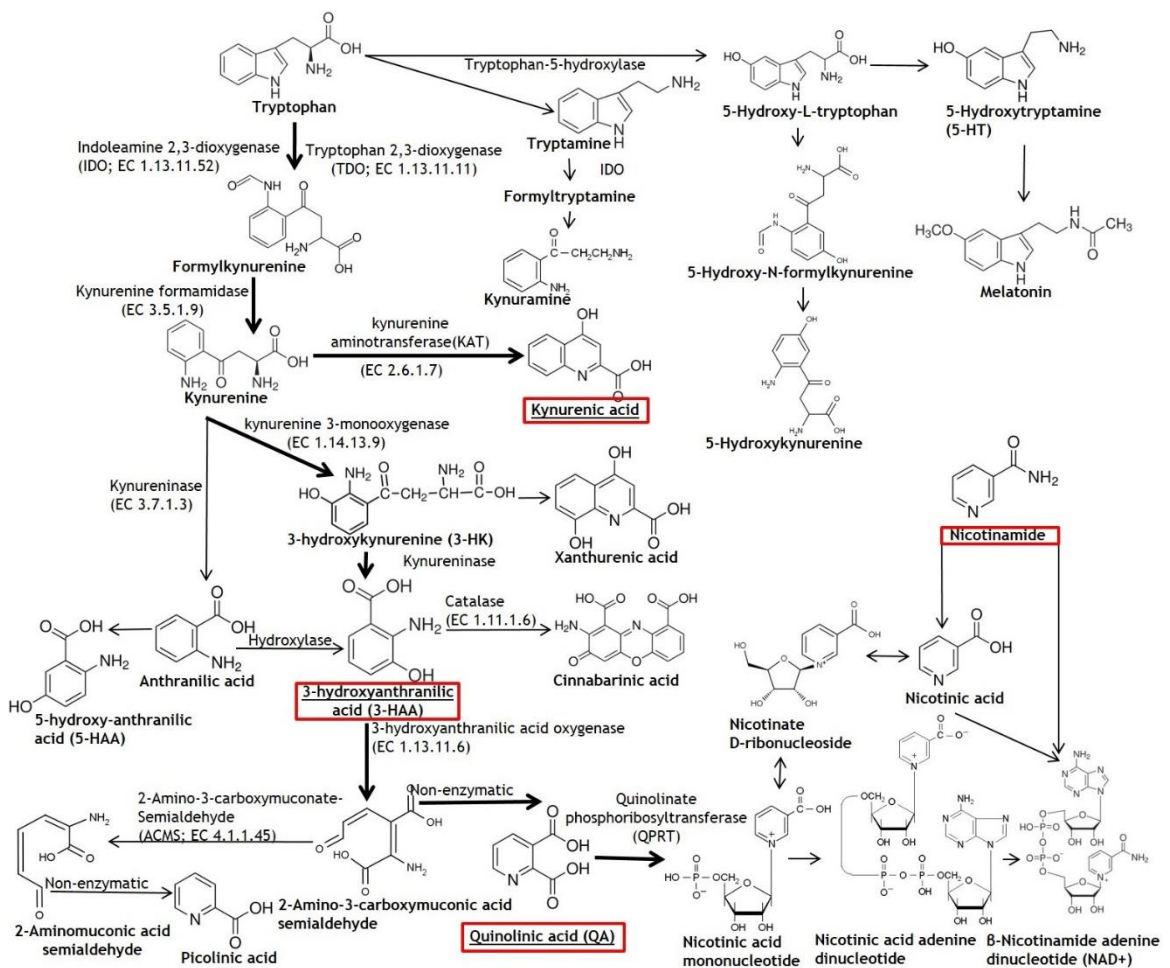


Figure 1. Tryptophan metabolism Kynurenine pathway and Methoxyindole pathway. Modified (Stone and Darlington, 2002).

The other route for the transformation of Trp is the methoxyindole pathway in which Trp is first hydroxylated, without the indole ring being lost, yielding 5-hydroxytryptophan and then decarboxylated forming the neurotransmitter 5-hydroxytryptamine (5-HT, serotonin). This conversion is conducted by tryptophan hydroxylase and by 5-hydroxytryptophan decarboxylase respectively, and this reaction is the rate-limiting step for the formation of serotonin. Serotonin can be subsequently N-acetylated and then O-methylated to form

Chapter 1

melatonin, a well-known CNS inhibitor of glutamatergic-induced damage (Lapin *et al.*, 1998).

In 1947 the kynurenine pathway was recognised as the major route of Trp transformation (Beadle *et al.*, 1947) and for a long time the interest in this pathway depended mainly on its role during the synthesis of nicotinamide adenine dinucleotide (NAD⁺) and NAD⁺ phosphate (NADP), which participate in various cellular processes related to hydride transfers and redox reactions.

It was not until 1973 that the psychoactive nature of some kynurenines was discovered regarding depression (Lapin, 1973) and shortly afterwards other neuroactive properties were attributed to kynurenines, specifically the ability of QA (QA) to cause convulsions when injected intraventricularly to mice (Lapin, 1978).

In 1981 it was finally discovered that QA excites glutamatergic neurons through activation of N-methyl- D-aspartate (NMDA) receptors (Stone and Perkins, 1981). It then became apparent that QA could be involved in the pathogenesis of various neurodegenerative diseases where such excitatory amino acid receptors had been implicated and excitotoxic damage observed (Mattson, 2007).

Further research on the kynurenine pathway led to the discovery of kynurenic acid (KA), a broad-spectrum inhibitor of excitatory amino acid receptors (Perkins and Stone, 1982; Nemeth *et al.*, 2005) which has neuroprotective properties. KA allosterically antagonises the NMDAR at the glycine site on the receptor complex and thus acts as a neuroprotectant against excitotoxic insults where NMDA overactivation occurs. KA can also presynaptically inhibit $\alpha 7$ nicotinic acetylcholine receptor (Schrocksadel *et al.*, 2003) thus regulating not only glutamatergic but also cholinergic synaptic transmission (Carpenedo *et al.*, 2001).

The enzymes involved in the kynurenine pathway have been the subject of much study as regulating their activity could shift the kynurenine metabolism towards either harmful (QA, 3-HK 3-Hydroanthranilic acid) or neuroprotective (KA) compounds. Indeed, the kinetics and substrate selectivity of most kynurenine

Chapter 1

enzymes has been elucidated and reasonable success has been made in the development of inhibitors.

1.3.1 Principal Metabolites and enzymes of the Kynurenine Pathway

Most Trp is metabolised in the liver, and substrate flux is regulated by tryptophan 2, 3-dioxygenase (TDO) which is the initial, rate-limiting and highly substrate-specific enzyme of the kynurenine pathway. TDO is responsible for the cleavage of the indole ring of Trp, forming N-formylkynurenine and then kynurenine (Bender and McCreanor, 1982; Stone, 2001). In extrahepatic tissues, the predominant enzyme carrying out the above transformation is a heme enzyme called indoleamine 2,3-dioxygenase (IDO) which, interestingly, is the only enzyme, aside from superoxide dismutase, that can use $O_2^{\cdot-}$ as a substrate.

Of particular interest, in neuroscience, is IDO since it is the enzyme found in neuronal cells. Nonetheless, it is worth noting that TDO is expressed in astrocytes and is of importance when considering the role of microglia in the physiology of the CNS, particularly during immune activation (Fuhrmann *et al.*, 2010).

The next step in the kynurenine pathway is the conversion from formylkynurenine to kynurenine (KYN) that is catalysed by formamidase (see Figure 1). KYN can be found throughout the mammalian body (in the liver, kidney, spleen, lung, intestine, blood and brain). It is well transported across the blood-brain-barrier by the neutral amino acid carrier (Fukui *et al.*, 1991). The exact function of KYN has eluded researchers for a long time since no direct cytoprotective or cytotoxic effects could be attributed to it.

Previous studies suggested that the binding of KYN (from the degradation of Trp by IDO) to the aryl hydrocarbon receptor (AHR) could lead to the generation of T_{regs} (Mezrich *et al.*, 2010). AHR is a xenobiotic receptor that functions as a transcriptional master molecule for drug-metabolizing enzyme genes. Interestingly, there had been some clues pointing to the possibility that an endogenous ligand of the AHR could be found among tryptophan metabolites of the kynurenines pathway. For instance, Tryptophan photo-derivatives and

Chapter 1

indigoids (indigo and indirubin) had previously been reported to be agonists of the AHR *in vivo* (Helferich and Denison, 1991; Peter Guengerich *et al.*, 2004). Tryptophan photo-derivatives, indigoids and kynurenines are all indole-derived compounds with a similar structure to xenobiotic ligands (planar halogenated aromatic hydrocarbons) of the AHR. Furthermore, an overlap had also been found between the roles of IDO and AHR in immune regulation, inflammation and carcinogenesis (Stevens *et al.*, 2009). Until recently, the relevance of KYN relied exclusively on the fact that it is a precursor of both KA and QA. However, a novel role for KYN in the facilitation of tumour-immune escape has been discovered in glioma cell lines and glioma-initiating cells, which will be discussed in section (1.3.5).

The transformation of kynurenine by kynurenine hydroxylase or kynureninase generates more than twenty kynurenine metabolites, classified initially as a) NMDA agonists (such as QA and picolinic acid) or b) free radical generators (such as 3-HK and 3-HAA), a classification that is nowadays obsolete considering the close interrelationship between kynurenine metabolites and the generation of oxidative stress (Oxenkrug, 2007).

1.3.2 Kynurenic Acid

Kynurenic acid (KA) is an endogenous molecule found in the human brain at a concentration of approximately 50 pmol/g under normal physiological conditions (Moroni *et al.*, 1988; Turski *et al.*, 1988; Turski *et al.*, 1989; Moroni *et al.*, 2012). It is believed that the astroglia are the main source of the KA found in the brain (Speciale *et al.*, 1989; Eastman *et al.*, 1994).

Kynurenic acid (KA) is produced by the transamination of kynurenine (KYN). In human, rat and mouse, this reaction can be catalysed by four kynurenine aminotransferases (KAT); KAT I/glutamine transaminase K/cysteine conjugate β -lyase 1, KAT II/aminoadipate aminotransferase, KAT III/cysteine conjugate β -lyase 2, and KAT IV/glutamic-oxaloacetic transaminase 2/mitochondrial aspartate aminotransferase (Stone, 1993; Han *et al.*, 2010).

It has been speculated that KATI and KATII are the main enzymes responsible for KA production in the mammalian brain, given their specificity and abundance in

Chapter 1

the brain (Guidetti *et al.*, 2007). The notion that KATII has a very high specificity for KYN has been challenged more recently. KATII is able to transaminate 16 out of 24 amino acids and it can use 16 α -oxo acids as amino-group acceptors (Han *et al.*, 2008). It is important to mention that a more recent review generated a substrate profile for all KATs. This study generated a comparison of the biochemical and structural characteristics of mammalian KATs proving that all four KATs are multifunctional enzymes that share many substrates and therefore have overlapping biological functions (Han *et al.*, 2010).

Even though KA is a compound that has been known for more than 150 years (Liebig, 1853; Asayama, 1916), its ability to antagonise the neuronal excitatory response to QA, quisqualate, NMDA and Glu was not described until 1982 (Perkins and Stone, 1982). Kessler and colleagues, using receptor binding assays, (Kessler *et al.*, 1989a; Kessler *et al.*, 1989b) discovered that KA binds to the glycine B site of the NMDAR.

Electrophysiological analysis in infant rat hemisected spinal cords showed that with increasing concentrations of KA, there were parallel shifts in the concentration-response curve to NMDA, and that dose ratios above 3×10^{-3} M produced a flattening of the NMDA curve (Birch *et al.*, 1988) This demonstrates that KA has an antagonist effect on the NMDAR. KA can efficiently inhibit glutamatergic neurotransmission. It blocks both the allosteric glycine B site, IC_{50} of 43 mM ([³H]glycine binding) and the Glu binding site (Danysz *et al.*, 1989a, b; Kessler *et al.*, 1989b; Danysz and Parsons, 1998). Interestingly, endogenous, physiological levels of KA have been shown to prevent Glu-induced neuronal death. It has been shown that when KA is applied exogenously, it decreases the activation of NMDARs (Birch *et al.*, 1988; Velisek *et al.*, 1995). It is still unclear whether the levels of KA found in the brain are sufficiently high to block the NMDAR and whether, under certain conditions, the levels can oscillate more, rendering KA a more powerful regulator of NMDAR.

There is data showing that the levels of KA are affected under several physiological conditions, for example in aging animals (Gramsbergen *et al.*, 1992), or pathological ones such as excitotoxic events (Wu *et al.*, 1992b; 1992a), epileptic seizures of the nucleus accumbens, system infection (Heyes and

Chapter 1

Lackner, 1990; Heyes *et al.*, 1990; Heyes *et al.*, 1992), Huntington's disease (Connick *et al.*, 1988; 1989) and Down's syndrome (Baran *et al.*, 1996).

The KA concentration, as well as that of other kynurenines, fluctuates during development. It is initially high in prenatal rodents (300 fmol/mg of protein), reduced at birth and up to the first postnatal week, and then finally increased again thereafter (Beal *et al.*, 1992; Cannazza *et al.*, 2001). Questions have been raised about the efficiency of KA on its own and whether this can be increased by co-administering KA with adjuvants or compounds like Probenecid that inhibit brain efflux, by administering KA precursors such as 4-chlorokynurenine, or by inhibiting the subsequent catabolic break down of KA.

It has been suggested that concentrations below the micromolar range of KA can interact with nicotinic acetylcholine (Schrocksnadel *et al.*, 2003) receptors, blocking the $\alpha 7$ -nACh subtype with a half-maximal inhibitory concentration of 7 μM ; this probably contributes to its protective properties during excitotoxicity (Hilmas *et al.*, 2001). This cross-talk between KA and nicotinic transmission could play a role in the development of some brain disorders, like schizophrenia and Alzheimer's disease, where KA levels are elevated and nicotinic functions are impaired (Nemeth *et al.*, 2005; Stone, 2007). Unfortunately, KA crosses the blood-brain barrier by passive diffusion at a considerably slow rate 1.16×10^{-5} ml/sec/gr (Fukui *et al.*, 1991). Therefore, the focus of much research has been on the theoretical development and synthesis of KA derivatives able to cross the blood-brain barrier.

It has also recently been reported that KA is an agonist of G-protein-coupled receptor 35 (Wang *et al.*, 2006; Cosi *et al.*, 2011) as well as an endogenous ligand for the human aryl hydrocarbon receptor (AHR); in this context, it is an efficient activator of IL6 production in MCF-7 cells. If this observation can be confirmed *in vivo*, it would have wide ranging implications in determining how the AHR may be activated in various cell type (DiNatale *et al.*, 2010)

1.3.2.1 KA derivatives

It is obvious that modifying the basic structure of KA and its analogues could lead to novel compounds with increased effectiveness. For instance, lipophilic and size-limited-disubstitutions with chlorine or bromine in the 5- and 7-positions of KA increases affinity for glycine B site in rat cortex/hippocampus P2 membrane and in a rat cortical wedge preparation (Foster *et al.*, 1992).

The effect of these substitutions seems to be additive, in terms of potency and selectivity. Chloro, bromo, and methyl groups were found to be the desirable substitutions at the 7-position and larger functional groups like iodo and ethyl seemed to work best at the 5-position. All compounds with substitutions at position 6 showed more affinity for the AMPA receptor, behaving as competitive antagonists. Substitutions at the 8-position rendered the entire compound inactive in all the receptors (Leeson *et al.*, 1991).

In rat cortical slices, the halogen substituted derivative 7-chlorokynurenic acid (7-Cl KA), in concentrations ranging from 10-100 μM , noncompetitively inhibits NMDA responses, yet this effect can be reversed by the addition of glycine to the preparations. Radioligand binding experiments showed that 7-Cl KA has a much higher affinity for the strychnine-insensitive glycine-binding site (Kemp *et al.*, 1988).

The halogenated KYN derivatives, 7-chlorokynurenic acid (7-Cl-KA) and 5,7-dichlorokynurenic acid (5,7-Cl₂-KA), show a very high potency and selectivity for NMDAR *in vitro* (Leeson *et al.*, 1991). 7-Cl KA also showed anticonvulsant and neuroprotective properties after intracerebroventricular administration (Singh *et al.*, 1990; Namba *et al.*, 1993; Bonina *et al.*, 2000).

However, once 7-Cl-KA and 5,7-Cl₂-KA are administered systemically, their potency and minimal blood brain barrier permeability render these derivatives inefficient (Leeson and Iversen, 1994). Administering direct precursors such as L-4-chlorokynurenine (4-Cl-KYN) and L-4,6-dichlorokynurenine (4,6-Cl₂-KYN), manages to increase the brain level of 7-Cl-KA and 5,7-Cl₂-KA, respectively (Hokari *et al.*, 1996).

Chapter 1

More recently, in an effort to generate masked compounds that go through the blood-brain barrier, three new esters have been synthesised by chemical conjugation with essential nutrients like glucose and galactose (Bonina *et al.*, 2000).

1.3.3 3-Anthranilic Acid (AA), Hydroxykynurenine (3-HK) and 3-Hydroxyanthranilic acid (3-HAA)

Kynurenine (KYN) is the substrate of three competing enzymes: KATs, kynurenine 3-monooxygenase and kynureninase. These enzymes catalyse the degradation of KYN to KA, 3-HK and anthranilic acid (AA), respectively. The activity of 3-monooxygenase is higher than that of kynureninase, therefore an increase in the levels of KYN will predominantly lead to an increase in the concentration of 3-HK rather than to that of AA.

Kynureninase (EC 3.7.1.3) is also able to catalyse the transformation of 3-HK into 3-HAA. Initially, it was believed that 3-HK was the main source of 3-HAA due to the fact that kynurenine 3-monooxygenase has a higher affinity than kynureninase for KYN (Bender and McCreanor, 1982). For instance, no labelled [13C6]QA was formed in medium containing labelled [13C6]AA, but [13C6]QA was produced in medium containing labelled L-[13C6]Trp (Saito *et al.*, 1993a). However, more recent pharmacokinetic studies suggest that it is the preference of kynureninase for 3-HK over KYN (265-fold preference) which explains why the majority of peripheral 3-HAA comes directly from 3-HK (Lima *et al.*, 2009; Phillips, 2011).

In DB/2 mice, Chiarugi *et al.* (1995) showed that inhibition of kynurenine 3-monooxygenase by intraperitoneal administration of m-nitrobenzoylalanine (mNBA) and of kynureninase by o-methoxybenzoylalanine (oMBA) increases the levels of KYN and KA in the brain, blood, liver, and kidney. Furthermore, the same treatment offers protection against spontaneous locomotor activity and audiogenic convulsions. These results indicate that the predominant pathway of 3-HAA formation is via 3-HK hydrolysis and that its pharmacological modulation has a positive effect on behavioural parameters.

Chapter 1

In Swiss male mice, intraperitoneal administration of KYN increases the brain and blood content of KA, 3-HK and AA. Inhibition of kynurenine 3-monooxygenase by mNBA decreases the brain content of 3-HK and 3-HAA but it increases the levels of KA and AA. Conversely, mNBA decreases the blood content of 3-HK but not that of 3-HAA which suggests that in peripheral tissues and in blood, hydroxylation of AA may be the predominant pathway of 3-HAA formation. The results regarding oMBA (the inhibitor of kynureninase) are inconsistent: oMBA did not reduce the levels of 3-HAA in either blood or brain and the concentration of AA was affected in a dose dependent matter not only in the brain but also biphasically in the periphery (Chiarugi *et al.*, 1996). It has recently been suggested that the synthesis of previous kynureninase inhibitors had been based on mechanistic considerations and ignored in the primary substrate binding mode and in substrate-enzyme interactions necessary for *in silico* directed drug design (Lima *et al.*, 2009). In fact, another molecule that acts as a kynureninase inhibitor has been recently synthesised, namely 3-hydroxyhippurate (Phillips, 2011).

There is evidence that challenges the predominance of 3-HK as the main precursor of 3-HAA in the brain and AA in the periphery. In blood, AA produces more 3-HAA due to the unspecific microsomal hydroxylation that occurs in the liver (Ueda *et al.*, 1978).

Exposure of rat cortical brain slices to 1mM of AA and 3-HK resulted in a rapid and transient increase in the concentration of 3-HAA (Baran and Schwarcz, 1990). In the brain, the maximal 3-HAA production from AA is 11-fold higher compared to the maximal 3-HAA production from 3-HK. Conversely, in the spleen, 3-HK is a better precursor of 3-HAA (Baran and Schwarcz, 1990). The conclusion from these studies is that, within the brain, AA is a better precursor of 3-HAA contrarily to what happens in the periphery (Schwarcz *et al.*, 2012).

Other studies, regarding the predominance of AA or 3-HK as a precursor of 3-HAA, suggest that no generalisations can be made in terms of localization (brain or periphery) since this will vary according to the species and the cell type analysed within these locations (Fujigaki *et al.*, 1998; 1999).

Chapter 1

Therefore, despite the fact that the degradation of 3-HK by 3-monooxygenase is the most recognised metabolic pathway of 3-HAA formation, the contribution and importance of AA in 3-HAA generation should not be ignored.

For many years, the focus of kynurenine research has been on the direct effects of QA and KA on NMDAR as electrophysiological studies of 3-HK and 3-HA have not been able to establish a direct effect on neuronal transmission (Stone, 1993). However, AA, 3-HK and 3-HAA have been described as pro- and antioxidant molecules in biological systems that can affect the complex processes in which the redox state of the cell is involved.

It has recently been discovered that xanthurenic acid (a product of 3-HK) and cinnabarinic acid (an oxidation product of 3-HAA) can activate Glu metabotropic receptors (Fazio *et al.*, 2012; Copeland *et al.*, 2013).

1.3.3.1 Role of 3-HK and 3-HAA in pathological events

3-HK and 3-HAA are both toxic to different cell types due to their conversion to quinonimines and subsequent generation of ROS (Okuda *et al.*, 1998; Goldstein *et al.*, 2000; Morita *et al.*, 2001; Fatokun *et al.*, 2008b; Lee *et al.*, 2010). 3-HAA can undergo autoxidation producing H_2O_2 , hydroxyl radicals and superoxide anion ($\text{O}_2^{\cdot-}$) all of which are ROS that have been widely implicated in cell death mechanisms (Manthey *et al.*, 1992).

The physiological levels of 3-HAA and 3-HK are within a nanomolar concentration, although micromolar levels have been detected in patients with hepatic encephalopathy, Huntington's disease, PD and (HIV)-1-associated dementia. It has been shown that 3-HK and 3-HAA cause cell death of primary cultures with apoptotic features, such as condensed and fragmented nuclear morphology, DNA fragmentation and an increase in caspase activity (Vamos *et al.*, 2009).

The treatment of monocyte-derived cell lines (U937 and THP-1) with 200 $\mu\text{mol/L}$ 3-HAA for 48 hours induced apoptosis. The toxicity induced by 3-HAA was reduced by the addition of the antioxidant trolox or α -tocopherol as well as by allopurinol, a xanthine oxidase inhibitor. Apoptosis was potentiated in the

Chapter 1

presence of ferrous and manganese ions. In this study, SOD was unable to rescue the cells from apoptosis and catalase provided only slight protection. These results suggest that 3-HAA acts through a mechanism that involves ROS production, most likely H₂O₂ (Morita *et al.*, 2001).

Different compounds such as epigallocatechin 3-gallate, N-acetylcysteine, catalase and allopurinol can protect against caspase activation and cell death induced by 3-HK. This indicates that the neurotoxic effects of 3-HK are mainly, if not entirely, due to an increase in the production of ROS which will lead to caspase activation (Okuda *et al.*, 1998; Nemeth *et al.*, 2005).

There also seems to be a difference on the susceptibility to these compounds depending on the cell type. For instance, in one study, it was shown that cortical and striatal neurons are more susceptible to 3-HK toxicity than cerebellar granule neurons. This difference in susceptibility may be due to the specific transporter activities present in these neurons. In the same study 3-HAA was also less potent at inducing damage than 3-HK. When 3-HAA was used, a concentration higher than 10µM for 48h was necessary to induce cell death as opposed to just 1µM when 3-HK was used (Okuda *et al.*, 1998). Interestingly, toxicity is attenuated by catalase, but not by either SOD or desferrioxamine (Smith *et al.*, 2007). In MC3T3-E1 osteoblast-like cells, 1mM 3-HK but not 3-HAA (also 1mM) significantly reduces viability 24 hours after treatment (Fatokun *et al.*, 2008b).

Changes in the concentration of AA, 3-HAA and 3-HK have also been reported to occur in some pathological conditions. For instance, patients with osteoporosis have lower baseline levels of 3-HAA and high levels of AA when compared with healthy individuals. In this study, the patients receiving therapy for a period of two years showed an improvement in bone density that correlates with a reversal of the 3-HAA:AA ratio to control levels (Forrest *et al.*, 2006).

In patients with advanced Huntington's disease, the ratio of 3-HAA and AA is also affected, with AA levels higher than those of 3-HAA when compared to healthy individual or to patients at early stages of the disease progression (Stoy *et al.*, 2005; Forrest *et al.*, 2010).

1.3.3.2 Autoxidation of 3-HAA

The complete autoxidation of 3-HAA involves several steps and transient intermediaries that produce various ROS. However, three main reaction steps can be outlined.

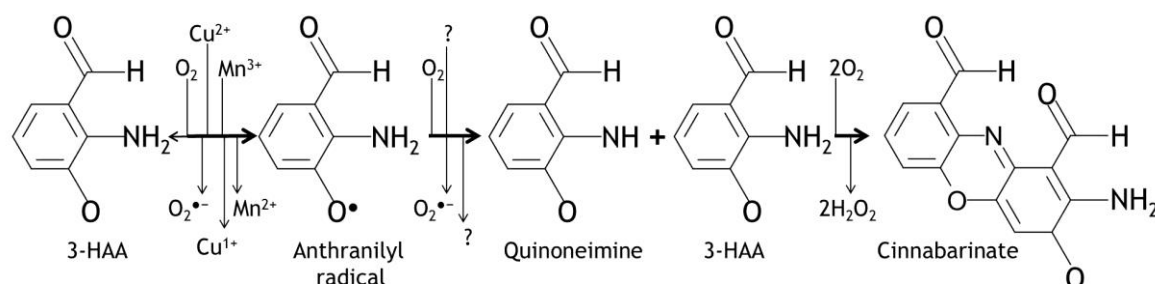


Figure 2 Three-step reaction for the complete oxidation of 3-HAA. First, 3-HAA is oxidised to anthranilyl radical, which upon a second oxidation forms quinoneimine. The imine is then condensed with another 3-HAA molecule to form cinnabarinic acid and H₂O₂. This Scheme is consistent with the fact that the cinnabarinic acid production is enhanced by manganese ions, copper and copper containing superoxide dismutase (SOD).

First, the *o*-aminophenol structure of 3-HAA is oxidised to form semiquinoneimine (anthranilyl radical) and superoxide (O₂^{•-}) followed by a second oxidation that produces the *p*-quinone dimer quinoneimine and O₂^{•-}. The quinoneimine formed is highly reactive and continues to oxidise. In the third part of the process, a series of oxidative modifications and a condensation with another molecule of 3-HAA form cinnabarinic acid and hydrogen peroxide (H₂O₂). Cinnabarinic acid is broken down by H₂O₂, a process that can be prevented by catalase (Dykens *et al.*, 1987). Labelling studies using ¹⁸O₂ show that the C-2 oxygen in the *p*-quinone dimer comes from molecular O₂, therefore aerobic conditions are necessary for the reaction to occur (Manthey *et al.*, 1990).

Cu-Zn-SOD increases the autoxidation of 3-HAA by a mechanism not fully characterised yet. One hypothesis is that the newly formed products of the first oxidation of 3-HAA (O₂^{•-} and anthranilyl radical) are involved in a backreaction. Alternatively O₂^{•-} could be neutralising other oxidant agents by switching its behaviour into reducing agents, therefore slowing down 3-HAA oxidation. Under these two possibilities the dismutation of O₂^{•-} by SOD would accelerate 3-HAA breakdown (Dykens *et al.*, 1987; Ishii *et al.*, 1990; Christen *et al.*, 1992).

Another possibility to explain the increased rate of cinnabarinic acid production, in the presence of SOD, is that the O₂^{•-}, produced during the autoxidation of 3-

Chapter 1

HAA degrades cinnabarinic acid. Thus the co-application of SOD causes an apparent increase in its concentration without the actual reaction rate being affected (Manthey *et al.*, 1990). This seems an unlikely explanation since it only takes into account the increase in the concentration of the final product (cinnabarinic acid) but it ignores the decrease in the concentration of the initial reactant (3-HAA) in the presence of SOD.

Interestingly, when added to a phosphate buffer solution, both 3HK and 3-HAA are able to generate $O_2^{\cdot-}$ and H_2O_2 in the presence of copper (Cu). At a physiological pH and under aerobic conditions, 3-HK and 3-HAA reduce Cu^{2+} to Cu^+ and Fe^{3+} to Fe^{2+} . The metal reduction observed could not be elicited by other kynurenines and therefore it is thought to be dependent on the presence of the *o*-aminophenol structure, which both 3-HK and 3-HAA share (Goldstein *et al.*, 2000).

In a more thorough study, it has been shown that in the absence of O_2 , 3-HAA reduces Cu^{2+} -Zn-SOD to Cu^+ -Zn-SOD with a subsequent reoxidation of Cu^+ -Zn-SOD by $O_2^{\cdot-}$ which provides Cu-Zn-SOD with the catalytic activity of a superoxide reductase to which 3-HAA serves a substrate. Furthermore, in the same study it is demonstrated that Mn-SOD does not affect the rate autoxidation of 3-HAA which categorically disproves the alleged back reaction of $O_2^{\cdot-}$ with the anthranilyl radical as a possible mechanism by which Cu-Zn-SOD accelerates the autoxidation of 3-HAA (Liochev and Fridovich, 2001).

Consequently, a more likely hypothesis has been put forward suggesting that SOD is directly affecting the rate of 3-HAA autoxidation by a mechanism in which the active site of Cu-Zn-SOD undergoes a series of reduction and oxidation cycles (just as Cu and Fe have been shown to do on their own). The mechanism proposed does not preclude the possibility that Cu-Zn-SOD may oxidise other radical intermediates besides 3-HAA. Furthermore, since the mechanism suggested requires the presence of $O_2^{\cdot-}$ (which may come from the oxidation of 3-HAA) for the reoxidation of Cu^+ -Zn-SOD, it may explain why in previous studies a direct role was attributed to $O_2^{\cdot-}$ in the autoxidation rate of 3-HAA.

1.3.3.3 Protection by 3-HAA

It has been reported that the redox behaviour of 3-HK and 3-HAA, and hence their toxicity, depends on different factors such as the presence of redox agents like O₂ and transition metal ions, in particular iron, manganese and copper.

The mechanism of action of 3-HAA, even though not as thoroughly studied as that of QA, has proven to be a complex process in which 3-HAA metabolism is subject to tight regulation. The importance of 3-HAA in healthy organisms is just beginning to be elucidated.

Toxicity for instance does not necessarily mean an overall deleterious effect. This is particularly true when discussing it from an organismic point of view, in which regionalised events of oxidative stress or even cell death guarantee the homeostasis of an organism. Superoxide for example is a very reactive and toxic molecule in biological systems and it could easily be considered as detrimental to organisms. However, during infection episodes, O₂^{•-} is used by the immune system to attack pathogens. Similarly, it has recently been reported that, despite the oxidising nature of 3-HAA and 3-HK, under certain conditions they can behave as antioxidants, protect cells against oxidative damage, inhibit inflammation in different models of autoimmune diseases, protect against atherosclerosis, and kill activated T cells (but not resting ones) after infection (Thomas *et al.*, 1996; Backhaus *et al.*, 2008; Chadha *et al.*, 2009; Lee *et al.*, 2010; Krause *et al.*, 2011; Piscianz *et al.*, 2011; Zhang *et al.*, 2012b).

In a model that mimics inflammation of the CNS by exposing human foetal brain tissue, or adult human glial cells, to cytokines (10 ng/ml of IL-1 with or without 1ng of interferon- γ), it was reported that adding 100 μ M 3-HAA suppressed glial cytokine and chemokine expression and reduced cytokine-induced neuronal death. This protection was attributed to the ability of 3-HAA to increase the expression of hemeoxygenase-1 (HO-1), an inducible enzyme with anti-inflammatory and cytoprotective properties. In this study it is suggested that the ability of 3-HAA to increase the expression of HO-1 is due to its oxidant properties. 3-HAA can induce the antioxidant response element, which is activated by the nuclear factor (erythroid-derived-2) like-2 (NRF2), which HO-1 depends on (Krause *et al.*, 2011).

Chapter 1

Most studies suggesting that 3-HAA has neuroprotective properties are based on the overall effect that 3-HAA has on cell cultures or *in vivo*; these results should be interpreted carefully since low concentrations of almost any drug can cause a favourable biological response, a phenomenon known as hormesis.

Nevertheless some studies have been able to attribute not only beneficial properties but also direct antioxidant properties to 3-HAA. One such study used a pulse radiolysis technique to investigate the behaviour of 3-HAA in oxidising conditions, and it was found that 3-HAA has a high affinity for nitrogen and oxygen radicals, and that it can repair the free radical modifications caused by the guanosine radical and the chlorpromazine cation radical (Chadha *et al.*, 2009).

It has been shown that interferon- γ -induced oxidation of the low density lipoprotein (LDL) causes the degradation of extracellular Trp with an increase in the levels of kynurenine (KYN), anthranilic acid and 3-hydroxyanthranilic acid (3-HAA). Furthermore, the oxidation induced by interferon- γ was potentiated in the absence of Trp, and the addition of exogenous 3-HAA was able to inhibit the oxidation of LDL (Christen *et al.*, 1994). Later studies by the same group showed that the inhibition of LDL oxidation by 3-HAA was due to the ability of its aminophenol ring to reduce the α -tocopheroxyl radical (α -TO \cdot) which propagates peroxidation during the initial stages of the lipid peroxidation. Under these conditions, 3-HAA was just as potent an antioxidant as ascorbate (Thomas *et al.*, 1996).

Murine RAW 264.7 macrophages that are stimulated with IFN-gamma and lipopolysaccharide (LPS) have enhanced levels of NO and increased expression inducible nitric oxide synthase (iNOS), heme oxygenase (HO)-1 and indoleamine 2,3-dioxygenase (IDO). It has been shown that both HO-1 and 3-HAA prevent these cells from generating NO by inhibiting the expression of iNOS (Sekkaï *et al.*, 1997). More recently, it has been shown that 3-HAA acts upstream of the HO-1 inhibition of iNOS, and not directly on iNOS. Indeed, 3-HAA acts by increasing the expression of HO-1, which in turn will decrease the expression of inducible nitric oxide synthase (Oh *et al.*, 2004).

Chapter 1

Additionally, another report shows that by becoming the main target of NO attack, 3-HAA is nitrosated forming o-quinone diazide; this can effectively reduce the negative impact that NO has on other component of the cellular machinery. In this study, 3-HAA proved to be a better scavenger than N-acetylcysteine (Backhaus *et al.*, 2008).

1.3.4 Quinolinic Acid (QA)

3-hydroxyanthranilic acid 3,4-dioxygenase (3-HAO; EC 1.13.11.6) catalyses the conversion of 3-HAA to 2-Amino-3-carboxymuconate semialdehyde from which QA is nonenzimatically formed by a spontaneous cyclisation reaction. Alternatively, 2-Amino-3-carboxymuconate semialdehyde can be converted to 2-aminomuconic semialdehyde by α -amino- β -carboxymuconate-epsilon-semialdehyde-decarboxylase (ACMSD; EC 4.1.1.45). 2-aminomuconic semialdehyde is the direct precursor from which picolinic acid is formed (PIC; also nonenzimatically). The non-enzymatic transformation of 2-amino-3-carboxymuconic semialdehyde to QA occurs when ACMSD is saturated with its substrate. It has been suggested that under normal conditions these two pathways control equal flux. Thus ACMSD is positioned at a key branching point that will determine whether 2-Amino-3-carboxymuconate semialdehyde will be converted to QA for NAD⁺ biosynthesis (discussed in section 1.4) or to picolinic acid (Grant *et al.*, 2009).

It has been shown that QA can induce excitotoxic damage, furthermore, when administered intracerebrally to rodents and non-human primates, it mimics Huntington's disease (Schwarcz *et al.*, 1983; Beal *et al.*, 1986; Stone, 1993). QA has been implicated in the pathogenesis of several inflammatory neurological diseases, e.g. Increased levels of QA and its producing enzymes has been reported in Alzheimer's disease, AIDS associated dementia, ischemia, epilepsy and Huntington's disease. In cell culture, acute damage by QA can be achieved at micromolar concentrations even after only a few hours' exposure and chronic damage occurs at nanomolar concentrations (Whetsell and Schwarcz, 1989).

One of the mechanisms underlying QA toxicity involves its ability to stimulate glutamatergic receptors which causes an increase in the intracellular concentration of Ca²⁺ and which in turn results in apoptosis and atrophy. For

Chapter 1

instance, the hippocampus has been found to be very susceptible to damage by this particular mechanism.

Even though QA is an agonist of the NMDAR, it only activates the NMDAR that has the right combination of subunits and it does so with very low affinity and efficacy. This was proven in *Xenopus* oocytes transfected with NMDAR, in this model, QA did not activate receptors containing GluN1/GluN2C but it did activate receptors containing GluN1/GluN2A and GluN1/GluN2B. Nevertheless, activation was only achieved at millimolar concentrations and therefore QA is considered to be a relatively weak NMDAR agonist (de Carvalho *et al.*, 1996).

It has been suggested that the toxicity of QA cannot be explained exclusively in terms of its excitatory properties on NMDAR, instead several other mechanisms may underlie its mechanism of action. For instance, toxicity has been observed to occur at doses below what would be necessary for effective NMDAR stimulation. In line with this, a growing body of evidence has accumulated that clearly shows that there are additional mechanisms involved in QA-mediated toxicity. For example, QA has the ability to induce oxidative stress independently of NMDAR activation (Rodriguez-Martinez *et al.*, 2000; Santamaria *et al.*, 2001) and it can directly disrupt energy metabolism (Ribeiro *et al.*, 2006; Schuck *et al.*, 2007b; 2007a). Furthermore, QA acts as a precursor of NAD⁺ in many tissues. For instance, QA will serve as a precursor to replenish NAD⁺ levels in activated leukocytes during immune response when the induction of oxidative stress leads to energy depletion in leukocytes (Moffett and Namboodiri, 2003)

For all these reasons, altering the concentration of QA can have an important impact on cellular physiology either by NMDA activation and signal transduction or by metabolic regulation of NAD and ROS production.

1.3.5 Regulating the metabolism of Trp metabolites.

It has been suggested that blocking Trp metabolism downstream of KYN, using inhibitors of kynureninase and kynurenine 3-monooxygenase, could represent a novel and successful therapy in the treatment of several diseases because the balance between QA and KA would shift towards the latter (Stone and Darlington, 2002).

The development of pharmacological tools to study the kynurenine pathway *in vivo* has proven to be a difficult task. For instance, many members of the kynurenine pathway and enzyme inhibitors currently available, do not cross the blood-brain barrier, thus their administration has to be performed intracerebrally.

The large neutral amino acid carrier (L-system) of the blood-brain-barrier efficiently transports 3-HK and KYN into the brain. AA uptake by the brain occurs by passive diffusion at a considerable rate. Passive diffusion of 3-HAA, KA and QA occurs at a lower rate and plasma protein binding interferes with their transfer (Fukui *et al.*, 1991). Despite the fact that the tools used so far are not ideal, they have been helpful in understanding the role that kynurenines have in the brain.

One such tool is γ -(3-pyridyl)- γ -oxo- α -aminobutyrate, referred to as nicotinyllalanine, which inhibits kynureninase and kynurenine 3-monooxygenase both *in vitro* and *in vivo* (Decker *et al.*, 1963). In rodents, nicotinyllalanine causes an increase in the brain levels of KA without a concomitant increase in QA within the brain (Moroni *et al.*, 1991).

Intraperitoneal injection of nicotinyllalanine protects mice against leptazol and shock-induced convulsions (Connick *et al.*, 1992) providing evidence to support the hypothesis that modulation of the kynurenine pathway can cause an increase in the endogenous concentration of KA to levels that can exert neuroprotection. Since then, other compounds have been found to successfully increase the level of KA, such as mNBA (inhibitor of kynurenine 3-monooxygenase) and oMBA (inhibitor of kynureninase) in the hippocampus (Chiarugi *et al.*, 1996).

Chapter 1

This modulation can be also accomplished with (R,S)-3,4-dichlorobenzoylalanine, formerly known as FCE 28833A and more recently as PNU156561. Systemic administration of PNU156561 (400 mg/kg) increases the maximal level of KA to 120 nM (Speciale *et al.*, 1996) which is much lower than the 15 μ M K_i of KA for the glycine B site of the NMDAR (Kessler *et al.*, 1989a). Furthermore, in a gerbil model of global ischemia, intraperitoneal administration of 1000 mg/Kg of KA leads to an increase in the brain levels of KA (30-40 μ M). This is the lowest concentration able to exert neuroprotection (Salvati *et al.*, 1999).

The evidence presented in this section shows that research on the kynurenine pathway has tended to focus on shifting the balance away from QA and towards kynurenic acid by means of inhibitors. However, the local and systemic effect that this shift has on the synthesis of nicotinamide adenine dinucleotide (NAD⁺) needs to be studied in greater detail.

1.3.6 The Kynurenine pathway in cancer pathogenesis

Over the past decade, there has been a dramatic increase in the experimental data supporting the role of IDO-1 as an important immunoregulatory enzyme that suppresses T-cell responses and promotes tolerance.

Early reports documented the ability of IDO to inhibit the proliferation of intracellular pathogens and tumour cells *in vitro* (Carlin *et al.*, 1989). For a long time, IDO continued to be considered as part of the host defence system against pathogens such as cytomegalovirus, *Toxoplasma spp.*, *Rickettsia conorii*, *Chlamydia psittaci*, *Mycobacterium avium* and class B streptococci (Gupta *et al.*, 1994; MacKenzie *et al.*, 1998; Hayashi *et al.*, 2001). However, the relevance of these observations *in vivo* has recently been questioned in the light of new discoveries that link IDO activation to the suppression of T-cell responses.

An additional immunoregulatory role for IDO was first proposed based on studies of mammalian pregnancy in which IDO activation was shown to be necessary to avoid spontaneous abortions caused by immune cells that fail to recognise the foetus (Munn *et al.*, 1998; Kudo and Boyd, 2001; Li *et al.*, 2003; Moffett and Nambodiri, 2003; Schrocksnadel *et al.*, 2003). Furthermore, low levels of IDO

Chapter 1

activity and hence high levels of Trp have been found during preeclampsia (Kudo and Boyd, 2001).

Subsequently, considerable experimental data from several models has accumulated demonstrating that IDO regulates innate as well as adaptive T-cell immunity. For example, IDO activation causes a reduction in proliferation in peripheral blood mononuclear cells co-cultured with IDO-expressing skin cells treated with IFN- γ (Sarkhosh *et al.*, 2003a). Human bone marrow stromal cells expressing IDO have an enhanced rate of tryptophan catabolism, which inhibits allogeneic T-cell proliferation. The addition of tryptophan in these cultures significantly restores the allogeneic proliferation of t-cells (Meisel *et al.*, 2004).

Fibroblasts expressing IDO and plated within collagen gel suppress the proliferation of allogeneic immune cells while remaining viable. The addition of an IDO-inhibitor (1-methyl-d-tryptophan) is able to counteract the inhibitory effects of IDO (Sarkhosh *et al.*, 2003b). On the other hand, when IDO is repressed in a model of animal HIV-1, elimination of infected macrophages is enhanced (Potula *et al.*, 2005).

It was initially proposed that the immunosuppression accompanying IDO activation could be explained solely in terms of Trp starvation given that T-cells growing in a conditioned medium (in co culture with macrophages) required the addition of Trp to proliferate after treatment with macrophage-colony-stimulating factor (Munn *et al.*, 1999). However, this hypothesis was based on largely indirect evidence and ignored the fact that other bioactive metabolites are produced downstream and as a consequence of IDO activation.

More recent studies provide evidence indicating that the immunosuppression caused by IDO activation involves at least three mechanisms: a) the removal of Trp necessary to proliferate; b) the production and/or accumulation of biological active downstream kynurenines; and c) the enhancement of the inhibitory potential of kynurenines as a direct consequence of Trp depletion (Munn *et al.*, 2005).

For instance, it has been shown that in the presence of extracellular Trp, treatment of peripheral blood lymphocytes with KYN and picolinic acid (but not

Chapter 1

QA) causes a dose-dependent inhibition of proliferation. Conversely, in the absence of extracellular Trp, all three metabolites effectively inhibit proliferation. (Frumento *et al.*, 2002). Similarly, the downstream metabolites of the kynurenine pathway 3-HAA and QA induce the selective apoptosis of murine thymocytes and of antigen-specific CD4⁺ T-helper 1 (T_{H1}) but not T_{H2} cells both *in vivo* and *in vitro* (Fallarino *et al.*, 2002; Fallarino *et al.*, 2003).

Interestingly, a new link has been established between IDO activation, the production of 3-HAA and the generation of tolerogenic foxp3⁺ T-regulatory cells (T_{regs}). *in vitro* studies have shown that in the presence of kynurenines (before T-cell cycle arrest due to a critical shortage of Trp) there is an early response that includes CD3 ζ downregulation and generation of T_{regs} from naïve CD4⁺ T-cells (Fallarino *et al.*, 2006). Furthermore 3-HAA from IDO induction by dendritic cells causes a reduction in CD4⁺ T_{H17} cells and a reciprocal increase in the fraction of T_{regs} (Favre *et al.*, 2010). These mechanisms act on specific T-cell subtypes to synergistically generate a unified immunosuppressive response with GCN2 (the general control non-derepressing 2 protein kinase) as one of the molecular sensors of intracellular tryptophan (Munn *et al.*, 2005; Fallarino *et al.*, 2006). T_{regs} in turn cause the induction of IDO in antigen-presenting cells via ligation of their CTLA4 (cytotoxic T lymphocyte-associated protein 4) with the CD80/CD86 found on antigen presenting cells. This has been suggested to be an important mechanism by which T_{regs} induce and maintain peripheral tolerance (Mellor *et al.*, 2004; Mellor and Munn, 2004; Puccetti and Grohmann, 2007). Furthermore, T_{regs} enforce dendritic cells and skin grafts to express enzymes that catabolize at least five different essential amino acids (including tryptophan), which also inhibits T-cells proliferation by decreased mammalian target of rapamycin (mTOR) signaling (Cobbold *et al.*, 2009) as well as GCN2.

This positive-feedback system involving the induction of IDO in dendritic cells, 3-HAA production, the differentiation of T_{regs} by 3-HAA and finally further IDO induction in dendritic cells, may play a significant role in suppressing an effective immune antitumour response. Especially in view of the fact that the ratio of T_{H17}-T_{regs} has replaced the twenty year-old T_{H1}-T_{H2} paradigm in cancer research (Peck and Mellins, 2010).

Chapter 1

An in-depth review of both paradigms is beyond the scope and aim of this study and a difficult one at that, in view of the fact that the exact molecular mechanism by which both subsets (T_H1 - T_H2 and/or T_H17 - T_{reg}) exert their actions, continues to be a matter of debate.

Briefly, the majority of tumours arise as a result of genetic and epigenetic changes in a particular tissue. These changes are often accompanied by an acute inflammation process, which involves the recruitment of granulocytes, lymphocytes (B-cell, T-cell and Natural killer cells), fibroblasts, endothelial cells as well as the release of inflammatory cytokines in the area surrounding the tumour. All these elements are indispensable participants in the neoplastic process and are collectively referred to as the tumour microenvironment. The tumour microenvironment determines the invasive potential of a newly formed tumour depending on the overall effect it has on cell proliferation, survival, angiogenesis and metastasis (Hanahan and Weinberg, 2000).

Several studies have demonstrated the presence of tumour-infiltrating lymphocytes in the lungs of patients with non-small cell lung cancer (Imahayashi *et al.*, 2002), in particular of $CD4^+$ T-cells. $CD4^+$ T-cells are significantly important in removing cancerous tissue or cells. $CD4^+$ T-cells can be functionally divided into T_H1 , T_H2 , T_H17 , and regulatory T cells (T_{regs}) based on the cytokines they secrete (Yusuf, 2014).

T_H1 cells (which produce interleukin-2, IFN- γ , and tumour necrosis factor-alpha) are tumour infiltrators that predominantly promote antitumour responses as opposed to T_H2 cells (which produce Interleukin- 4, 5, 6, 10 and 13) and predominantly inhibit antitumour responses. Both have been implicated in the development of different types of cancer (Dennis *et al.*, 2013).

T_H17 cells predominantly induce antitumour immunity by facilitating T-cell recruitment to the tumour site and $CD8^+$ T-cell priming. In contrast, T_{regs} promote acquired tolerance to tumours. Multiple lines of evidence have indicated that T_{regs} are involved in the control of the local immune response and in the growth of human lung cancer (Woo *et al.*, 2002; Erfani *et al.*, 2012; Ganesan *et al.*, 2013). *In vitro*, lung interstitial antigen-presenting cells suppress T-cell mediated response by overexpressing IDO. Inhibition of IDO activity results

Chapter 1

in the spontaneous proliferation of lung T-cells and inflammation. Similarly, immunotolerance after transplant is increased when overactivation of IDO occurs (Swanson *et al.*, 2004).

The studies presented thus far demonstrate that the kynurenine pathway plays an important role in the regulation of cellular immune responses. This opens up the possibility that a link may also exist between the kynurenine pathway and cancer pathogenesis. In support of this view, it has been shown that in a syngeneic model of Lewis lung carcinoma, the expression of IDO is increased in mononuclear cells that surround the tumours as well as in tumour-draining lymph nodes. In this study, it is shown for the first time that the inhibition of IDO (with 1-methyl D-tryptophan; 1-MDT) effectively delays tumour growth (Friberg *et al.*, 2002).

In a series of elegant experiments, Uyttenhove and collaborators (2003) provided extensive evidence that directly links the expression of IDO with tumoural progression; more specifically, that IDO confers suppressor activity to tumours and tumour cell lines. First, the constitutive expression of INDO (the gene that codifies for IDO) and its presence, as a functionally active protein, was found in several tumour cell lines (LB1610-MEL, melanoma line; MZ-PC-1, pancreatic carcinoma; NCI-H596, non-small-cell lung carcinoma; LB1263-SCCHN, laryngeal carcinoma; LB1165-SCCHN, pharyngeal squamous-cell carcinoma) at comparable levels to those found in human placenta. Similarly, IDO expression was detected in several human tumours (prostatic, pancreatic, colorectal carcinomas and gliomas) but not in normal stromal cells which suggests that IDO expression is relegated to the tumour microenvironment (Uyttenhove *et al.*, 2003). The intraperitoneal inoculation of syngeneic DBA/2 mice with P815 cells (a mastocytoma cell line) induces the formation of tumours. Pre-immunisation with P1A antigen protects these mice against tumour formation (Van den Eynde *et al.*, 1991). However, when injected with modified P815 cells (in which the expression of IDO had been enhanced) the majority of pre-immunised mice developed progressive tumours. A positive correlation was demonstrated between the rate of tumour progression and the expression of IDO as well as a concomitant decrease in the number of P1A-specific T-cells in the tumoural cavity (Uyttenhove *et al.*, 2003).

Chapter 1

It has recently been suggested that the evaluation of tryptophan accumulation by positron emission tomography (PET) can improve pre and post-treatment delineation of glioblastomas and metastatic brain tumours because it improves the delivery of radiotherapy and chemotherapy to more efficient levels. (Kamson *et al.*, 2013).

Moreover, the evaluation of IDO-1 expression has been shown to be a powerful predictor of patient outcome in various cancers (Mellor *et al.*, 2005). In the particular context of brain tumours, it has been shown that IDO over-expression correlates with poor patient outcome which opens up the possibility of using IDO as a prognostic indicator and as a discriminatory tool to decide the course of treatment (Wainwright *et al.*, 2012).

Based on preclinical studies showing that IDO inhibition causes tumour regression, pharmacologic IDO inhibitors such as 1-DMT and INCB024360 alone or in combination with other standard of care chemotherapeutic drugs (Docetaxel) are currently being used in phase II clinical trials on patients with advanced solid tumours (Wainwright *et al.*, 2013). The results from the two initial studies using IDO inhibitors have been long awaited and to date remain unpublished. Preliminary results indicate that 1-DMT treatment is well tolerated by patients treated with both INCB02436 and ipilimumab (IPI) and may have better outcomes as compared to IPI monotherapy (Gibney *et al.*, 2014). Similarly, a phase I trial (NCT01219348) has been completed in which the effects and optimal dose of a synthetic peptide vaccine that targets IDO was assessed in patients with metastatic non-small cell lung cancer (Iversen *et al.*, 2014). It has also been suggested that the ratio of KYN/Trp in serum could be used as an alternative non-invasive biomarker for evaluating the efficacy of IDO inhibitors in the clinic (Muller *et al.*, 2005).

To date, there are twenty-six clinical trials studying the effect and efficacy of cancer therapies targeting IDO alone or in combination with other standard of care drugs as part of a multidrug-treatment therapy. For a comprehensive table, showing a list of ongoing clinical trials targeting IDO alone or as an adjuvant immunotherapy, refer to section 6.2 of the Appendix (page 198 Table 8).

Chapter 1

As previously mentioned, in addition to IDO, Tryptophan 2,3-dioxygenase (TDO) metabolises Trp as well. Although initially believed to be present exclusively in the liver, there is now evidence suggesting that it is also expressed in brain tissue where it may locally alter the concentration of several kynurenines (Kanai *et al.*, 2009).

Two recent studies outline a critical role for TDO in regulating immune responses (Schmidt *et al.*, 2009) and its constitutive expression has been found in several cancers (hepatocellular carcinoma, melanoma, and bladder cancer) including brain tumours (malignant glioma) (Opitz *et al.*, 2011; Pilotte *et al.*, 2012). In the first study, another mechanism for facilitating tumour-immune evasion is reported in glioma cell lines and glioma-initiating cells (GICs), where TDO-2 is frequently activated and constitutively expressed leading to the production of KYN which suppresses anti-tumour immune responses and promotes tumour-cell survival and motility by acting as a ligand of the human aryl hydrocarbon receptor (AHR) in an autocrine manner (Opitz *et al.*, 2011). The second study provides additional evidence supporting the role of TDO expression by cancer cells in the promotion of tumoural growth. The authors show that TDO expression by tumours prevents their rejection in immunized mice and that, upon systemic treatment with a TDO inhibitor, these mice regain the ability to reject implanted cancerous cells (Pilotte *et al.*, 2012).

Both studies provide evidence suggesting that the enzymatic activity of TDO is sufficient to alter Trp metabolism and suppress antitumour immune responses which may also explain why, in previous studies, no aberrant immunological phenotype was found in IDO and GCN2 null mice (Cobbold *et al.*, 2009; Prendergast *et al.*, 2010). These recent developments will surely bring with them the advent of a new plethora of cancer research trials, this time, targeting TDO instead of IDO. Indeed, several studies have suggested that it is of the utmost importance to explore the possibility of a combined therapy using IDO and TDO inhibitors in order to increase the efficacy of restoring tumoural immune responses (Platten *et al.*, 2012; Ott *et al.*, 2014; Pantouris and Mowat, 2014).

Other than the previously direct effect of 3-HAA, QA, and picolinic acid (PIC) on immunosuppression (Fallarino *et al.*, 2002; Frumento *et al.*, 2002; Fallarino *et*

Chapter 1

al., 2003; Fallarino *et al.*, 2006; Favre *et al.*, 2010), the involvement of the metabolites and enzymes of the lower segment of the kynurenine pathway in the development of cancer has remained virtually unexplored. Nevertheless, several descriptive studies have shown that there is a difference in the concentration of several kynurenines between healthy and pathological states such as cancer (Schwarcz *et al.*, 2012).

In patients with primary cervical cancer (PCC), it has been reported that there is a change in the systemic concentration of several Kynurenines. For instance, whereas there are no changes in Trp and KA concentration between healthy and patients with PCC, the activity of IDO and the levels of kynurenic acid are significantly lower in PCC patients when compared to controls while the levels of QA are significantly higher. Overall the ratio of QA to KA is markedly different between healthy individuals and those with PCC (Fotopoulou *et al.*, 2011). Additionally, several studies have shown that KA inhibits proliferation and migration of Caki-2 and human glioblastoma T98G Cells (Walczak *et al.*, 2011; Walczak *et al.*, 2012; Walczak *et al.*, 2014)

Within and around brain tumours, variable numbers of QA immunoreactive cells have been detected. It has been suggested, that this may aid inflammatory cell infiltrates during immune tumoural response (Moffett *et al.*, 1997).

It has been shown that exogenous administration of kynurenines such as KYN and QA causes the activation of β -catenin and concomitant proliferation of human colon cancer cells as well as increased tumour growth in mice.(Thaker *et al.*, 2013)

It has been shown that kynurenines (N-formylkynurenine, N-formylanthranilic acid, KYN, AA, 3-HAA) can be detected after Interferon- γ induction of IDO in the SK-N-SH neuroblastoma cell line, proving that they possess the main set of enzymes of the kynurenine pathway (Werner-Felmayer *et al.*, 1989). Several other groups have confirmed this observation (Saito *et al.*, 1993b; Heyes *et al.*, 1997; Guillemin *et al.*, 2007).

Guillemin and colleagues (2007) carried out the first complete characterization of the kynurenine pathway in primary neurons and in the neuroblastoma cell line

Chapter 1

SK-N-SH. The authors found that both in primary and SK-N-SH cells, there is a balance between TDO and IDO expression whereby in the absence of one, the other's expression is increased. Whereas certain kynurenine pathway enzymes were shown to be downregulated (KAT-I, KAT-II) other were upregulated (KMO) in SK-N-SH cells. Perhaps most importantly, the authors show that QA increases the proliferation of SK-N-SH cells and conversely, PIC reduces it (Guillemin *et al.*, 2007).

Drawing on an extensive range of sources, Adam and collaborators (2012) have proposed a compelling new hypothesis that if confirmed, directly links QA production to the progression of cancer. The authors suggest that increased levels of QA confer a selective advantage to cancerous cells by maintaining a high supply of NAD⁺ (Adams *et al.*, 2012).

1.4 Nicotinamide metabolism

In order to make this section easier to understand it is necessary to make a brief list of the common names and synonyms used in the literature to refer to the components of the nicotinamide pathway, which is independent from the earlier list of abbreviations and easier to refer to, if necessary:

- **NAD⁺**: β -Nicotinamide adenine dinucleotide, β -DPN, β -NAD, Coenzyme 1, Cozymase 1, DPN, Diphosphopyridine nucleotide, Nadide.
- **NADH**: nicotinamide adenine dinucleotide reduced.
- **NADP⁺**: β -Nicotinamide adenine dinucleotide phosphate, Coenzyme 2, Cozymase 2, Codehydrogenase 2, Codehydrase 2 and finally, in the earlier literature Triphosphopyridine nucleotide.
- **NADPH**: Nicotinamide adenine dinucleotide phosphate reduced.
- **NaMN**: Nicotinic acid mononucleotide.
- **NaAD**: nicotinic acid adenine dinucleotide, nicotinic acid adenine dinucleotide.
- **NaADP**: Nicotinic acid adenine dinucleotide phosphate.
- **Nam**: Nicotinamide, Niacinamide, Nicotinic acid amide, Pyridine-3-carboxylic acid amide, vitamin B3.
- **MNam**: 1-Methylnicotinamide
- **NMN**: Nicotinamide mononucleotide, Nicotinamide ribonucleotide.
- **NA**: Nicotinic acid, 3-Carboxylpyridine, 3-Pyridylcarboxylic acid, Niacin, vitamin B3.
- **NR**: Nicotinamide Riboside, Nicotinamide- β -ribose, N-Ribosylnicotinamide, 1-(β -D-Ribofuranosyl)nicotinamide.

Chapter 1

- **Qprt**: quinolinic acid phosphoribosyltransferase.
- **Nmnat**: nicotinamide-nucleotide adenylyltransferase 2, Nicotinamide mononucleotide adenylyltransferase 2 (EC 2.7.7.1; EC 2.7.7.18).
- **NNMT**: Nicotinamide N-methyltransferase (EC 2.1.1.1).
- **Nadsyn1**: glutamine-dependent NAD⁺ synthase (EC 6.3.5.1).
- **PBEF**: nicotinamide phosphoribosyltransferase, Nampt (EC 2.4.2.12).
- **NRK1**: nicotinamide/nicotinate riboside kinase (EC 2.7.1.22; EC 2.7.1.173).

NAD⁺ is an oxidizing agent; it accepts electrons from other molecules and becomes reduced. NADH can be used as a reducing agent to donate electrons. NAD⁺ and NADH are mainly used by enzymes catalysing substrate oxidation whereas NADP⁺ and NADPH are mainly used by the enzymes catalysing substrate reduction. The ratio of NAD⁺/NADH in the cytosol is approximately 700 to 1 while the mitochondrial one is approximately 7 to 8. Contrastingly the concentration of NADPH is much higher than the concentrations of NADP⁺, NAD⁺, NADH.

NADP⁺ and NADPH are molecules involved in redox metabolism, reductive biosynthesis, antioxidation and posttranslational modification of several proteins (Nelson, 2013).

Additionally, increasing evidence has pointed to several new biological functions that are directly regulated by NAD⁺ and NADP⁺ (Belenky *et al.*, 2007). For example: a) NAD⁺ dependent histone deacetylases (sirtuins) regulate mechanisms that range from caloric restriction to differentiation; b) poly(ADP-ribose) polymerase-1 (PARP-1) which has been widely implicated in DNA-repair mechanisms and different types of cell death; c) cyclic ADP-ribose and NaADP, both synthesised from NAD⁺, mobilise calcium from intracellular pools (Ying, 2008); and finally d) NADPH oxidase (NOX) generation of ROS is implicated in processes such as infection cellular response, growth, differentiation and death (Maejima *et al.*, 2011).

Chapter 1

SIRT1 stands for sirtuin (silent mating type information regulation 2 homolog 1). It is also known as NAD⁺-dependent deacetylase sirtuin-1. *SIRT1* is the human homolog of the protein *SIRT2* which is found in *S. cerevisiae* (Frye, 1999). *SIRT1* functions as a sensor of the ratio of cytosolic NAD⁺/NADH during episodes of glucose deprivation or caloric restriction (when the ratio of NAD⁺/NADP⁺ increases). For instance, in response to low nutrients or stress conditions, *SIRT1* inhibits skeletal myoblast differentiation (a decrease of the NAD⁺/NADH ratio coincides with skeletal myogenesis, whereas its increase inhibits it). Glucose restriction activates 5'-AMP-activated protein kinase (AMPK) which in turn activates nicotinamide phosphoribosyltransferase (PBEF), this activation shifts the ration of NAD⁺, NADP⁺ and nicotinamide and prevents differentiation, however *SIRT1*^{+/-} myoblasts are less sensitive to either glucose restriction or AMPK activation and differentiate even under conditions of extremely low caloric intake. (Fulco *et al.*, 2008; Saini *et al.*, 2012). *SIRT1* deacetylates histones and promotes both DNA and histone methylation, therefore increasing the positive charges of the histone's tails and in doing so enables high-affinity binding to occur between the histones and the DNA backbone. When this occurs, chromatin becomes tightly packed and transcription factors cannot attach to the specific DNA sequences of the genes that they regulate, causing transcription repression. By affecting chromatin structure, *SIRT1* negatively regulates chromatin remodelling and gene expression.

SIRT1 can also deacetylate transcription factors and co-regulators, thereby affecting target gene expression positively and negatively; some of these transcription factors are p53, forkhead transcription factors (FOXO), p300 histone acetyltransferase, tumour suppressor protein p73, E2F transcription factor 1 (E2F1), DNA repair factor Ku antigen 70-kDa subunit (Ku70), nuclear factor kappa-B (NF-κB), and androgen receptor (AR). Since the number and type of transcription factors that *SIRT1* interacts with is so large, *SIRT1* has been shown to be involved in diverse cellular processes such as reaction to metabolism, stressors, development, longevity, cell cycle, response to DNA damage,, apoptosis, autophagy and differentiation (Luo *et al.*, 2001; Brunet *et al.*, 2004; Wang *et al.*, 2008; Blander *et al.*, 2009; Ou *et al.*, 2011; Saini *et al.*, 2012). In mammalian cells *SIRT1* also mediates stress adaptation by

Chapter 1

deacetylating stress-response elements such as FOXO proteins and p53 (Luo *et al.*, 2001; Brunet *et al.*, 2004).

The role of Poly (ADP-ribose) polymerase (PARP) in DNA repair mechanisms has been widely documented (Sousa *et al.*, 2012). However, prolonged PARP activation markedly reduces cellular NAD⁺ and ATP content culminating in cellular death due to energy deficiency. Interestingly, both PARP-1 and sirtuins compete for NAD⁺ as a substrate and crosstalk between the two has been reported to occur (Canto *et al.*, 2013). The interaction between the two could therefore determine cell cycle progression, differentiation or death.

Intracellular NAD homeostasis is maintained by an equilibrium between NAD⁺ degradation and NAD⁺ synthesis. There are four known NAD⁺ biosynthesis pathways in vertebrates: *de novo* (from QA formed through the kynurenine pathway), Preiss-Handler (salvage from nicotinic acid), salvage from nicotinamide and salvage from nicotinamide riboside (NR). All of these pathways have one enzyme in common, Nmnat.

Of particular interest for this project are the *de novo* pathway and the nicotinamide salvage pathway. In the *de novo* pathway a phosphoribose group is added to QA by Qprt to form nicotinic acid mononucleotide (NaMN) by a series of enzymatic reactions. An adenylate group is then transferred by Nmnat1, Nmnat2 and Nmnat3 to form nicotinic acid adenine dinucleotide (NaAD). The final step in the reaction is the amidation of the nicotinic acid group in NaAD to a nicotinamide (Nam) group by Nadsyn1, forming NAD⁺. For instance, it has been shown that in neurons 3-HK, 3-HAA, QA and PIC significantly increase intracellular NAD⁺ at concentrations below 100 nM but substantially decrease it at higher concentrations, which coincides with an increase in extracellular LDH activity (Braidy *et al.*, 2009).

In a further step, some NAD⁺ is phosphorylated into NADP⁺ by NAD⁺ kinase. Both NAD⁺ and NADP⁺ are oxidising agents involved in a myriad of cellular processes such as energy metabolism, mitochondrial function, calcium homeostasis, oxidative state, gene expression, differentiation, aging and cell death.

Chapter 1

All the enzymes that use NAD^+ as a substrate will form Nam (which can also be ingested) as a by-product. Nam is transformed into NMN by PBEF and then adenylated by Nmnat1-3 to form NAD^+ (Figure 3).

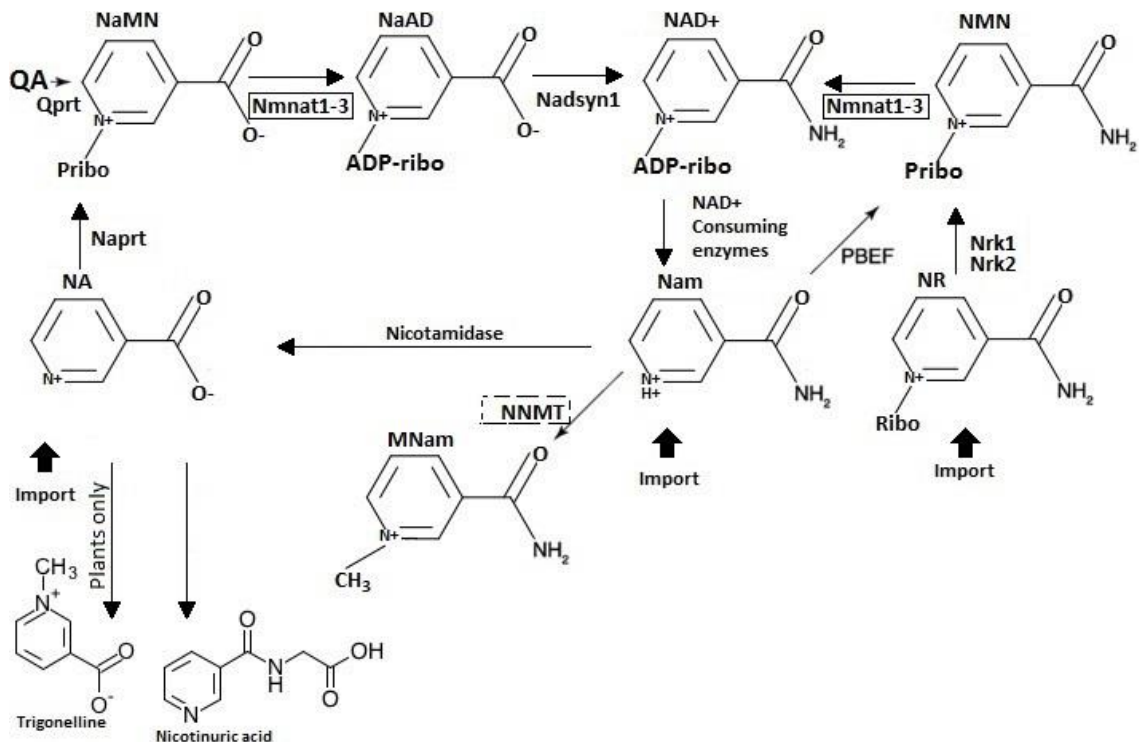


Figure 3- Intracellular NAD^+ metabolism. *de novo* (QA), Preiss-Handler (Nicotinic acid, NA), salvage (Nam) and Salvage nicotinamide riboside (Nr) pathways. Modified from Belenky *et al.* (2007).

Nam can be N-methylated by nicotinamide N-methyltransferase (NNMT) to form 1-methylnicotinamide. Alternatively, nicotinamide can be transformed into nicotinic acid (NA) by nicotinamidase. NA acid can be catabolised into two elimination products: trigonelline (in plants only) nicotinic acid (in humans) by Glycine N-acyltransferase and Glycine N-acyltransferase-like protein 1,2,3.

There are two main mechanisms by which NADP^+ can be formed, one is the *de novo* mechanism involving NAD^+ kinases which phosphorylate NAD^+ or alternatively through the action of NADPH-dependent enzymes.

NADPH in turn can be formed from NADH and NADP^+ by mitochondrial transhydrogenases or from NADP^+ by a multiple sequence of steps involving different NADP^+ dependent enzymes (glucose 6-phosphate dehydrogenase, 6-gluconate phosphate dehydrogenase, NADP^+ -dependent isocitrate dehydrogenases, NADP^+ dependent malic enzymes, mitochondrial dehydrogenase).

Chapter 1

NAD⁺ is used by a vast number of protein families, like the mammalian ADP-ribosyl cyclase CD38. CD38 acts as an ectocyclase that converts NAD⁺ to the Ca²⁺-releasing second messenger cyclic ADP-ribose (cADPR). CD38 knockout mice exhibit high levels of NAD⁺, which suggests that under physiological conditions NAD⁺ levels are regulated by CD38. The expression of CD38 is also tissue dependent, it is widely expressed on thymocytes, activated T cells, terminally differentiated B cells (plasma cells), it is high in kidney and cardiac tissue and it is thought to be involved in cellular proliferation and adhesion (Aksoy *et al.*, 2006).

NADPH has three main biological functions: a) it is part of the cellular antioxidant defence mechanism; b) it donates electrons necessary for the reductive synthesis of fatty acids, steroids and DNA (Pollak *et al.*, 2007); c) it is a substrate of NADPH-oxidase (discussed in more detail in chapter 1.5.2.2)

1.4.1 Role of NAD⁺ in cancer

It has been suggested that certain inherent properties of tumours (high metabolic activity, increased ROS production, increased DNA damage and need for reparative enzymes, etc.) result in a high rate of NAD⁺ consumption. Thus having a high NAD⁺ supply has been suggested to be crucial for the survival and proliferation of tumour cells (Holen *et al.*, 2008; Travelli *et al.*, 2011).

Conversely, low levels of NAD⁺ potentially jeopardize the ability of transformant cells to maintain ongoing cell division. Indeed, tumour's NAD⁺ dependency has been the target of several successful therapies in which the application of NAD⁺-consuming enzymes (PARPs and sirtuins) causes the intracellular depletion of NAD⁺ with concomitant tumoural death (Haigis and Sinclair, 2010; Rouleau *et al.*, 2010).

Cancer cells have acquired several adaptations (metabolic transformation) in order to meet their particular metabolic requirements. Accordingly, it has been shown that several enzymes involved in NAD⁺ metabolism are differentially expressed in tumours when compared to normal tissue. One such enzyme is PBEF, which is overexpressed in several solid tumours (Yang *et al.*, 2007; Reddy *et al.*, 2008; Bi *et al.*, 2011; Wang *et al.*, 2011) where it may promote

Chapter 1

angiogenesis by inducing the expression of growth factors and metalloproteinases (Dreves *et al.*, 2003; Kim *et al.*, 2007).

In preclinical studies, two PBEF inhibitors (FK866 and CHS 828) exhibited antitumour properties through a mechanism involving NAD⁺ depletion followed by ATP depletion (Hasmann and Schemainda, 2003; Olesen *et al.*, 2008). Furthermore, it has been shown that FK866 induces autophagy in SH-SY5Y cells (Travelli *et al.*, 2011). These results have subsequently led to the entering of both compounds in phase I/II clinical trials for patients with advanced malignancies (www.clinicaltrials.gov).

There are several enzymes involved in the synthesis of NAD⁺ (approximately nine including isoforms) yet only a few of them have been studied as possible therapeutic targets in the management of neoplastic malignancies (Chiarugi *et al.*, 2012). Thus, it is conceivable that cancer cells can potentially compensate for the effect of a single inhibitor and relieve the induced NAD⁺ deficit. Additionally it has been suggested that metabolic targeting represents a great selective pressure for the emergence of new, more resistant phenotypes (Oliveras-Ferraros *et al.*, 2014). Conversely, the molecular challenges of a multifaceted treatment (acting at multiple levels on cellular metabolism) reduce the probability of cells adapting and developing resistance (Cantor and Sabatini, 2012).

As previously mentioned (Section 1.3.4), ACMSD is the rate limiting enzyme for QA production and an inverse relationship has been found between ACMSD activity and QA production/excretion in rats (Egashira *et al.*, 2003) and humans (Ikeda *et al.*, 1965).

Adam and collaborators (2012) have proposed that due to the subsequent transformation of QA to NAD⁺ (*de novo* pathway), ACMSD could also play an important role in the maintenance of elevated NAD⁺ levels in cancer (Adams *et al.*, 2012). In support of this hypothesis, the authors present evidence by Guillemín (2007) showing that a) in contrast to normal neurons, SK-N-SH cells do not express ACMSD which results in the preferential production of QA over PIC; b) exogenous application of QA increases the number of cells whereas PIC decreases it (Guillemín *et al.*, 2007). Further strengthening the possibility that

Chapter 1

in certain cancers QA production is favoured over that of PIC, the authors present evidence showing that PIC has neuroprotective (Coggan *et al.*, 2009) and antiproliferative properties in transformed cells both *in vitro* (Fernandez-Pol and Johnson, 1977) and *in vivo* (Leuthauser *et al.*, 1982), the latter probably due to an increase in the production of tumoricidal NO^-_2 by macrophages (Melillo *et al.*, 1994).

Additional evidence exists supporting the role of QA in cancer pathogenesis. For instance, Qprt (the enzyme transforming QA into NaMN) has been put forward as a novel biomarker for thyroid carcinomas (Hinsch *et al.*, 2009). Furthermore, the SH-SY5Y cell line (subclone of SK-N-SH) has no endogenous expression of NNMT (Parsons *et al.*, 2011) which transforms Nam into 1-methylnicotinamide (MNA_m). This could represent a metabolic adaptation that prevents the loss of Nam thereby securing that enough precursor is available for NAD^+ formation.

In a study that set out to determine the role of NNMT on neuronal differentiation, the transfection of SH-SY5Y cells with a plasmid encoding for NNMT increased the number of neurites and the expression of synaptophysin without the induction of terminal differentiation (mitotic stop). Interestingly, incubation of wild-type SH-SY5Y cells with 1-methylnicotinamide (MNA_m) also caused an increase in neurite branching (Thomas *et al.*, 2013).

1.5 Reactive Oxygen Species (ROS) and Oxidative Stress

1.5.1 Reactive Oxygen species

Oxygen (O_2) is a chemical element with the electronic configuration of $1s^2 2s^2 2p^4$ which under standard conditions for temperature and pressure is found as diatomic molecule with the chemical formula O_2 . O_2 is the final acceptor of electrons during oxidative phosphorylation to generate the proton gradient necessary for the synthesis of ATP. During oxidative phosphorylation, which involves the reduction of O_2 to H_2O , many partly reduced products are formed; these are known as reactive oxygen species (ROS). ROS are also generated during the cyclooxygenase pathway or by cellular enzymes such as p450-oxidase, xanthine-oxidase and NADPH-oxidase (Halliwell, 2006; Fatokun *et al.*, 2008a).

The electrons found surrounding atoms and molecules occupy spatial regions that are known as orbitals. Each orbital can only fit two electrons at a given time. For example, in a covalent bond there are two electrons being shared, these electrons are present in the same orbital but have opposite spins. When only one electron is present in an orbital, it is said to be unpaired. A free radical is a chemical species capable of independent existence and that has one or more unpaired electrons (Halliwell, 2006).

Free radicals generally short-lived molecules as their reactivity allows them to remove an electron from other compounds, oxidise it, or yield one of its electrons to a recipient compound, rendering it more reactive. For this reason, the direct quantification of these compounds is very difficult and the techniques used for their study in biological systems is generally based on indirect indicators of the oxidative modification of biomolecules and rarely by compounds that emit fluorescence after having being oxidised.

The term reactive species (RS) is a broad category which includes both the reactive oxygen species (ROS), as well as the reactive nitrogen species (RNS). The term ROS refers to both the free radicals of O_2 and to some non-radical derivatives of O_2 that are oxidant agents and that can be easily converted into radicals such as: $HOCl$, $HOBr$, O_3 , $ONOO^-$, 1O_2 , H_2O_2 . Following a simple categorical syllogism: all O_2 radicals are ROS but not all ROS are O_2 radicals. The

Chapter 1

term reactive species (RS) is wider and it includes the reactive species of O₂, nitrogen, chlorine, bromine and those of sulphur (Stadtman, 1992; Halliwell, 2006; Fatokun *et al.*, 2008a). Table 3

Free radicals	Non-radicals
<p style="text-align: center;"><u>ROS</u></p> <p>Superoxide O₂^{•-} Hydroxyl OH[•] Hydroxyperoxyl HO₂[•] Carbonate CO₃^{•-} Peroxyl RO₂^{•-} Radical carbon dioxide CO₂^{•-} Singlet oxygen ↑O₂(1Σg) Alcoxy RO[•]</p>	<p style="text-align: center;"><u>ROS</u></p> <p>Hydrogen peroxide H₂O₂ Organic peroxides ROOH Hypobromous acid HOBr Hypochlorous acid HOCl</p>
<p style="text-align: center;"><u>RNS</u></p> <p>Nitric Oxide NO[•] Nitrogen dioxide NO₂[•] Nitrate NO₃[•]</p>	<p style="text-align: center;"><u>RNS</u></p> <p>Peroxynitrite ONOO⁻ Peroxynitric Ion (O₂NOO⁻) Peroxynitrous acid ONOOH Nitrous acid HNO₂ Nitrosyl cation NO⁺ Nitrosyl anion NO⁻</p>

Table 3 Radical and non-radical reactive species. Table listing examples of radical and non-radical reactive oxygen species (ROS) and reactive nitrogen species (RNS).

1.5.2 Superoxide Anion

O₂^{•-} is a diatomic molecule in which one electron is unpaired. This radical is formed under several physiological conditions such as in the electron transport chain where electrons passing through the different complexes can escape and attach to O₂. Furthermore, O₂^{•-} is capable of acting as both a reducing and oxidizing agent depending on the nature of the molecule it acts upon. Even though O₂^{•-} reacts with a limited number of molecules, it is the precursor of far more noxious ROS like H₂O₂. (Valentine *et al.*, 1984; Sawyer *et al.*, 1985).

1.5.2.1 Xanthine Oxidoreductases

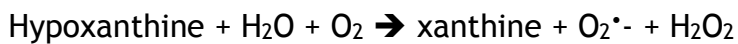
Another Source of O₂^{•-} is through the oxidation of non-radical molecules such as epinephrine, dopamine, 6 hydroxydopamine and molecules that contain thiol groups like cysteine (Spencer *et al.*, 1998).

Xanthine oxidoreductases consist of two subunits, with each subunit containing three domains: a molybdenum (Mo) containing domain, an iron-sulphur

Chapter 1

containing domain and a flavin adenine dinucleotide (FAD) containing domain. In mammals xanthine oxidoreductases exist in two forms: xanthine dehydrogenase (XDH), which is the predominant form *in vivo*, and xanthine oxidase (XO). XDH and XO interconvert by the action of sulphide reagents (thiosulfates). However upon proteolysis the transformation of XDH to XO is irreversible (Harrison, 2002).

Xanthine oxidoreductase catalyses the hydroxylation of hypoxanthine to xanthine and of xanthine to uric acid. During the transformation of hypoxanthine to xanthine, $O_2^{\cdot-}$ and H_2O_2 are formed by the following reaction:



During the conversion of xanthine to uric acid which is catalysed by the enzyme xanthine oxidase $O_2^{\cdot-}$ and H_2O_2 is formed by the following reaction:



The reduction of O_2 by either form of the enzyme will produce $O_2^{\cdot-}$ and H_2O_2 . XDH reduces NAD^+ preferentially but it can also reduce O_2 . Contrastingly, XO cannot reduce NAD^+ and will use O_2 instead. Xanthine oxidase is activated by the Ca^{2+} entry that follows NMDAR activation (Hille and Nishino, 1995).

1.5.2.2 NADPH-oxidase (NOX)

$O_2^{\cdot-}$ can also be produced by nicotinamide adenine dinucleotide phosphate-oxidase (NOX)/ dual oxidase (DUOX) family. NOX is an enzymatic complex made up of 6 subunits: the catalytic subunit gp91^{phox}, the small GTPase RAC (both membrane bound) together with the regulatory subunits p22^{phox}, p47^{phox}, p40^{phox}, p67^{phox} (all of which are cytosolic). For the complex to be active, all the subunits need to be present on the membrane, only then will NOX catalyse the formation of $O_2^{\cdot-}$ from O_2 . Diphenylene iodonium chloride (DPI) is the most common NOX inhibitor used. DPI abstracts an electron from an electron transporter to form a radical, which in turn inhibits the respective electron transporter through a covalent binding step (Bedard and Krause, 2007).

NOX plays an important role in many physiological and pathological processes through the generation of ROS. During a pathogen infection, phagocytic NOX is

Chapter 1

activated and the generated ROS have an antibacterial effect. For instance, chronic granulomatous disease is characterised by reduced antibacterial capacity in phagocytes which is due to their inability to activate NOX. Furthermore, catalase-positive organisms (*Staphylococcus aureus*) can only be killed by neutrophils expressing NOX2. The exact mechanism by which NOX-produced ROS kill pathogens is not completely understood but it is believed to be partly due to changes in phagosomal pH and ionic concentrations.

There are many reports that show that NOX-produced ROS alter intracellular signaling pathways by inhibiting the activity of protein tyrosine kinases and changing intracellular Ca²⁺ homeostasis (Chan *et al.*, 2009).

1.5.3 Hydrogen Peroxide

H₂O₂ is a non-radical ROS present in various biological systems. It can be produced through many enzymatic reactions such as those catalysed by superoxide dismutase (SOD), the oxidases of D-amino acids, the amino oxidases, the glycolate oxidases and by the cyclic redox reactions of compounds like catecholamines. Being a far more powerful oxidant, H₂O₂ is therefore more reactive; its targets are also limited but among them is methionine and certain reactive cysteines. In the presence of transition metals it can generate OH[•]- by Fenton reactions (Halliwell and Gutteridge, 1992; Koppenol, 2001).



1.5.4 Hydroxyl radical

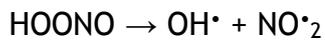
OH[•]- is a highly reactive compound that can cause oxidative damage in different biomolecules by chain reactions of free radicals. It can initiate lipid peroxidation as well as generate free radicals in proteins and polynucleotides by the abstraction of hydrogen atoms. •-

OH[•]- can be formed by three mechanisms:

1. Fenton reactions as shown above.

Chapter 1

2. The homolytic fission of water by ionizing radiation (Sonntag, 1987).
3. The homolytic fission of peroxyntrous acid

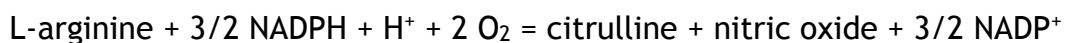


1.5.5 Nitric oxide

NO^\bullet is a radical that does not possess an electric charge. Since it is a hydrophobic compound, NO^\bullet has the ability to easily pass through cellular membranes (Beckman and Koppenol, 1996). NO^\bullet acts as a vasodilator (Moncada and Higgs, 2006), neurotransmitter and second messenger (Stamler, 1994; Halliwell, 1999).

NO forms stable high affinity bonds with heme and non-heme-iron, the binding between NO and the ferrous heme groups is rapid and of high affinity and this has considerable biological implications in the activation of the soluble guanylate cyclase to form Cyclic guanosine monophosphate (cGMP).

The exact stoichiometry of the nitric oxide synthase (Cecchi *et al.*) reaction, its mechanism, products, prosthetic groups, cofactors (FAD, FMN, tetrahydrobiopterin, and heme) and specific favourable conditions continue to be a matter of debate. However, it is clear that NO^\bullet is generated by NOS enzymes that catalyse the NADPH- and O_2 -dependent oxidation of L-arginine to L-citrulline and NO as follows, (Moncada and Higgs, 2006):



NOS can be activated by the increase in the intracellular concentration of Ca^{2+} by the calcium-calmodulin complex (Alderton *et al.*, 2001).

Nitric oxide can react with the $\text{O}_2^{\bullet -}$ radical to form peroxyntrite:



Chapter 1

Nitric oxide can attach itself to cytochrome oxidase c reducing its affinity to O₂ and therefore affecting the mitochondrial electron flow and the synthesis of ATP (Poderoso *et al.*, 1996).

1.5.6 Peroxynitrite

ONOO⁻ can be rapidly formed by the molecular interaction of O₂^{•-} and nitric oxide. ONOO⁻ is a powerful oxidative agent which can cause the nitration of guanine and the formation of carbonyl groups as well as other oxidised products of proteins like nitrotyrosine (Squadrito and Pryor, 1995)

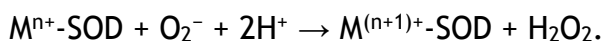
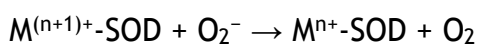
The protonation of peroxynitrite leads to the formation of peroxynitrous acid (Alvarez *et al.*, 2002).

1.6 Antioxidant Defences

Given that ROS are constantly being generated in biological systems as part of their normal physiology, a healthy organism needs to remove them to avoid oxidative damage. Cells have developed detoxifying mechanisms that will turn highly reactive compounds into more stable innocuous ones.

1.6.1 Superoxide dismutase (SOD)

SOD dismutates O₂^{•-} by adding to it two protons (Fridovich, 1989) as shown in the following reaction:



Where M = Cu (n=1); Mn (n=2); Fe (n=2); Ni (n=2).

There are 4 isoforms of this enzyme depending on the cofactor that it is attached to. Mn-SOD or SOD2 is mainly found in the mitochondria and requires manganese on its active site.

Chapter 1

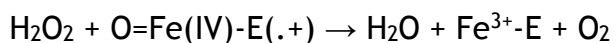
Cu-Zn-SOD requires copper and zinc on its catalytic site and it can be intracellular (SOD1) or extracellular (SOD3). SOD3 is released to the extracellular space and it is mainly expressed on vascular smooth muscle.

Since the reaction catalysed by SOD produces another non-radical ROS, H₂O₂, its action must be tightly linked to that of other antioxidants (peroxidases, catalase, and glutathione peroxidase) that will ultimately turn H₂O₂ into a less reactive compound.

Alterations in the functioning and structure of SOD have been found to underlie the pathogenicity of some neurodegenerative diseases, such as amyotrophic lateral sclerosis (Canals *et al.*) and Friedreich's ataxia (Beal and Shults, 2003; Hart *et al.*, 2005)

1.6.2 Catalase

Catalase (Gedik *et al.*) is an enzyme found in the peroxisomes of mammalian cells (Chance *et al.*, 1979) and it catalyses the conversion of H₂O₂ to water and O₂ depending on the concentration of H₂O₂. When the concentration of H₂O₂ is high, the following reaction takes place:



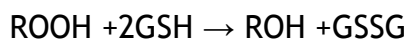
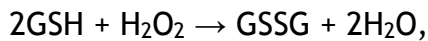
However, if the concentration of H₂O₂ is low and hydrogen donors such as methanol, ethanol, phenol, formaldehyde, formic acid and acetaldehyde, are present then catalase removes the H₂O₂ by oxidising its substrate as follows:



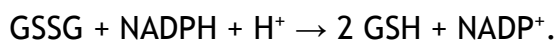
Catalase acts in conjunction with SOD. However, the levels of catalase in the brain are very low when compared to those found in other tissues.

1.6.3 Glutathione Peroxidase (GPx)

GPx is the main enzyme that detoxifies peroxides; it reduces lipid hydroperoxides to their corresponding alcohols and reduces free H₂O₂ in the brain (Brigelius-Flohe, 1999). It is found in the cytoplasm and the mitochondrial matrix. GPx contains selenium on its catalytic site (Maiorino *et al.*, 1995) and breaks down peroxides through the following reactions:

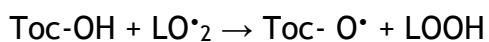


Glutathione needs to be reduced again by glutathione reductase to complete a cycle of oxidation and reduction:



1.6.4 A-tocopherol

Vitamin E refers to four tocopherols and four tocotrienols that are liposoluble molecules and constitutive components of membranes. Tocopherols and tocotrienols prevent the lipid peroxidation of membranes by eliminating the peroxide radicals using OH (Parks and Traber, 2000). They also convert the alkyperoxy radicals into hydroxyperoxides and simultaneously into tocopheroxyl radicals:



The tocopheroxyl radical is not very reactive and it is partly reduced by ascorbate, turning it into tocopherol



α -tocopherol is the most important tocopherol in the brain, if not the only one (Roy *et al.*, 2002; Hayton and Muller, 2004) and its deficiency affects the CNS more than the peripheral one. This indicates that there exists a tight regulation of its levels in the brain (Halliwell, 2006).

1.7 Oxidative stress

Oxidative stress has been defined as a state in which an unbalance between the cellular pro-oxidant and antioxidant defences occurs (Chandra *et al.*, 2000; Fatokun *et al.*, 2008a), triggering different effects which depend on the cellular type and the cell context.

An intracellular increase and accumulation of ROS can occur both under physiological (cell signaling or cell metabolism) and pathological (toxic insults and neurodegeneration) conditions. This means that oxidative stress can cause cell damage but this damage is not necessarily an intrinsic condition linked to an episode of oxidative stress. For instance, several ROS are not removed immediately after their generation because they have very important biological functions (Gutteridge and Halliwell, 2000). Oscillations between the cellular pro-oxidant and antioxidant balance are very common in healthy organisms under various circumstances. For example: following an infection; during an inflammatory response; or, in fibroblasts where $O_2^{\cdot-}$ regulates cell division and halts the chain reaction of lipid peroxidation as it reacts with the alcohoxyl radical.

The existence of enzymes involved in the generation and removal of ROS (NOX, dual oxidase, myeloperoxidase, NOS, heme oxygenase) and the controlled regulation and induction of ROS formation in response to growth factors, cytokines and Ca^{2+} -dependent signals, suggests a positive selection of pro-oxidant mechanisms throughout evolution, given its importance in cellular physiology. For example, one of the physiological roles of ROS is the modulation in the expression of genes that are activated by transcription factors sensitive to the intracellular redox state as is the case for the nuclear factor kappa-light-chain-enhancer of activated B cells (NF- κ B) (Remacle *et al.*, 1995; Cimino *et al.*, 1997).

Once ROS have acted upon their targets, it is necessary to remove them to avoid cell damage because of their high reactivity with biomolecules. To accomplish this, there are several antioxidant systems within the cell such as glutathione and enzymes like SOD and catalase. Some experimental models have shown how important these antioxidant systems are for the normal physiology of cells. This

Chapter 1

is the case for SOD2 (mitochondrial isoform) knockout mice presenting, as a result, cardiomyopathy and neurodegeneration (McCord, 1994).

One of the consequences of ROS unbalance is the structural and functional modification of biological macromolecules (DNA, lipids and proteins). These modifications can be direct, when ROS act upon the cell's molecular machinery, or indirect when other subproducts of ROS attack the cell's components. Oxidised biomolecules can pose a threat to the cell since they can interfere with the normal functioning of the cell's molecular machinery and also because they can propagate the damage onto other biomolecules through free radical's chain reactions (Stark, 2005).

1.7.1 Lipid Peroxidation

Lipid peroxidation has been implicated in the pathogenesis of several degenerative diseases like atherosclerosis, diabetes, inflammation, neurodegenerative disorders, ischemic-reperfusion insults and spinal damage (Farooqui and Horrocks, 1998; Stark, 2005; Farooqui *et al.*, 2007). Lipid peroxidation disrupts the organization of the cell membrane, which causes changes on its properties such as fluidity and permeability; this inhibits certain metabolic processes as well as ionic transport (Stark, 2005).

Oxidative damage to mitochondrial membranes causes a positive feedback loop in which more ROS are generated (Green and Reed, 1998). For example, it has been shown that the production of lipid peroxides and its aldehydic products, depletes the cell of GSH and renders the cell more vulnerable to oxidative insults since these compounds are detoxified through the GSH-Px and glutathione S-transferase systems. (Arakawa *et al.*, 2007)

The final products of lipid peroxidation such as malondialdehyde (Lopes *et al.*), 4-HNE and acrolein are able to react with diverse molecules, such as proteins, through covalent reactions with thiol groups or with the amine group of guanosine to form cyclic adducts. Out of all the α , β -unsaturated aldehydes, acrolein is the most electrophile and hence it shows great reactivity with proteins (Uchida, 1999; Kehrer and Biswal, 2000).

1.7.2 Protein Oxidative Modifications

Oxidative modification of proteins by the action of ROS and RNS is implicated in the pathogenesis associated with natural ageing and in the development and progression of neurodegenerative diseases (Stadtman, 1992; Stadtman and Berlett, 1997).

The radical OH^{\bullet} is able to attack the amino acid residues in proteins; these reactions induce an extensive protein-protein cross-linking. $\text{O}_2^{\bullet-}$ can react with NO to generate peroxynitrite. This compound, although not a free radical, behaves similarly to OH^{\bullet} inducing protein oxidation and nitration to form 3-nitrotyrosine (3-NT). 3-NT formation is markedly favoured in the presence of CO_2 and is widely used as a marker of oxidative stress.

Protein oxidation in various tissues, including the brain, has been proposed as one of the underlying mechanisms that explain the functional deficit associated with ageing, in particular the oxidative modification and inactivation of mitochondrial proteins involved in the electron transport chain. The functional repercussions that oxidative damage has on biomolecules depend in great measure on the levels of ROS involved, on the level of antioxidant defences present and on the rate of exchange of the molecules involved. If the exchange rate is continuous, then oxidative damage does not accumulate and it may not have critical repercussions on cell functioning.

1.7.3 DNA Oxidative Damage

This is not the case for nuclear DNA (NDNA), which possesses all the information necessary for the cell to carry out its functions, and which will not be replaced during the cell's life span. Thus, DNA damage represents a serious threat to cellular homeostasis. If DNA damage is severe or if its accumulation exceeds the cell's capacity to repair it, then mechanisms of senescence or programmed cell death are induced to ensure tissue and systemic homeostasis (Liu *et al.*, 2009).

It has been observed that sub-lethal doses of H_2O_2 can cause double-strand rupture of the DNA followed by an increase in the levels of p53 and p21 which in turn leads to cell cycle arrest (Chen *et al.*, 2004; Chen *et al.*, 2005). If the DNA is successfully repaired by the cellular machinery, then progression of the cell

Chapter 1

cycle can occur; but if the damage cannot be repaired, then senescence or programmed cell death mechanisms will be executed (Chen *et al.*, 2004; Chen *et al.*, 2007). Contrarily, if the cell cycle proceeds, then cancer transformation is likely to occur.

Since ROS are the main endogenous agents causing DNA damage, any oscillations in their levels or in the levels of antioxidants will have repercussions over the cell's state. For instance, it has been reported that mutations on SOD1 are associated with the familial form of Amyotrophic lateral sclerosis (Canals *et al.*, 2005) and of premature senescence in fibroblasts (Rosen *et al.*, 1993; Blander *et al.*, 2003). Similarly, the oxidative damage induced by ROS has been proposed as one of the main events underlying the brain damage that follows a transient/permanent ischemic process (Chen *et al.*, 1997; Nagayama *et al.*, 2000).

The formation and accumulation of 8-hydroxyl-2'-deoxyguanosine (8-oxo-dG) in the DNA is one of the most common oxidative base modifications. This modification is caused by the OH[•]- radical and it affects the integrity, expression and function of active genes within the cells presenting it (Cui *et al.*, 1996). Thus, the levels of 8-oxo-dG have been used as a parameter to determine the amount of oxidative lesions on the DNA. It has been argued however, that the exact contribution of oxidative damage by ROS is hard to determine because some of the guanosine oxidation may occur during the DNA preparation, previous to its analysis. This has resulted in significant differences (sometimes three orders of magnitude apart) in the results published for 8-oxo-dG (Collins *et al.*, 2004; Gedik *et al.*, 2005).

In response to DNA oxidative damage, several widely characterised repair mechanisms are activated in order to maintain the genomic integrity and overall functioning of the affected genes. One of these repair mechanisms is carried out by 8-oxoguanine glycosylase, also known as OGG1, an enzyme present in the mammalian brain that works through the base excision pathway and that eliminates 8-oxo-dG from DNA (Araneda *et al.*, 2005).

When discussing DNA damage caused by ROS, it is important to include mitochondrial DNA (mtDNA) as well. The mitochondrial genome is a double helix

Chapter 1

of circular DNA of approximately 16kpb. The mtDNA of mammals contains 37 genes which codify for the 13 polypeptide components of the electron transport chain, the RNAr and the RNAt necessary for intramitochondrial protein synthesis (Lin and Beal, 2006).

MtDNA is extremely vulnerable to ROS attack for several reasons; it is located near the internal mitochondrial membrane which is the site of maximal ROS production, it has no protecting histones, and mitochondria do not have the enzymes necessary for base excision repair (Balaban *et al.*, 2005). Indeed, it has been shown that the levels of oxidative damage found in MtDNA are ten-fold higher than that found in nuclear DNA for different brain regions (Wallace, 1992). There is evidence that suggests that MtDNA damage can cause an uncoupling of the electron transport chain that further increases the levels of ROS, for instance mutation to MtDNA causes such an increase in the intracellular levels of ROS (Beal, 2005; Kujoth *et al.*, 2007).

1.8 ROS in Cancer

In 1981, Oberley *et al* determined, for the first time, that a link exists between ROS and cancer cell proliferation (Oberley *et al.*, 1981). These observations formed the basis for the “free radical theory of cancer”. Since then, numerous studies have corroborated that ROS promote uncontrolled cell growth, genomic instability and migration (Szatrowski and Nathan, 1991; Petros *et al.*, 2005; Kumar *et al.*, 2008; Ralph *et al.*, 2010; Bauer, 2014).

ROS are potent carcinogens because of their ability to cause DNA damage, gene mutations and DNA hypomethylation (previously described in section 1.7.3, page 85). The most common oncogenic mutations affect several signaling molecules such as p53, Raf, retinoblastoma (Rb), protein phosphatase 2A, telomerase, Ral-GEFs, phosphatidylinositol 3-kinase (PI3K), Ras, Rac, cellular v-myc myelocytomatosis viral oncogene homolog (c-Myc), STAT3, NF-κB, and HIF-1a (Ralph *et al.*, 2010). In addition to this genotoxic effect, ROS can also promote carcinogenesis by acting as second messengers in several signaling pathways or by directly activating redox-sensitive transcription factors ultimately modifying gene expression (Yang *et al.*, 2013).

Chapter 1

The exact role that ROS play in cancer has remained hard to determine and continues to be a matter of debate because there is evidence indicating that ROS can also be detrimental to cancer cells. For instance ROS can induce: a) the activation of tumour suppressors such as p53 (Maillet and Pervaiz, 2012; Vurusaner *et al.*, 2012; He and Simon, 2013); b) the activation of cell cycle inhibitors (Ramsey and Sharpless, 2006; Takahashi *et al.*, 2006); c) DNA damage and proliferative arrest (Ogrunc *et al.*, 2014); d) apoptosis (Raj *et al.*, 2011). It has also been demonstrated that almost all standard of care chemotherapeutic and radiotherapeutic agents induce cell death partly by causing an increase in ROS (Gorrini *et al.*, 2013).

It is becoming increasingly evident that these responses are dependent upon the levels of ROS, the duration of exposure, their source and localization, and the nature of the ROS involved. Furthermore, even under the same pro-oxidant conditions, the cellular response will depend on the specific cellular context of each cancer such as the presence of intrinsic levels of antioxidant defences and the particular somatic mutations. Ultimately, the ability to execute a particular programme after any given stimulus depends on the molecular components within each cell and on possible alterations of the cell's functional properties during transformation.

The two extremes of this broad spectrum of responses, namely proliferation vs. cell death, are perhaps the two best studied. The clear pattern that has emerged is that, at low levels, ROS contribute to tumour formation by acting as signaling molecules that sustain cell proliferation by activating stress-responsive survival pathways (Gorrini *et al.*, 2013). On the other hand, high levels of ROS cause massive oxidative damage to cellular components and, consequently induce the activation of several mechanisms of cell death. As an example, ROS are essential for Fas activation and phosphorylation in the extrinsic pathway of apoptosis (Medan *et al.*, 2005) and also for the disruption of the mitochondrial pore in the intrinsic pathway (Martindale and Holbrook, 2002; Gloire *et al.*, 2006). At more moderate levels, ROS can induce irreversible senescence-induced tumour suppression by blocking cytokinesis acting on the p16INK4a-RB axis (Takahashi *et al.*, 2006).

Chapter 1

More complicating factors in further understanding the role of ROS in cancer originate from studies offering evidence that ROS induce differentiation and autophagy in normal and transformant cells. The biological significance of differentiation in cancer and how it relates to its physiological and developmental counterpart in non-transformant cells remains to be determined. There is evidence, that partly addresses these questions, which suggests that in cancer cells (that have lost the ability to exit the cell cycle normally and/or to die) differentiation may represent the only available response to excessive oxidative stress and DNA-damage (Yang *et al.*, 2011; Santos *et al.*, 2014). Similarly, autophagy may represent either a cellular strategy to temporarily withstand stress or an alternative mechanism of cellular death (Filomeni *et al.*, 2014). It has been suggested that several autophagic pathways may not be compromised in cancer because, to a certain extent, their activation guarantees cell survival during episodes of metabolic stress. However, when autophagic pathways are overstimulated, they can have a detrimental effect on cell survival and the rate of tumoural growth. The contrasting cellular responses elicited by ROS also indicate that there is an overlap in the pathways that promote cancer survival/proliferation and those that cause cancer cells to arrest/differentiate and to die (Gupta *et al.*, 2012).

Stem cell research may offer some information regarding the effect of ROS on cellular differentiation. As previously mentioned, (page 23) cancer stem cells (CSCs) share several characteristics with normal stem cells such as self-renewal and differentiation capacity. Interestingly, it has been suggested that another shared attribute between CSCs and normal stem cells is their response to ROS (Dayem *et al.*, 2010; Shi *et al.*, 2012).

Since hematopoietic stem cells (HSCs) are the first and best characterised type of adult stem cells, they will be used as an example to illustrate the similarities between stem cells and cancer stem cells with regard to ROS. HSCs and mammary epithelial stem cells have lower levels of ROS than their differentiated progeny (Naka *et al.*, 2008; Zhang *et al.*, 2008). It has been shown that these lower levels prevent their differentiation and early exhaustion which is partly due to their remaining under hypoxic conditions in a quiescent state (Wilson *et al.*, 2009). Furthermore, Human Embryonic Stem Cells (HESCs) continue to proliferate and remain undifferentiated when cultured under hypoxic conditions;

Chapter 1

however, upon transfer to a normoxic atmosphere, spontaneous differentiation is induced (Ezashi *et al.*, 2005). This behaviour is believed to be dependent on the effect of ROS since O₂ alters the rate of oxidative phosphorylation and in turn on ROS production (Sauer and Wartenberg, 2005; Zhang *et al.*, 2012a).

Analogously, CSCs in human and mouse breast tumours maintain lower levels of ROS than their cancerous epithelial-like progeny (Toyokuni, 2006; Diehn *et al.*, 2009; Kim *et al.*, 2012). It has been suggested that whereas high levels of ROS are essential for malignant initiation and progression, maintaining low levels of ROS is necessary to prevent differentiation and to guarantee the survival of the pre-neoplastic foci (Ghaffari, 2008; Gorrini *et al.*, 2013). In line with this, it has been shown that ROS induce the differentiation of pheochromocytoma PC12 cells (Katoh *et al.*, 1997) through activation of MAPK/ERK (Katoh *et al.*, 1999; Goldsmit *et al.*, 2001) and through the direct activation of PKC ϵ (Gopalakrishna *et al.*, 2008). Furthermore, the production of ROS seems to be a common occurrence in several models of cancer differentiation with a CSC component including, but not limited to, human monoblastic leukaemia cells (Kikuchi *et al.*, 2010) and SH-SY5Y cells (Nitti *et al.*, 2010; Li *et al.*, 2013).

The main pathways controlling proliferation and/or differentiation in cancer and normal stem cells involve the activation of redox-sensitive factors such as nuclear factor kappa-light-chain enhancer of activated B cells (NF- κ B), nuclear factor (erythroid-derived 2)-like factor 2 (NRF2), c-Jun, and hypoxia-inducible factor-1 α (HIF-1 α), Bach1, activator protein-1 (AP-1), signal transducer and activator of transcription 3 (STAT3), and others (Martindale and Holbrook, 2002; Ranjan *et al.*, 2006; Tiligada, 2006; Zhou *et al.*, 2013).

1.8.1 NF- κ B

NF- κ B was the first transcription factor shown to be redox-regulated. NF- κ B is a multiprotein complex that regulates many genes involved in inflammation, cell survival and differentiation. It is comprised of homo or heterodimers of five groups of proteins: NF- κ B1 (p50 and its precursor p105), NF- κ B2 (p52 and its precursor p100), p65/RelA, c-Rel and RelB. Inactive NF- κ B is sequestered in the cytoplasm when bound to an inhibitory kappa-B protein (I κ B; I κ B α , I κ B β , I κ B γ , I κ B ϵ , Bcl-3, p100 and p105). Upon stimulation (i.e. interleukin-1 β , TNF- α ,

Chapter 1

viruses, TPA, UV light, ionizing radiation, ROS) I κ B is phosphorylated and target for proteasomal degradation which in turn allows the nuclear translocation of NF- κ B. Once in the nucleus, NF- κ B acts as transcription factor for several target genes such as cytokines, chemokines, adhesion molecules and inhibitors of apoptosis (Gloire *et al.*, 2006). Additionally, ROS trigger signaling cascades leading to the activation and phosphorylation of mitogen activate protein kinases (MAPKs; such as ERK). which in turn activates NF- κ B and the induction of early response genes such as c-jun and c-fos, which are involved in differentiation (Bours *et al.*, 2000). See Figure 4.

Interestingly, it has been shown that NF- κ B is activated in certain regions of the brain during neurogenesis. Similarly, the expression and activity of NF- κ B increases during differentiation of human embryonic stem cells (Kang *et al.*, 2007). Furthermore, in SH-SY5Y cells, NF- κ B activation is an early event (preceding the appearance of neuronal characteristics) required for differentiation to occur after RA and TPA treatment (Feng and Porter, 1999). It has been demonstrated that these two compounds increase the levels of ROS (Yen and Albright, 1984; Konopka *et al.*, 2008; Kikuchi *et al.*, 2010; Nitti *et al.*, 2010). Ra-induced differentiation is enhanced in SH-SY5Y cells by IL-1 as it causes an increase in the binding activity of NF- κ B (Kania *et al.*, 2003). H₂O₂ has also been shown to significantly increase the activity of NF- κ B, which coincides with the enhanced expression of the dopamine D2 receptor in differentiated SH-SY5Y cells (Larouche, Berube *et al.* 2008).

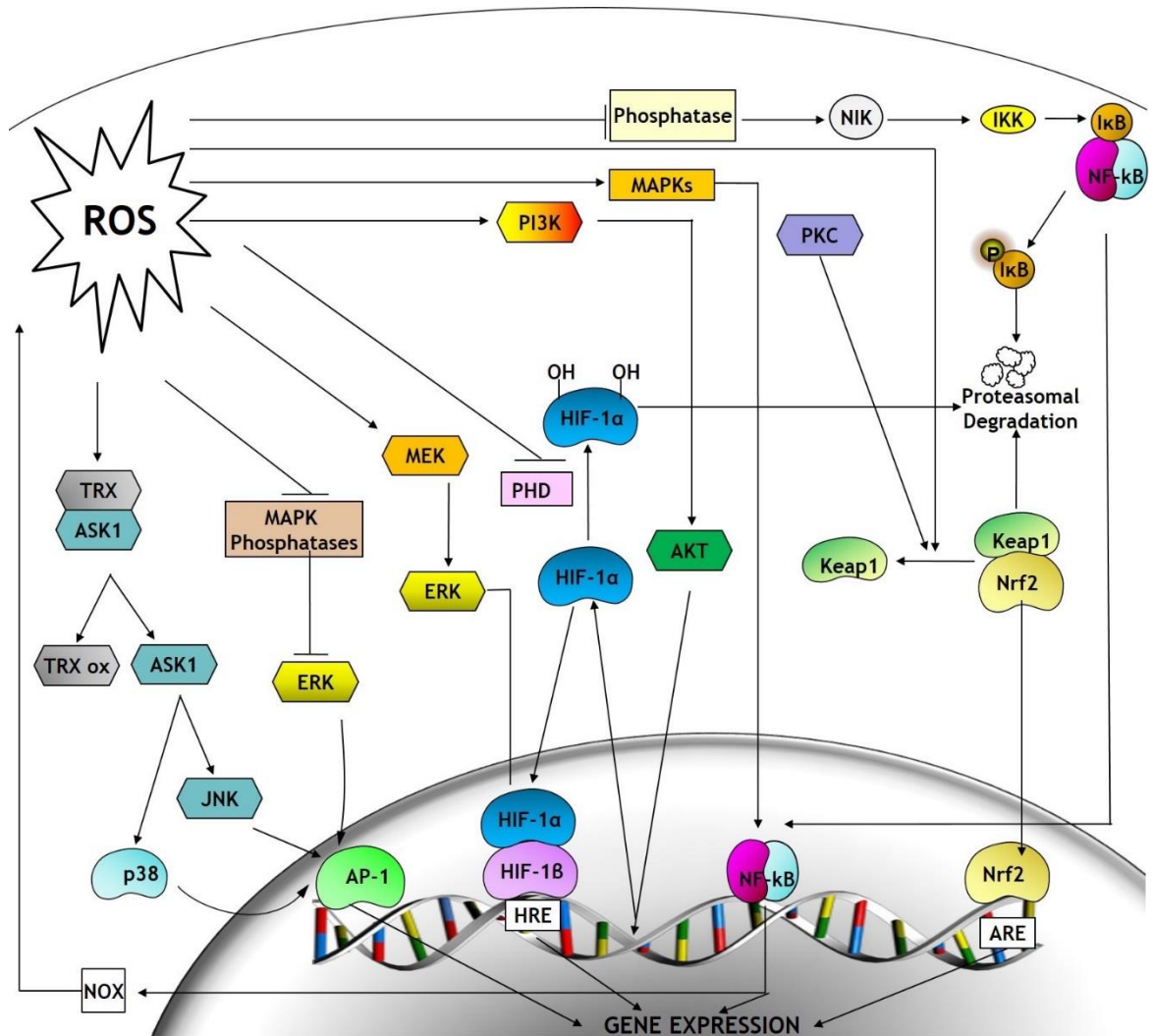


Figure 4 Transcription factors activated by ROS. ROS activation of four classical redox-sensitive transcription factors involved in differentiation, described in text. Abbreviations used (in alphabetical order): ARE, antioxidant response element; AP-1, activator protein-1; ASK1, apoptosis signal-regulating kinase-1; ERK, extracellular signal-regulated kinase; HIF-1, hypoxia-inducible factor 1; HRE, hypoxia responsive element; IKK, I κ B kinase; JNK, c-Jun N-terminal kinase; Keap1, Kelch-like ECH associated protein 1; MAPK, mitogen-activated protein kinase; NIK, NK- κ B-inducing kinase; NRF2, nuclear factor erythroid 2-related factor 2; PHD, prolyl hydroxylase; PKC, protein kinase C; TRX, thioredoxin.

1.8.2 NRF-2

NRF2 is a redox-sensitive transcription factor involved in the cellular response to environmental toxicants and carcinogens (Zhao *et al.*, 2009). Under normal conditions, NRF2 is constitutively targeted for proteasomal degradation by Keap1 (Kelch-like ECH associated protein). However, upon exposure to ROS, NRF2 disassociates from Keap1, leading to an increase in its protein stability and its nuclear translocation where it forms a heterodimer with one of the small Maf proteins. The NRF2/Maf heterodimer activates the antioxidant response element (ARE) in the promoter of its target genes (such as HO-1, Trx) Additionally, it has been shown that PKC phosphorylates NRF2 in its Neh2 domain at Ser-40 which

Chapter 1

also causes its disassociation from Keap1 (Hayes *et al.*, 2010; Bryan *et al.*, 2013). Also presented in Figure 4.

The role of NRF2 as a promoter of cell survival has been extensively examined on normal (Reddy *et al.*, 2007) and transformant cells (DeNicola *et al.*, 2011). However, recent evidence shows that ROS activation of NRF2 can also promote differentiation in B-cells, mouse primary peritoneal macrophages, RAW 264.7 cells, and mouse neural stem cells (Bertolotti *et al.*, 2010; Kanzaki *et al.*, 2013; Santos *et al.*, 2013). In SH-SY5Y cells, an early response following RA treatment is the increase in the expression of NRF2 prior to a clear appearance of differentiation signs. Furthermore, overexpression of NRF2 alone induces differentiation in SH-SY5Y and in primary neuronal cultures (Zhao *et al.*, 2009). Similarly, it has been reported that NRF2 is a positive regulator of differentiation in U937 human monoblastic leukaemia cells (Bobilev *et al.*, 2011).

1.8.3 HIF-1

Hypoxia inducible factor (HIF) is another redox-sensitive transcription factor activated during episodes of hypoxia. The extent to which hypoxia increases the levels of ROS still remains a matter of debate. However, there is evidence indicating that hypoxia (but not anoxia) causes an increase in the production of ROS at the mitochondrial complex III (Vieira *et al.*, 2011). Additionally, HIF-1 can be activated by hypoxia-independent but ROS-dependent mechanisms (Zhao *et al.*, 2014).

HIF is a heterodimeric protein complex formed by the assembly of α/β subunits. The most common HIF isoforms are HIF-1 and HIF-2. Under normal conditions the α subunits are targeted for proteasomal degradation by HIF prolyl-hydroxylases (PHD) and von Hippel-Lindau protein. ROS promote the stabilisation of the α subunits by modulating the activity of PHD (Niecknig *et al.*, 2012) which in turn enables the nuclear translocation of HIF and its binding to hypoxia response-elements in the DNA, thus altering gene transcription. Additionally, ROS activate PI3K/Akt and MEK/ERK signaling which increases the expression of the α subunit and, as a consequence, increases the transcriptional activity of HIF (Agani and Jiang, 2013). It has been reported that ROS regulate normal and malignant

hematopoietic differentiation through the activation of HIF-1 (Desplat *et al.*, 2002; Jiang *et al.*, 2005; Liu *et al.*, 2006; Song *et al.*, 2008; Yin *et al.*, 2011).

1.8.4 AP-1

The AP-1 transcription factor is a dimeric complex formed by members of the basic region-leucine zipper (bZIP) protein group such as Jun (c-Jun, JunB, JunD), Fos (c-Fos, FosB, Fra-1, Fra-2), CREB/ATF (CREB, ATF2, ATF3/LRF1, CREB, Maf and others). The target genes and regulation of this transcription factor is very complex because there are clearly several possible combinations of subunits that will form AP-1 homo- heterodimers (Remacle *et al.*, 1995; Cimino *et al.*, 1997; Echlin *et al.*, 2000).

AP-1 (c-jun/c-fos) is induced in response to ROS such as $O_2^{\bullet-}$ and H_2O_2 (Maki *et al.*, 1992; Aggeli *et al.*, 2006) by MAPKs (ERK, JNK, p38 kinase) via two main mechanisms: a) thioredoxin (TRX) oxidation and b) inhibition of MAPK phosphatases. In the first mechanism, reduced thioredoxin (TRX) inhibits apoptosis signal-regulating kinase-1 (ASK-1). However, upon accumulation of ROS, TRX becomes oxidised and ASK-1 is activated, leading to the downstream activation of MAPKs (JNK and p38) and AP-1 (Cheng *et al.*, 2014). The second mechanism involves the oxidation and inhibition of MAPK phosphatases by ROS, leading to the increased activity of ERK1/2 and in turn of AP-1 (Yang *et al.*, 2013), presented in figure 4. There are several important studies showing that the activation of AP-1 by ROS induces differentiation in several lines such as P19 CL6 embryonal carcinoma cells (Murray *et al.*, 2013), immortalised SV-HUC-1 cells (Liu *et al.*, 2013) and F9 teratocarcinoma stem cells (Yamaguchi-Iwai *et al.*, 1990; Jin *et al.*, 2002). Additionally, AP-1 inhibition severely enhances the aggressiveness of hepatomas (Bitton-Worms *et al.*, 2010).

From Figure 4 it can be inferred that there is considerable crosstalk between these signaling pathways and indeed, this has been experimentally proven and also extensively reviewed (Trachootham *et al.*, 2008). A notable example of crosstalk between these pathways, in regard to differentiation, comes from a study in which the effect of NRF2 on the differentiation of AML cells was shown to be tightly regulated by AP-1 activity. (Bobilev *et al.*, 2011).

Chapter 1

Taken together, these studies provide evidence that ROS play an important role in the differentiation of normal stem cells, cancer stem cells, as well as in several cell lines that maintain the ability to differentiate, including the SH-SY5Y neuroblastoma cell line used in this project.

1.9 Rationale of Study

1.9.1 Reasons for Study

The literature suggests that a link exists between dysregulation of Glu signaling, enhanced Trp metabolism and ROS production in the context of cancer development and progression. Consequently, the current study set out to investigate how these processes may interact and affect the biology of the neuroblastoma-derived SH-SY5Y cell line.

1.9.2 Reasons for the use of SH-SY5Y cells

There are many advantages to using SH-SY5Y cells in research, both practical and empirical. Besides the obvious advantages that any cell model provides: such as low cost, the ability to proliferate for a long time and genetic homogeneity, the SH-SY5Y line has the ability to convert Glu to the neurotransmitter GABA, and L-tyrosine to L-3,4-dihydroxyphenylalanine (L-DOPA). This last characteristic makes this cell line an ideal neuronal model to study PD dopaminergic transmission, among others (Youdim et al., 2003; Xie et al., 2010).

Furthermore, the fact that the SH-SY5Y cells transition from a malignant phenotype into a neuronal phenotype when treated with any of various compounds (such as RA), makes this cell line an excellent model system to study tumour regression and the effect that various drugs have on this process.

1.9.3 General Aims

The initial aim of this PhD project was to determine a method and a cell line validation in order to ascertain whether both the SH-SY5Y cell line and the methods available could be used to study the effect of kynurenines on the survival and differentiation of said cell line.

Then, based on preliminary results, this study set out to determine the effect of some kynurenines (QA, KA, 3-HAA) on the survival and differentiation of the neuroblastoma SH-SY5Y cell line. This study also set out to examine the extent to which the effect of QA and KA was mediated by their opposite actions on the

Chapter 1

NMDAR. The involvement of ROS was studied as well. Specifically an attempt was made to establish a link between ROS production and the differentiation of SH-SY5Y cells.

Finally, this research sought to examine the emerging role of NAD⁺ metabolism in cancer and whether there was evidence suggesting that a relationship existed between QA and NAD⁺ metabolism in the survival and differentiation of SH-SY5Y cells.

Chapter 2 – MATERIALS AND METHODS

2.1 SH-SY5Y culture procedures

General laboratory consumables and chemicals were purchased from different sources depending on the availability in the stores of the College of Medical, Veterinary and Life Sciences (MVLS).

The following list contains the consumables that were used to maintain the SH-SY5Y cells:

2.1.1 Materials

BD Falcon™; 6-well Multiwell; Plate. Tissue-culture treated polystyrene, flat-bottom, with low-evaporation lid (353046)

BD Falcon™; 12-well Multiwell™; Plate. Tissue-culture treated polystyrene, flat bottom, with low-evaporation lid (353043).

BD Falcon™; 24-well Multiwell™; Plate. Tissue-culture treated polystyrene, flat bottom, with low-evaporation lid (353047).

BD Falcon™ 96-well Microtest™ Plate. Tissue-culture treated polystyrene, U-bottom, with low-evaporation lid (353227).

Millipore filters (Minisart, 0.2µm pore size).

Corning® 75cm² Rectangular Canted Neck Cell Culture Flasks with Plug Seal Cap (Product #430720).

Corning® CellBIND® 75cm² Rectangular Canted Neck Cell Culture Flask with Vent Cap (Product #3290).

Corning® 150cm² Rectangular Canted Neck Cell Culture Flasks with Plug Seal Cap (Product #430823).

Chapter 2

Corning® 150cm² Rectangular Canted Neck Cell Culture Flasks with Vent Cap (Product #430825).

Corning® 15mL PP Centrifuge Tubes, Rack Packed with Plug Seal Cap (430052).

Corning® 50mL PP Centrifuge Tubes, Conical Bottom with Plug Seal Cap, Rack Packed, Sterile, 25/Rack, 500/Case (430290).

Laminar flow hood.

Different sizes of automatic pipettes.

CO₂ incubator.

Water bath.

The following list containing all the chemicals used to grow and plate the SH-SY5Y cells.

2.1.2 Chemicals

All the solutions necessary to culture the SH-SY5Y cells were purchased from the sources suggested by the European Collection of Cell Cultures.

From Sigma-Aldrich Company Ltd., Poole, Dorset, UK:

Foetal bovine serum -heat inactivated (F9665).

DEPC-Treated water (95284).

L-Glutamine 200 mM solution (G7513).

Minimum Essential Medium Eagle (M2279).

Nutrient Mixture F-12 Ham (N4888).

MEM Non-essential Amino Acid Solution (M7145).

Chapter 2

Penicillin 10,000 U and Streptomycin 10mg/ml (P4333).

Poly-D-lysine (P7280).

Trypan Blue dye (T8154).

Trypsin-EDTA solution from porcine pancreas 0.25% (T4049).

Water sterile-filtered (W3500)

All chemicals were stored at the appropriate conditions (temperature, humidity and light exposure) recommended by the suppliers and/or according to the available literature regarding the stability of each compound.

2.1.3 Medium preparation

The medium used to resuscitate, grow and differentiate the SH-SY5Y cells was a mixture of Eagle's minimum essential medium and Ham's F-12 medium 1:1 (vol/vol), supplemented with 2 mM glutamine, penicillin-streptomycin (1%), non-essential amino acids (1%) and foetal bovine serum (FBS) at different concentrations.

To maximise the number of cells obtained after resuscitation, the medium used contained 15% FBS (resuscitation medium). Once the cell line was established and after having been allowed to expand for three days, the concentration of FBS was decreased to 10%. This is the FBS concentration in the medium that was used to feed growing cultures, as well as to routinely passage them (growing medium). Finally, a third concentration of FBS was used when evaluating the effect that certain compounds have on differentiation; for these treatments, the concentration was decreased to 1% (differentiation medium) to avoid interference from mitogenic factors present in the serum.

To avoid l-glutamine degradation and changes in the initial pH due to nutrient breakdown, the medium was used within 5 days from its preparation. All the experiments carried out were designed to assess the effect of treatments at various time points occurring within 7 days. Therefore it was necessary to prepare two batches of medium per experiment. All the reagents used to

Chapter 2

prepare the medium were of culture quality and the medium was prepared under sterile conditions and kept at 4 °C.

2.1.4 Overview

SH-SY5Y human neuroblastoma cells were purchased from the European Collection of Cell Cultures (ECACC, Salisbury, UK) and kept in growing medium. Cells were maintained in T75 flasks at an atmosphere of 95% air and 5% CO₂ at 37 °C.

Cells were subcultured every 72 h, this is approximately the number of days necessary for the cultures to reach a confluence of 70-80% which corresponds to their log phase of growth and consequently to an optimum viability.

2.1.5 Cell line Resuscitation.

SH-SY5Y cells from passage 18 were acquired from ECACC. Upon arrival, vials were kept in liquid nitrogen at -240 °C and thawed whenever they were needed according to the following protocol.

First, the cryovial was removed from the liquid nitrogen and immediately placed in a cooler containing dry ice. The cryovial was then placed in a water bath at 37 °C for two minutes until about 80% of the volume had thawed. The content of the cryovial was pipetted out into a T15 flask containing medium with 15% FBS and placed in an incubator at 37 °C with an atmosphere of 95% air and 5% CO₂. 24 hours after plating, once the majority of the viable cells had attached to the flask, the medium was changed in order to remove dead and non-adherent cells and to replenish nutrients. Cells were allowed to grow for 2 more days before following the cell harvesting protocol, see 2.1.6

2.1.6 Cell harvesting

Once the cultures reached the desired confluence, the growing medium was removed and the cells were washed with 15mL of PBS at 37 °C. Cells were dissociated by adding 2mL of a solution containing 0.5% trypsin/EDTA. The excess of trypsin solution was removed and the cells were incubated at 37 °C for 1 minute. Once detached, cells were transferred to a 50mL centrifuge tube and

Chapter 2

the trypsin was neutralised with 10mL of medium containing 10% FBS. A sample of 100 μ L was taken from this cell suspension and mixed with Trypan blue dye 1:1 (vol/vol). A cell count of viable cells was performed under the microscope using a Neubauer haemocytometer.

Finally, one part of the cell suspension was transferred to T75 flasks at a final concentration of 1×10^5 cells/ml (to keep the cultures growing) and another to multiwell plates at various concentrations depending on the experimental setting, (see chapter 2.1.7). To avoid the loss of neuronal characteristics that has been reported to occur in the SH-SY5Y cell line after numerous passages, cultures were only split up to twelve times (passages eighteen to thirty).

2.1.7 Culture plating

The cells harvested were seeded in different plates depending on the experiments performed.

For all viability assays, cells were plated in 96-well plates at a density of 1×10^5 cells/ml. For all of the microscopic photography experiments, cells were plated in 24-well plates at a density of 1×10^5 cells/ml; this proved to be the ideal setting to take good quality micrographs. Micrographs were taken for neurite count experiments as well as for the DHE assay. For the latter, poly-D-lysine coated cover slips were used during plating. For the neurite outgrowth, assay cells were plated in 12-well plates and Millipore inserts at a density of 1×10^6 cells/ml. To meet the protein requirement for western blotting, cells were plated at a density of 2×10^6 cells/ml. All cultures were treated with the compounds of interest 48-72 hours after having been plated as this was the time when cultures reached a confluence of 70-80%. The only exception was the neurite outgrowth assay for which the manufacturer's guidelines were followed (see section 2.3.2.)

2.1.8 Poly-D-Lysine coating

Poly-D-Lysine is a polymer that provides cells with a substrate to adhere to otherwise smooth surfaces such as glass. Some cell types cannot form a monolayer when they are plated unless the surfaces are coated with poly-lysine.

Chapter 2

SH-SY5Y cells adhere easily to plastic plates but not when glass coverslips are used.

Poly-D-lysine was diluted in sterile water to a final concentration of 15 µg/ml. The coverslips were submerged in this solution for two hours at 37°C and then rinsed thoroughly since it has been shown that an excess of monomeric poly-D-lysine can be toxic to certain cell types.

72 hours after seeding, foetal calf serum (FBS) levels in the medium were reduced to 1% and retinoic acid (10 µM) was added to induce a neuronal phenotype (Pahlman *et al.*, 1984; Nicolini *et al.*, 1998). RA treated cells are the positive control for differentiated SH-SY5Y cells. Unless otherwise stated, all treatments were performed on the undifferentiated state. A final concentration of 50 nM of QA was used to treat SH-SY5Y cells. In some experiments, cells were co-incubated with SOD (300 U/ml) to investigate the role of ROS during differentiation,

2.2 Probes for Cell viability/proliferation

2.2.1 Fluorescein diacetate (FDA)

FDA (Sigma F7378), is an esterified compound that can be taken up by living cells. In the presence of functional intracellular esterases, the acetate groups are removed producing fluorescein which can be quantified spectrophotometrically. (Valencia and Moran, 2001).

A final FDA concentration of 5µg/ml, and 1% ethanol was added to 96 well plates. Plates were then incubated for 10 minutes at 37°C and read in a plate reader (Fluoroskan Ascent microplate fluorometer, Thermo Scientific) with the excitation set at a wavelength of 485nm and the emission at a wavelength of 538nm. Unless otherwise stated, all viability assays were carried out using this method.

2.2.2 AlamarBlue®

Alamar blue is an oxidation-reduction indicator that changes colour from blue to red, and fluoresces, when reduced by cellular metabolic activity. It has been

Chapter 2

used to study the proliferation of tumour cell lines and the effects of chemotherapeutic drugs, and has been found to provide a rapid, sensitive and non-toxic fluorescence assay of cell viability (White *et al.*, 1996). It detects cell viability by the transformation of non-fluorescent resazurin into a fluorescent dye (resorufin) in response to chemical reduction of culture medium resulting from cell growth. Continued cell growth maintains a reduced environment while inhibition of growth maintains an oxidised environment. Reduction related to growth causes the redox indicator to change from oxidised (non-fluorescent, blue) form to reduced (fluorescent, red) form.

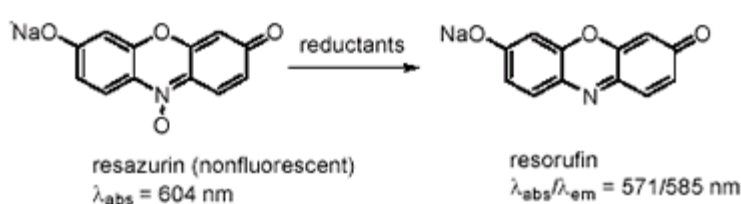


Figure 5- The reduction of non-fluorescent resazurin. The transformation yields a highly fluorescent red compound, resorufin.

The alamarBlue® (AB) assay (BioSource International, Nivelles, Belgium) was used to determine cell viability. Briefly, after each treatment period, the medium was replaced with 100 μl of medium containing 10% v/v of AB. The plates were then put back in the incubator for another 6 hours after which the absorbance was determined by reading the plates at both 540 nm and at 595 nm wavelengths using a spectrophotometric plate reader (DYNEX Technologies, UK). The absorbance value of a blank well containing only medium was subtracted from all the experimental values. Since there was an overlap in the absorption spectra of the oxidised and reduced forms of AB, it was necessary to read at two different wavelengths. The two different values from the reading and the molar extinction coefficient were used in the following equations to establish the concentration of both the oxidised and reduced form of AB.

$$1. \text{ \% of reduced AB} = \frac{[(\epsilon_{\text{OX}})\lambda_2 A\lambda_1 - (\epsilon_{\text{OX}})\lambda_1 A\lambda_2]}{[(\epsilon_{\text{RED}})\lambda_1 A'\lambda_2 - (\epsilon_{\text{RED}})\lambda_2 A'\lambda_1]} \times 100$$

Chapter 2

2. % difference in reduction between treated and control cells = $[(\epsilon_{OX})\lambda_2 A\lambda_1 - (\epsilon_{OX}) \lambda_1 A\lambda_2]$ of test agent dilution $\div [(\epsilon_{RED})\lambda_1 A'\lambda_2 - (\epsilon_{RED})\lambda_2 A'\lambda_1]$ of untreated positive growth control $\times 100$

Where:

CRED = concentration of reduced alamarBlue® (RED)

COX = concentration of oxidised alamarBlue® (BLUE)

ϵ_{OX} = molar extinction coefficient of oxidised alamarBlue (BLUE)

ϵ_{RED} = molar extinction coefficient of reduced alamarBlue (RED)

A = absorbance of test wells

A' = absorbance of negative control well (media + alamarBlue without cells).

A* = absorbance of positive growth control well

λ_1 = 540 nM

λ_2 = 595nm

All the data was normalised to control values (Fatokun *et al.*, 2006).

2.3 Neurite Extension.

2.3.1 Morphology of SH-SY5Y cells

To study the morphology of living SH-SY5Y cells, the cells were visualised 72 h after treatment using an Olympus DP50 inverted phase-contrast microscope which was fitted with a digital camera system. The cells were photographed using the DPSoft software (Olympus UK Ltd., Southall, UK). For all the morphology experiments, cells were plated in 6 well plates at a density of 1.5×10^6 per well. This particular setting allows a better visualization of the cell bodies and neurites with minimum interference from the plate itself. Micrographs were taken immediately after treatments. For all the experiments in which a count of the number of cell bodies and neurites was performed, 3 images from at least 3 separate experiments were analysed. A neurite was defined as an outgrowth longer than twice the cell body diameter. The results are presented as the ratio of neurites/cell bodies.

2.3.2 Neurite Outgrowth assay

To further assess the degree of neurite formation, the Millipore's NS230 Neurite Outgrowth Assay Plus Kit (3 μm) was used. This assay is based on the use of a microporous tissue culture insert which contains a permeable membrane with a pore size of 3 μm . This assay is ideal for cells projecting neurites and with a cell body diameter larger than 3 μm , like the SH-SY5Y cell line as the cell bodies remain in the upper side of the insert while the neurites continue to extend through the insert membrane. After differentiation occurred, the cell bodies were scraped off keeping only the fraction containing neurites. This guaranteed that all the measurements came from the neuritic fraction. The kit was used according the manufacturer's guidelines, briefly;

Cultures are passaged normally and maintained in a growing medium until they reach a confluence of approximately 70%. Once the cultures are confluent, differentiation is induced for 24 hours by changing the medium of the cultures to one containing the differentiation factor of interest (RA 10 μM , 50 ng/ml NGF, QA). Cells are then briefly washed with PBS buffer and dissociated using the Cell Dissociation Buffer provided (Part No. CS202683). Once the cells have detached from the flask they are centrifuged at 200 x g. The pellet is collected and

Chapter 2

resuspended at a concentration 1×10^6 cell/ml. The cells obtained are then plated in the Millicell inserts provided. For each condition two inserts are used, one coated with laminin (1mg/ml), which promotes neuritic adhesion to the plate, and another one coated with BSA 100mg/ml (as a negative control).

After 72 h in the differentiation media, an indirect immunocytochemistry protocol is performed against β 3-tubulin, using TMB, (3,3',5,5'-tetramethylbenzidine) as the horseradish peroxidase substrate and sodium fluoride as the stop solution. All materials, aside from the methanol used for fixing the cells, are provided by the manufacturer as part of the kit. There is only one modification in the immunocytochemistry protocol which involves the removal of the cell bodies following the antibody incubation. Briefly, to visualise the cell bodies, an inactive stain solution is added to the top part of the insert, the cell bodies are then scraped off using cotton swabs.

The OD readings for both the laminin and the BSA coated inserts are read at 450 nm wavelengths with a spectrophotometric plate reader (DYNEX Technologies, UK). The OD readings obtained were then used to calculate signal (laminin) to noise (BSA) ratios for each treatment.

2.4 DHE ROS quantification

Cytosolic DHE exhibits blue fluorescence. However, upon oxidation, this compound is converted to ethidium, mainly by $O_2^{\cdot-}$, and it intercalates within the cell's DNA. DNA-bound ethidium exhibits bright red fluorescence. After treatment, cells were incubated with DHE at a final concentration of $3.2 \mu\text{M}$ for 20 min, washed twice with PBS and then fixed in 4% fresh paraformaldehyde. Cells were then mounted with PBS:Glycerol 1:1 (v/v) and examined with an epifluorescence microscope using a Rhodamine filter. Results are expressed as a relationship between ethidium positive cells and the total number of cells per field. Alternatively, after DHE, incubation cells were washed twice with PBS buffer and read in a fluorescence plate reader with the filters set at 535nm absorption and 610 nm emission.

2.5 Immunocytochemistry

2.5.1 Materials

0.1 M phosphate buffer solution

0.2 M PBS

0.3% triton solution (in 0.1M PBS)

1.5% blocking serum solution in PBS and 0.3% triton

4% or 8% paraformaldehyde solution (in 0.1M phosphate buffer)

Olympus DP50 Digital camera

Olympus IX50 Phase-contrast microscope

Olympus TH3 Light source

Olympus U-RFL-T Fluorescent light source

2.5.2 Antibodies

Anti-NeuN Antibody (mouse), clone A60, Alexa Fluor®488 conjugated (MAB377X)

FITC-conjugated donkey anti-rabbit antibody (Jackson 711-095-152)

2.5.3 Immunocytochemistry protocol

After treatments, cells were removed from the incubator and washed once with PBS at 37°C. PBS was aspirated and cells were fixed for 15 minutes with 100µL of a 4% paraformaldehyde (PFA) solution (at 4°C) and gently pipetted into the cultures to avoid cell detachment. In order to completely remove PFA, cells were washed 3 times for 5 minutes with 0.1M PBS. To prevent non-specific binding, the plates were blocked with 1.5% donkey serum in 0.3% Triton for 1 hour (50 µL). All incubations were performed at room temperature for one hour on a gyratory rocking platform to ensure that all the solutions were covering the cultures and that the motion was gentle enough to prevent detachment of the fixed cells.

The blocking serum was then removed and 50µl per well of primary antibody was added (1:100 dilution in PBS and 0.3% triton). This was followed by an overnight incubation at 4°C. A set of wells were incubated as negative controls with just 50µl of PBS and triton solution, the negative controls were used to calibrate the exposure time when photographing the cultures.

After the primary antibody incubation, the plates were washed 3 times for 5 minutes with 50µl of 0.1M PBS. From this moment on, the plates were handled with care to reduce exposure to direct light. The samples were viewed and photographed under the microscope with fluorescent light at a wavelength of 495 nm/521 nm.

2.6 Microscopy photography

For all the experiments requiring micrographs to be taken, the software used to capture and process the images was Cell D, (Soft Imaging System GmbH). This program has the basic tools to capture, measure and edit. The contrast and brightness of some phase-contrast micrographs was modified with Photoshop. However, special care was taken to maintain intact all the images from fluorescent assays since adjusting them would have interfered with quantification. For fluorescent microscopy photography, the exposure time was set using the negative control. A first picture was taken in which all the background is bright and the exposure time was lowered until there was no

Chapter 2

background in the image. Once set, the exposure was not changed across different fields or wells. Image J (<http://imagej.nih.gov/ij/>) was used to perform cell counts. This software is considered very useful to perform cell counts as it saves a layer that can be reviewed later, along with all the marks for all the counted individual cells, without modifying the original picture.

2.7 Protein sample preparation and quantification

2.7.1 Materials

BIORAD® protein assay dye (BIORAD®, 500-0006)

BSA (Sigma, A2153)

Costar disposable cell scraper (Corning, 3010)

Eppendorf 5417R centrifuge

IGEPAL (Sigma, I7771)

PBS (Gibco, 1010)

Protease Inhibitor cocktail tablets (Roche, 11 836 170 001)

Sodium chloride powder (BDH, 102415K)

Sodium dodecyl sulphate powder (BDH, 442444H)

Tris powder (Boehringer Mannheim, 708976)

Triton X-100 (Sigma, T8787)

2.7.2 Protein preparation

For the preparation of protein lysates, SH-SY5Y cells were plated in six-well plates at a density of 2×10^6 cells/well.

Chapter 2

After treatments, culture plates were removed from the incubator and placed on ice. The culture medium was aspirated by pipette and the cultures were washed once with ice-cold PBS. PBS was also removed and 200 μ L of radio-immune precipitation assay (RIPA) buffer was added to the plates to lyse the cells. RIPA buffer was prepared by making a solution containing 50 mM Tris, 150 mM NaCl, 0.5% Triton, 0.1% SDS, 1% IGEPAL in distilled water. The pH was adjusted to 7.4.

After 1 minute in RIPA buffer, the cells were scraped off and the buffer/cell suspension for each condition was transferred into different Eppendorf tubes. This cell suspension was centrifuged at 16,000 X g for 5 minutes at 4°C in an Eppendorf 5417R centrifuge. The supernatant was collected and the pellet containing the membranes was discarded.

2.7.3 Protein quantification

The protein concentrations were determined using the Coomassie Blue Protein Assay (BioRad®)

A protein concentration curve was produced using BSA as a standard. A BSA stock solution was prepared by diluting 1 in 10 BSA in distilled water (20mg/100mL). From this stock solution further dilutions were prepared in duplicate to have a range of protein concentrations (0, 0.25, 0.5, 1.0, 1.5, 2.0mg/ml).

In order to determine the protein concentration of the experimental samples and express it in terms comparable to the concentration curve generated (mg/ml), dilutions of the samples had to be prepared, all in duplicate. This was done by taking a volume of 4 μ L of sample and adding 396 μ L of distilled water (1/100). 200 μ L of BioRad reagent diluted in water (1:1) was added to the samples, then vortexed and both the standard curve and the samples were transferred into a 96-well plate. The plate was read at 595nm on a plate reader (Dynex). A linear regression was performed using the O.D. from the standard solutions. The linear equation obtained was then used to calculate the total protein concentration in each sample. A total of 20 μ g of protein was loaded into each lane.

Chapter 2

Using the lowest concentration found in the samples as a standard, all the other samples could then be diluted to contain the same amount of protein per ml.

2.8 Western Blotting

2.8.1 Materials

'Hypercassette' film cassette (Amersham RPN12642)

'PowerEase® 500' pre-cast gel system includes powerease® power supply, temperature monitoring probe, xcell surelock® mini-cell and Xcell II™ blot module (Invitrogen EI8675UK)

Sponge pad for blotting (Invitrogen EI9052)

Blotting Roller, 8.6 cm wide (Invitrogen LC2100)

'Restore' stripping buffer (Pierce, 21059)

Gel Spatula (Invitrogen)

Photosensitive films (Amersham, RPN3103K)

Protein transfer chamber (Invitrogen, E19051)

2.8.2 Chemicals

PVDF membrane (Invitrogen, LC2005)

NuPAGE® Novex 12% Bis-Tris gel 1.0 mm, 15 well (Invitrogen, NP0343BOX)

Antioxidant (Invitrogen, NP0005)

Methanol (Fisher, M/4056/17)

Milk powder (Upstate, 20-200)

MOPS running buffer (Invitrogen, NP0001)

Chapter 2

Ponceau stain (Sigma, P7170)

Sample buffer (Invitrogen, NP0007)

Sample reducing agent (Invitrogen, NP0004)

SeeBlue protein marker (Invitrogen, LC5925)

Transfer buffer (Invitrogen, NP0006)

Tween-20 (Sigma, 27,434-8)

2.8.3 Antibodies

All antibodies were obtained from their UK distributors (Millipore, Watford; R&D Systems, Abingdon; Santa Cruz, Insight Biotechnology, Wembley).

Actin, goat polyclonal (Santa Cruz, sc-1615).

Anti- β 3-tubulin, mouse monoclonal clone 2G10 (Millipore, 05-559).

Donkey anti-goat HRP (Santa Cruz, sc-2020)

Doublecortin, goat polyclonal (Santa Cruz, sc-8066).

Goat anti-mouse HRP (Santa Cruz, sc-2005).

Goat anti-rabbit HRP (Millipore, 12-348).

GluN1, mouse monoclonal (Millipore, 05-432)

NRF2, goat polyclonal (Santa Cruz, sc-30915)

Synaptophysin, mouse monoclonal (Millipore, MAB368).

VAMP-1/synaptobrevin, goat polyclonal (R&D Systems, AF4828).

2.8.4 Gel running procedure

Loading samples were prepared as follows: 65% adjusted experimental sample, 25% sample buffer, and 10% reducing agent. The loading samples were then vortexed and heated at 70°C in a water bath for 10 minutes.

While the samples were heating, the gel cassettes were washed with distilled water to remove the packing buffer and the lanes were rinsed with MOPS running buffer (50mL NuPage MOPS running buffer to make a final volume of 1000mL with distilled water). Next, the gel assembly was set up by placing 2 gel cassettes facing each other in the gel tank. The middle reservoir formed by the 2 gel cassettes was then filled with 200mL of MOPS running buffer supplemented with 0.5mL of antioxidant. Finally, the outside reservoir of the gels, formed between the gel cassettes and the tank itself, was filled with MOPS running buffer without antioxidant.

10µL of see plus 2 (Invitrogen) marker was added to a marker lane at the side of the gel as a standard of location/weight in the gel. In the remainder of the lanes, 15µL of the adjusted experimental sample was loaded, after ensuring that that each lane in fact had 20µg of protein.

The tank was run at 175V for 1hr and 10 minutes which was found to be the optimum condition for the appropriate separation of the proteins studied in this project. The intensity of electric current was set to 120mAMP for one gel and 240mAMP when two were run in one tank.

2.8.5 Protein transfer procedure

While gels were running, transfer buffer was prepared by mixing 50mL of NuPage® transfer buffer, 200mL of methanol, 1 ml of antioxidant and enough distilled water to make a final volume of 1000mL. 800mL of this solution was transferred to a tray alongside with all the equipment for gel transfers (sponge pads, blotting roller, and filter paper).

A spatula was used to crack open the gel cassette, half of the cassette was removed and the gel indentations that form the lanes were cut and removed. A square of filter paper was placed on the gel surface; at this point the other half

Chapter 2

of the cassette was removed, leaving the gel suspended over the filter paper. A PVDF membrane, previously soaked in methanol, was placed on the other surface of the gel and on top of this another square of filter paper. This membrane sandwich of filter-gel-membrane-filter was then placed on top of the sponge pads which, up to this point, had been resting on the cathode core of the blotting module. Two more sponge pads were placed on top of the membrane sandwich. Finally, the lid or anode core of the transfer assembly was placed on top, and the entire blot module was placed in the tank.

The remainder 200mL of the transfer buffer solution was then added to the middle compartment of the Xcell II™ blot module, approximately 1cm above the membrane sandwich. The outer compartment, formed by the assembly module and the walls of the tank, was filled with distilled water. The volume of distilled water used was enough to cover up to $\frac{3}{4}$ of the blot module

The powerpack was attached and the unit was run at 30V for 1 hour at 450mAMP

After this time, the transfer unit was disassembled, the polyacrylamide gels and the filters were securely disposed of and the PVDF membrane was soaked in distilled water.

2.8.6 Ponceau staining

The Ponceau staining technique is a simple and rapid procedure that allowed corroboration of the loading uniformity of the samples across the lanes as well as confirming that the transfer had been successful. This technique, using Ponceau S solution (Sigma, Poole, UK), always followed the transfer of the blots.

The PVDF membrane were rinsed twice with distilled water, drained and submerged in 5mL of Ponceau solution for 5 minutes. The PVDF membrane was then quickly rinsed and the protein bands examined and photographed. After this, the distilled water was drained and the PVDF membrane was immersed in a solution of 0.1M of NAOH for approximately 30 seconds or until the stained bands had faded. To ensure that all the Ponceau stain and NAOH had been removed, the PVDF membranes were washed twice for 3 minutes

2.8.7 Antibody incubation

The membrane was blocked to avoid non-specific antibody binding with 5% skimmed milk in Tris Buffer Saline Tween-20 (TBST; 10 mM Tris pH 8.0, 150 mM NaCl, 0.05% Tween-20) at room temperature for 1 hour.

Incubation with primary antibodies was typically done overnight with agitation at 4°C for the following specific antibodies: B3-tubulin (1:1000), synaptophysin (1:1000), GAP-43 (1:1000), doublecortin (1:1000), NRF2 (1:500) and GAPDH (1:10,000) as a loading control.

The following day, the membrane was washed with TBST three times for 15 minutes (with agitation) to remove any unbound primary antibody from the membrane and from the dishes where the membranes were kept.

The membrane was then immersed and stirred for 1 hour in 5mL of a solution containing horseradish peroxidase coupled secondary antibody (1:3000) and 5% skimmed milk in TBST. Next, the membrane was washed 5 times for 15 minutes in TBST in a shaker to remove any unbound secondary antibody.

2.8.8 Enhanced Chemiluminescence

To quantify the amount of specific binding between the target protein, the primary antibody and the secondary antibody, a chemiluminescence detection system was used. A luminol peroxide detection reagent was added to the membrane for 5 minutes, during which time the HRP enzyme present in the secondary antibody would catalyse the oxidation of luminol. This reaction was accompanied by the emission of a low intensity light. Commercially available chemiluminescence kits enhance the signal by the addition of other chemicals to the reaction; this process is called enhanced chemiluminescence (ECL). The signal was visualised using ECL PLUS (GE Healthcare). The kit was used according to the manufacturer's guidelines, briefly;

The detection reagents (solution A and solution B) were removed from the fridge and allowed to reach room temperature. Solutions A and B were mixed in a ratio of 40:1 (2 ml solution A and 50µL solution B). Once mixed, the solution was kept away from direct light at all times, this was achieved by shielding all the

Chapter 2

containers used (centrifuge tube and dish) with tin foil. The mixed detection reagent was pipetted onto the protein side of the PVDF membrane and covered with a square of parafilm® to ensure an even distribution of the solution across the membrane. After incubation for 5 minutes, the excess solution was removed and the membrane was placed in a developing cassette.

The cassette was taken into a red-light room, where photosensitive film paper was cut to the correct size and placed over the membrane. The time of exposure varied according to the intensity of the signal, but in general was between 30 seconds and 1 minute. Films were then fed into a developing machine (KODAK).

Quantification of the blots' size and intensity was measured using the program image J (<http://imagej.nih.gov/ij/>). Corrections accounting to loading differences were made using the intensity of the “housekeeping” proteins (actin and GAPDH).

2.9 Statistical analysis

Data were analysed using one-way ANOVA as almost all the experiments were designed to ensure the existence of only one independent variable (drug) and one response variable (effect). The exception to this rule was time courses, for which a two-way ANOVA was used, followed by a Dunnett's test (when comparing against control only) and Tukey's post hoc test (when multiple comparisons were performed).

The experiments performed included a very large number of experimental conditions, it was therefore not possible to use a follow-up test of planned comparisons which, in theory, should have a $k-1$ number of comparisons. Furthermore, there was no strong theoretical basis to design experiments with a reduced number of conditions.

Most of the research conducted was aimed at determining the possibility of significant differences occurring within groups (generally speaking this refers to the different doses used). Therefore, all the groups were compared equally by applying a post-hoc test after the one-way ANOVA.

Chapter 2

Data are expressed as means \pm SE. Statistical significance was set at $P < 0.05$. Preliminary statistical analyses were performed using StatView software.

One-way ANOVA followed by Dunnett's multiple comparisons test was performed using GraphPad Prism version 6.00 for Windows, GraphPad Software, La Jolla California USA, www.graphpad.com

A minimum number of conditions and a two-way ANOVA was used for the experiments designed to determine whether delivering the drugs in 1% FBS or 10% FBS medium caused a different cellular response.

2.10 Treatments

2.10.1 Chemicals.

From Sigma-Aldrich Company Ltd., Poole, Dorset, UK:

Catalase powder, bovine liver (C1345)

Diphenylene iodonium chloride (D2926)

Hydrogen peroxide 30% solution (H1009)

3-Hydroxyanthranilic acid powder (H9391)

Kynurenic acid powder (K3375)

MK-801 maleate (M107)

N-methyl-D-aspartate powder (M3262)

QA powder (Q104)

Retinoic Acid (R2625)

Superoxide dismutase powder, bovine erythrocyte (S5395)

Xanthine (X4002)

Xanthine oxidase (from bovine milk, X4376)

The majority of compounds used to treat the cells were dissolved in stock solutions using sterile water (culture grade). The exception was 3-HAA, KA, RA, DHE and H₂O₂.

3-HAA can only be solubilised when it is in a protonated state. Hydrochloric acid (HCl) 1N was used followed by a pH adjustment to 7.4 using 1M of Tris-HCl, pH 8.8.

Chapter 2

To dissolve KA, 1 M NaOH was used; the solution was back titrated with 0.1 M HCl to pH 7.4.

RA was dissolved in ethanol to a final stock solution of 0.01 M (3 mg/ml). To treat SH-SY5Y cells, subsequent dilutions were made in the growth medium to get a final RA concentration of 10 μ M; this in turn yielded a final ethanol concentration of 0.1% (v/v) that has no effect on cultures.

DHE was solubilised in methanol making sure that once treated, the final concentration of methanol would not exceed 0.05% (v/v).

H₂O₂ was diluted in fresh 10% FBS medium to prepare the desired final concentrations. Preparing stock solutions for long-term storage by diluting them in culture media is not recommended. However since the prepared solutions were used soon afterwards, diluting them in medium reduces stress on the cells caused by changes in osmolarity.

All the solutions used to treat the cells were prepared under sterile conditions, heated to 37°C using a water bath (Grant Instruments, Cambridge) and filtered prior to use.

The time spent changing the medium and treating the cells never exceeded five minutes after which the cells were always placed in an incubator set to inject 95% air and 5% CO₂ at 37 °C.

2.11 Methods (carried out by others)

2.11.1 High performance liquid chromatography (HPLC).

The concentration of 3-HAA in cultures and in cell-free preparations was measured by HPLC and carried out by Dr. Alexandra Ferguson at the University of Glasgow. The methodology described here is only a brief summary based on the more complex methodology described and developed by Dr. Gillian Moira Mackay for her PhD dissertation (Mackay *et al.*, 2006; Mackay, 2007).

Method details are given in the Appendix (section 6.1 under “Methods carried out by others”).

2.11.1.1 Sample's origin

The samples analysed came from solutions that were used to treat cells seeded on 96-well plates. One single treatment was made on day 0 and no medium changes were performed. The same solutions that were used to treat the cells were pipetted into plates that had no cells growing on them to discern the actual cellular contribution to the process. The solutions added to the cells and to the wells without cells were: 3-HAA (50 μM and 100 μM) in 1% FBS medium with or without SOD (300 U/ml), 3-HAA (50 μM and 100 μM) in 10% FBS medium with or without SOD (300U/ml). Cells were treated on day 0 with the solutions mentioned above. 900 μL per condition were put aside on Eppendorf tubes to be used as the 3-HAA concentration present on day 1. Samples were collected thereafter on day 1, 2 and 3. A total of 900 μL were collected for each condition (16 per day), labelled in code (for example, 1D0a meant the sample for day 0 containing 100 μM 3-haa in 10% FBS without SOD) and frozen. At this point, samples were given to Dr. Ferguson to be run through the HPLC knowing only in general the range of concentrations used (to adjust the standard curve) and of course, that the compound used was 3-HAA (double blind). At the end of the HPLC run the data received was 1D0a = 87.95622338 μM .

Chapter 3 – OPTIMISING CULTURE CONDITIONS AND ASSESSING THE OVERALL STATE OF SH-SY5Y CELLS

3.1 Introduction

According to Good Laboratory Practice recommendations (Li *et al.*, 2006) this chapter intends to validate the SH-SY5Y cell line as a reliable *in vitro* model to study toxicity and/or differentiation. The findings of this section focus on the three key aspects: a) optimization of the culture conditions necessary to grow the SH-SY5Y cell line; b) confirmation that the methods employed to evaluate a specific parameter (survival and differentiation) are suitable for their intended use; and c) comparability studies confirming that the SH-SY5Y cell line acquired behaves in accordance to what has been reported in the literature in terms of survival and differentiation.

During the initial stages of this project, it was noted that SH-SY5Y cells are highly dependent on serum to proliferate. For instance, the data sheet from the cell line's supplier (ECACC) specifically encourages plating the cells in a medium containing up to 15%FBS when first resuscitated. The relevance of finding an adequate FBS batch to supplement the medium to be used to grow and treat the cells was therefore of the highest priority.

The SH-SY5Y cell line had already been established in the laboratory and tests to find the optimal culturing conditions had already been performed by Dr. Caroline Forrest. However, the FBS used to prepare the medium to feed the cells had to be changed due to an exhaustion of the FBS batch initially reserved (Sigma F9665 batch 011k3396).

Since SH-SY5Y cells can be induced to differentiate into neurons through various chemical treatments, it was decided to test the effect of QA on differentiation; but first it was necessary to establish a reliable method of inducing and evaluating differentiation.

Chapter 3

In view of the above and aware that the loss of neuronal characteristics has been described with increasing passage numbers, we followed the recommendation of not using them after passage 38. In this study, two factors (RA and NGF) were tested and reported to have neuronal differentiating properties. The use of 10 μ M RA resulted in cells with apparent neuronal morphology (with long, extensive network of neurites). This effect was less pronounced after treatment with NGF.

In order to confirm that the results obtained from the morphological analysis had a molecular basis and that cells were indeed undergoing neuritogenesis and not simply transient changes in shape the expression of neuronal and proliferation markers was evaluated. The expression of cytoskeleton proteins is known to increase with the development of neuritic processes (Heraud *et al.*, 2004), in particular that of β 3-tubulin. As differentiation occurs, the number of proliferating cells decreases and so does the expression of doublecortin (DCX). DCX is a microtubule associated protein found in migrating neuronal precursors as well as in brain areas with high neurogenesis (Couillard-Despres *et al.*, 2005). This is also the case in neuroblasts where an inverse correlation between the acquisition of a mature neuronal phenotype and the expression DCX has been reported (Galderisi *et al.*, 2003)

For this reason the use of antibodies against β 3-tubulin and DCX was evaluated after treatments with RA and NGF and it became an essential tool for identifying the degree of neurite extension or conversely of proliferation.

Neuronal synapses are characterised by the presence of synaptic vesicles, neurotransmitters, receptors and exocytotic machinery. The synaptophysin (SYN)-synaptobrevin (VAMP1) complex is found in mature synaptic vesicles and its presence has been used as a marker of functional synapses. In order to determine if cell differentiation is also associated with an acquisition of functional synapses, the expression of VAMP1 was assessed.

After a 7 day treatment with 10 μ M RA and 50 ng/ml NGF, the expression of β 3-tubulin and VAMP1 increased and there was a decrease in the expression of DCX.

3.2 Aims and objectives

- Establish the optimal culture conditions for the SH-SY5Y cell line.
- Determine what the optimum serum for growing SH-SY5Y cells is
- Familiarise with the lag, log, and stationary phase of the SH-SY5Y cell line in order to establish the best time to subculture and treat the cells.
- Establish that the acquired SH-SY5Y cell line is able to differentiate when treated with RA
- Confirm that the acquired SH-SY5Y cell line responds the same way as in the literature reports regarding H₂O₂ toxicity.
- To ascertain if a correlation exists between the morphology and the β 3-tubulin/DCX ratio after differentiation has been induced.

3.3 Results

3.3.1 SH-SY5Y cells show different growing profiles depending on the batch of foetal bovine serum (FBS).

Two different serum batches were tested: Sigma F9665 batch 018k3396 against Sigma F9665 batch 098K3396. First, a new vial was unfrozen and plated in a T15 flask containing medium with 15% FBS from the initial batch (011k3396). After resuscitation, SH-SY5Y cells remained in suspension for 24 hours, their cell bodies at this stage were bright, round and very small. However, over the next 24 hours after having been plated, they reattached to the dish surface and resumed growth. Cells were fed daily and passaged after three days into a T150 flask containing 10% FBS from the original batch (011k3396).

Cells were fed on the third day and subcultured on the 7th day in order to have a sufficient number of cells to be plated in 2 different T75 flasks and two 6-well plates at a final density of 1×10^5 cells/ml. One flask and one of the 6-well plates contained medium with 10% FBS from batch 018K3396 and the other flask and 6-well plates contained 10% FBS medium from batch 098K3396. The plates were photographed daily and the micrographs obtained were used to count the number of cells present in the optic field. After having been photographed, 2 wells in each plate were scraped and a total cell count was performed by trypan blue on day 1, 2 and 3.

The cell count obtained from both serum batches was compared to the average cell count recorded up to that day, making sure it belonged to the cultures grown in the original batch of FBS (011k3396).

After 1 DIV, there were not any apparent qualitative differences the cultures grown in batches 018K3396 and 098K3396. The morphology of the SH-SY5Y cells in either one of the media was neuroblastic. Approximately 70% of the cells present had attached to the plate surface while 30% could still be found in suspension (Figure 6 a). Also after 1DIV, the micrograph cell count of the culture grown in batch 018K3396 was 42 cells and for the culture grown in batch 098K3396 was 43 cells (Figure 6 b). Similarly the trypan blue cell count yielded a total of 2.2×10^5 cells/ml in the medium with serum 018K3396 and 2.4×10^5 cell/ml in the 098K3396 one, but this difference was not significant (Figure 6c).

Chapter 3

At day 2 however, there were significant changes in all of the evaluated parameters. Cells grown in the medium containing 018K3396 serum looked similar to the way they did the day before; there were no changes in the proportion of attached cells vs. the ones in suspension. There were only 45 cells per micrograph and the total cell count using trypan blue was 330,381 cells/ml. On the other hand, cells grown in medium with 098K3396 serum were bigger (30 μ M), started associating together in clumps of cell bodies and the number of cells per micrograph had increased to 70. Similarly, the trypan blue count yielded a total of 5.2×10^5 cells/ml (Figure 6).

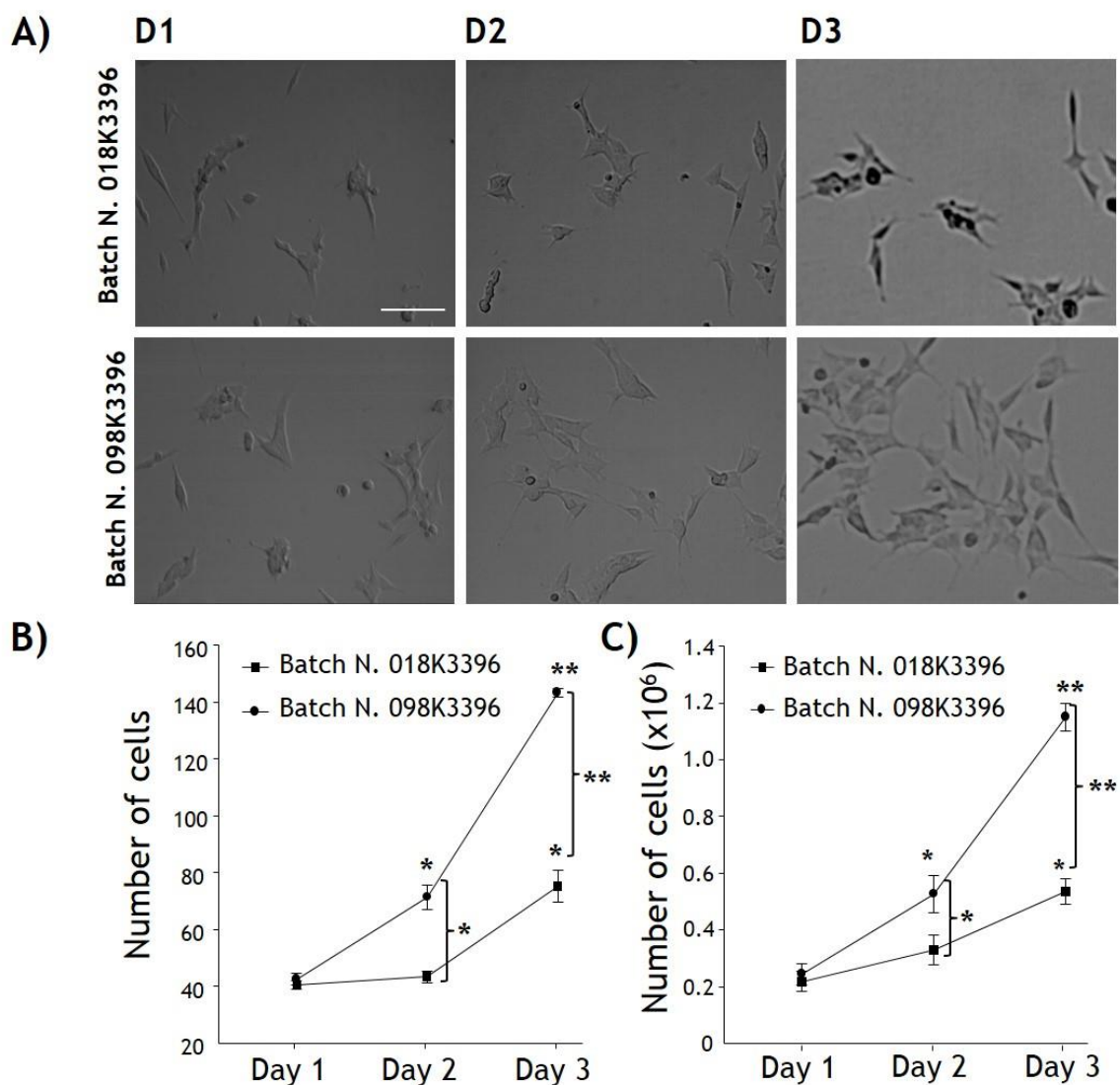


Figure 6. Foetal bovine serum affects the growth rate of SH-SY5Y cells. A) Phase-contrast micrographs of SH-SY5Y cells corresponding to 1, 2 and 72 h after plating B) Graphs indicating the number of cells counted from micrographs (by triplicate) taken 1, 2 and 72 h after plating. C) Haemocytometer cell count (Trypan blue) 1, 2 and 72 h after plating. Results are expressed as percentage of control. Point in graph represent mean \pm SEM. * $P < 0.01$, ** $P < 0.001$ Two-way ANOVA followed by Tukey's test. $n = 5$. Scale bar = 50 μ m.

Chapter 3

The difference in cell proliferation between both sera was more noticeable on the 3rd day. Cells in medium from batch 018K3396 were still precariously scattered on the plate surface. The number of cells increased only by approximately 60% regardless of the counting method used (micrograph count or by haemocytometer).

In contrast, cells plated in medium prepared from batch 098K3396 had already reached 70% confluence, approximately. The cells were distributed evenly on the plate surface. The micrograph cell count yielded 140 cells per optic field and 1.2×10^6 cells/ml.

3.3.2 RA and NGF induce differentiation in SH-SY5Y cells

3.3.2.1 Qualitative assessment of the morphology

SH-SY5Y cells were plated in 6-well plates and cultured for 72 h in 10% FBS medium after which they were transferred to a 1% FBS medium alone (control) or supplemented with either 10 μ M RA or 50 ng/ml NGF. Cells were incubated for 72 h before being collected for western blotting. Alternatively, cells were incubated under the same conditions for 7 days, with a change of fresh medium, RA or NGF on the 3rd day, before being collected for western blotting. A total of 4 independent experiments were carried out each time, using fresh solutions prepared from well preserved stocks.

Since exposure of SH-SY5Y cells to 10 μ M RA is the most widely reported inducer of differentiation, this treatment was used in several experiments as a positive control of differentiation. When cells were differentiated for a period longer than 72 h, they were always fed with fresh 1% FBS containing 10 μ M RA on the 3rd day.

Undifferentiated SH-SY5Y cells grew in clusters of neuroblastic cells presenting flat cell bodies that adhered to the surface onto which they were plated. Their cell bodies were elongated and star-shaped with some of the multiple vertices thinning until they formed short processes. During the first 24 hours there were no obvious differences between control cells (kept in 10% medium) and treated cells (Figure 7).

Chapter 3

Cultures reached a high density within 72 h, this was evidenced by groups of cells growing on top of each other, forming a series of multilayers. This effect could be observed even before cells reached 70% confluence.

Despite the fact that SH-SY5Y cells are an adherent cell type, the number of adherent and non-adherent cells increased with time. It was not uncommon to see some clumps of viable cells sporadically detaching from the plates and remaining in suspension as evidenced by the larger round spots in the micrographs (Figure 7).

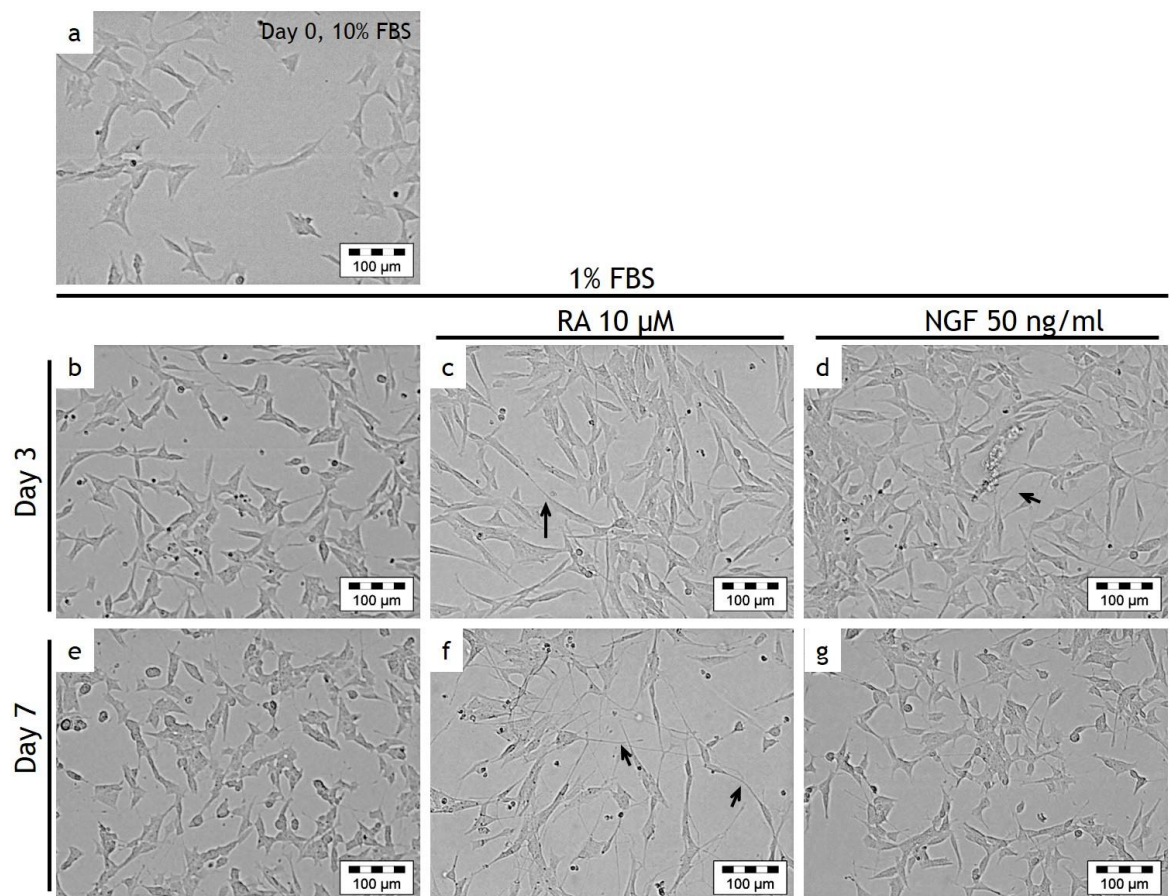


Figure 7. RA and NGF alter the morphology of SH-SY5Y cells. Bright-field micrographs taken 3 and 7 days after treatment with 10 μM RA and 50 ng/ml NGF in which morphological changes can be observed (neurite, arrow). Scale bar = 100 μm

24 hours after cells were transferred to a medium containing 1% FBS and 10 μM RA, there was an increase in the length of the processes. Some of them were at least twice the length of their cell body. The cell body itself began to compact and adopted a more circular shape. SH-SY5Y cells were induced to differentiate into a more neuronal phenotype by RA and to a lesser extent by 50 ng/ml NGF. Cells treated with 50 ng/ml NGF maintained a typical epithelial morphology (Figure 7) 3 and 7 days after treatment.

Chapter 3

To demonstrate that differentiation with RA had occurred, as in several previous reports, SH-SY5Y cells were treated with 10 μM of RA and an increase in the number of neurite-bearing cells was confirmed. This effect was initially observed 24 hours after treatment and up to a maximal 7 days after treatment. During the first 48 hours, the cell bodies changed from a flat, triangular shape to a more rounded one (Figure 7). RA is a light sensitive compound that is not very stable under culture conditions therefore cells had to be fed with fresh medium containing 10 μM RA every 48 hours. In preliminary experiments, feeding the cells less than twice a week dramatically reduced the degree of RA-induced differentiation observed in the cultures.

It was important to test whether the morphological differences observed had a molecular basis that could be measured. Therefore, changes in specific neuronal ($\beta 3$ -tubulin, VAMP1) and non-differentiated cell markers (DCX) were evaluated by Western blotting.

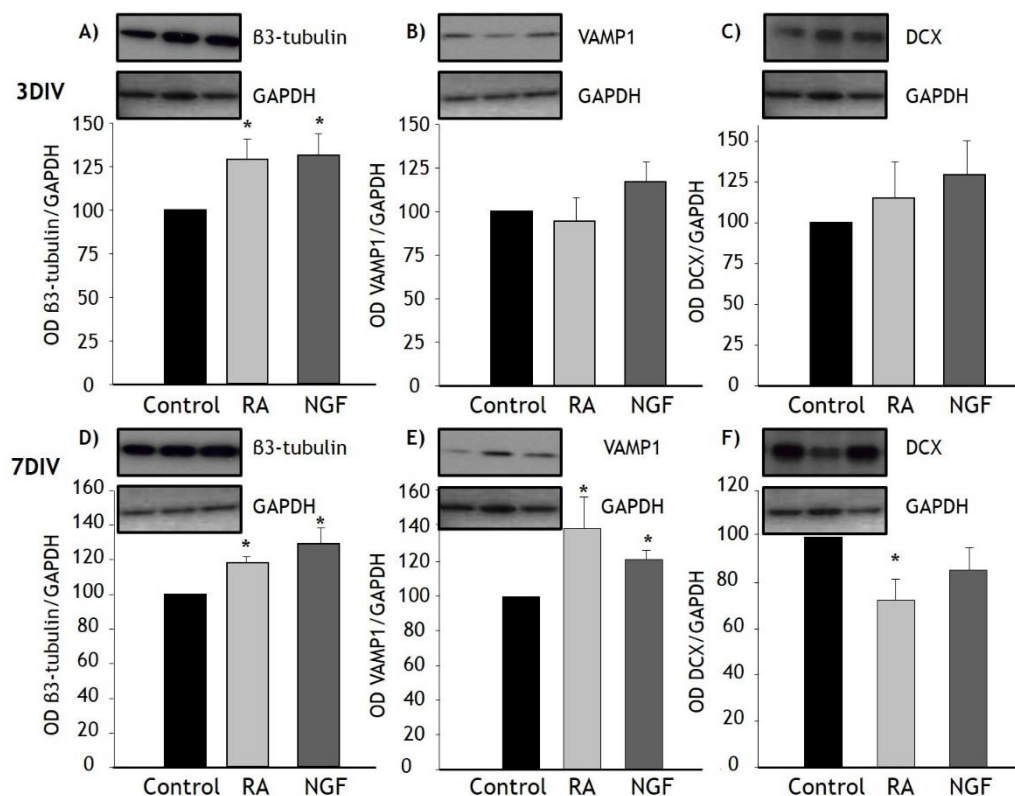


Figure 8. RA and NGF increase the expression of neuronal markers in SH-SY5Y cells. Western immunoblotting and histograms of the quantification analyses of $\beta 3$ -tubulin (A, D), synaptic protein VAMP1 (B, E) and proliferation marker doublecortin (DCX; C, F) after 3 and 7 day treatments with RA (10 μM) or NGF (50 ng/ml). Bars represent mean \pm SEM in arbitrary units of optical density (OD). GAPDH was used as a house-keeping protein and results were normalised to the control. * $p < 0.05$ One-way ANOVA followed by Dunnett's test. $n = 4$.

Chapter 3

Cells treated with 10 μ M RA showed an increase in the expression of β 3-tubulin as early as 72 h after treatment (Figure 8-a). This increase was maintained up to 7 days after treatment (Figure 8-d). In contrast, the expression of VAMP1 was not different from control levels after 72 h of treatment (Figure 8-c). However, 7 days after treatment, the expression of VMAP-1 was significantly increased when compared to control cells (Figure 8-e). Accordingly, RA successfully caused a decrease in the expression of the proliferation marker DCX (Figure 8-f) 7 days after treatment.

Cells treated with 50 ng/ml NGF showed a significant increase in the expression of β 3-tubulin three days after treatment (Figure 8-a). The expression of β 3-tubulin remained high 7 days after treatment (Figure 8-a, d). The expression of VAMP1 did not change during the first three days. NGF significantly increased VAMP1 expression 7 days after treatment (Figure 8d, e) when compared to proliferative cells. Contrastingly to what happened with RA treatment, NGF did not cause changes in the expression of DCX at any of the time points evaluated (Figure 8-c, f).

3.3.3 Hydrogen peroxide is a potent inducer of cell death in SH-SY5Y cells

SH-SY5Y cells were grown for 72 h in medium containing 10% FBS. After this time, the medium in the plates was gently aspirated and replaced with fresh medium containing 10% FBS alone (control) or with H₂O₂ at 3 different concentrations (100 μM, 250 μM, 500 μM). Cells were placed back in the incubator for 2 hours after which viability was assessed by FDA. Additionally, the same treatments were delivered in medium containing either 1000U/ml CAT or 300U/ml of superoxide dismutase (SOD). The initial stock was a 30% aqueous solution of H₂O₂ (9.79M), this was diluted in fresh 10% FBS medium to prepare the desired final concentrations. A total of 3 independent experiments were carried out, using fresh solutions each time

To rule out any interference of catalase (Gedik *et al.*, 2005) with the FDA readings, it was decided to design a cell-free preparation using a 96-well microplate. Each well contained 10μL of CAT at different concentrations (2500U/ml, 3125U/ml, 6250U/ml, 12500U/ml and 25000U/ml) and 100μL of growing medium (10% FBS). The volumes chosen were similar to the ones generally used to treat cells in a 96-well microplate. The plate was incubated for 2 hours and a normal FDA assay performed (see chapter 2.2.1). A total of 6 independent experiments were carried out, using fresh solutions each time.

Indeed, the presence of CAT at concentrations higher than 3125 u/ml caused an increase in the optical density readings (Figure 9a). The relationship between the optical density obtained and the concentration of CAT applied was dose-dependent. This relationship was nonlinear and, once plotted, it exhibited a sigmoidal behaviour that was best described ($R^2= 0.972$) by the following 4 parameter logistic nonlinear regression (Figure 9a, insert):

$$f = -52.8788 + \frac{241.9217}{1 + \left(\frac{x}{2798.1819}\right)^{-0.9978}}$$

This increase in the reading was not caused by cellular esterase activity since there were no cells in the wells treated. Therefore, to avoid any interference in future FDA readings, which could be wrongly interpreted as an increase in cell viability, the final concentration of CAT used in all experiments was 1000 U/ml.

Chapter 3

This having been established, SH-SY5Y cells were exposed to H₂O₂ (100-500 μM) for 2 hours and cell viability was assessed by FDA. After 2 hours, exposure to 100 μM, 250 μM and 500 μM H₂O₂ decreased cell viability, when compared to control, in a dose dependent manner to 79% ± 2.8, 60% ± 3.8, 38% ± 3.9 respectively (Figure 9b), $P < 0.0083$ for 3 different experiments.

The effect of SOD and CAT on H₂O₂-induced cell death was evaluated. As expected, incubation with 300U/ml SOD did not exert any protection from H₂O₂-induced cell death. The same doses 100 μM, 250 μM and 500 μM in combination with 300U/ml SOD continued to reduce cell viability to 79% ± 2, 69% ± 2.9, 39% ± 1.9 respectively (Figure 9c), $P < 0.0014$ for 6 different experiments.

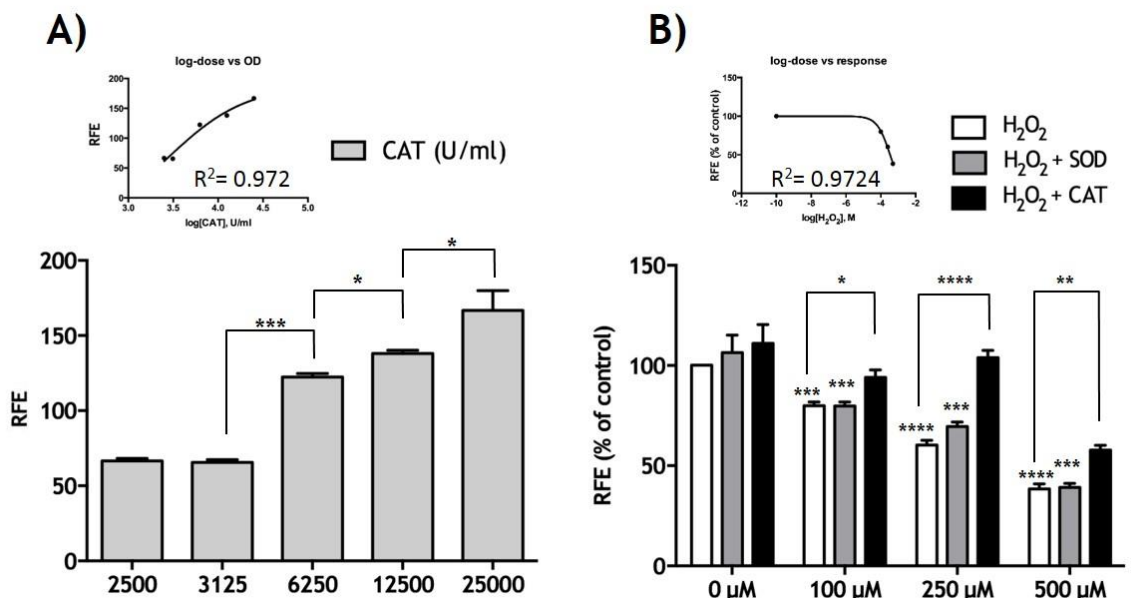


Figure 9. Catalase protects SH-SY5Y cells against H₂O₂-induced toxicity. A) Histogram indicating the FDA relative fluorescent emission values of a cell-free preparation containing medium plus catalase (2500-25000 U/m. B) Viability of SH-SY5Y cells treated for 2 h with different concentrations of H₂O₂ (100-500 μM) in the presence of either catalase (Black bar; 1000U/ml) or SOD (grey bar; 300U/ml). For graph A) results are expressed as FDA relative fluorescence emission (RFE). For graph B), results are expressed as percentage of control RFE. Bars represent mean ± SEM. * $P < 0.05$, ** $P < 0.0083$, *** $P < 0.0014$, **** $P < 0.0001$. One-way ANOVA followed by Dunnett's test (A) and Two-way ANOVA followed Tukey's test (B). n=6.

Contrastingly, 1000 U/ml CAT rescued the SH-SY5Y cells from H₂O₂-induced damage at 100 μM and 250 μM, restoring the viability to a level comparable to that of control wells. For the highest concentration of H₂O₂ used (500 μM), CAT protection was only partial, managing to increment the viability by approximately 10% when compared to cells treated with 500 μM H₂O₂ only.

The same experiments were carried out using the Alamar blue viability assay. The results obtained were similar to the FDA results. Therefore, it was decided to continue using the FDA assay for future experiments.

3.4 Discussion

This set of experiments confirmed that the SH-SY5Y cell line acquired from ECACC behaves similarly to what has been reported in the literature in terms of its growing profile, its ability to differentiate as well as its susceptibility to toxic insults (Constantinescu *et al.*, 2007; Weinreb *et al.*, 2008; Cheung *et al.*, 2009).

An article by Lin *et al.* (2009) shows that exposure of SH-SY5y cells to 100 μM H_2O_2 for 3 hours results in approximately a 40% reduction of cell survival (Lin *et al.*, 2009). The data herein contained confirmed that exposure to 100 μM H_2O_2 for 2 hours causes a 20% reduction in cell viability (Figure 9-b).

Furthermore, it was confirmed that differentiation of SH-SY5Y cells could only occur in medium with a low serum concentration. It has been suggested that the presence of growth and mitogenic factors (cAMP, NGF, bFGF, PDGF, EGF, steroids, insulin, IGF-I and II.) in serum inhibit differentiation of SH-SY5Y cells (Glick *et al.*, 2000; Zheng *et al.*, 2006)

The data gathered in this study are in agreement with previous reports that show that an increase in the expression of neuronal markers occurs with the concomitant decrease in the expression of proliferation markers in SH-SY5Y (Lopes *et al.*, 2010). Although an increase in the immunoccontent of β 3-tubulin was found as early as 72 h after differentiation was initiated, there was an equal amount of DCX in proliferative cells and in those treated for 72 h with RA, which means that cells were at a very early differentiation stage. Seven days after treatment with RA, there was a clear decrease in the expression of DCX, which points out to a cease in cellular division, and the adoption of a fully mature neuronal phenotype. The period of time in which RA effectively induced the expression of β 3-tubulin and a decrease in DCX is similar to what has been shown in previous reports (Leondaritis *et al.*, 2009; Agholme *et al.*, 2010).

Chapter 3

There are conflicting reports regarding SH-SY5Y cell's responsiveness to NGF. It has been classically accepted that the SH-SY5Y cell line does not respond to NGF due to its low expression of TRKA receptors, high affinity NGF receptor pp140^{crk}, and the low affinity neurotrophin receptor p75^{LNGFR} (Pahlman *et al.*, 1995; Encinas *et al.*, 1999; Olsson *et al.*, 2000; Simpson *et al.*, 2001; Xie *et al.*, 2010). However there are several studies that show that SH-SY5Y cells do respond to NGF and extend neurites after treatment (Chen *et al.*, 1990; LoPresti *et al.*, 1992; Poluha *et al.*, 1995). A potential explanation for these contradictory reports comes from data showing that, within the SH-SY5Y cell line, there are some genetically different cellular subpopulations that are more responsive to NGF than others (Oe *et al.*, 2005). Similarly, there is evidence suggesting that other differentiating factors influence the responsiveness of the SH-SY5Y cells to NGF, such as brain derived neurotrophic factor, neuregulin B1 and vitamin D3 (Agholme *et al.*, 2010).

The data presented in this project shows that exposure to 50 ng/ml NGF stimulates neurite extension when compared to controls, but to a lesser extent than RA does. NGF treatment increased the expression of β 3-tubulin and VAMP1 which supports the morphological assessment proving that cells are differentiating. On the other hand, NGF treatment failed to reduce the levels of DCX, indicating that proliferation is not completely halted in the cultures. It has been suggested that NGF differentiation can be enhanced by blocking cell proliferation with inhibitors of α and δ polymerase such as aphidicolin (LoPresti *et al.*, 1992). Because of the partial differentiation observed with NGF, RA was used instead as a positive control of differentiation as treating SH-SY5Y cells with 10 μ M RA is one of the most widely accepted stimulus to differentiate SH-SY5Y cells (Pahlman *et al.*, 1984; Schneider *et al.*, 2011)

After 7 days of RA differentiation, the expression of DCX decreased significantly. DCX, a microtubule associated protein, is expressed in a cell-cycle-dependent manner. DCX is downregulated as cells stop dividing and differentiate.

3.5 Conclusion

- Based on the growth curve analysis, the serum from batch 098K3396 is an ideal serum to grow, passage and treat SH-SY5Y cells.
- High concentrations of CAT caused an increase in the optical density readings of FDA. Special care has to be taken when using other compounds to ensure that they do not interfere with the assays at the used concentration. It was also decided to conduct other cell-free experiments throughout this study to guarantee that the results obtained are not an artefact.
- RA induces differentiation and so does NG, though to a lesser extent. RA treatment can therefore be effectively used as a positive control for differentiation in this study.

Chapter 4 – CONTRASTING EFFECTS OF QUINOLINIC AND 3-HYDROXYANTHRANILIC ACID

4.1 Introduction

QA is a highly toxic metabolite of Trp; even millimolar concentrations of QA are able to cause selective nerve cell degeneration (Schwarcz *et al.*, 1983) either by over stimulating the NMDAR or by causing oxidative stress.

Whetsell and Schwarcz (1989) showed that caudate nucleus cultures or a combination culture of frontal cortex and caudate nucleus could be maintained in the presence of 100 nM QA for up to 7 weeks without any obvious loss in the number of cells. However, upon ultrastructural morphological analysis, they demonstrated that cells exhibit increased vacuolization (Whetsell and Schwarcz, 1989).

It has been shown that the concentration of enzymes and metabolites of the kynurenine pathway is altered in the SK-N-SH neuroblastoma cell line (from which the SH-SY5Y cell line was subcloned). For instance, in the SK-N-SH line IDO-1 is not constitutively expressed, the concentration of ACMSD is low and QA is preferentially metabolised (Guillemin *et al.*, 2007).

Adams and collaborators (2012) hypothesised that a shift in the kynurenine pathway towards QA provides neuroblastomas with an adaptive advantage. Briefly, they state that favouring QA production provides neuroblastomas with a more steady and reliable source of the NAD⁺, which in turn sustains the enhanced activity of PARP1 (which is found in many cancers) and ultimately promotes tumour cell viability and proliferation (Adams *et al.*, 2012).

This study provides evidence suggesting, for the first time, that QA induces neuritogenesis in SH-SY5Y cells. It is proposed that QA induces differentiation through a ROS-dependent mechanism. The source of these ROS is believed to be NOX (at least partly) since DPI prevented QA-induced differentiation. An early consequence of QA treatment was an increase in the expression of NRF2 (12 h

Chapter 4

after treatment) followed by an increase in the expression of β 3-tubulin and neurite extension (72 h after treatment). A prospective hypothesis is presented in which both ROS production and NAD^+ are necessary to induce differentiation of the SH-SY5Y line. NAD^+ could support neuronal differentiation both metabolically and by inhibiting SIRT1 (which represses NRF2).

If ROS were to play an important role in the differentiation of SH-SY5Y cells, then perhaps other oxidant molecules could affect SH-SY5Y survival and/or differentiation. Thus, given the effect of QA on the production of ROS and neuritogenesis, it was decided to evaluate if other kynurenines such as 3-HAA (a well-known inducer of oxidative stress) could exert a similar effect on the viability and neuritogenesis of SH-SY5Y cells. Cells were treated with different concentrations of 3-HAA and the morphology and viability were assessed 24 h 48 h and 72 h after treatment. No changes in the morphology or survival could be observed 24 h after treatment with 3-HAA. However, after 48 h, cells showed clear signs of cellular damage and death

There are no reports about the effect of 3-HAA on the SH-SY5Y cell line despite the fact that 3-HAA has been, to a certain extent, implicated in the pathologies that the SH-SY5Y cell line is a model for.

4.2 Aims and objectives

- Determine the effect of QA on differentiation.
- Determine if QA is acting on the NMDAR or affecting the oxidant state of the cell.
- Ascertain whether there exists a relationship between the expression of neuronal markers and QA treatments.
- Evaluate the effect of 3-HAA on cell survival.
- Ascertain factors involved in the cellular response to 3-HAA.

Chapter 4

- Determine the effect of 3-HAA on SH-SY5Y cells and whether there is a differential response between differentiated and undifferentiated SH-SY5Y cells.
- Establish if the levels of ROS are affected by 3-HAA treatment

4.3 Results

4.3.1 QA effect on SH-SY5Y survival and neuritogenesis

4.3.1.1 QA does not negatively affect the survival of SH-SY5Y cells

In order to establish if QA had a detrimental effect on cell survival, undifferentiated SH-SY5Y cells were fed with fresh 10% FBS medium (control) or treated for 72h with increasing concentrations of QA (50 nM, 300 nM, 500 nM, 25 μ M, 50 μ M, 100 μ M, 500 μ M, 1mM and 5mM), after which survival was assessed.

Figure 10 shows that, contrary to what was expected, QA did not have a toxic effect on SH-SY5Y cells 72 h after treatment regardless of the concentration used. At doses above 25 μ M, there seemed to be 10% decrease in the viability; nevertheless, after statistical analysis, these differences were not significant.

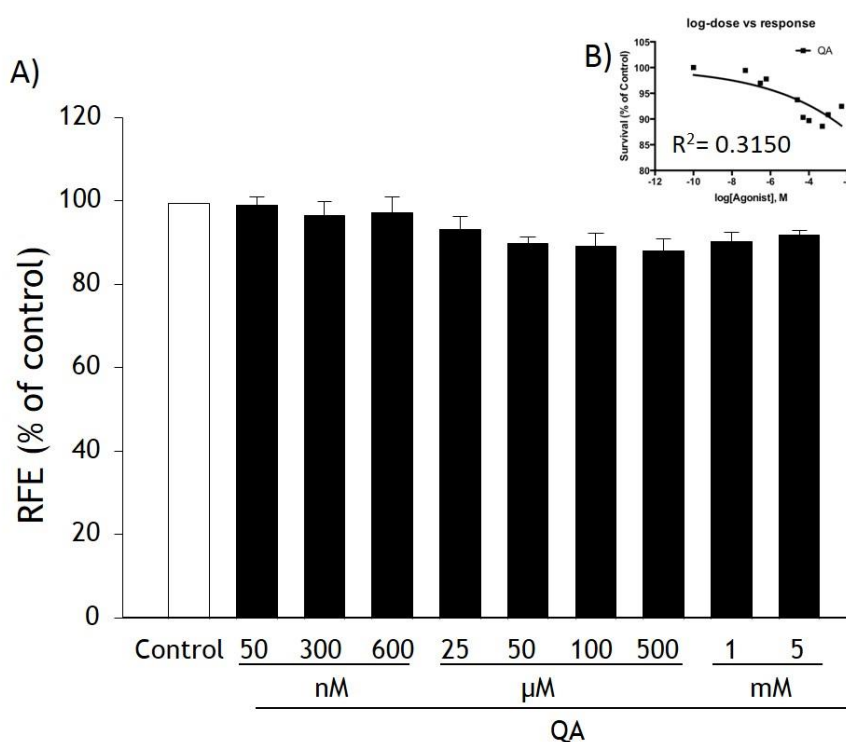


Figure 10. QA does not promote cell death in SH-SY5Y cells. A) Histogram indicating the viability of undifferentiated control SH-SY5Y cells (untreated) and cells treated for 72 h with QA (50nM-5mM) in 10% FBS. **B)** Dose-response curve fitting with a variable Hill slope. $R^2=0.3150$. Results are expressed as a percentage of control RFE. Bars represent mean \pm SEM. No significant differences were found using One-way ANOVA followed by Dunnett's test. $n=4$.

The same data were fitted to a dose-response curve (Figure 10, insert) which had an R^2 value of 0.3150, further confirming that QA does not negatively affect cell survival in a dose-dependent manner.

4.3.1.2 SOD treatment increases the number of cells in culture.

Since the original aim of these experiments was to ascertain whether QA could affect RA-induced cell differentiation, it was first necessary to establish whether a sublethal dose of QA had a toxic effect when administered in combination with RA. Therefore SH-SY5Y cells were treated after 3DIV with RA 10 μ M, QA 50 nM and a combination of both. These treatments were delivered in both 1% FBS medium and 10% FBS medium.

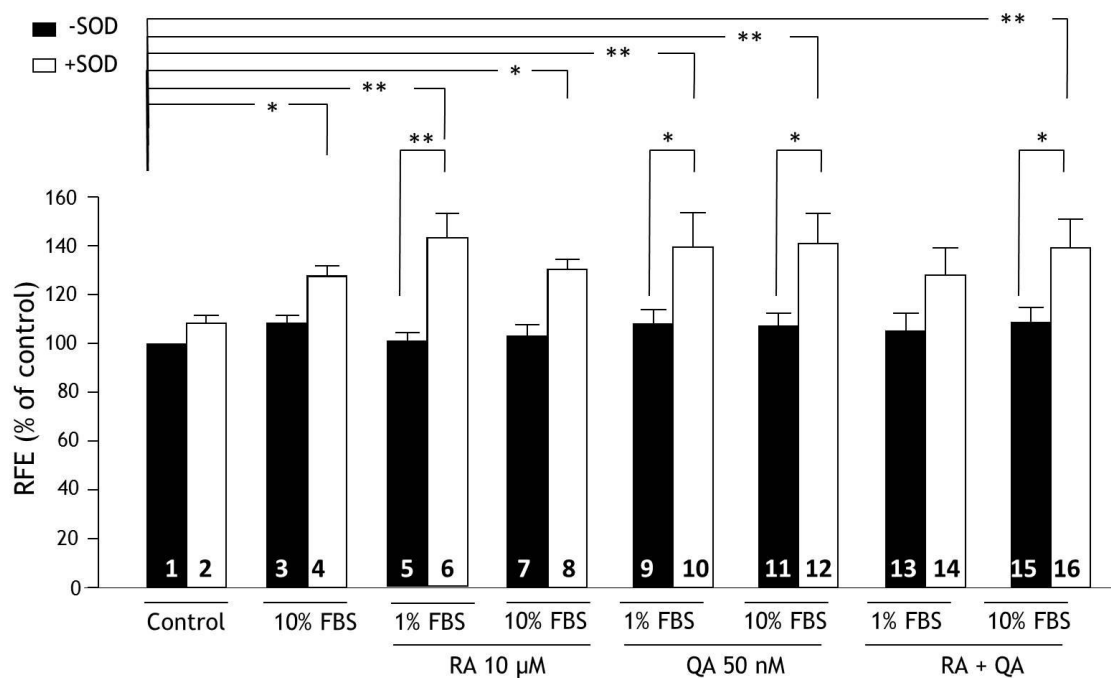


Figure 11- SOD increases the number of cells after 72 h treatment with QA plus RA. Histogram indicating the viability of undifferentiated SH-SY5Y control cells, and cells treated with RA (10 μ M) and/or QA (50 nM) in 1 or 10% FBS medium supplemented with SOD (300 U/ml, white bars). Control wells received 1% FBS medium exchanges only. The results are expressed as a percentage control RFE. Bars represent mean \pm SEM. * p <0.05, ** p <.0072. Two-way ANOVA followed by Tukey's test. $n=4$.

Consistently with previous results (Figure 10), there were no significant changes in the number of cells after 72 h of QA incubation when compared to untreated cells (Figure 11, 1st bar vs. 9th and 11th). Furthermore, when comparing control cell with those treated with both QA and RA, (Figure 11, 1st bar vs. 13th and 15th) there were no significant differences in the number of cells. Survival was not affected by the concentration of foetal bovine serum in the medium in which RA and/or QA was delivered (Figure 11, 5th vs. 7th bar; 9th vs. 11th bar; 13th vs 15th bar).

Chapter 4

When $O_2^{\cdot-}$ was removed by supplementing the medium with 300U/ml SOD, there was a significant increase in cell viability for the majority of the conditions tested. In the previous chapter, it was shown that high concentrations of catalase interfered with the FDA readings. Thus to rule out the possibility that the effect of SOD observed was an artefact, the FDA assay was performed on cell-free plates using solutions of identical composition to the ones used for treatments (QA, RA, QA+RA with and without SOD). There were no differences in the relative fluorescent emission between either of the tested solutions.

Compared to untreated controls, a relatively high increase in cell viability was noted when SOD was added to cells treated with 10% FBS medium, RA (in 1% and 10% FBS medium), QA (in 1% and 10% FBS medium) and finally, RA+QA in 10% FBS medium (Figure 11, 1st vs. 4th, 6th, 8th, 10th, 12th, 14th and 16th bar).

Compared to controls, there was a marked and significant increase in the viability of cells treated with RA in 10% FBS medium containing SOD. However, there were no differences in the viability between cells treated with RA in 10% FBS medium and those co-treated with SOD (Figure 11, 7th vs. 8th bar). A possibility is that cells in both groups continued to grow, making the net differences in viability less pronounced. This is in accordance with several reports showing that a high FBS concentration sustains cell growth despite the presence of a differentiation-inducing agent.

Interestingly, when RA+QA+SOD was delivered in 1% FBS medium there were no differences in the viability when compared against controls or against the same treatments but without SOD (Figure 11, 1st vs. 14th bar; 13th vs 14th bar). This may suggest that the joint effect of RA and QA effectively neutralizes the proliferative effect of SOD.

On the other hand, when RA+QA+SOD was delivered in 10% FBS medium, there was a significant increase in the viability as compared against controls or against the same treatment but without SOD. This may suggest that the proven mitogenic effect of a high concentration of FBS in addition to the observed proliferative effect of SOD, nullify the joint effect of RA and QA.

Chapter 4

These initial results suggest that $O_2^{\cdot-}$ may directly or indirectly affect the growth and/or differentiation of SH-SY5Y cells. To test this hypothesis, the degree of differentiation (or acquisition of a neuronal phenotype) was evaluated by counting the number of neuritic processes in cells treated with 1% and 10% FBS medium containing RA plus QA, with and without SOD.

4.3.1.3 SOD reduces QA and RA-induced neuritogenesis.

Three independent experiments were performed to evaluate the cellular morphology under the aforementioned conditions. The neurite to soma ratio is presented (Figure 12A) along with a set of representative micrographs showing the morphological changes and lack of signs of cellular death or damage of treated SH-SY5Y cells (Figure 12B).

Unlike controls, cells treated with 10 μ M RA in 1% FBS medium showed a 150% increase in the neurite/soma ratio (Figure 12A, 1st vs. 3rd bar). However, cells treated with RA in 1% FBS medium containing SOD showed only a 50% increase in the neurite/soma ratio when compared to control cells (Figure 12A, 1st and 4th bar). When the same drugs were delivered in 10% FBS medium, no differences were found in the neurite/soma ratio between treated and untreated controls (Figure 12A, 1st and 5th /6th bar). Observations of SH-SY5Y morphology 72 h after treatment with 10 μ M RA in 1% FBS medium indicated that these cells started to acquire a neuronal phenotype with extensive neurite networks (Figure 12B 3rd and previously shown in Figure 7, micrograph C and F).

Similarly, in cells treated with 50 nM QA delivered in 1% FBS, there was an increase in the neurite/soma ratio of approximately 150% as compared to control cells (Figure 12A, 1st and 7th bar). Furthermore, the changes in morphology caused by QA were more pronounced when the treatment was delivered in medium containing 1% FBS rather than in 10% FBS medium (Figure 12B, 7th and 9th micrograph). Whereas cells treated with QA (50 nM) did not exhibit any morphological signs of damage, they did suffer other morphological changes such as rounding of the cells bodies, increased number of neurites and phase-bright cell bodies. This morphology was very similar to the phenotype of cells treated with 10 μ M RA which is associated with cell differentiation (Figure 12B, 3rd and 7th micrograph).

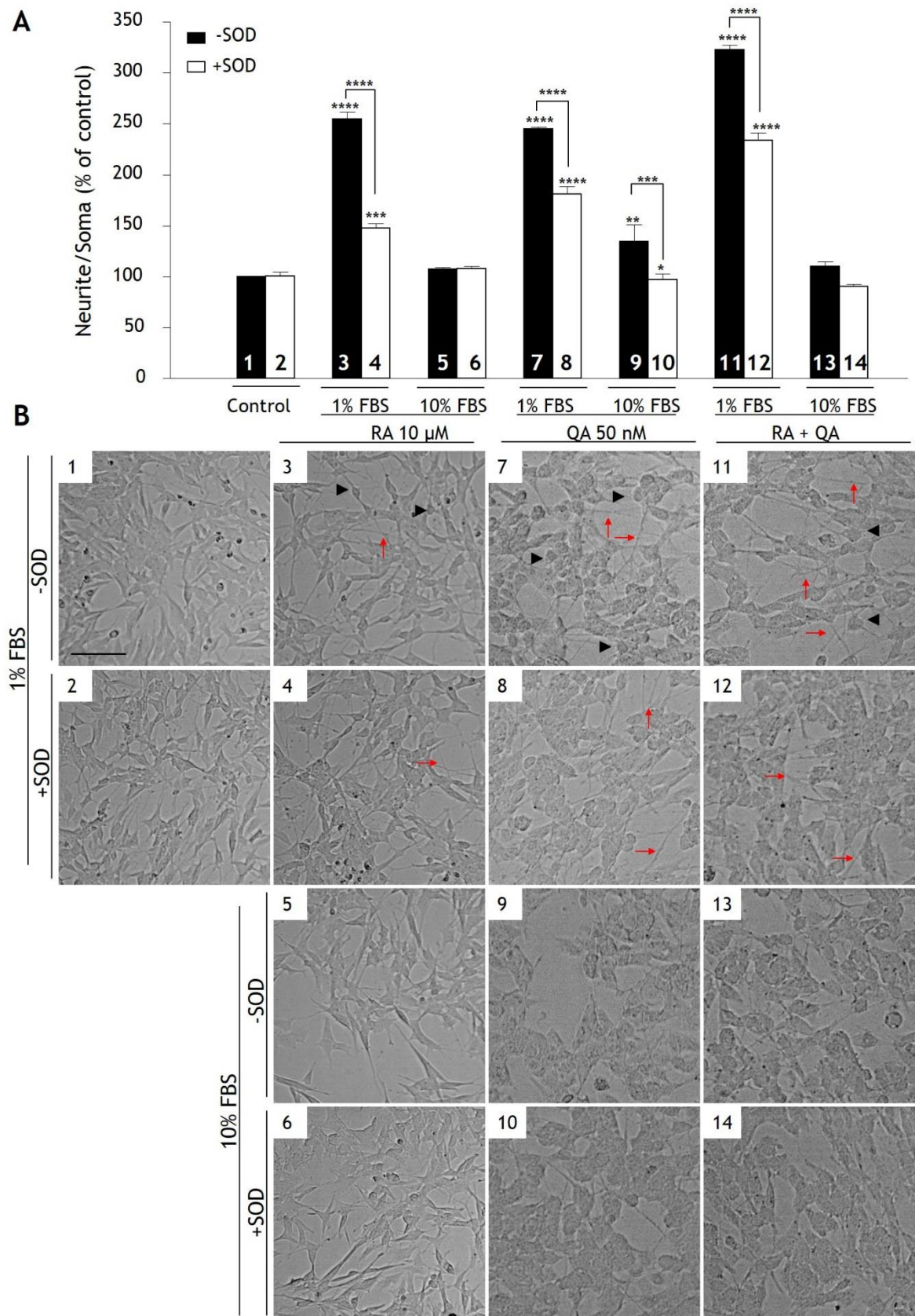


Figure 12 Inhibitory effect of SOD on QA and RA-induced neuritogenesis. **A)** Histogram indicating the neurite/soma ratio of SH-SY5Y cells counted from micrographs (by triplicate) taken 72 h after treatments with RA (10 μ M) and/or QA (50 nM) in medium (1% FBS or 10% FBS) supplemented with SOD (300 U/ml, white bars). Control wells received 1% FBS medium exchanges only. **B)** Bright-field micrographs corresponding to the aforementioned treatments (neurite, arrow; round soma, arrowhead). Results are expressed as percentage of the control. Bars represent mean \pm SEM. * p <0.05, ** p <.0072, *** p <.0006, **** p <0.0001 Two-way ANOVA followed by Tukey's test. $n=3$. Scale bar = 50 μ m

Chapter 4

Under these conditions, the addition of SOD reduced the neurite/soma ratio by 1/3, therefore now at 100% above control levels (Figure 12A, 1st and 8th bar). However, when cells were treated with QA, in 10% FBS medium, there was only a 50% increase in the neurite/soma ratio when compared against controls (Figure 12A, 1st vs 9th bar). This is in contrast to what was observed for RA, delivered in 10% FBS, where no changes in the neurite ratio were found. The increase in the neurite ratio after QA, in 10% FBS medium, was completely eliminated by the addition of SOD (Figure 12A, 10th bar).

Co-treatment with QA and RA in 1% FBS medium further increased the neurite/soma ratio (Figure 12A, 1st vs. 11th bar) regardless of the presence of SOD (Figure 12A, 12th bar). However when the same drugs were delivered in 10% FBS medium, there were no changes in the neurite/soma ratio (Figure 12A, 1st vs 13th and 14th bar). In contrast, in cultures where serum was reduced at the time of addition of RA QA, a homogeneous population of cells with neuronal morphology was obtained. In these cultures, cells showed rounded, phase-bright bodies and a profuse neuritic arborisation forming extensive networks over the culture dish surface (Figure 12B).

A correlation analysis between cell viability and the number of neurites was performed using the results presented in Figure 11 and Figure 12, respectively. However, no significant correlation between these two variables was found ($p=0.1855$). A possibility is that the time point selected (72 h) was too early for either proliferation to be completely halted or for terminal differentiation to occur. Another possibility is that, under certain circumstances, an increase in the number of viable cells results in an increase in the number of neurites and vice versa; an ending of proliferation can lead to an increase in the number of neurites.

To gain a better insight into the molecular basis sustaining the morphological changes caused by QA, the expression of β 3-tubulin and DCX was evaluated. Additionally MK-801 was used in order to ascertain whether blocking NMDAR activation affects QA-induced differentiation. Taking into account that a low FBS concentration is needed for the induction of differentiation, after 3DIV, cells were treated with RA, QA, RA+QA in 1% FBS medium. In accordance with previous experiments (Figure 8), 72 h after RA treatment there was an increase

Chapter 4

in the expression of β 3-tubulin of approximately 140% above control levels (Figure 13A). However, at this time point, RA did not downregulate the expression of DCX (Figure 13C). In cells treated for 7 days with RA, the expression of β 3-tubulin continued to be above control levels but only by 40%, at this time point, RA significantly decreased the expression of DCX.

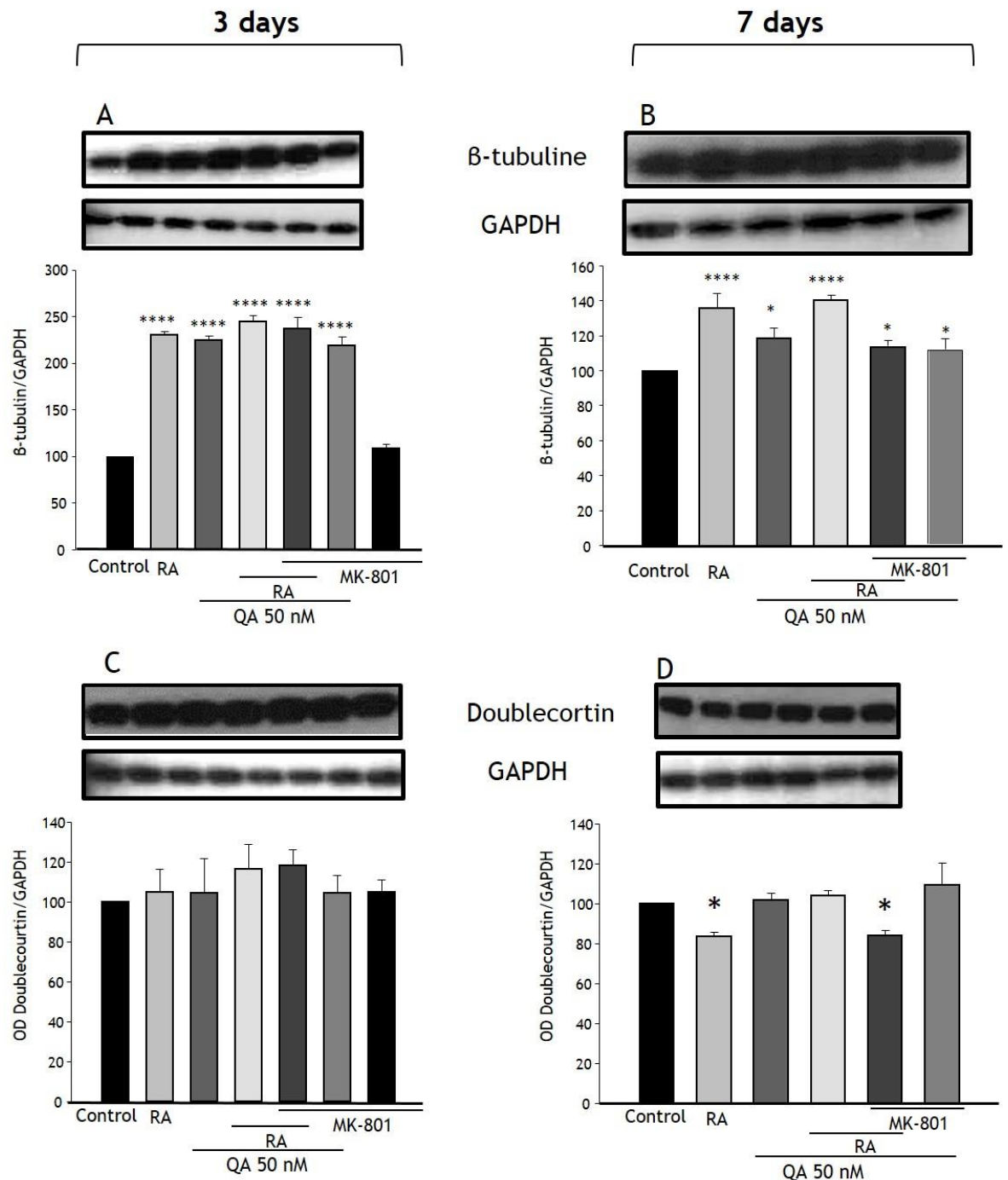


Figure 13 QA increases the levels of β 3-tubulin without decreasing those of doublecortin. Western immunoblotting and quantification analyses of β 3-tubulin (A, B), Doublecortin (C, D) after 3 and 7 day treatments with QA (50 nM), RA (10 μ M), MK-801 (400 nM) in 1% FBS medium. Bars represent mean \pm SEM in arbitrary units of optical density (OD). GAPDH was used as a house-keeping protein and results were normalised to the control. * p <0.05, ** p <0.005, **** p <0.0001. One-way ANOVA followed by Dunnett's test. $n=4$.

Chapter 4

The addition of MK-801 had no effect on QA-induced neuritogenesis or DCX expression at any of the time points evaluated.

Similarly, treatment with QA for 72 h and 7 days caused a significant increase in the expression of β 3-tubulin, comparable to the levels obtained with RA. However, the expression of DCX was not affected at either of the time points evaluated (Figure 13). There are several possibilities as to why QA did not reduce proliferation (viability and DCX): a) in SH-SY5Y cells, the expression of β 3-tubulin could perhaps be independent of the cell cycle phase, which would allow QA to induce neuritogenesis without leading to terminal differentiation, b) There are different subpopulations within the SH-SY5Y cell line with different responsiveness to QA-induced differentiation.

Whereas RA alone reduced the expression of DCX, the co-application of RA+QA did not reduce the expression of DCX at either 72 h or 7 days. A possibility is that the process by which QA induces neuritogenesis interferes with RA-induced differentiation or alternatively QA promotes cell growth in a specific SH-SY5Y subpopulation.

4.3.1.4 QA causes an early and transient increase in the level of ROS

Given that the presence of SOD caused an increase in the viability for all of the conditions tested (except for RA+QA in 1% FBS medium) as well as a decrease in the neurite/soma ratio for all of the tested conditions, it was decided to further study the involvement of ROS in these processes. To evaluate if QA had an effect on the level of ROS, the DHE assay was used (see chapter 2.4). For this set of experiments, cells were treated with two concentrations of QA (50 nM and 300 nM) alone or in combination with 10 μ M RA. All treatments were delivered in 1% FBS with and without 300 U/ml of SOD.

For all experiments the xanthine (Xa)/xanthine oxidase (XO) system was used as a positive control of $O_2^{\cdot-}$ production as previously described by Schuck (2007a). Briefly, 2 hours before the DHE assay was started, the medium was changed with one containing 100 μ M Xa. Cells were left in this medium for 1 hour before adding 0.05 U/ml of XO to the cells. Cells were incubated for an additional hour after which the ethidium fluorescence was analysed using a microplate reader.

Chapter 4

Xa/XO treatment significantly increased ROS production in all of the experiments (Figure 14A, C, D; 13th bar). The addition of SOD effectively decreased the levels of O₂⁻ produced by Xa/XO (Figure 14 A, C, D; 14th bar)

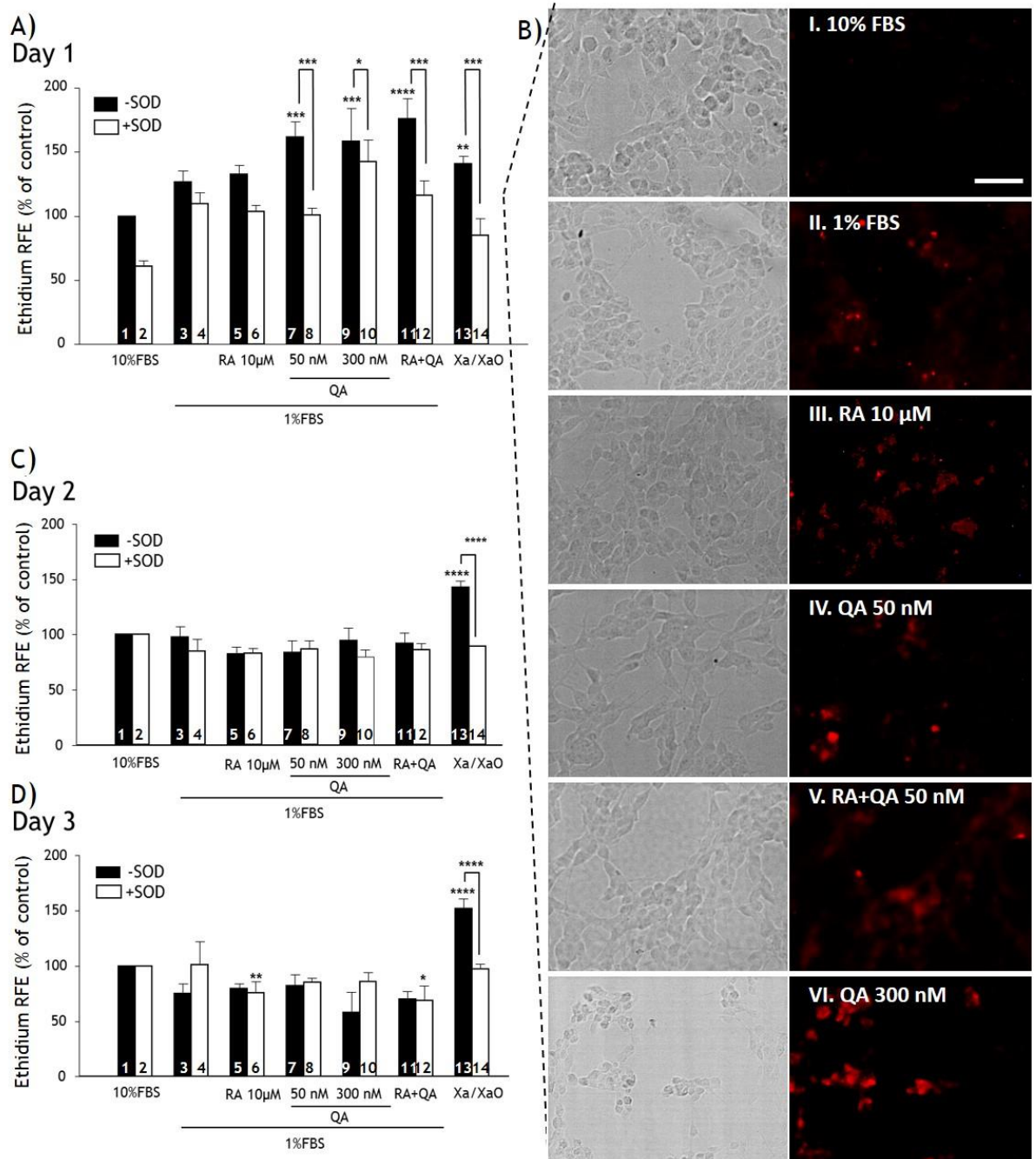


Figure 14- QA promotes the early formation of ROS in SH-SY5Y cells. Time course evaluation of ROS production in undifferentiated SH-SY5Y cells measured by ethidium fluorescence on a micro-plate reader 24 (A), 48 (C) and 72 h (D) after treatment with QA (50 or 300 nM) and/or RA (10 μM) with and without SOD (300 U/ml), Control wells received medium exchanges only. Xanthine (50 μM) Xanthine oxidase (0.05 U/ml) served as a positive control. b) DHE fluorescence and corresponding bright field micrographs of SH-SY5Y cultures photographed 24 h after incubation with QA and/or RA. Results are expressed as percentage of control. Bar graphs represent mean ± SEM. **p*<0.05, ***p*<.0072, ****p*<.0006, *****p*<.00001. Two-way ANOVA followed by Tukey's test, n=5(A), n=8(C), n=6 (D). Scale bar = 50 μm.

Chapter 4

24 h after QA treatment, there was a significant increase in the levels of ROS when compared to control cells (Figure 14A, 1st vs 7th column). This effect can also be observed in the corresponding micrographs as bright red fluorescence in the nucleus of the cells (Figure 14B). The increase in ROS was not so clearly reflected in the micrographs for the 10 μ M RA in 1% FBS treatments, yet when the experiments were performed using a micro-plate reader, a peak of ROS was observed at 24 hours for both conditions. No significant changes in the levels of ROS were found 48 or 72 h after treatment (Figure 14C, D).

Co-applying SOD with RA and QA, alone or in combination, significantly decreased the levels of ROS 24 h after treatment. This effect was more pronounced in cells treated with 50 nM QA than in those treated with 300 nM QA, which indicates that small fluctuations in the concentration of QA had a big impact on the oxidant state of the cell. When cells were treated with 300 nM QA, SOD was unable to significantly decrease the concentration of ROS.

A significant ($p=0.0041$) positive correlation ($r=0.6845$) was found between the number of neurites and the amount of ROS produced 24 h after QA. Conversely, a significant ($p= 0.0062$) negative ($r= -0.4735$) correlation was found between the number of cells and the levels of ROS for all tested conditions, further strengthening the prospective role of ROS in the regulation of proliferation and neuritogenesis in SH-SY5Y cells.

4.3.1.5 NMDA does not affect the survival or neuritogenesis of SH-SY5Y cells.

The effect of NMDA on differentiated and undifferentiated SH-SY5Y cells was studied in order to establish whether there were similarities as to the effect of QA on the cultures. The initial hypothesis was that if NMDA could elicit the same cellular response as QA treatment, then perhaps QA could be acting on the NMDAR. SH-SY5Y cells were grown for 72 h in 10% FBS after which they were treated with different concentrations of NMDA (50 μ M, 100 μ M, 500 μ M, 1mM, 2mM, 5mM, 10 mM,) delivered in 10% FBS medium. Alternatively cultures were differentiated for 7 days with 10 μ M RA before treating them with NMDA (50 μ M, 100 μ M, 500 μ M, 1mM, 2mM, 5mM, 10 mM,) in 1% FBS medium. For all

Chapter 4

experiments, the viability and morphology were analysed on the 3rd day after treatment.

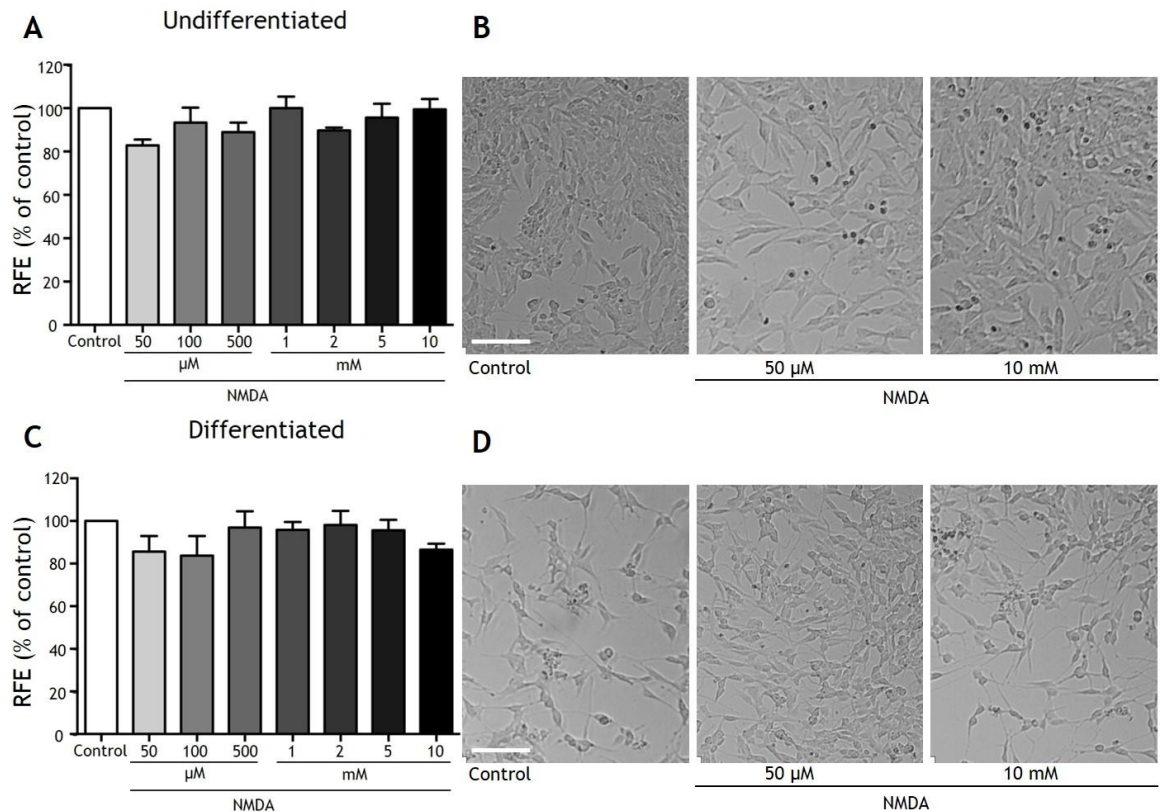


Figure 15- NMDA does not induce cell death in SH-SY5Y cells. A, B) Histogram and micrographs showing the viability and morphology of undifferentiated control cells (untreated) and cells treated with the indicated concentrations of NMDA for 72 h in 10% FBS medium. C, D) Histogram and micrograph showing the viability and morphology of cells previously differentiated with RA for 7 days and then treated with fresh 1% FBS medium containing the indicated concentrations of NMDA for 72 h. Results are expressed as a percentage of the RFE with respect to control. Bars represent mean \pm SEM. One-way ANOVA followed by Dunnett's test, no significant differences were found. n=3 (A). n=4 (C). Scale bar= 100 μ m

In these experiments, NMDA did not cause a significant decrease in cell viability (Figure 10 and Figure 15). However, in some experiments there seemed to be a slight decrease in the viability of cells (approximately 20%). It was expected that NMDA would be a more potent inducer of cell death than QA since QA is a weak NMDAR agonist.

There were no evident morphological signs of damage in cells treated with NMDA for three days. However, in all of the micrographs of undifferentiated cells treated with NMDA, some dead cells can be observed (dark round bodies) which could represent a small fraction of the cell population that is susceptible to NMDA toxicity (Figure 15B) or, more likely, it represents the normal fraction of

cells that die in growing cultures. These micrographs show that there are fewer cells in the differentiated state when compared to the undifferentiated ones, yet, there were no marked differences in the viability between these two groups (Figure 15). Therefore, the difference in the number of cells is not caused by NMDA treatment but rather by 7 days of RA-induced differentiation which ends proliferation.

4.3.1.6 Kynurenic acid (KA) does not affect cell survival

It has been reported that KA, an NMDA antagonist, reduces the proliferation of certain cancerous cells (Walczak *et al.*, 2012; Walczak *et al.*, 2014). For this reason, and in order to further characterise the lack of toxicity of QA and NMDA as well as the lack of effect of MK-801, undifferentiated cells were treated with different concentrations (1 μM , 10 μM , 100 μM , 500 μM , 1 mM, 5 mM, 10 mM) of KA delivered in 1 and 10% FBS.

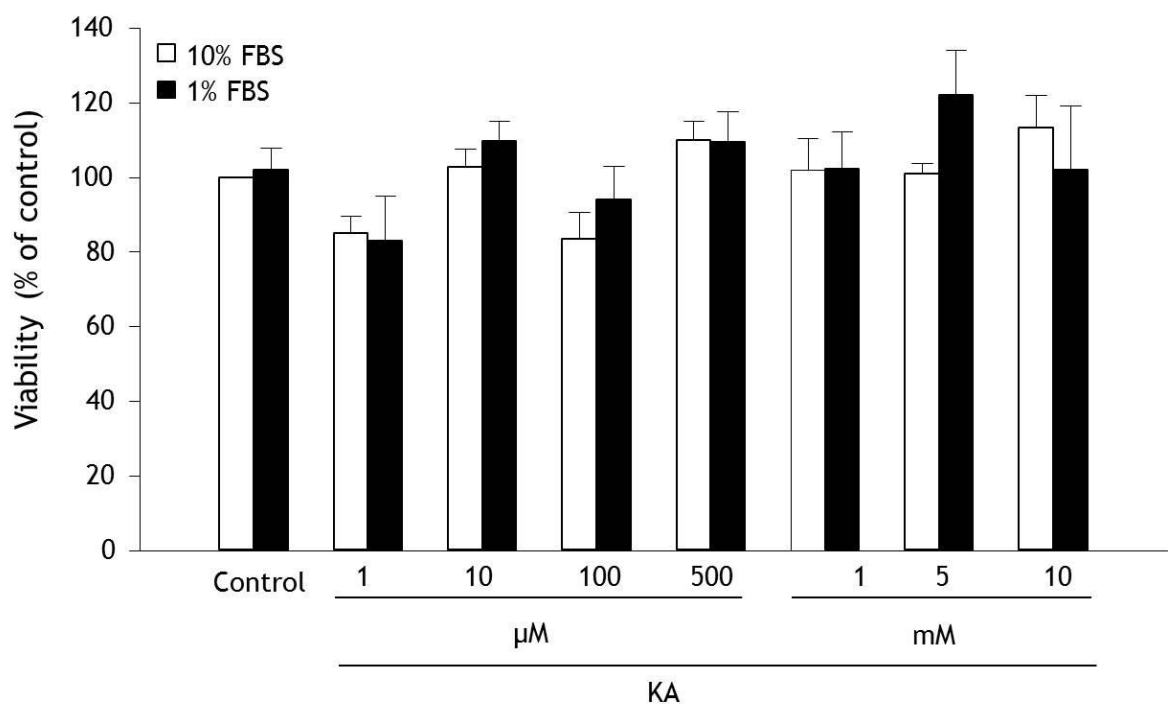


Figure 16 Lack of effect of KA on the survival of SH-SY5Y cells. Undifferentiated cells were treated for 72 h with KA (1 μM -10 mM) in 10% and 1% FBS medium. Results are expressed as percentage of control RFE. Bars represent mean \pm SEM. No statistical differences were found with one-way ANOVA followed by Dunnett's test. n=8.

The assessment of SH-SY5Y treated with KA did not show any significant changes in the viability of cells at either of the tested concentration. Furthermore, when cells were observed under the microscope, there were no evident differences in

any of the parameters of interest (toxicity, neurite number and length) between control and treated cells.

4.3.1.7 GluN1 expression was not detected in SH-SY5Y cells

An antibody against all the isoforms of the GluN1 subunit (predicted to react in human, rats and mice) was used for western blotting, yet no expression could be detected on SH-SY5Y cells at either 72 h or 7 days, regardless of the given differentiation stimuli. The positive control for these experiments was rat brain homogenate and this band could be easily quantified. The lack of NMDAR explains the low toxicity of both NMDA and QA. It also explains why MK-801 and KA had no effect on the cultures.

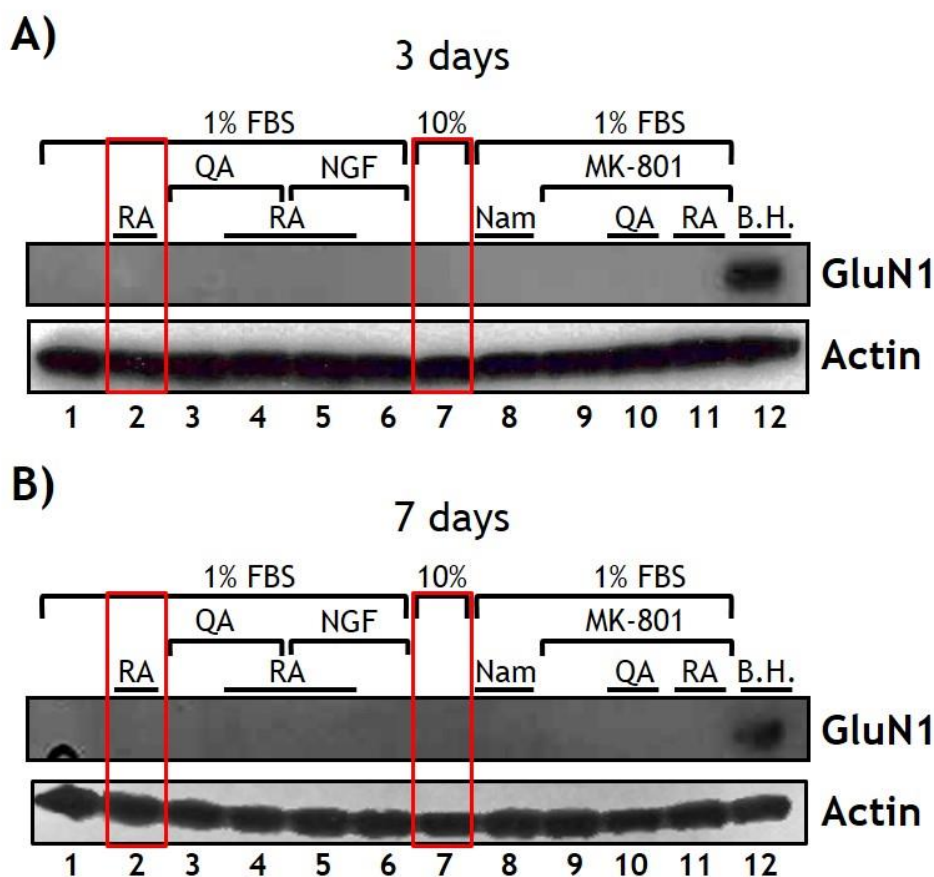


Figure 17. Western blotting showing the lack of GluN 1 expression in SH-SY5Y cells. Cells were incubated for 3 (A) and 7 (B) days in 10% FBS medium (Lane 7, red box) or induced to differentiate with RA (10 μ M) in 1% FBS medium (Lane 2, red box). Cells were also treated with QA (50 nM), RA plus QA, NGF (50 ng/ml), NGF plus RA, nicotinamide (Nam; 100 μ M), MK-801 (400 nM), QA plus MK-801 and RA plus MK-801 for the indicated durations. Rat's whole brain homogenate (B.H.) was used as a positive control. Actin was used as a loading control.

4.3.1.8 Nam increases the number of neurites in a dose-dependent manner

Cells were treated with nicotinamide (Nam; 100 nM, 1 μ M, 100 μ M, 1 mM) in 1% FBS medium for 72 h. After treatment, cells were photographed and the expression of neuronal markers assessed. A total of 4 experiments were used for the western blot analysis.

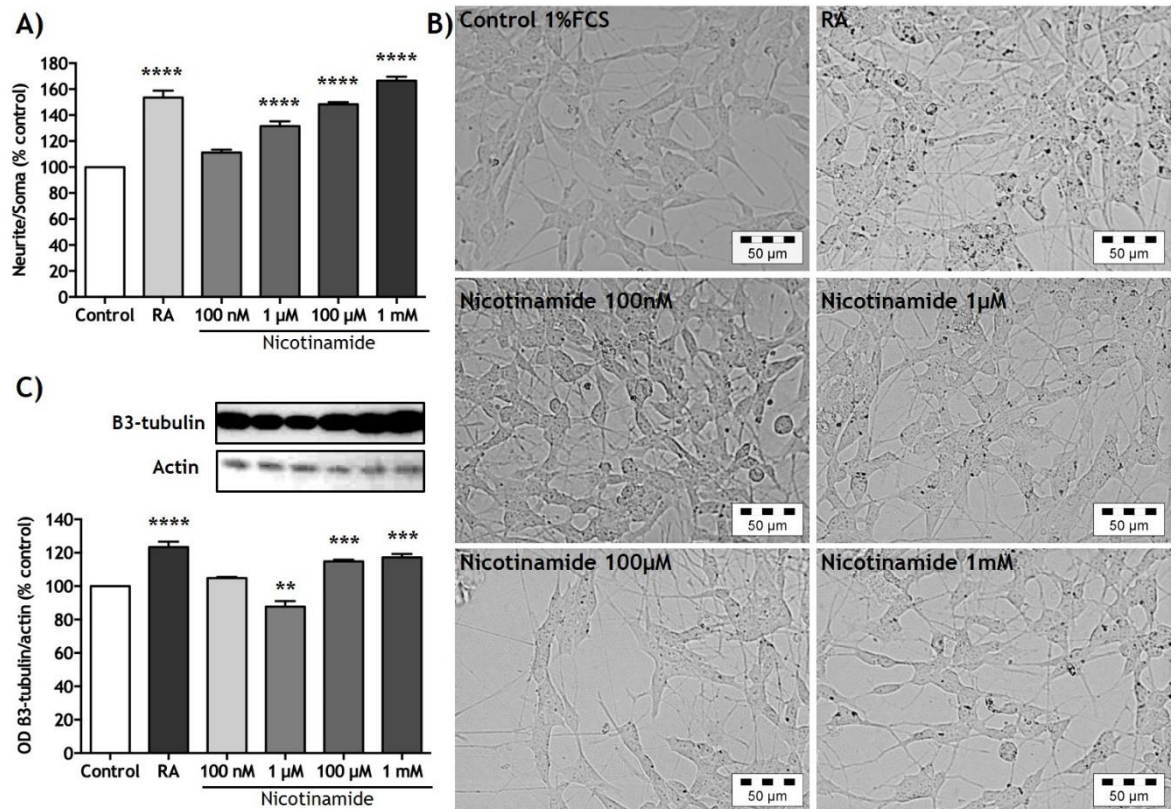


Figure 18. Nicotinamide increases the number of neurites and the expression of β 3-tubulin in SH-SY5Y cells. Cells were treated with nicotinamide (Nam; 100 nM, 1 μ M, 100 μ M and 1 mM) delivered in 1% FBS medium for 72 h, after which the neurite/soma ratio was established (A). Control cells received 1% FBS medium exchanges only. Results are expressed as percentage of the control, bars represent mean \pm SEM. **** $P < 0.0001$ vs. control One-way ANOVA followed by Dunnett's test. $n=3$. B) Corresponding micrographs of the aforementioned treatments. Bar 50 μ m. C) Representative blots and quantification of β 3-tubulin from cells exposed to the same Nam treatment. Bars represent mean \pm SEM in arbitrary units of optical density (OD). Actin was used as a house-keeping protein and results were normalised to the control. ** $p < 0.0038$, *** $p < 0.0008$, **** $p < 0.0001$. One-way ANOVA followed by Dunnett's test. $n=4$.

Nam, another precursor of NAD^+ besides QA, mimicked the neuritogenesis observed after QA treatment as evidenced by an increase in the neurite/soma ratio (Figure 18A). The micrographs of SH-SY5Y cells clearly show that there is an increase in the number of neurites as well as a reduction in the number of cells after Nam treatment (Figure 18B). This morphology is consistent with the phenotype adopted by SH-SY5Y cells after differentiation is induced. Furthermore, 72 h after treatment, Nam increased the overall expression of the

Chapter 4

neuronal marker β 3-tubulin. The neurite outgrowth assay confirmed that Nam promotes neurite extension (Figure 18C).

Based on these results, two Nam concentrations (100 μ M and 1mM) were selected to be delivered in 1% FBS medium and used in the experiments evaluating neurite projection by means of the neurite outgrowth kit. A total of 6 samples belonging to 3 different experiments were used for this purpose (section 4.3.1.9, Figure 19C).

4.3.1.9 Neurite Outgrowth assay and DPI inhibition of neuritogenesis

The neurite/soma ratio method, previously used as an indicator of cell differentiation, tends to underestimate the total content of neurites present in culture as it only takes into account the number of neurites that exceed a given length and ignores the differences that may exist in networks with a different architecture. For example, branched neurites with several branch points and neurite bifurcations tend to be severely underestimated. Conversely, the neurite/soma ratio tends to overestimate the neurite extension of cells in which elongation, rather than neuritogenesis, occurs. To overcome this limitation, it was decided to use a neurite outgrowth assay-kit that effectively quantifies the total content of neurite mass, as previously described in the methods' section (section 2.3).

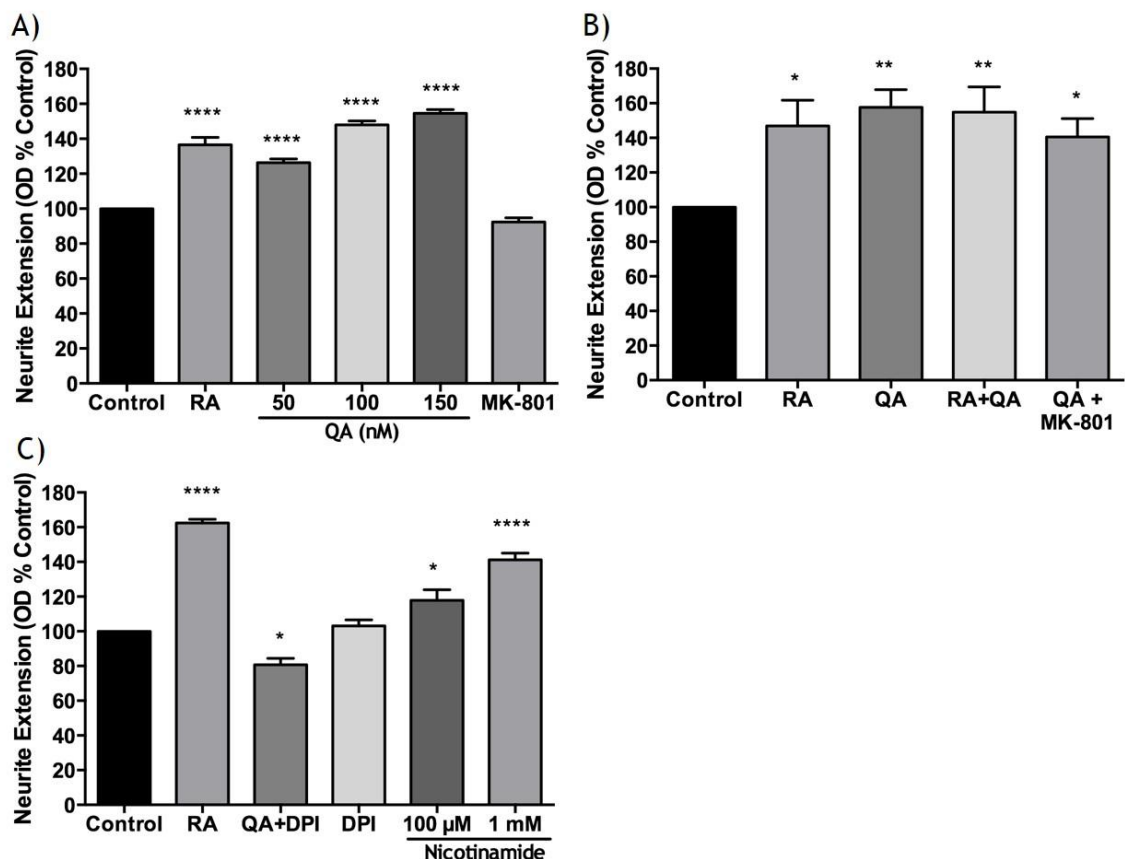


Figure 19. Inhibitory effect of DPI (but not MK-801) on QA-induced neuritogenesis. The neurite outgrowth assay was performed 72 h after treating the SH-SY5Y cells with: A) RA (10 μM), QA (50, 100 and 150 nM), and MK-801 (400 nM); B) RA+QA (50nM), and QA (50nM) + Mk-801 (400nM); C) RA, QA (50nM), QA (150nM) + DPI (1 μM) and nicotinamide (Nam; 100 μM and 1 mM). All drugs were delivered in 1% FBS medium, thus, sham controls were also switched 1% FBS medium. Results are expressed as percentage of controls. Bars represent mean ± SEM in arbitrary units of optical density (OD). *P < 0.022, **P < 0.004, ****P < 0.0001 One-way ANOVA followed by Dunnett's test. n=3 for A, B and C.

Chapter 4

Similarly, in order to corroborate that the mechanism of action of QA is not through NMDAR activation, cells were treated with 50 nM QA alone or in combination with 400 nM MK-801, delivered in 1% FBS medium. The untreated control for this set of experiments received 1% FBS medium exchanges only and the positive control of differentiation selected was 10 μ M RA.

In accordance with previous experiments, treatment with RA alone or in combination with QA caused an increase in neurite mass. Treatment with MK-801 on its own did not have a negative effect on cells. Interestingly, the degree of neurite extension never exceeded 50% above control levels (Figure 19A). In contrast to what had been previously shown to occur using the neurite/soma ratio, the degree of neurite extension induced by QA alone (or in combination with RA) was not of a higher magnitude than that of RA alone (Figure 19A and Figure 12A). Similarly, the estimate of neuritogenesis obtained by Western blotting quantification of β 3-tubulin (Figure 13) was much higher than the one obtained using the neurite outgrowth assay. This could be partly due to the fact that the Western blot analysis yields the total amount of β 3-tubulin present (in both soma and neurites) whereas the neurite outgrowth assay quantifies only the amount of the neuritic fraction.

Figure 19B presents the dose-dependent increase in neurite mass after QA treatment as well as the lack of effect of MK-801 on QA-induced neuritogenesis. The effect of DPI (a NOX) on QA-induced neuritogenesis was assessed. DPI treatment on its own had no significant effect on the cells but in contrast to NMDAR antagonists, DPI significantly reduced the neurite extension of cells treated with QA (Figure 19C). In accordance with previous experiments, nicotinamide (100 μ M and 1 mM) caused a significant increase in neurite mass.

4.3.1.10 QA increases NRF2 expression

Preliminary results showed that the expression of the NRF2 was markedly enhanced 12 h after treatment with RA (10 μ M). The increase in the expression of NRF2 using different doses of QA (50, 100, 150 nM) seemed to be dose-dependent. The expression of NRF2 did not seem to be affected by NGF (50 ng/ml) treatment (Figure 20).

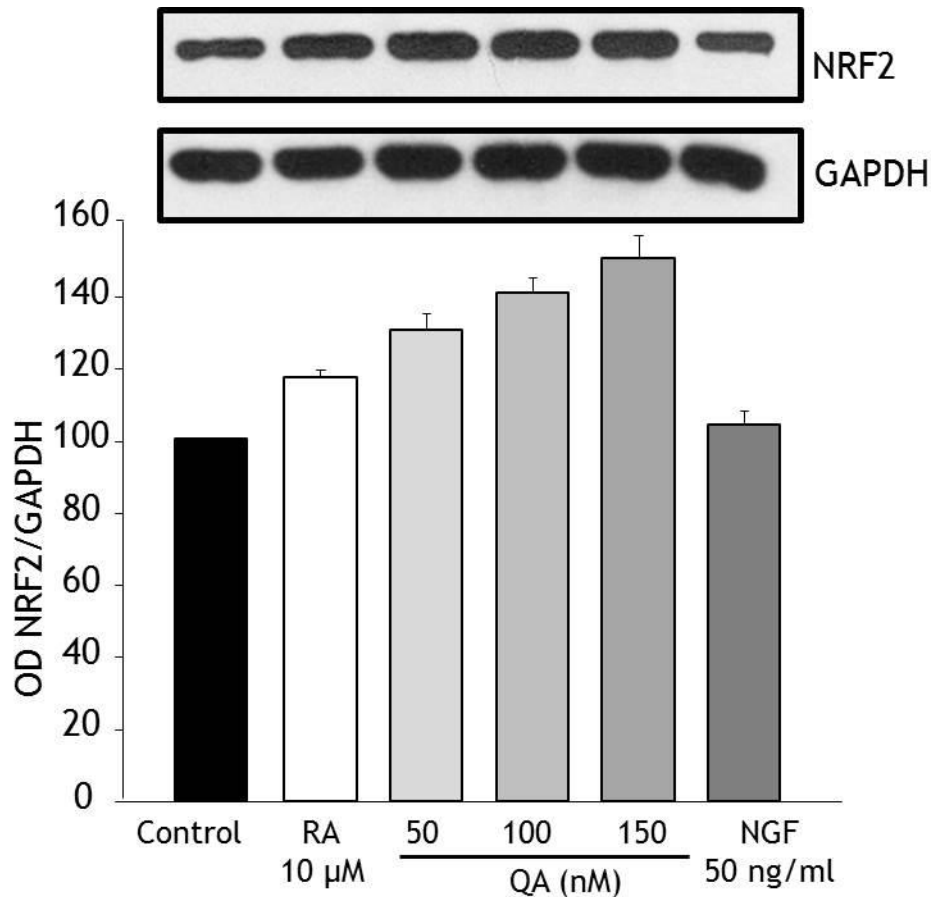


Figure 20 QA increases the expression of NRF2 in SH-SY5Y cells. Western blot and quantification analysis of undifferentiated control cells (untreated) and cells treated with QA (50, 100, 150 nM), RA (10 μM) or NGF (50 ng/ml) for 12 hours. Controls received 1% FBS medium exchanges only. Bars represent mean \pm SD (n=2) in arbitrary units of optical density (OD). GAPDH was used as a house-keeping protein and results were normalised to the control.

The number of experiments should have been increased in order to confirm that the results are significant. However, for data with a normal distribution, approximately 95% of the samples will have values within 2 standard deviations of the mean. Therefore, given the small dispersion from the mean (standard deviation) of the data presented, it is expected that future experiments will fall within similar values, not majorly changing the interpretation of these results.

4.3.2 Effect of 3-HAA on SH-SY5Y survival and neuritogenesis

4.3.2.1 3-HAA induces cell death in SH-SY5Y cells

In order to establish if 3-HAA had a detrimental effect on cell survival, undifferentiated SH-SY5Y cells were fed with 10% FBS medium (control) or treated with increasing concentrations of 3-HAA (1 μ M, 10 μ M, 50 μ M, 100 μ M, 500 μ M, 1 mM, 10 mM) for 48 h or and 72 h, after which the viability was assessed by FDA and a dose-response curve was plotted (Figure 21A, B).

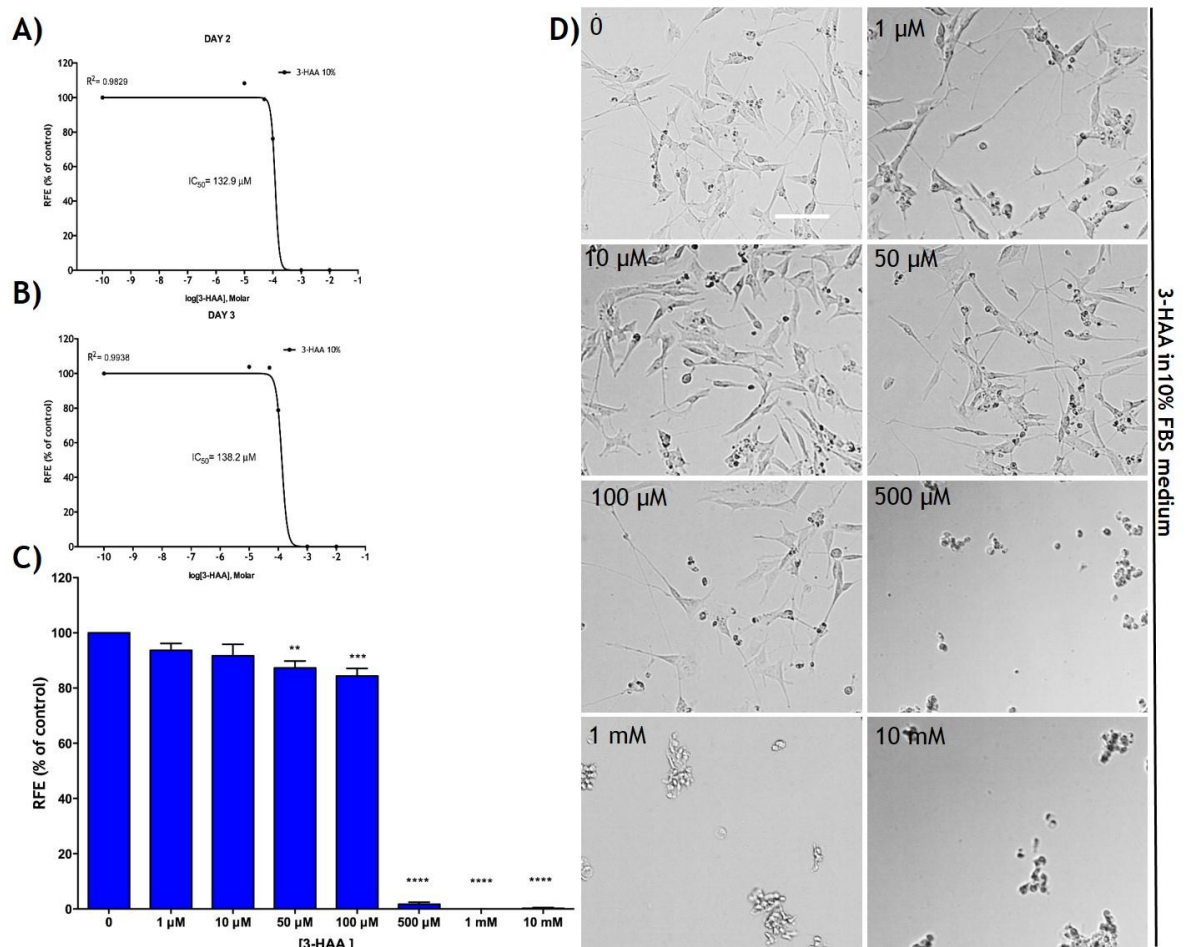


Figure 21. Cellular death is induced by 3-HAA in SH-SY5Y cells. A Fitted Log(inhibitor) vs normalised response curve is displayed for cells incubated for either 48 h (A) or 72 h (B) with 3-HAA delivered in 10% FBS after which the toxicity was evaluated by FDA. IC_{50} values were obtained by non-linear regression analysis (Dose-response inhibition; Prism Graphpad v. 6.0f. The average IC_{50} are listed in each graph and are summarized in Table 4. For graph (C) results are expressed as percentage of control RFE. Bars represent mean \pm SEM for 3 different experiments ($n=3$). ** $p < 0.004$, *** $p < 0.0005$, **** $p < 0.0001$. One-way ANOVA followed by Dunnett's test. D) 72 h after treatment cells were photographed without fixing using a phase-contrast microscope (Bar=100 μ M).

No signs of cellular death could be observed 24 h after treatment with 3-HAA. However 48 h after treatment, 3-HAA in 10% FBS caused a dose-dependent decrease in the viability of cells. It became immediately clear that 3-HAA

Chapter 4

induced cell death and not neuritogenesis or differentiation, as it had been the case for QA and RA, respectively.

The IC₅₀ value for 3-HAA, delivered in 10 % FBS medium, was calculated by a non-linear regression analysis of the toxicity-concentration curve, obtaining a value of 132.9 ± 15.55 μM and 138.2 ± 16.74 μM after 48 h and 72 h of exposure, respectively (Table 4). No significant changes in the IC₅₀ values were found between cells exposed for 48 h and those exposed for 72 h. Thus, the latter time point was selected to assess the viability and the IC₅₀ values in subsequent experiments.

SOD has been shown to protect against the toxic effects caused by ROS production in several models, therefore a first approximation was conducted to determine the mechanism through which 3-HAA induced toxicity: its aim was to co-apply SOD and evaluate whether it exerted any protection. Surprisingly, the addition of SOD caused a shift in the IC₅₀ value for 3-HAA delivered in 10% FBS medium. The IC₅₀ value for 3-HAA + SOD, delivered in 10 % FBS, decreased to 81.87 ± 15.55 μM after 72 h exposure, which suggested that the combined treatment with 3-HAA and SOD was more toxic to the cells (Table 4). This can be clearly observed in Figure 25, in both the histogram graphs for day 2 and 3 (A, B) and in the presented micrographs (C).

1 Treatment	3-HAA 10%		3-HAA 10% SOD		3-HAA 1%		3-HAA 1% SOD			
DAY	2	3	≠ p ^{2,3} =0.0001	2	3	≠ p ^{2,3} =0.0001	2	3		
IC ₅₀ (μM)	132.9	= 138.2		78.83	= 81.87		142.9	= 150.1	66.65	= 69.01
R ²	0.9829	0.9938		0.9859	0.9882		0.9874	0.9951	0.9519	0.9748

Table 4. SOD causes a shift in the IC₅₀ values for 3-HAA treatment. A one-way ANOVA followed by Sidak's test was used to compare the difference of the IC₅₀ values between 48 h and 72 h exposure to 3-HAA. Pooled data from dose-response curves, generated from the different responses to 3-HAA in the presence of 1% and 10% FBS with and without SOD. Shown in Figure 22. SOD shifted the 3-HAA concentration–response curves to the left with and with highly similar slopes.

Similarly, an assessment of cell viability was performed 48 h and 72 h after exposure to 3-HAA ± SOD but this time treatments were delivered in 1% FBS medium. The concentration of FBS did not have a significant effect on the

Chapter 4

toxicity of 3-HAA. The IC_{50} for 3-HAA delivered in 1% had a value of 150.1 ± 17.7 (Table 4).

Interestingly, the co-treatments with 3-HAA and SOD delivered in 1% FBS medium, increased the toxicity caused by all previous 3-HAA concentrations delivered in 1% FBS. The addition of SOD caused a significant reduction ($p < 0.0001$) of the IC_{50} ($69.01 \pm 4.33 \mu\text{M}$) value for the 3-day exposure to 3-HAA in 1% FBS medium (Table 4).

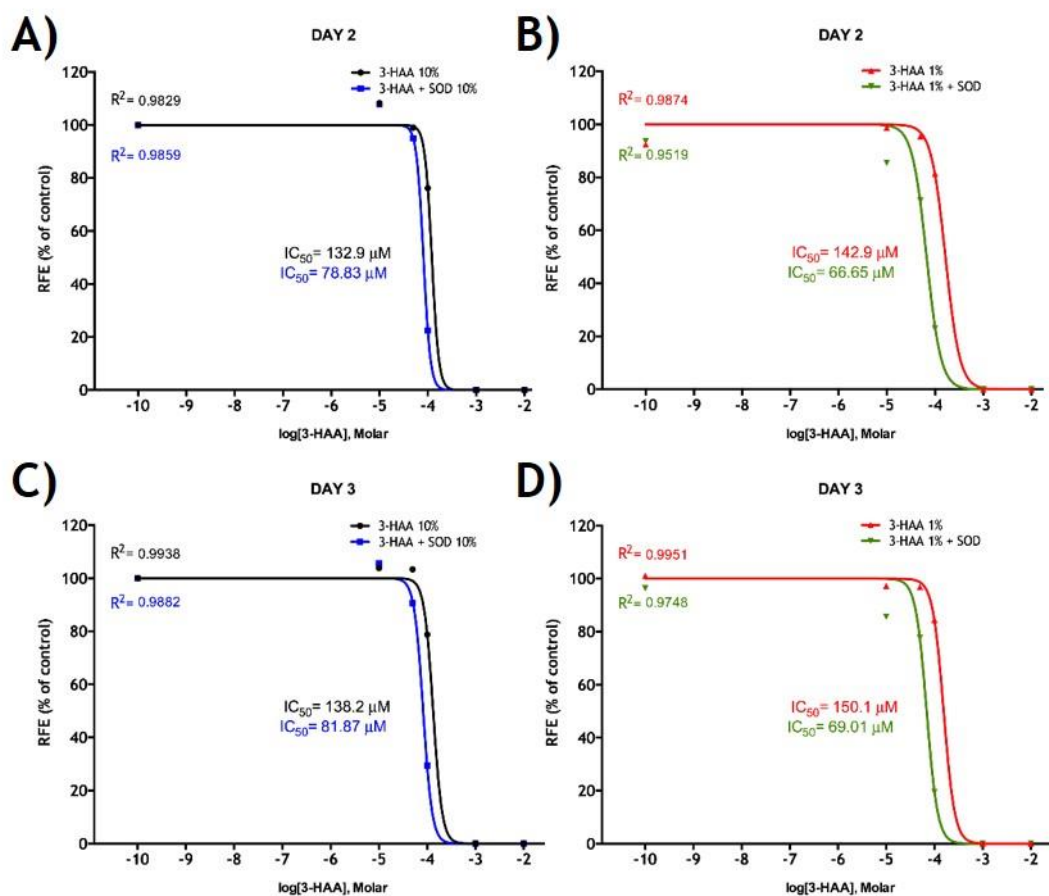


Figure 22 The IC_{50} of 3-HAA is reduced when co-applied with SOD. Effect of single 3-HAA treatment delivered in 1 and 10% FBS medium supplemented with SOD (300 U/ml) on cell viability after 48 h and 72 exposure. A Fitted Log(inhibitor) vs normalised response curve is displayed for cells incubated for either 48 h (A, B) or 72 h (C, D) with 3-HAA delivered in 10%(A, C) and 1% (B, D) FBS medium supplemented with SOD (Solid Blue and Green lines) after which the toxicity was evaluated by FDA. IC_{50} values were obtained by non-linear regression analysis (Dose-response inhibition; Prism Graphpad v. 6.0f. The average IC_{50} are listed in each graph and are summarized in Table 4.

Observations of SH-SY5Y morphology after 72h exposure to 3-HAA provided confirmation of the viability assay findings. A clear relationship could be observed between the concentration of 3-HAA and the reduction in the number of cells per optic field. The appearance of opaque spots in the micrographs are an indication that dead cells are present in the cultures (Figure 21D). The lowest

Chapter 4

3-HAA dose to cause a significant decrease in the viability was 50 μM (Figure 21C). However, morphologically, signs of damage were more obvious when cells were treated with 100 μM . At this concentration, there were more detached cells as well as cellular debris. The following concentration used (500 μM) completely obliterated the cell population and only cellular debris could be observed on the plates (Figure 21D).

4.3.2.2 SOD increases the levels of ROS in cells treated with 3-HAA

To better understand the mechanism through which SOD (300 U/ml) interacts with 3-HAA (10 μM -100 μM) to generate damage, the level of ROS in cultures was studied using the DHE assay. The presence of ROS was determined in cells treated with 3-HAA delivered in 1% FBS (Figure 24) and 10% FBS (Figure 23) containing medium.

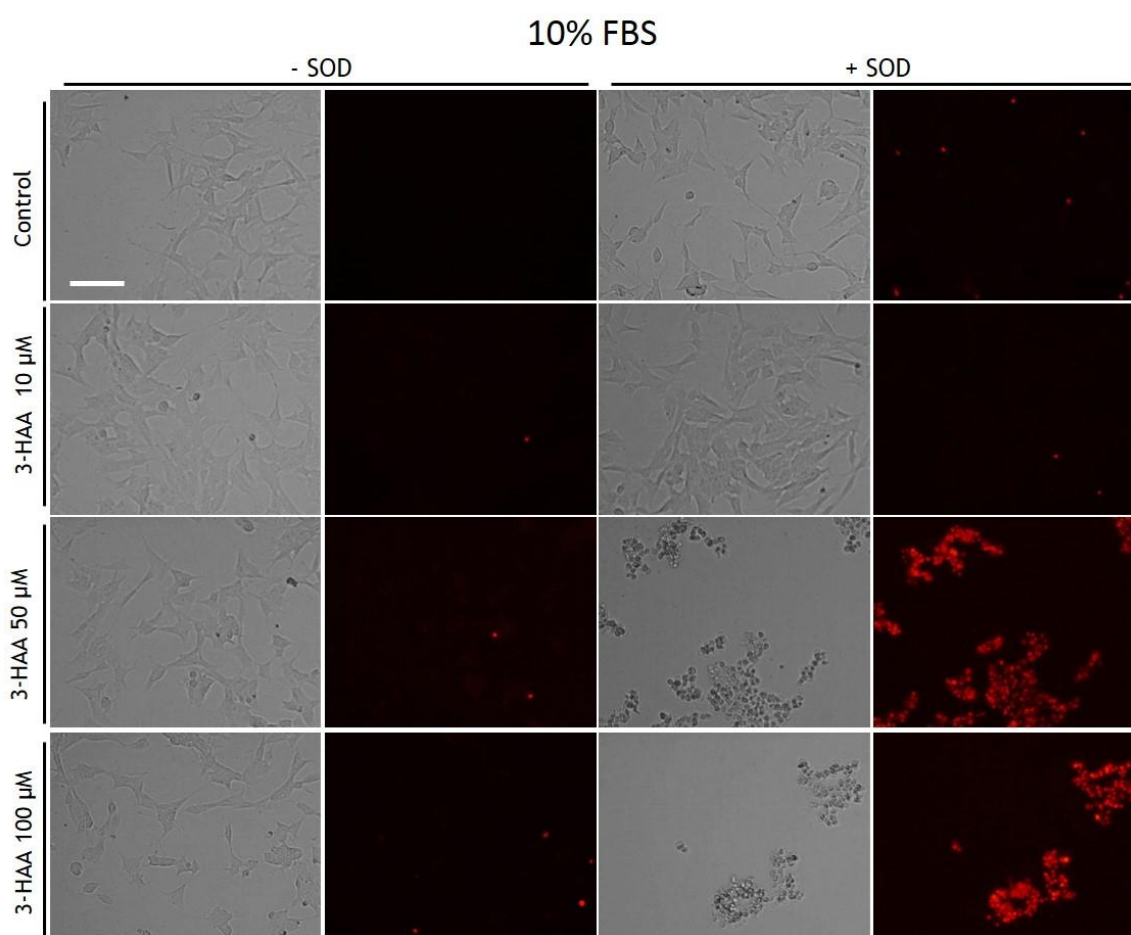


Figure 23. SOD exacerbates the production of ROS induced by single 3-HAA treatment. Evaluation of ROS production in undifferentiated SH-SY5Y cells assessed by ethidium fluorescence 24 h after treatment with 3-HAA (10 μM , 50 μM and 100 μM) in 10% FBS medium supplemented with SOD (300 U/ml). Control wells received 10% FBS medium exchanges only. DHE fluorescence and corresponding bright field micrographs taken 24 h after incubation with the aforementioned treatments in 10% FBS medium with or without SOD. Scale bar = 100 μm .

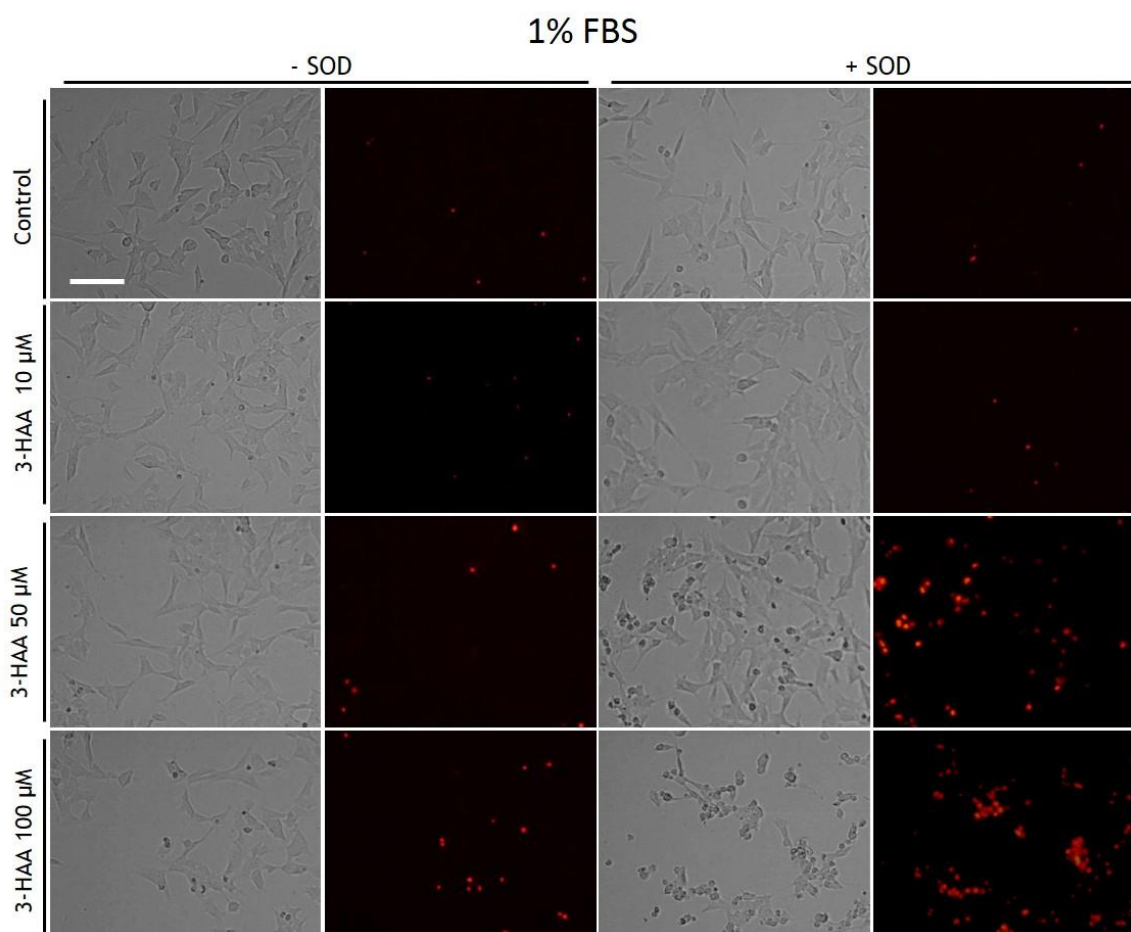


Figure 24. SOD exacerbates the production of ROS induced by single 3-HAA treatment
 Evaluation of ROS production in undifferentiated SH-SY5Y cells assessed by ethidium fluorescence 24 h after treatment with 3-HAA (10 μ M, 50 μ M and 100 μ M) in 1% FBS medium supplemented with SOD (300 U/ml). Control wells received 1% FBS medium exchanges only. DHE fluorescence and corresponding bright field micrographs taken 24 h after incubation with the aforementioned treatments in 1% FBS medium with or without SOD. Scale bar = 100 μ m.

3-HAA treatment caused an increase in the levels of ROS (Figure 24). When cells were treated with 3-HAA and 300 U/ml SOD, there was a marked increase in the DHE fluorescence indicating that the production of ROS is exacerbated by co-applying 3-HAA. SOD and 3-HAA increased ROS production in both 1% and 10% FBS medium (Figure 23). These results, however, do not provide evidence as to the identity of the ROS involved but do confirm that there is an increase in the levels of ROS following 3-HAA treatments. This condition was intensified by the addition of SOD.

4.3.2.3 Catalase prevents the death of SH-SY5Y induced by 3-HAA+SOD

Due to the upsurge of cellular death and ROS production when 3-HAA was co-applied with SOD, it was initially expected that 3-HAA could be increasing the levels of $O_2^{\cdot-}$ and that the addition of SOD, by dismutating it, could be increasing

Chapter 4

the levels of H₂O₂. To test this hypothesis, cells were treated on day 0 with 3-HAA (100 µM) alone or in combination with catalase (CAT; 1000U/ml) in either 1% or 10% FBS medium with and without SOD (300 U/ml), obtaining the following combination of treatments:

- 100 µM 3-HAA 10% FBS
- 100 µM 3-HAA+CAT 10% FBS
- 100 µM 3-HAA+SOD 10% FBS
- 100 µM 3-HAA+CAT+SOD 10% FBS
- 100 µM 3-HAA 1% FBS
- 100 µM 3-HAA+CAT 1% FBS
- 100 µM 3-HAA+SOD 1% FBS
- 100 µM 3-HAA+CAT+SOD 1% FBS

Viability was assessed by FDA 48 h and 72 h after treatments and a total of 3 independent experiments were carried out, using fresh solutions prepared each time.

48 h and 72 h exposure to 100 µM 3-HAA in 10% FBS medium caused a ≈20% reduction in the viability when compared to untreated controls which was prevented by CAT only in cells exposed for 48 h but not in those exposed for 72 h. In cells treated with 100 µM 3-HAA+SOD 10% FBS there was a further decrease in the viability (80%) when compared to control cells; the addition of catalase completely averted SOD-induced death (Figure 25A, B).

A similar reduction in cell viability (≈20%) was observed in cells exposed for 48 h and 72 h to 100 µM 3-HAA 1% FBS. Under these conditions, CAT protected cells exposed for 48 h as well as those exposed for 72 h to 3-HAA (Figure 25A, B) which may indicate that whereas the concentration of FBS in the medium does not affect the IC₅₀ of 3-HAA (Table 4), it does affect the mechanism by which cells die.

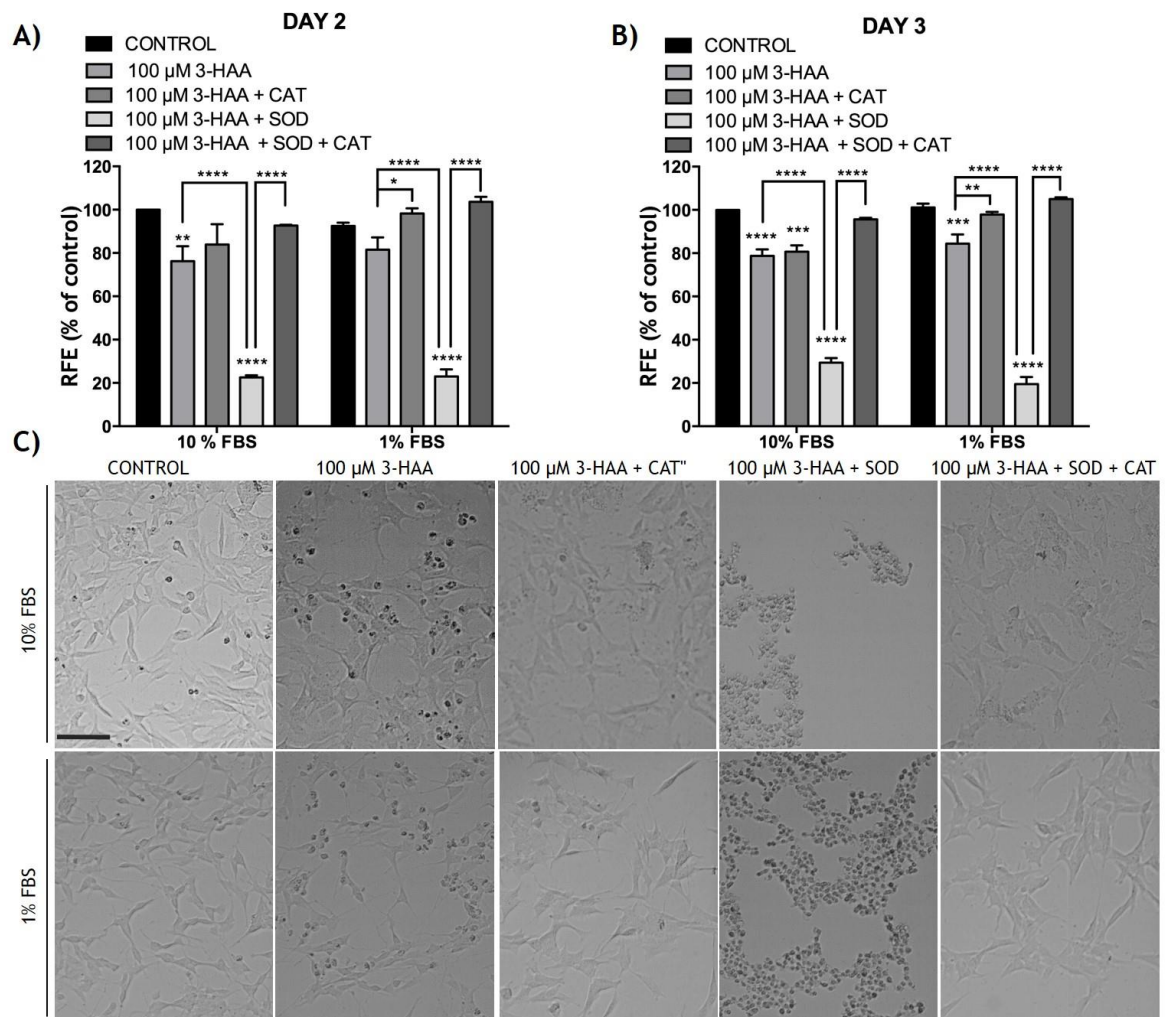


Figure 25. Catalase protects against the exacerbated toxicity of combined treatment with 3-HAA and SOD. Cells were treated for 48 h (A) or 72 h (B) with 3-HAA (100 μM) in 1% and 10% FBS medium supplemented with SOD (300 U/ml) alone or in combination with CAT (100 U/ml). Control wells received medium exchanges only. C) Corresponding bright field micrographs of SH-SY5Y cultures photographed 72 h after the aforementioned treatments. Results are expressed as percentage of control. Bars represent mean \pm SEM. ** $P < 0.0078$, *** $P < 0.0003$, **** $P < 0.0001$ Two-way ANOVA followed by Tukey's test. $n = 3$. Scale bar = 100 μm.

The toxicity results, obtained by FDA and previously described, are in accordance to the morphology of cells exposed to the different combinations of 3-HAA treatments. In the micrographs presented, it is clearly observed that 100 μM 3-HAA causes cell death, as evidenced by the presence of dark spots. Similarly, in wells treated with 100 μM 3-HAA+SOD, all cells have completely detached from the plates (Figure 25C).

4.3.2.4 3-HAA affects RA-induced differentiation in SH-SY5Y cells

Some cultures were specifically plated to be photographed under a bright field microscope at day 1, 2 and 3. Using these micrographs, a corresponding neurite count was performed.

Chapter 4

The same methodology used to assess neuritogenesis in QA-treated cells was applied to cell treated with 3-HAA. However, the neurite/soma ratio did not reflect the cellular processes that were taking place. In some cases, neurites remained attached to the culture plates despite the large number of dead cells present. This could be wrongly misinterpreted as an increase in neuritogenesis. For this reason, the data from the neurite/soma ratios is presented in section 6.3 of the appendix (Figure 32 and Figure 33). Instead, the expression of NeuN (post-mitotic neuronal marker) is presented below in which a clear dose-dependent effect can be observed.

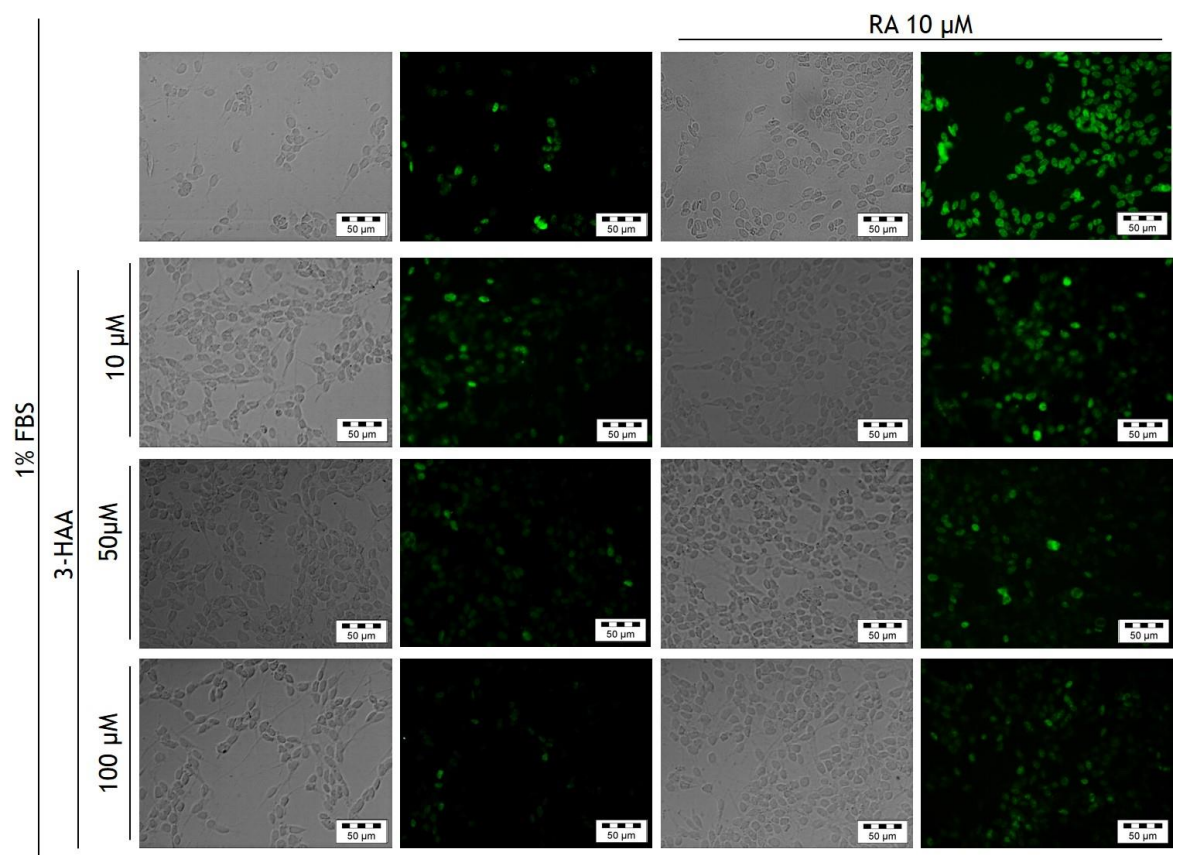


Figure 26. Effect of a single 3-HAA treatment delivered in 1% FBS medium on the expression of NeuN 72 h after treatment. Immunocytochemistry was performed 72 h after SH-SY5Y cells were treated with various concentrations of 3-HAA (10 μ M, 50 μ M and 100 μ M) in 10% FBS medium alone, or in combination with 10 μ M RA.

In these experiments cells were treated once at day 0 with 1% FBS (Figure 26) or 10% FBS (Figure 27) medium alone (control), or either one of those supplemented with 3-HAA (10 μ M, 50 μ M and 100 μ M) or RA (10 μ M). The cultures were incubated under these conditions for 72 h.

As expected, the FBS concentration in the medium affected the degree of differentiation of the cells. The expression of NeuN was reduced when the

Chapter 4

medium used had a higher concentration of FBS (10%). The higher the concentration of 3-HAA used, the less expression of NeuN was found.

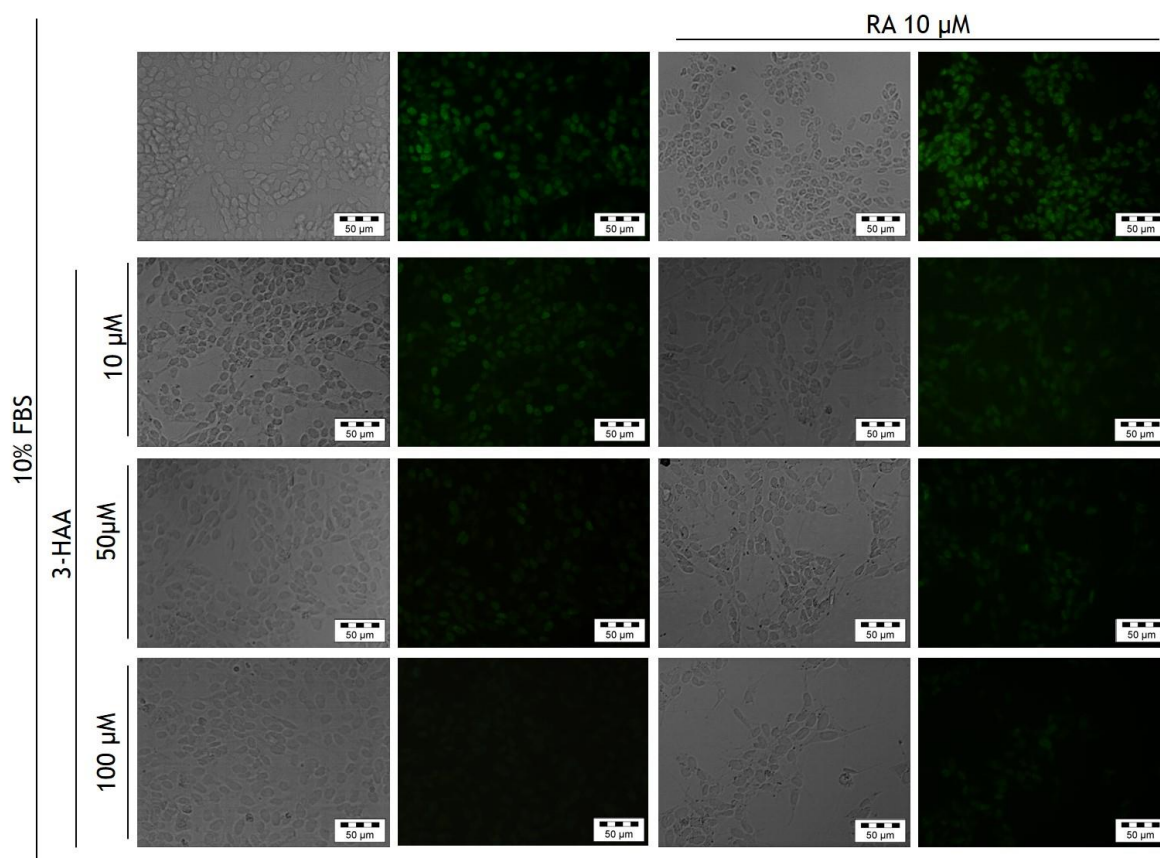


Figure 27- Effect of a single 3-HAA treatment delivered in 10% FBS medium on the expression of NeuN, 72 h after treatment.

Immunocytochemistry was performed 72 h after SH-SY5Y cells were treated with various concentrations of 3-HAA (10 μ M, 50 μ M and 100 μ M) in 1% FBS medium alone, or in combination with 10 μ M RA.

4.3.2.5 SH-SY5Y cells recover from a single 3-HAA treatment

It has been widely reported that differentiation alters the way SH-SY5Y cells respond to toxic insults (Cecchi *et al.*, 2008; Cheung *et al.*, 2009; Xie *et al.*, 2010; Schneider *et al.*, 2011). Therefore it was decided to evaluate whether there were differences in the toxicity of 3-HAA between differentiated and undifferentiated SH-SY5Y cells. All the results presented in this section originate from experiments in which a single 3-HAA treatment was applied on day 0 and the viability assessed 72h and 7 days after the initial treatment.

After 3DIV, undifferentiated SH-SY5Y cells growing in 10% FBS medium were treated with 10% FBS medium alone (control) or medium containing different concentrations of 3-HAA (1 μ M-10 mM). After an additional 72 h or 7 days, phase-contrast micrographs were taken and the viability assessed. The cultures that

Chapter 4

had been growing for 7 days were fed on the 3rd day with 10% FBS medium without 3-HAA. This was done to study whether cells were able to recover from the initial treatment. A total of 3 independent experiments were carried out, using fresh solutions prepared each time.

Another set of experiments studied whether RA-induced differentiation had an effect on the cell's susceptibility to damage and recovery following exposure to 3-HAA. For these experiments, cells were differentiated for 7 days with RA and then transferred to medium containing 1% FBS alone (control) or the same medium containing 3-HAA (1 μ M-10 mM) and incubated for either 72 h or 7 days before viability was assessed. Similarly, cells that were incubated for 7 days were fed on the 3rd day with 1% FBS medium alone. A total of 3 independent experiments were carried out, using fresh solutions each time

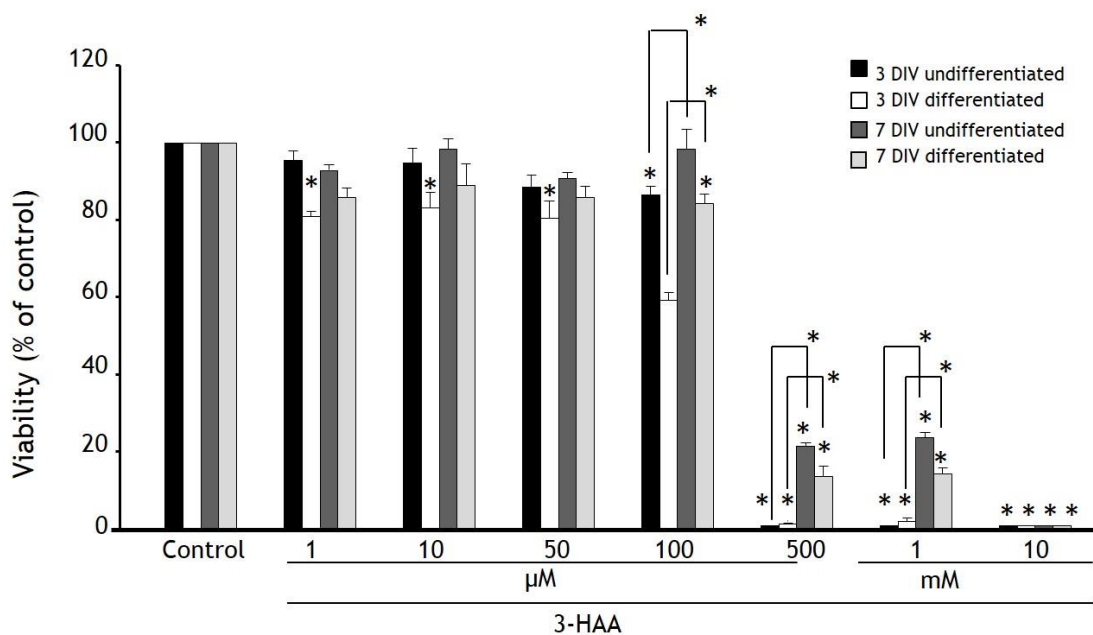


Figure 28- Viability recovery from single 3-HAA treatment. The viability of differentiated and undifferentiated cells treated for 3 or 7 days with 3-HAA. Undifferentiated cells treated with fresh 10% FBS medium alone (control) or in combination with 3-HAA (1 μ M-10 mM) for 72 h (black bars) or 7 days (dark grey bars). Differentiated cells switched to 1% FBS medium alone (control) or in combination with 3-HAA (1 μ M-10 mM) for 72 h (white bars) or 7 days (light grey bars). Results are expressed as percentage of control. Mean \pm S.E.M. for 5 different experiments. * P <0.0001 vs. control, * P <0.0001 vs. 7 days undifferentiated. * P <0.0001 vs. 7 days differentiated.

When cells were treated with 3-HAA either in the differentiated or undifferentiated state there were no apparent changes in toxicity susceptibility at the highest dose used. 10 mM 3-HAA was lethal in both states (Figure 28).

Chapter 4

When differentiated and undifferentiated cells were treated with 500 μM and 1mM 3-HAA for 72 h, no metabolic activity was detected by the FDA assay. However, when the assessment was performed 7 days after the initial and only treatment, there was a 20% increase in the viability (Figure 28). This shows that the few cells that survive the initial 3-HAA treatment slowly manage to repopulate the dishes.

As expected, the undifferentiated cells showed a faster rate at repopulating the dishes than the differentiated cells (dark grey bar compared to light grey bar). The fact that cells, that had been differentiated for 7 days with RA, manage to grow again indicates that 10 μM RA and 1% FBS need to be constantly present to avoid de-differentiation.

Another interesting observation is that, in the group of cells that had been differentiated for 7 days, low doses of 3-HAA which previously had been innocuous (1 μM and 10 μM) to the cells, now successfully caused a 20% decrease in viability when assessed 72 h after treatment (Figure 28, white bars). This effect was no longer noticeable when assessed 7 days after treatment (light grey bars) which once again indicates that even though cells had been differentiated for 7 days, they can continue to grow if given enough time without RA.

It is important to note that the ability of differentiated cultures to repopulate the petri dish following 3-HAA treatment is more pronounced in cells treated with 10% FBS containing medium than those treated with 1% FBS medium. This can be seen more clearly when comparing the 100 μM concentration (Figure 28).

4.3.2.6 HPLC quantification of 3-HAA in medium of cultures and cell-free preparation (Samples were processed by Dr. Alexandra Ferguson)

The recovery results presented above suggested that that 3-HAA was being broken down within the first 3 days after treatments as recovery successfully occurred between day 3 and day 7. Similarly these results indicate that the addition of SOD increased the toxicity of 3-HAA probably by increasing H_2O_2 production as catalase afforded total protection. In view of all presented thus far, it was hypothesised that SOD could be promoting the autoxidation of 3-HAA, as per descriptions in section 1.3.3.2). To test this hypothesis, the concentration of 3-HAA was measured by HPLC. Four time points were chosen; day 0, day 1, day 2 and day 3.

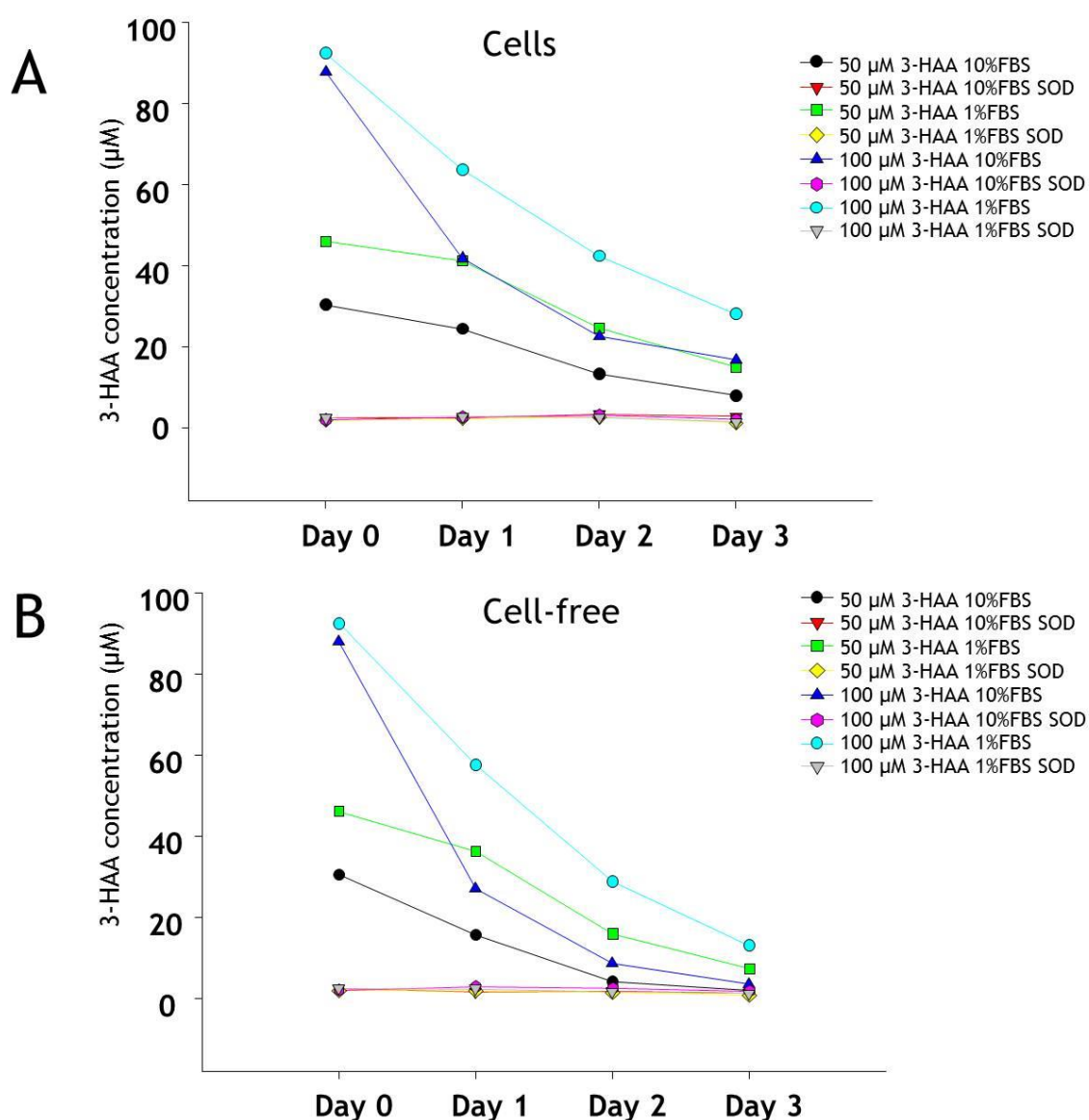


Figure 29- Concentration of 3-HAA in cultures and cell-free preparation determined by HPLC. The samples were obtained as described previously in section 2.11.1.1 processed and analysed by Dr Alexandra Ferguson (see Appendix).

Chapter 4

The HPLC analysis shows that 3-HAA with the addition of SOD did promote the breakdown of 3-HAA in both cell-free preparations as well as in cultures. Additionally, it can be observed that 3-HAA breaks down slightly faster in 10% FBS medium than in 1% FBS medium in accordance with the cellular viability results, which points to the induction of different mechanisms of death (yet not overall toxicity) depending on the serum concentration used to deliver 3-HAA. Contrary to what was expected, 3-HAA was degraded faster in cell-free preparations than in the presence of cells. This could be due to many factors including O₂ availability, pH levels, metabolic activity, etc. Based on these results, a non-linear regression was performed from which the half-life of 3-HAA (100 µM) was determined:

FBS []	Cell-Free		Cell cultures	
	10%	1%	10%	1%
Half-life (in days)	0.49	1.06	0.84	1.52
R ²	0.9677	0.9763	0.9389	0.9754

Table 5. Half-life values for 3-HAA in cell-free preparations and in cell cultures. Data obtained by non-linear regression (One phase decay, Prism Graphpad v. 6.0f), from the HPLC analysis of the concentrations of 3-HAA in 1% and 10% FBS with and without SOD.

An important observation resulting from this data is that the greater part of 3-HAA decay occurs within the first 24 h after treatment which explains why the toxicity did not increase in cells exposed for longer periods of time. The presence of SOD increased the breakdown rate of 3-HAA; from the HPLC analysis, it can be inferred that this process occurs within minutes. Since the experiment was not designed to evaluate short time points, a non-linear regression could not be applied to evaluate the decay rate. A different setting would have been required to evaluate 3-HAA breakdown in real time. Nevertheless, it became evident that the cellular death observed in cells treated with 3-HAA and SOD is not directly caused by 3-HAA but by a product(s) of its degradation.

4.3.2.7 SH-SY5Y cell viability after daily 3-HAA treatment for 72 h

Taking into account the HPLC results showing that 3-HAA breakdown occurs within the first 24 h after treatment, it was decided to examine the effect of daily 3-HAA treatments on the survival of undifferentiated SH-SY5Y cells. In

Chapter 4

order to ensure the frequent replenishment of 3-HAA, cells were treated on day 0, 1 and 2 with 10% FBS medium (control) or with increasing concentrations of 3-HAA (1 μ M, 10 μ M, 50 μ M, 100 μ M, 500 μ M, 1 mM 10 mM). Cells were then incubated for an additional 24 h after the initial treatment, at which point the viability was assessed by FDA and a dose-response curve was plotted. Thereby cells, in which the viability was evaluated at day 2 (Figure 30), received two treatments (first on day 0 and then again 24 h afterwards) and cells assessed at day 3 (Figure 31) received 3 treatments (first on day 0, then 24 h after that, and finally 48 h after the initial treatment).

In contrast to the effect observed with a single treatment of 3-HAA, the addition of fresh drugs on a daily basis further reduced the IC₅₀ for 3-HAA-treated cells. There were no differences in the effect of the drugs regardless of the medium in which they were delivered. Since damage levels had increased, all the other subtle differences caused by the concentration of FBS in the medium were no longer noticeable.

3 Treatments	3-HAA 10%		3-HAA 10% SOD		3-HAA 1%		3-HAA 1% SOD	
DAY	2	3	2	3	2	3	2	3
IC ₅₀ (μ M)	131.8	82.18	51.99	38.76	144.1	68.39	41.23	36.74
R ²	0.9746	0.9054	0.9408	0.9566	0.9735	0.8317	0.9030	0.9416

Table 6. Daily treatments cause a shift in the IC₅₀ values for 3-HAA. One-way ANOVA followed by Sidak's test was used to compare the difference of the IC₅₀ values between 48 h and 72 h exposure to daily 3-HAA treatments. Pooled data from dose-response curves, generated from the different responses to daily 3-HAA treatments in the presence of 1% and 10% FBS with and without SOD. Shown in Figure 30 and Figure 31. *p<0.0189.

A one-way ANOVA was used to test the difference among IC₅₀ values from single and daily 3-HAA treatments (Table 6). The IC₅₀ of 3-HAA daily treatments delivered in 10% FBS medium (82 μ M) was significantly different (p=0.0424) than the IC₅₀ of a single 3-HAA treatment delivered in 10% FBS medium (138.2 μ M). Similarly, the IC₅₀ of 3-HAA+SOD daily treatments delivered in 10% FBS medium (38.76 μ M) was significantly different (p=0.0016) than the IC₅₀ of a single 3-HAA+SOD treatment delivered in 10% FBS medium (81.87 μ M).

This was also the case for the comparison performed between single and daily 3-HAA treatments delivered in 1% FBS. For instance, the IC₅₀ of 3-HAA daily

Chapter 4

treatments delivered in 1% FBS medium (68.39 μM) was significantly different ($p=0.00010$) to the IC_{50} of a single 3-HAA treatment delivered in 1% FBS medium (150.1 μM). The IC_{50} of daily 3-HAA+SOD treatments delivered in 1% FBS medium (36.74 μM) was significantly different ($p=0.0079$) than the IC_{50} of a single 3-HAA+SOD treatment delivered in 1% FBS medium (69.01 μM).

Similarly, the effect of daily treatments with 3-HAA (100 μM) alone, or in combination with catalase (CAT; 1000U/ml), in either 1% or 10% FBS medium, with and without SOD (300 U/ml) was assessed 48 h (Figure 30) and 72h (Figure 31) after the initial treatment, obtaining the following combination of treatments:

- 100 μM 3-HAA 10% FBS
- 100 μM 3-HAA+CAT 10% FBS
- 100 μM 3-HAA+SOD 10% FBS
- 100 μM 3-HAA+CAT+SOD 10% FBS
- 100 μM 3-HAA 1% FBS
- 100 μM 3-HAA+CAT 1% FBS
- 100 μM 3-HAA+SOD 1% FBS
- 100 μM 3-HAA+CAT+SOD 1% FBS

As expected, daily 3-HAA treatments caused a cumulative decrease in cell viability and a reduction in the protection afforded by catalase. In cells treated 2 and 3 times with 100 μM 3-HAA 10% FBS there was a $\approx 40\%$ reduction in the viability when compared to untreated controls (Figure 30 and Figure 31). The addition of CAT no longer afforded any protection in cells treated either 2 or 3 times. In cells treated twice with 100 μM 3-HAA+SOD in 10% FBS medium, there was a decrease in the viability (80%) when compared to control cells (Figure 30), however a third treatment did not cause any further reduction in cell viability (Figure 31). In this third treatment, the addition of catalase exerted some protection, however the viability was not restored to control levels (Figure 31).

A similar reduction in cell viability ($\approx 40\%$) was observed in cells treated twice and three times with 100 μM 3-HAA 1% FBS (Figure 30 and Figure 31). Under these conditions, CAT protected cells treated twice but not those receiving an additional treatment (Figure 31). Interestingly, the viability of cells treated with 100 μM 3-HAA+SOD in 1% and 10% FBS medium did not change between day 2 and day 3.

Chapter 4

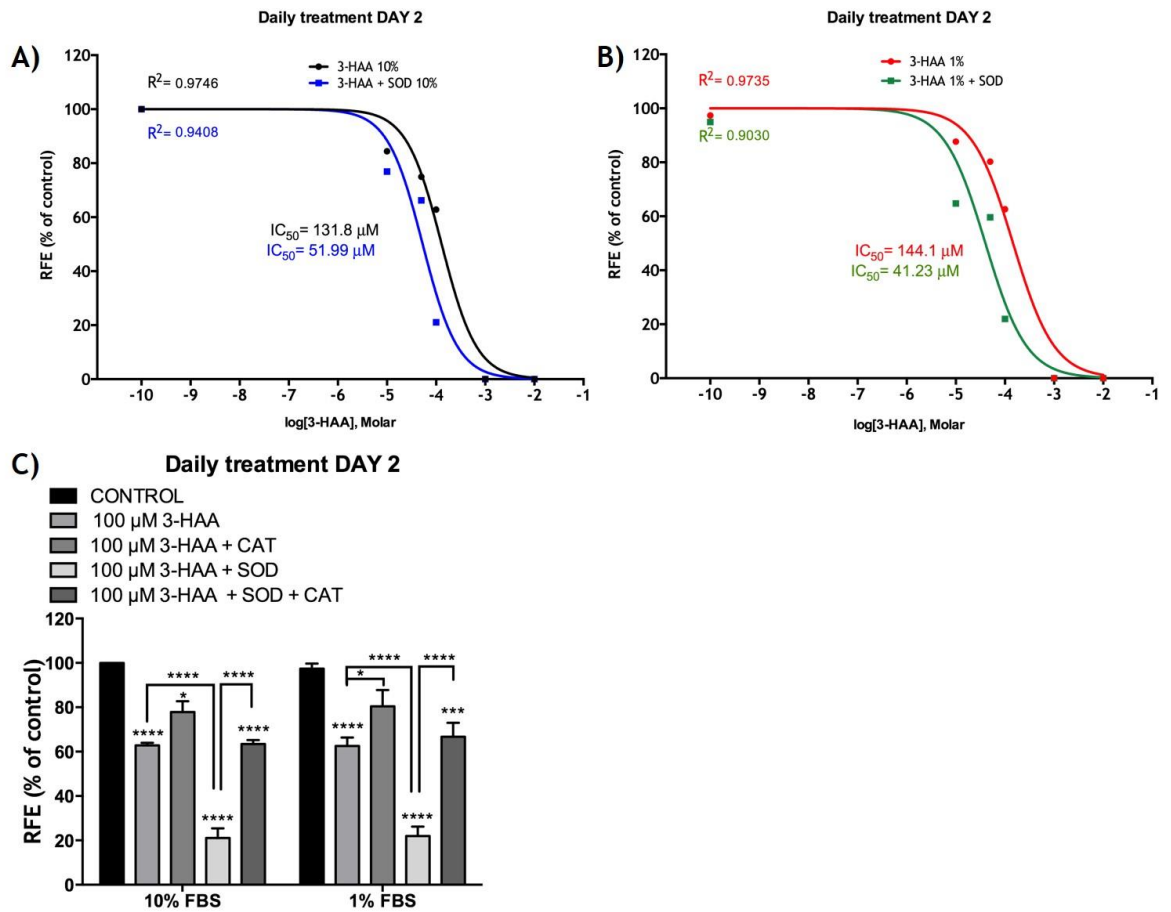


Figure 30. Catalase protects against the exacerbated toxicity of 2 daily 3-HAA treatments. SH-SY5Y cells were treated on day 0 and day 1 with 3-HAA delivered in 1 and 10% FBS medium supplemented with SOD (300 U/ml). The toxicity was assessed 48 h after the initial exposure. A Fitted Log(inhibitor) vs normalised response curve is displayed for cells incubated for 48 h (treated twice) with 3-HAA delivered in 10%(A) and 1% (B) FBS medium supplemented with SOD (Solid Blue and Green lines) after which the toxicity was evaluated by FDA. IC_{50} values were obtained by non-linear regression analysis (Dose-inhibition; Prism Graphpad v. 6.0f). C) Cells were treated with 3-HAA (100 μM) in 1% and 10% FBS medium with/without SOD (300 U/ml) alone or in combination with CAT (100 U/ml). Control wells received medium exchanges only. Results are expressed as percentage of control. Bars represent mean \pm SEM. * $P < 0.05$, *** $P < 0.0004$, **** $P < 0.0001$ Two-way ANOVA followed by Tukey's test. $n = 3$. The average IC_{50} are listed in each graph and are summarized in Table 6.

Chapter 4

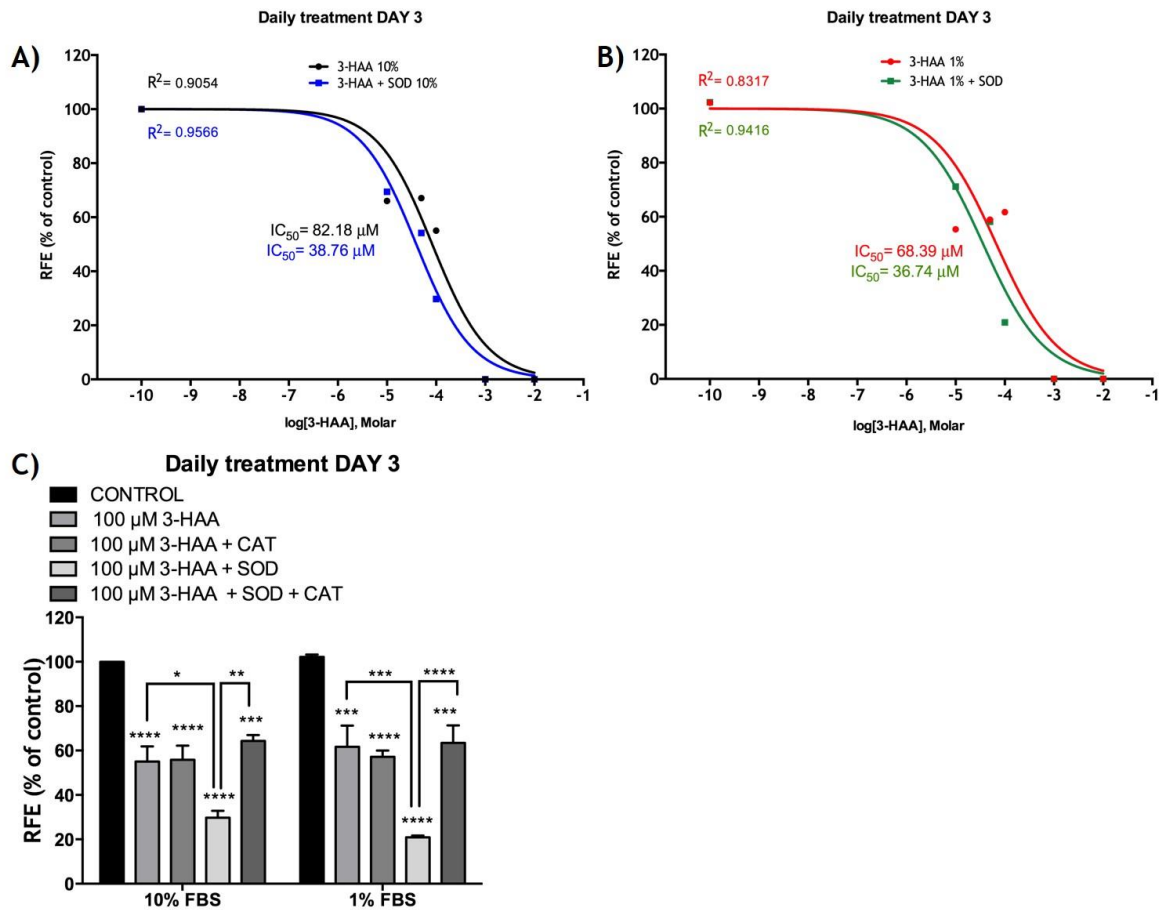


Figure 31. Catalase protects against the exacerbated toxicity of 3 daily 3-HAA treatments. SH-SY5Y cells were treated on day 0, day 1 and day 2 with 3-HAA delivered in 1 and 10% FBS medium supplemented with SOD (300 U/ml). The toxicity was assessed 72 h after the initial exposure. A Fitted Log(inhibitor) vs normalised response curve is displayed for cells incubated for 72 h (treated three times) with 3-HAA delivered in 10%(A) and 1% (B) FBS medium supplemented with SOD (Solid Blue and Green lines) after which the toxicity was evaluated by FDA. IC_{50} values were obtained by non-linear regression analysis (Dose-response inhibition Prism Graphpad v. 6.0f). C) Cells were treated with 3-HAA (100 μM) in 1% and 10% FBS medium with/without SOD (300 U/ml) alone or in combination with CAT (100 U/ml). Control wells received medium exchanges only. Results are expressed as percentage of control. Bars represent mean \pm SEM. * $P < 0.0183$, ** $P < 0.001$, *** $P < 0.0008$, **** $P < 0.0001$ Two-way ANOVA followed by Tukey's test. $n = 3$. The average IC_{50} are listed in each graph and are summarized in Table 6.

4.4 Discussion

The results of the QA experiments show that there are no changes in the viability of SH-SY5Y cells at any of the concentrations tested which was an exciting discovery. However, during the development of this project, the resistance of SH-SY5Y cells against QA toxicity was reported (Wszelaki and Melzig, 2011). Since QA selectively activates NMDAR with the subunit combination GluN1+GluN2A and GluN1+GluN2B (de Carvalho *et al.*, 1996), it was initially thought that perhaps the specific subunit composition in SH-SY5Y cells could account for the lack of toxicity of QA.

Furthermore, the QA-induced expression of β 3-tubulin and DCX was not affected by blockade of the NMDAR with MK-801 or KA, at neither of the time points evaluated. KA (NMDAR antagonist) has been reported to affect cancer growth (Walczak *et al.*, 2012; Walczak *et al.*, 2014), thus its effect on the survival of SH-SY5Y cells was evaluated. Consistently with the lack of effect of MK-801, the viability of cells treated with KA was not affected at any of the concentrations tested.

Since QA is a weak agonist of the NMDAR, the effect of NMDA on the survival and neuritogenesis of SH-SY5Y cells was evaluated. NMDA treatment of undifferentiated SH-SY5Y cells for 72 h had no significant effect on cell survival. In some experiments, NMDA caused a small decrease in the viability but not in a dose-dependent manner. Since it had previously been reported that QA-induced differentiation correlated with the appearance of GluN1 mRNA in the SH-SY5Y cells (Kulikov *et al.*, 2007), it was decided to assess whether differentiation modified the susceptibility of cells to NMDA. Surprisingly, the response to NMDA was identical in differentiated and undifferentiated cells. There are discrepancies in the literature regarding the lethal concentration of NMDA in SH-SY5Y cells. Park and collaborators (2012) report a 20% decrease in cell viability after a 24 hour incubation of 100 μ M NMDA (Park *et al.*, 2012). Contrastingly, other reports show that 24 h exposure to NMDA at doses below 1 mM have no consistent effect on SH-SY5Y cell viability and that high doses (5mM) are necessary to cause an increase of LDH leakage (Tetich *et al.*, 2004).

Chapter 4

The lack of effect of NMDA (and its antagonists) suggests that no functional NMDARs exist in the SH-SY5Y cell line, which would be in accordance with two previous studies that specifically selected this cell line as a negative control for the presence of GluRs (Uberti *et al.*, 1997; Glantz *et al.*, 2007). However, these authors provide no direct evidence or references to support their claim. Furthermore several other studies on SH-SY5Y cells have implicated NMDAR activation to a myriad of processes, from toxicity to preconditioning stimulation which indirectly provided evidence that this receptor is present in the SH-SY5Y cell line (Nair *et al.*, 1996b, a; Singh and Kaur, 2005, 2007; Park *et al.*, 2012).

The results presented in this dissertation provide evidence to demonstrate that the GluN1 subunit is not present in the SH-SY5Y cell line. It could be argued that the antibody used in this study does not recognise human GluN1, given that the positive control used was rat brain homogenate while the SH-SY5Y cells are of human origin. However this is an unlikely possibility as that the epitope (highly conserved) recognised by the antibody is identical in both human and rat. Furthermore, the GluN1 antibody used in this project has been shown to bind to the GluN1 subunit in human embryonic stem cells (Francis and Wei, 2010) and in cells from human cerebrospinal fluid (Gleichman *et al.*, 2012).

The absence of GluN1 subunit could explain the low toxicity of both of QA, NMDA and KA in these cells. Another possibility to explain the low toxicity of QA, NMDA and the lack of response to MK-801 and KA could be the presence of an alternative form of NMDAR with a different subunit composition. For instance, there are studies showing that co-expression of the GluN1/GluN3A-B will form excitatory glycine receptors insensitive to Glu, NMDA, MK-801, memantine and competitive antagonists (Chatterton *et al.*, 2002). In human embryonic kidney cells (HEK293), the GluN1/GluN3A or GluN1/GluN3B receptor combination does not express well on the surface (Smothers and Woodward, 2007). Therefore, if this subunit combination is present in the SH-SY5Y cells, then the lack of detection could possibly be explained.

Unfortunately, the expression profile, localization, arrangement and functional characterisation of the NMDAR has never been fully studied in the SH-SY5Y cell line. The majority of studies of SH-SY5Y cells, which attribute an effect to the NMDR, base their theoretical framework on research performed on RA-

Chapter 4

differentiated SK-N-SH cells (Pizzi *et al.*, 2002). However, the SK-N-SH cell line is morphologically and biochemically different to the SH-SY5Y cell line (Cohen *et al.*, 2003); therefore the possibility exists that functional NMDARs exist in one cell line but not in the other.

As previously mentioned, in one report it is suggested that functional NMDARs are present in SH-SY5Y cells. However, the only supporting evidence provided, was the presence of GluN1 mRNA (interestingly, not that of GluN2A-D and GluN3) yet, the actual levels of GluN1 protein were not reported (Kulikov *et al.*, 2007). A more recent report shows that the constitutive expression of GluN2A increases after RA-induced differentiation and that *in vitro* ischemia-reperfusion increases its tyrosine-phosphorylation (Beske and Jackson, 2012). Conflictingly, a microarray study, evaluating the transcriptional changes that occur in SH-SY5Y after RA-induced differentiation, shows that whereas GRIN1 (the gene codifying for GluN1) expression can be detected, its expression does not change among undifferentiated and RA-differentiated cells SH-SY5Y (Korecka *et al.*, 2013).

Furthermore, electrophysiological studies of the NMDAR in SH-SY5Y cell lines are virtually non-existent. In a study that set out to determine the effect of Binteigrin-1 on amyloid- β_{1-42} (AB_{1-42}) enhancement of NMDAR activation in SH-SY5Y cells, Uhasz and collaborators (2010) report that Binteigrin-1 blocks the increase in the intracellular concentration of Ca^{2+} (measured using the Fluo-4NW Calcium Assay Kit) that generally follows AB_{1-42} treatment (Uhasz *et al.*, 2010). However, in a previous patch-clamp study, it is reported that NMDA treatment does not evoke any detectable ionotropic responses in these cells, indicating that either the NMDAR is absent or that it is found in an inactive state (Jantas *et al.*, 2008). The same authors then report that NMDA has antiapoptotic actions against staurosporine and salsolinol-induced death (Jantas and Lason, 2009) by a mechanism that would require functional NMDAR. It is therefore recognised that research performed using the SH-SY5Y cell line would greatly benefit from a full and exhaustive characterization of the NMDAR composition and its electrophysiology.

It is surprising that despite accumulating evidence suggesting that the NMDAR is not present in SH-SY5Y cells, there are still several reports in which the effects observed are attributed to NMDAR activation (Masuko *et al.*, 2012; Shin *et al.*,

Chapter 4

2014; Zhou *et al.*, 2014). Partially addressing these inconsistencies, Sun and collaborators propose that some of the effects of Glu and its antagonists on SH-SY5Y cells could be attributed to oxidative Glu toxicity and not calcium disturbances mediated by NMDARs (Sun *et al.*, 2010).

It has been reported that QA can cause an increase in the levels of ROS by inactivating endogenous antioxidant molecules (Rodriguez-Martinez *et al.*, 2000). Furthermore, in rat cerebral slices (cortex, hippocampus and striatum) MK-801 does not prevent the QA-induced formation of ROS, which suggests a mechanism independent of NMDAR activation (Dobrachinski *et al.*, 2012). It has been suggested that QA directly activates NOX thus increasing the levels of $O_2^{\bullet-}$ (Santamaria *et al.*, 2001). There is an increasing body of evidence that points to ROS as promoters of cell differentiation at low concentrations; this has been observed in immortalised human fibroblast lines (Takahashi *et al.*, 2006). More directly, in SH-SY5Y cells, a recent report showed that docosahexaenoic acid induces neuritogenesis via activation of ERK1/2 through the generation of ROS (Wu *et al.*, 2009).

The results herein contained suggest that QA-induced neuritogenesis occurs independently of NMDAR activation. Therefore, the role of ROS in the differentiation induced by RA and QA was studied. Several probes have been designed to quantify the intracellular levels of ROS. For example, the oxidation of dihydroethidium (DHE) as an indicator of $O_2^{\bullet-}$ production has been widely used since the 1980s (Robinson *et al.*, 2008). Despite controversies regarding the specificity of DHE to react with $O_2^{\bullet-}$, the DHE oxidation assay is still considered a valid method to study the overall oxidative state of the cell. This is especially true when DHE is used in combination with a pharmacological approach (use of antioxidants) to discern the particular ROS that is being produced. Therefore, the oxidation of DHE was the method selected to evaluate ROS production in SH-SY5Y cells.

SOD treatment increased the number of cells present in the cultures. This increase in viability and decrease in the number of neurite bearing cells by SOD points to an involvement of reactive oxygen species (ROS), in particular $O_2^{\bullet-}$, in the proliferation of SH-SY5Y cells. In this sense, ROS could be slowing down cell proliferation, perhaps through the action of tumour suppressors hence allowing

Chapter 4

differentiation to occur or they could be directly inducing differentiation through the activation of transcription factors responsive to oxidative stress. The transient and oscillating levels of ROS suggest that they may be acting as signaling molecules during the first day after QA treatment.

These data may indicate that SH-SY5Y cells have a high intrinsic production of ROS that maintain a balance between proliferation and differentiation and that a small shift towards an oxidant condition could be down-regulating cell growth and therefore promoting differentiation. Indeed, there is evidence suggesting that decreasing the amounts of ROS with antioxidants promotes proliferation in precancerous cells and in cancer cell lines that have not yet lost p53 function (via a mechanism involving NRF2) which occurs late in tumour progression (Sayin *et al.*, 2014). Notably, whereas loss of p53 function is a common feature in human cancers, it is of rare occurrence in neuroblastoma and its derived cell lines. Mutations in p53 are found almost exclusively in progressive and relapsed neuroblastoma (Janardhanan *et al.*, 2009). However further experiments would be needed to explain the increase in viability caused by SOD in SH-SY5Y cells and whether SOD addition has a down-regulating effect on p53 and NRF2.

When cells are treated with RA in medium containing SOD, there was a clear reduction in the soma/neurite ratio as compared to medium without SOD. These results offer additional evidence to support that ROS are involved in the differentiation exerted by RA and QA. In accordance with this, it has been previously demonstrated that RA has a pro-oxidant effect one week after treatment and that reducing the levels of ROS reduces the degree of differentiation (Konopka *et al.*, 2008). A more recent report shows that RA increases differentiation and ROS through the activation of NADPH oxidase (Nitti *et al.*, 2010)

Da Frota and collaborators (2011) reported that the addition of Trolox to SH-SY5Y cultures increases both the proliferation (cell number) and neuritogenesis (neurite/soma ratio) however it is not mentioned how both processes can simultaneously occur. Coincidentally, under these conditions, the levels of SOD are reduced. Furthermore the authors suggest that an antioxidant-strategy could avoid the premature death of cells entering differentiation programmes (da Frota Junior *et al.*, 2011) though they do not take into account the neoplastic

Chapter 4

nature of the SH-SY5Y cell line and the negative outcome that such strategies would have in reality.

Furthermore, the time-course assessment presented here indicates that 24 hours after RA treatment there is an increase in the levels of ROS, which is completely eliminated by co-incubation with SOD. Serum reduction also increases the levels of ROS in SH-SY5Y cells but this stimulus is not sufficient to cause differentiation on its own. The levels of ROS in QA-treated cells are significantly higher than the levels of ROS found in cells kept in 10% FBS medium (control), 1% FBS medium or RA. The effect of RA and QA on ROS production is additive as evidenced by increased DHE fluorescence.

SOD significantly decreased the levels of free radical generation and differentiation in all of the experimental conditions. The effect of SOD as well as the positive DHE signal, which preferentially reacts with $O_2^{\cdot-}$, suggested that this is the main ROS involved in the differentiation observed after RA and QA treatment. RA caused an increase in the number of neurites which correlated with an increase in the expression of β 3-tubulin after 3 and 7 days and a decrease in the expression of DCX after 7 days. Furthermore, by using a neurite outgrowth assay, it was possible to determine that the changes in β 3-tubulin come from the neuritic fraction and that indeed RA promotes neurite extension as early as 72 h after treatment.

As expected, none of the treatments delivered in 10% FBS induced differentiation, this had been previously reported and it is due to the action of mitogenic factors present in the serum (Zheng *et al.*, 2006) that promote cell growth. Differentiation only occurs when the cells are treated with 1% FBS (Meghani *et al.*, 1993) since proliferation signals are incompatible with the differentiation programme (Strehl *et al.*, 2002).

Surprisingly, cells treated with QA showed morphological similarities to cells treated with RA, such as an increase in the length and number of neurites and rounding of the cell bodies.

Since most of the evidence supporting a differentiating effect of QA came from a morphological assessment, and taking into account the sample bias from

Chapter 4

choosing random fields, other molecular tools were used to confirm these observations. If indeed cells are acquiring a more neuronal phenotype with QA and RA, then this ought to be reflected by an increase in neuronal markers.

QA treatment caused an increase in β 3-tubulin at 3 and 7 days. The results obtained from the neurite outgrowth assay indicate that QA treatment promotes cell differentiation, which is dose dependant. This is a very relevant discovery since it is the first time that QA has been shown to have a positive effect on neuritogenesis in mammalian cells. From an oncogenic point of view, it may suggest that it induces tumour regression (at least in a significant fraction of the cells) which contributes to the accumulating body of evidence suggesting that whereas persistently high levels of ROS promote cell growth, an acute oxidising condition decreases it.

QA failed to significantly decrease the expression of DCX at either 3 or 7 days, which indicates that some cells retain the ability to divide. This may suggest that the differentiation induced by QA is only partial and that inducing a complete stop in proliferation may be necessary to elicit a fully differentiated phenotype.

The inability of QA to reduce proliferation may suggest that as regards to SH-SY5Y cells, at least two independent stimuli are necessary for complete neuronal differentiation. This could be due to the transformant nature of the SH-SY5Y cell line in which the ability to exit the cell cycle in the absence of exogenous mitogens has been lost. For instance, NGF-induced differentiation is also partial unless aphidicolin is added to the cultures (LoPresti *et al.*, 1992). Similarly, a homogenous population of neural cells can be obtained when SH-SY5Y cells are sequentially treated with RA and brain-derived neurotrophic factor (BDNF). These cells adopt a neuronal morphology which correlates with a termination of DNA replication (Encinas *et al.*, 2000; Jamsa *et al.*, 2004). Other differentiation-inducing compounds behave in a similar manner. For example, in the absence of mitotic inhibitors, SH-SY5Y cells treated with RA or 12-O-tetradecanoyl phorbol-13 acetate (TPA) continue to proliferate and thus far only staurosporine has been able to induce terminal differentiation that is neurotrophin-independent (Prince and Oreland, 1997). Interestingly, RA increases the levels of Bcl-2 and

Chapter 4

decreases those of p53, whereas staurosporine decreases Bcl-2 and increases p53 levels in SH-SY5Y (Tieu *et al.*, 1999).

According to the clonal expansion model, both N-type and S-type cells are simultaneously present in a normal SH-SY5Y culture (Cohen *et al.*, 2003). Thus, it seems more likely that the neuritogenic effect of QA is exerted on the N-type fraction of the cultures which is more susceptible to differentiating stimuli. It has also been shown that after differentiation is induced in SH-SY5Y cells, the S-type subpopulation continues to divide leading to its selection (over the non-dividing N-type) and clonal expansion (Encinas *et al.*, 2000) which would explain why the expression of β 3-tubulin decreased 7 days after QA treatment when compared to its expression 3 days after treatment. Furthermore, it has been suggested that the SH-SY5Y cell line provided by ATCC (American Type Culture Collection) differentiates more easily than the one provided by ECACC due to an increased presence of the S-type subpopulation in the latter (Nishida *et al.*, 2008).

Interestingly, it has been reported that QA is preferentially produced (over PIC) in SK-N-SH cells, where it causes an increase in cell proliferation (Guillemin *et al.*, 2007). To what extent and how this relates to the results obtained in this study is hard to determine given the many genetic and functional differences between the SK-N-SH cell line and the SH-SY5Y cell line. The more obvious one is the unquestionable presence of functional NMDARs (Pizzi *et al.*, 2002) in the SK-N-SH cell line, which could potentially confer this cell line with the ability to use both Glu and QA to stimulate growth in an autocrine manner (Adams *et al.*, 2012). However it is tempting to speculate that the dissimilar response elicited by QA in the SK-N-SH and SH-SY5Y cell line may underlie, at least in part, the enhanced capability of the SH-SY5Y cell line to undergo differentiation as opposed to the SK-N-SH cell line, where 80% of the population (the S-type) does not differentiate (Nishida *et al.*, 2008)

Given that both the neurite/soma ratio evaluation and the neurite outgrowth assay produced results consistent with an increase in neuritogenesis, it was of interest to establish whether the results attained with each method were comparable. The estimates of neurite extension obtained with the neurite outgrowth assay were more conservative compared to the neurite/soma ratio

Chapter 4

and the β 3-tubulin western blot quantification. This suggests that QA causes a major change in the neuritic architecture; mainly by causing the elongation of neurites and, to a lesser (yet still significant) extent, by causing an increase in the overall neuritic mass. Similarly, the differences in the expression of β 3-tubulin between the Western blot analysis and the neurite outgrowth assay may indicate that QA causes an increase in the expression of β 3-tubulin mainly in the soma and to a lesser but still significant extent in the neurites.

QA (a precursor of NAD^+) has been reported to induce oxidative stress through NOX-activation (Maldonado *et al.*, 2010) and NOX has been shown to mediate the differentiation of stem cells (Chan *et al.*, 2009), it was decided to study the role of NOX in QA-induced neuritogenesis.

The neurite outgrowth assay showed that when cells are treated with QA and DPI, differentiation is eliminated. The data presented here is consistent with reports showing that, in SH-SY5Y cells treated with RA, the acquisition of a neuronal phenotype is accompanied by an increase in the activity of NOX and that its inhibition with DPI decreases RA-induced neurite elongation (Nitti *et al.*, 2007; Nitti *et al.*, 2010). However, since $\text{O}_2^{\bullet-}$ can be generated by other mechanisms that do not involve NOX, the possibility of additional sources of $\text{O}_2^{\bullet-}$ during QA-induced differentiation cannot be discarded.

For instance, when xanthine/xanthine-oxidase was used as a positive control for $\text{O}_2^{\bullet-}$ formation, there was no indication that differentiation was taking place which further strengthens the hypothesis that in addition to oxidative stress another stimulus is necessary to promote cell differentiation. Nevertheless, the effect of xanthine/xanthine-oxidase on neuritogenesis was never quantitatively studied. The study of the xanthine/xanthine oxidase system may represent an important element to elucidate the role of ROS in the differentiation of SH-SY5Y.

NRF2 is a protein that mediates the cellular response to oxidative stress and which has been shown to play a role in differentiation. NRF2 is released when Keap-1 is oxidised at several cysteine residues. NRF2 then migrates to the nucleus where it activates the transcription of genes with antioxidant response element box (ARE) in their promoters. In a liver carcinoma cell line and in a

Chapter 4

myelogenous leukaemia line, SIRT1 decreases acetylation of NRF2 as well as NRF2-dependent gene transcription. Furthermore, selective inhibitors of SIRT1 (EX-527 and Nam) increase the transcription of genes regulated by NRF2 whereas activating Sirt1 with resveratrol inhibits NRF2 (Kawai *et al.*, 2011).

Since QA treatment caused a marked increase in the levels of ROS, it was decided to evaluate the expression of NRF2. QA induced a marked increase in the expression of NRF2 which was detectable 12 hours after treatment. This is in accordance with reports showing that ROS-mediated differentiation induces the expression of NRF2 in SH-SY5Y cells (Zhao *et al.*, 2009). More recently, it has been shown that neuronal differentiation of SH-SY5Y cells causes an increase in NRF2, a transcription factor regulating the endogenous antioxidant response and neuronal differentiation (Korecka *et al.*, 2013)

To further study the process by which QA induces differentiation, it was decided to treat SH-SY5Y cells with different concentrations of Nam, another precursor of NAD⁺ (and an inhibitor of SIRT1). Nam treatment induced differentiation as evidenced by an increase in neurite formation and expression of β 3-tubulin. The fact that QA increased the levels of NRF2 and that Nam mimicked the effect of QA may indicate that the mechanism through which QA is exerting its actions is by altering the metabolism of NAD⁺/Nam/Nicotinic acid.

Interestingly, trigonelline (essentially a methylated form of nicotinic acid found in plants) and 1-Methylnicotinamide cause an increase in the number of neurites in SK-N-SH cells (Tohda *et al.*, 1999; Thomas *et al.*, 2013). Trigonelline increases the susceptibility of pancreatic cancer cells to apoptosis through a mechanism that involves the inhibition of NRF2 (Arlt *et al.*, 2013).

The exact mechanism by which Nam promotes cell neuritogenesis was not studied rigorously. However, based on the data presented in this project, a prospective series of hypotheses are presented, which could form the basis for future venues of research.

Hypotheses:

Chapter 4

1.- QA may induce neuritogenesis and an increase of ROS through the activation of NOX followed by activation of antioxidant response elements. The results presented here show an increase in NRF2 after QA treatment. NRF2 binds to the antioxidant response element in the promoter of genes such as NAD(P)H:quinone oxidoreductase (Vomhof-Dekrey and Picklo, 2012).

2.- QA may cause differentiation by increasing the intracellular concentration of NAD⁺, thereby affecting the NAD⁺/NADH ratio.

3.- An increase in the availability of NAD⁺ will in turn affect the intracellular concentration of Nam (since Nam is both a product and a precursor of NAD⁺). The hypothesis that Nam accumulates in the SH-SY5Y cell line is partly supported by the fact that the pathway involved in Nam elimination is compromised. The SH-SY5Y cell line lacks nicotinamide N-methyltransferase, an enzyme that is involved in the elimination of Nam by causing its N-methylation to form 1-methylnicotinamide (Parsons *et al.*, 2011). Interestingly, trigonelline (essentially a methylated form of nicotinic acid found in plants) and 1-Methylnicotinamide cause an increase in the number of neurites in SK-N-SH cells (Tohda *et al.*, 1999; Thomas *et al.*, 2013). Trigonelline increases the susceptibility of pancreatic cancer cells to apoptosis through a mechanism that involves the inhibition of NRF2 (Arlt *et al.*, 2013).

4.- An increase in the intracellular concentration of Nam decreases the activity of SIRT1 which in turn will increase the activity of NRF2. Even though the mutual cooperation of SIRT1 and NRF2 has been extensively reported, in particular the activation of NRF2 by SIRT1 (Huang *et al.*, 2013; Kulkarni *et al.*, 2014), it has also been shown that Sirt1 causes a decrease in the acetylation of NRF2 and a reduction in the expression of genes regulated by NRF2 (Kawai *et al.*, 2011). Furthermore, there is evidence suggesting that sirtuins may be involved in carcinogenesis based on a recent study which shows that cancer cells require SIRT1 for survival (Ford *et al.*, 2005; Deppert, 2008). Taking into account the transformant nature of the SH-SY5Y cell line, the hypothesis that Nam is inhibiting SIRT1 and that this is causing proliferation to stop and an increase in NRF2 is further strengthened. In any case, the importance of studying the interaction between NRF2 and SIRT1 during QA-induced differentiation in SH-SY5Y cells is evident. A link between SIRT1 and neuroprotection has also been

Chapter 4

found in several models including *in vivo*, *in vitro* and *ex vivo*. For instance, in mice with Wallerian degeneration slow (Wlds), the overexpression of *Nmnat1*, protects cells against axonal degeneration through a pathway that involves SIRT1 as a downstream effector (Araki *et al.*, 2004).

5.-NRF2 is affecting the expression of genes involved in differentiation. It has already been shown that NRF2 plays a role in the RA-induced differentiation of SH-SY5Y cells (Zhao *et al.*, 2009).

Based on the results obtained using QA to treat the SH-SY5Y cells, it was decided to evaluate the effect of 3-HAA on SH-SY5Y differentiation. However, SH-SY5Y cells presented signs of damage upon exposure to 3-HAA. 3-HAA caused cell death and increased the levels of ROS. This damage was potentiated upon addition of SOD to the cultures which is in agreement with reports showing that SOD promotes the autoxidation of 3-HAA and further production of ROS (Liochev and Fridovich, 2001). It needs to be noted that DHE preferentially labels $O_2^{\bullet-}$ however this can only be irrefutably proven when the assay is used in combination with drugs that specifically detoxify a particular ROS (as it was done for QA with SOD). Since SOD increased DHE fluorescence, other antioxidants should have been used to identify the ROS in cultures. Alternatively a different method to identify ROS could have been used.

Whereas CAT protected against 3-HAA-induced cellular death, SOD enhanced its cytotoxicity. This is also in agreement with previous reports showing that at physiological pH, 3-HAA generates $O_2^{\bullet-}$ and H_2O_2 in a copper-dependent manner which can be detected by DHE (Goldstein *et al.*, 2000). SH-SY5Y cells are very sensitive to H_2O_2 attack (Weinreb *et al.*, 2008).

The data herein contained suggest that both $O_2^{\bullet-}$ and H_2O_2 could account for 3-HAA toxicity depending on the concentration of FBS in the media in which the treatment is delivered. FBS did not cause a shift in the IC_{50} but it did affect the response to catalase.

One possibility is that H_2O_2 is not the main ROS responsible for the induction of cellular death in cells treated with 3-HAA in 10% FBS, and that therefore CAT treatment cannot exert protection. Conversely, the protective effect of catalase

Chapter 4

indicates that H_2O_2 is the main ROS produced in cells exposed to 3-HAA in 1% FBS as well as in those exposed to 3-HAA+SOD in either 1% or 10% FBS for 48 and 72 h.

Cu-Zn-SOD is extracted from bovine erythrocytes and foetal bovine serum (FBS) is also obtained from blood plasma. It is therefore a very likely possibility that Cu-Zn-SOD is present in bovine serum. Indeed, early reports have shown that Cu-Zn-SOD is present in FBS at concentration ranging from 12-4400 ng/ml, enough to exert an anticlastogenic effect, depending on the batch and heat inactivation protocol used (Baret and Emerit, 1983). Given that the specific activity of SOD is not disclosed, it was not possible to convert ng/ml to U/m in order to ascertain how this concentration compares to the ones used and what its effect would be. Alternatively, it has also been shown that FBS has an effect on the level of SOD produced by cell in cultures (Rahman *et al.*, 2011), which may also explain why in our preparation FBS had an effect on the extent to which catalase could protect.

As mentioned in the introduction, the autoxidation of 3-HAA leads to the production of $\text{O}_2^{\cdot-}$ and H_2O_2 . The results herein contained confirmed that the addition of SOD promotes the autoxidation of 3-HAA but that there is also a significant production of H_2O_2 during 3-HAA autoxidation, perhaps caused by the dismutation of $\text{O}_2^{\cdot-}$ into H_2O_2 .

When cells were treated only once, at day 0 with 3-HAA, recovery was observed. Thus, it was hypothesised that 3-HAA could be breaking down within the first 24 hours. The HPLC results showed that indeed, this is the case. When cells were treated every day with 3-HAA for three days, the viability was reduced and no signs of recovery were observed.

It has been widely reported that differentiation alters the way SH-SY5Y cells respond to toxic insults (Cecchi *et al.*, 2008; Cheung *et al.*, 2009; Xie *et al.*, 2010; Schneider *et al.*, 2011). However, this effect has also been reported to be due to the lack of appropriate controls and adjustments necessary to compare the viability or cytotoxicity between undifferentiated (proliferative) and differentiated cells (arrested). This is particularly relevant for studies such as

Chapter 4

this one in which cell death occurs several days after the initial treatment with 3-HAA whereby untreated controls continue to grow.

It has been suggested that in growing cultures, the cells are unsynchronised, which causes uncertainty in toxicity measurements. For example, the MTT assay of A β -peptides might lead to false results when non-differentiated neuroblastoma cells are used, because A β -peptides act mostly on the neurites of the neuroblastoma cells (Datki *et al.*, 2003).

Furthermore, when determining the differential toxicity of a compound between proliferative and non-proliferative cells it is necessary to determine if the decrease in “viability” is due to an increase in the number of dead cells, less proliferation or less metabolic activity without death. If the number of cells cannot be kept constant, then an adjustment/correction needs to be performed unless the redox activity of the cells is confirmed to be directly proportional to the toxicity

Working with non-differentiated cells involves some disadvantages since the number of cells is continuously growing during the experiments. This makes undifferentiated SH-SY5Y cells a less than ideal neuronal model to evaluate the events that follow an initial toxic insult since some cells will recover after time. Using differentiated cultures to assess toxicity has been presented by some as an alternative (Datki *et al.*, 2003; Cecchi *et al.*, 2008). However, differentiated SH-SY5Y cells can dedifferentiate after time even when maintained in 1% FBS medium supplemented with RA (Constantinescu *et al.*, 2007). Then there is also the risk that the drug being analysed is interfering with RA differentiation and cell proliferation resumes which can cause misinterpretation of data.

For instance, the differences in viability found 72 h after a single 3-HAA treatment between differentiated and undifferentiated cells could have been interpreted as a different susceptibility to 3-HAA between differentiated and undifferentiated cells when in fact the mechanism behind this difference in viability was the different proliferation rates of differentiated cells vs undifferentiated cells. A more exact estimate of the toxicity could have been obtained by using propidium iodide or LDH release to adjust the data. Even then, the total number of cells would have continued to skew the values.

Chapter 4

Direct oxidation of unidentified substrates by Cu-Zn-SOD has been proposed to account for the deleterious effects sometimes reported to accompany overproduction or overadministration of this enzyme (Liochev and Fridovich, 2001; Lindskog *et al.*, 2006). This work supports this hypothesis by establishing that Cu-Zn-SOD is capable of causing such oxidations. A possibility exists that both $O_2^{\cdot-}$, H_2O_2 and cinnabarinic acid caused the toxicity associated with co-treatment with 3-HAA and SOD (Hiramatsu *et al.*, 2008).

4.5 Future Avenues

This study leaves abundant room for further progress in kynurenine research in the context of cancer pathogenesis. In future investigations, it might be possible to use a different cell line like the SK-N-SH, in addition to the SH-SY5Y, to compare their responses to kynurenines and attempt to determine the reason behind any possible differences.

There are several experimental approaches to test each of the aforementioned hypothetical points. For instance, an important issue would be determining the precise effect of QA on cell proliferation, for instance assessing proliferation by bromodeoxyuridine (BRDU) to determine whether cells continue to proliferate after QA treatment.

Assessing the activity of NOX after QA treatment can further strengthen the hypothesis that NOX is the source of $O_2^{\bullet-}$ since DPI caused a decrease in neurite extension.

Several questions remain at present unanswered, for instance it would be necessary to determine whether the increase in NRF2 expression is causing differentiation or whether it is an independent antioxidative response against the increase in ROS caused by QA. To accomplish this, the activity of NRF2 would need to be blocked and quantified in order to determine if neuritogenesis is affected. Even though recent advances have been made in the development of a direct inhibitor of Keap1-NRF2 (Arlt et al., 2013; Hu et al., 2013), the main reliable method to inhibit it continues to be through siRNA gene silencing.

In order to ascertain if the effect of QA is mediated by downstream metabolites of NAD⁺ metabolism, an initial approach could be to measure the ratio of NAD⁺/NADH and NADP/NADPH after QA treatment as well as the concentration of Nam. An additional approach would be to inhibit the enzymes that transform QA into NAD⁺ (quinolinate phosphoribosyltransferase, nicotinamide mononucleotide adenylyltransferase, nicotinamide methyltransferase and NAD⁺ synthetase) and assess if neuritogenesis is affected.

Chapter 4

It is necessary to evaluate the expression and activity of SIRT1 after QA treatment. The use of resveratrol during RA and QA treatment could shed some light on its role during differentiation and NRF2 expression.

Assessing whether NRF2 expression alone is sufficient to induce cell differentiation. This could be performed using a recently described method in which the Neh2 domain of NRF2 is deleted, thereby eliminating the Keap1 binding site, which in turn generates a constitutively active transcription factor (Vargas et al., 2013).

The results obtained from exposing SH-SY5Y cells to 3-HAA are a first approximation to what could be a very interesting mechanism of cell death. To determine the mechanism of cell death induced by 3-HAA, the use of ZVAD could determine whether apoptosis is being induced. If this is the case, as it is in other cell lines, this could turn out to be a model to study the induction of apoptosis in neuroblastoma by an increase in ROS production.

Chapter 5 – GENERAL DISCUSSION

Throughout the development of this study, it was noted that many fundamental aspects of SH-SY5Y biology remain a matter of debate. The most relevant to this study were discussed (presence of NMDAR, NGF responsiveness, effectiveness of differentiating protocols, genetic make-up, karyotyping, etc.). Several attempts have been made to unify and explain previous and ongoing inconsistencies (Ross *et al.*, 1995; Encinas *et al.*, 2000; Spengler *et al.*, 2002; Cohen *et al.*, 2003; Sun *et al.*, 2010; Kovalevich and Langford, 2013). Perhaps all these contradictions *in vitro* are a reflection of the multilevel heterogeneity found in neuroblastomas *in vivo* (Speleman *et al.*, 2011), which is another reason why this cell line is a wonderful tool to study the molecular basis of neuroblastoma.

However, the research to date has tended to focus on how to render the SH-SY5Y cell line into a more reliable neuronal model (Xie *et al.*, 2010) for the study of toxicity and neurite extension. A major problem with this type of approach is that the transformant nature of the SH-SY5Y cell line is often ignored and may, in fact, underlie these discrepancies. This attitude is beginning to change, as evidenced by an increase in the number of articles concerned with establishing the transcriptional profile of SH-SY5Y cells in order to determine if they are indeed a good dopaminergic neuronal model (Korecka *et al.*, 2013). Yusuf and collaborators (2013) have recommended that neuroscientists using neuroblastoma cell lines (to study Parkinson's, Alzheimer's or Autism spectrum disorders), ensure that their research is passage number- and karyotype-informed, precisely because of the genetic aberrations that these cell lines are prone to as they continue to proliferate.

As previously mentioned, there is a wide gap between the study of differentiation in SH-SY5Y cells and its applicability in the treatment of neuroblastomas. SH-SY5Y cells have been used to study either the molecular pathways that cause tumour regression or, neuronal toxicity and neuronal differentiation. How the information regarding the SH-SY5Y cells is interpreted depends upon the particular goals of each research group. For instance the effect of (-)-epigallocatechin-3-gallate on SH-SY5Y cells has been reported to be

Chapter 5

neuroprotective by some research groups (Levites et al., 2001; 2002; 2003) and anticarcinogenic by others (Mohan et al., 2011; Hossain et al., 2012).

In this thesis, special care was taken to highlight the results of differentiation and toxicity while bearing in mind the intrinsic transformant nature of the SH-SY5Y cell line. The main finding of this study was that SH-SY5Y neuroblastoma cells were very susceptible to both QA and 3-HAA treatment. These compounds had an effect on the oxidative state of the cells, with profound and varied consequences to their physiology.

For instance, in this study it was shown that ROS elicit at least 3 different responses in SH-SY5Y cells: 1) they slow down proliferation (as evidenced by a marked increase in the viability after SOD treatment); 2) they induce neuritogenesis (Correlation between neurites and ROS production after QA treatment); 3) they induce cell death (by 3-HAA). Even though these may seem contradictory effects, they are all separate but fully compatible processes.

Persistently high ROS levels in cancer cells often lead to increased cell proliferation and adaptive responses that may contribute to tumourigenesis, metastasis, and treatment resistance. Further exposure to exogenous ROS is hypothesized up to a threshold whereby tumour cells (with already very high levels of ROS) can no longer cope with oxidative stress, cell division is then halted and, depending on the severity of the oxidative-associated damage, cell death is induced. Therefore, regulation of the intracellular redox state with neuritogenic QA and toxic 3-HAA (by forcing their intracellular accumulation or by direct administration) may represent an additional strategy to selectively sensitize cancer cells (oxidative stress-inducing therapy).

Small molecules targeting specific components of NAD⁺ and Trp metabolism are rapidly transitioning into the clinic for neuroblastoma. Furthermore, it may be possible to exploit the unique features of neuroblastoma differentiation with respect to QA. In this sense, QA could represent an example of differentiation therapy whereby malignant cells could become benign. However, differentiation therapy only targets a subgroup of cancer cells that are already more susceptible to differentiating stimuli (transit-amplifying cells). Although metabolites used in single-agent-targeted strategies may provide some relief, their curative

Chapter 5

potential in neuroblastoma is likely to require multifaceted treatments exploiting multiple metabolic pathways and careful integration with other agents, such as chemo/radio/immunotherapy, to actively induce cell death. The results herein contained demonstrate, for instance, that not all SH-SY5Y cells respond homogeneously to 3-HAA yet that their repopulating capabilities are extraordinary.

The possibility of using compounds that induce cellular death and differentiation in neuroblastoma cell lines opens exciting therapeutic perspectives: if these observations can be confirmed *in vivo* they could impact the treatment of patients with neuroblastoma where inhibitors of Trp metabolism are currently being used.

Appendix

6.1 Methods carried out by others

HPLC (Dr A. Ferguson, IBLS, University of Glasgow, Glasgow, UK)

Since 3-HAA is a highly unstable and light sensitive compound an antioxidant was added to the samples before being processed and analysed. 250 μ L of cell culture supernatant were mixed with 25 μ L of ascorbic acid (AA, 1.3mM) and 25 μ L of 3-nitrotyrosine (3NTYR, 240 μ M). The samples were then vortexed and 25 μ l perchloric acid (PCA, 2M) were added in order to change the isoelectric point and precipitate any proteins present in the medium. After treatment with PCA the samples were vortexed for exactly 30 seconds to avoid differences in the samples due to extraction efficiency. After mixing samples were centrifuged at 5000g for 10 minutes at 4°C (to get rid of all the protein precipitates that if left in the samples could cause the HPLC machinery to block).

The supernatants were transferred to Alltech filter tubes using centrifugation at 10,000g for 10 minutes at 4°C. The filtered samples were then transferred to chilled autosampler vials. The injection volume of filtered sample extract was 100 μ l. The analysis of 3-HAA was performed with isocratic reverse phase HPLC at 30°C, using a Synergi Hydro column C18. The mobile phase was a solution of 25mM sodium acetate buffer (pH 5) pumped at a flow rate of 1ml/min. 3-HAA was detected by fluorescence using an excitation wavelength of λ_{ex} 320 nm and emission wavelength of λ_{em} 420 nm.

The internal standard, 3NTYR, was determined by the absorbance detector at 365nm, which was connected in series with the fluorescence detector. 0.1357gr of 3NTYR were dissolved in 1mL HCL (1M) and 49mL HPLC-grade water, from this stock solution (12mM). 1 ml of NTYR 12mM was diluted in 49mL HPLC-grade to have a final concentration of 240 μ M.

A standard solution of 3-HAA (2mM) was prepared, since 3-HAA has to be protonated to dissolve, 40 mM hydrochloric acid was used as a solvent. Ascorbic

acid (μM) was added to stop 3-HAA breakdown. These stock solutions were frozen in aliquots of $600\mu\text{L}$ at -40°C .

For each experimental run, a standard curve was prepared. The stock solutions of standard 3-HAA were defrosted and mixed together using serial dilutions of up to 1 in 20 as follows:

$200\ \mu\text{M} = 0.5\text{mL } 2\text{mM } 3\text{-HAA} + 0.5\text{ml AA} + 4\text{mL } 100\ \mu\text{M ascorbic acid}$

$20\ \mu\text{M} = 0.5\text{mL } 200\ \mu\text{M } 3\text{-HAA} + 4.5\text{mL } 100\ \mu\text{M ascorbic acid}$

$4\ \mu\text{M} = 1\text{ml } 20\ \mu\text{M } 3\text{-HAA} + 4\text{ml } 100\ \mu\text{M ascorbic acid}$

To make the standards comparable with the experimental samples, various volumes of these mixed standards were diluted with water, ascorbic acid and PCA. A blank of ascorbic acid and PCA was also prepared (see Table 7).

STD	3-haa (nM)	AA (nM)	Mix STD	Vol STD	100 μM vol asc acid	300 μM vol asc acid	3-NTYR VOL IS (μL)	1 M Vol PCA (μL)
1	1	1	3	25	225	25	25	25
2	4	4	3	100	150	25	25	25
3	7	7	3	175	75	25	25	25
4	12	12	2	37.5	212.5	25	25	25
5	16	16	2	50	200	25	25	25
6	24	24	2	75	175	25	25	25
7	32	32	2	100	150	25	25	25
8	40	40	1	25	225	25	25	25
BLANK	0	0	-	0	275	25	25	25

Table 7 Preparation of standard solutions for calibrations curves of 3-HAA. Standard (Std), 4M perchloric acid (PCA)

The 8 standards plus the blank were filtered using $0.2\mu\text{m}$ Alltech filter tubes by centrifugation at $10,000\text{g}$ for 10 minutes at 4°C .

The standard solutions were intercalated with the experimental samples (every 8 or 10 vials) to check for any changes in the retention times of the metabolites. A new calibration curve was run after any shutdown of the HPLC. A blank, containing only water, ascorbic acid and PCA was run with each calibration curve to ensure the baseline was completely flat at the retention times for the peaks of interest

6.2 Table of clinical trials targeting IDO in the treatment of cancer

Title	Identifier	Status	Goal
1.- IDO Inhibitor Study For Relapsed Or Refractory Solid Tumours	NCT00739609	Terminated	Determine the safety and efficacy of D1-MT in patients with recurrent or refractory solid tumours. Establish the toxicities of D1-MT and define any dose-limiting toxicities
2.- IDO2 Genetic Status Informs The Neoadjuvant Efficacy Of Chloroquine (CQ) In Brain Metastasis	NCT01727531	Recruiting	Phase I trial to study effects and optimal dose of 1-DMT in treating patients with metastatic or refractory solid tumours that cannot be removed by surgery.
3.- D1-MT and Docetaxel in treating patients with metastatic solid	NCT01191216	Recruiting	Phase I trial to study the effects and best dose for giving D1-MT and Docetaxel together in treating patients with metastatic solid tumours.
4.- Vaccine therapy in treating patients with metastatic breast cancer	NCT01042535	Recruiting	Randomized Phase I/II trial to study the side-effects and best dose of giving vaccine therapy and to assess the effectiveness in treating patients with metastatic breast cancer.
5.- Study Of Chemotherapy In Combination With IDO Inhibitor In Metastatic Breast Cancer	NCT01792050	Recruiting	To compare the effects of Docetaxel(standard treatment) with/without the co-administration of 1-DMT. Metastatic Breast Cancer
6.- Phase II study of Sipuleucel-T and Indoximod for patients with refractory metastatic prostate cancer	NCT01560923	Recruiting	Phase II trial studying the effect of Indoximod or placebo after the completion of standard of care treatment Sipuleucel-T.
7.- Peptide Vaccine And Temozolomide For Metastatic Melanoma Patients	NCT01543464	Recruiting	Phase II studying the clinical benefit rate of an IDO/survivin peptide vaccine malignant melanoma Malignant Melanoma
8.- A Phase 1/2 Randomized, Blinded, Placebo Controlled Study Of Ipilimumab In Combination With INCB024360 Or Placebo In Subjects With Unresectable or Metastatic Melanoma	NCT01604889	Recruiting	Study the safety, tolerability, optimal dose and effect of the combination of INCB024360 and ipilimumab in patients with metastatic Melanoma
9.- A Phase 2 Study Of The IDO Inhibitor INCB024360 Versus Tamoxifen For Subjects With Biochemical- Recurrent-Only EOC, PPC Or FTC Following Complete Remission With First-Line	NCT01685255	Active, Not Recruiting	Phase II trial to study the safety and tolerability of INCB0243602 as well as the progression of solid tumours by assessing the expression of cancer antigens and imaging techniques.
10.- 1-Methyl-D-Tryptophan In Treating Patients With Metastatic Or Refractory Solid Tumours That Cannot	NCT00567931	Completed	Phase I trial studying the expression of IDO, the pharmacokinetics of 1-DMT as well as changes in the Trp/kynurenine ratio and in the number of circulating CD4+ CD25+ T _{reg} cells in unspecified adult solid tumours.

11.- Phase II INCB024360 Study For Patients With Myelodysplastic Syndromes (MDS)	NCT01822691	Active Not Recruiting	Phase II trial studying the best overall response rate and progression of Myelodysplastic Syndromes treated with INCB024360
15.- Indoleamine 2,3-Dioxygenase (IDO) Activity In Patients With Chronic Lymphocytic	NCT01397916	Completed	Prospective study assessing the activity of IDO in patients with CLL
16.- IDO Peptide Vaccination for Stage III-IV Non Small-cell Lung Cancer Patients.	NCT01219348	Completed	Phase I trial assessing the toxicity and the immunological /clinical responses after peptide IDO vaccination in Non-small-cell-lung-carcinoma
17.- INCB024360 and Vaccine Therapy in Treating Patients With Stage III-IV Melanoma	NCT01961115	Recruiting	Phase II trial evaluating the immune response (number/character/transcriptome of CD8+, CD4+, T and NK cells) as well as the adverse effects following peptide vaccination (12 class I MHC-restricted melanoma peptides and a class II MHC-restricted tetanus toxoid helper peptide) and IDO inhibitor in melanoma
18.- Vaccine Therapy and IDO1 Inhibitor INCB024360 in Treating Patients With Epithelial Ovarian, Fallopian Tube, or Primary Peritoneal Cancer Who Are in Remission	NCT01982487	Withdrawn	Phase I/II trial studying the maximum tolerated dose of IDO1 inhibitor INCB024360 and the related immunological response in several types of uterine cancer.
19.- INCB024360 Before Surgery in Treating Patients With Newly Diagnosed Stage III-IV Epithelial Ovarian, Fallopian Tube, or Primary Peritoneal Cancer	NCT02042430	Recruiting	Pilot clinical trial studying the number/character/transcriptome change in tumour infiltrating cells, peripheral blood mononuclear cells, and ascites as well as the change viral responses and the Trp/Kyn ratio in fallopian tube cancer following pre-surgical treatment with an IDO inhibitor
20.- IDO Inhibitor Study for Advanced Solid Tumours	NCT02048709	Recruiting	Phase I studying the safety, maximum tolerated dose and pharmacokinetics of IDO-1 inhibitor as well as the overall survival of patients with solid Lung, Breast, pancreas
21.- Study of IDO Inhibitor and Temozolomide for Adult Patients With Primary Malignant Brain Tumours	NCT02052648	Recruiting	Phase I/II trial comparing the safety/tolerability/pharmacokinetics of IDO inhibitors and temozolomide treatment against historical controls of temozolomide alone in patients with glioblastoma.
22.- Study of IDO Inhibitor in Combination With Ipilimumab for Adult Patients With Metastatic Melanoma	NCT02073123	Recruiting	Phase I/II trial studying safety/tolerability as well as overall survival and the mechanisms underlying the activity/resistance to IDO/CTLA-4 inhibitor therapy.
24.- Study of IDO Inhibitor in Combination With Gemcitabine and Nab-Paclitaxel in Patients With Metastatic Pancreatic Cancer	NCT02077881	Not yet recruiting	Phase I/II trial studying dosing/toxicity of IDO inhibitor co-administered with a chemotherapeutic agent (gemcitabine) and a microtubule stabiliser (nab-paclitaxel) as well as the overall survival and response time.

25.- Intraperitoneal Natural Killer Cells and INCB024360 for Recurrent Ovarian, Fallopian Tube, and Primary Peritoneal Cancer	NCT02118285	Recruiting	Phase I trial evaluating the maximum tolerated dose of INCB024360, the initial tumour response (and duration) as well as overall survival and progression-free survival in patients with ovarian Cancer, fallopian tube carcinoma and Primary Peritoneal Carcinoma
26.- DEC-205/NY-ESO-1 Fusion Protein CDX-1401, Poly ICLC, and IDO1 Inhibitor INCB024360 in Treating Patients With Ovarian, Fallopian Tube, or Primary Peritoneal Cancer in Remission	NCT02166905	Recruiting	Phase I/II trial assessing the maximum tolerated dose, overall survival as well as the frequency and functioning of memory t-cells/CD8+ and CD4+ T-cells recognizing the tumour antigen NY-ESO-1.

Table 8 Clinical trials targeting the kynurenine pathway enzyme Indolamine 2,3-dioxygenase. Information obtained and modified from <http://Clinicaltrials.gov>.

6.3 Neurite/soma ratio after 3-HAA treatment

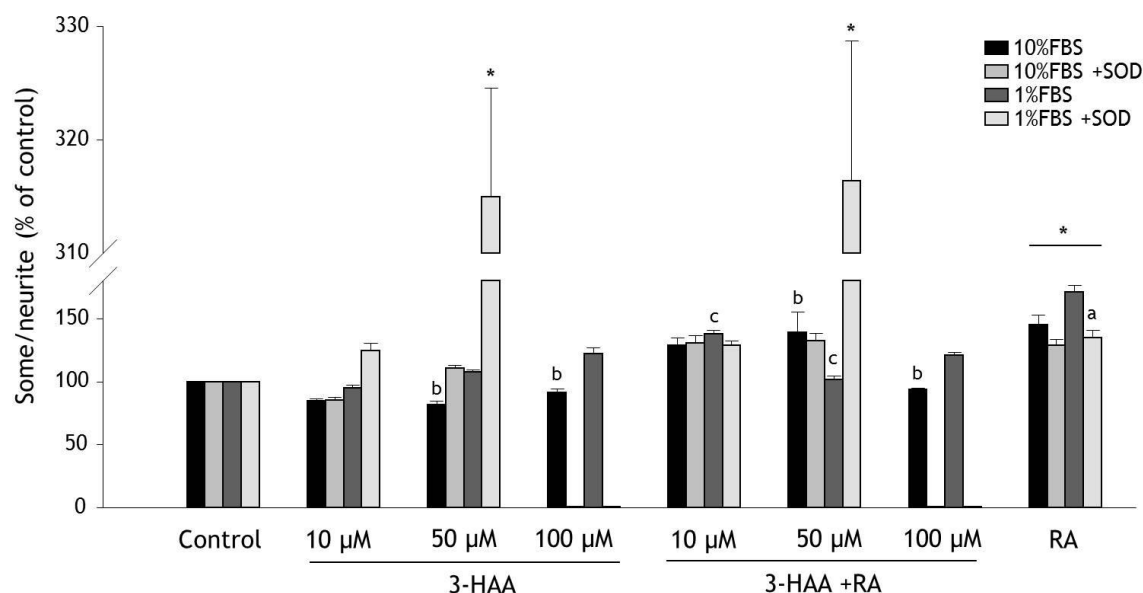


Figure 32 Effect of a single 3-HAA treatment on the Neurite/Cell body ratio, 48 h after treatment. Micrographs were taken 48 h after treatment with different concentrations of 3-HAA (10 μM, 50 μM and 100 μM) in 1% FBS medium or 10% FBS medium. Some cultures were co-incubated with 300u/ml SOD and 10 μM RA. Results are expressed as percentage of control. Mean ± S.E.M. for 4 different experiments. * $P < 0.05$ vs. control. a $P < 0.05$ vs. same treatment with SOD. b $P < 0.05$ vs. same treatment in 1% FBS medium. c $P < 0.05$ vs. RA in 1% FBS medium

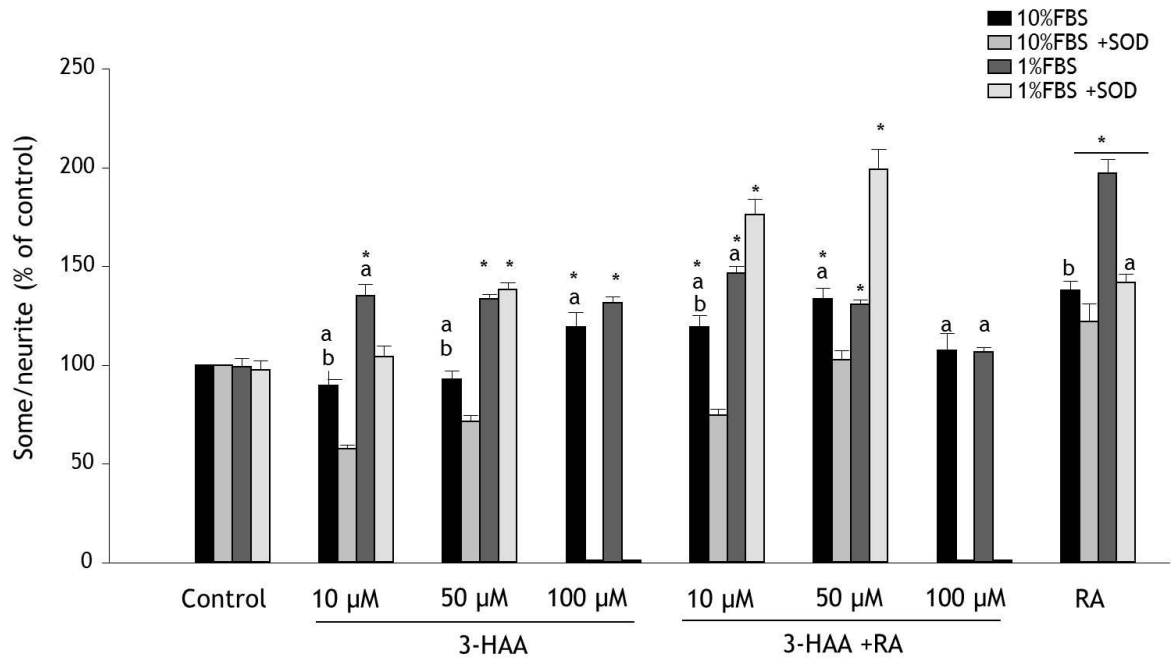


Figure 33 Effect of a single 3-HAA treatment on the Neurite/Cell body ratio, 72 h after treatment. Micrographs were taken 72 h after treatment with different concentrations of 3-HAA (10 μ M, 50 μ M and 100 μ M) in 1% FBS medium or 10% FBS medium. Some cultures were co-incubated with 300u/ml SOD and 10 μ M RA. Results are expressed as percentage of control. Mean \pm S.E.M. for 4 different experiments. * $P < 0.05$ vs. control. a $P < 0.05$ vs. same treatment with SOD. b $P < 0.05$ vs. same treatment in 1% FBS medium. c $P < 0.05$ vs. RA in 1% FBS medium.

List of References

- Aanerud J, Borghammer P, Chakravarty MM, Vang K, Rodell AB, Jonsdottir KY, Moller A, Ashkanian M, Vafae MS, Iversen P, Johannsen P, Gjedde A (2012) Brain energy metabolism and blood flow differences in healthy aging. *Journal of cerebral blood flow and metabolism : official journal of the International Society of Cerebral Blood Flow and Metabolism* 32:1177-1187.
- Adams S, Braidy N, Bessede A, Brew BJ, Grant R, Teo C, Guillemin GJ (2012) The kynurenine pathway in brain tumor pathogenesis. *Cancer research* 72:5649-5657.
- Agani F, Jiang BH (2013) Oxygen-independent regulation of HIF-1: novel involvement of PI3K/AKT/mTOR pathway in cancer. *Current cancer drug targets* 13:245-251.
- Aggeli IK, Gaitanaki C, Beis I (2006) Involvement of JNKs and p38-MAPK/MSK1 pathways in H₂O₂-induced upregulation of heme oxygenase-1 mRNA in H9c2 cells. *Cellular signalling* 18:1801-1812.
- Agholme L, Lindstrom T, Kagedal K, Marcusson J, Hallbeck M (2010) An in vitro model for neuroscience: differentiation of SH-SY5Y cells into cells with morphological and biochemical characteristics of mature neurons. *Journal of Alzheimer's disease : JAD* 20:1069-1082.
- Aksoy P, White TA, Thompson M, Chini EN (2006) Regulation of intracellular levels of NAD: a novel role for CD38. *Biochemical and biophysical research communications* 345:1386-1392.
- Aktipis CA, Boddy AM, Gatenby RA, Brown JS, Maley CC (2013) Life history trade-offs in cancer evolution. *Nature reviews Cancer* 13:883-892.
- Alderton WK, Cooper CE, Knowles RG (2001) Nitric oxide synthases: structure, function and inhibition. *The Biochemical journal* 357:593-615.
- Alexander SP, Mathie A, Peters JA (2011) *Guide to Receptors and Channels (GRAC)*, 5th edition. *Br J Pharmacol* 164 Suppl 1:S1-324.
- Aloe L, Rocco ML, Bianchi P, Manni L (2012) Nerve growth factor: from the early discoveries to the potential clinical use. *Journal of translational medicine* 10:239.
- Alvarez MN, Trujillo M, Radi R (2002) Peroxynitrite formation from biochemical and cellular fluxes of nitric oxide and superoxide. *Methods in enzymology* 359:353-366.
- Arakawa M, Ishimura A, Arai Y, Kawabe K, Suzuki S, Ishige K, Ito Y (2007) N-Acetylcysteine and ebselen but not nifedipine protected cerebellar granule neurons against 4-hydroxynonenal-induced neuronal death. *Neuroscience research* 57:220-229.

- Araki T, Sasaki Y, Milbrandt J (2004) Increased nuclear NAD biosynthesis and SIRT1 activation prevent axonal degeneration. *Science* 305:1010-1013.
- Araneda S, Pelloux S, Radicella JP, Angulo J, Kitahama K, Gysling K, Forray MI (2005) 8-oxoguanine DNA glycosylase, but not Kin17 protein, is translocated and differentially regulated by estrogens in rat brain cells. *Neuroscience* 136:135-146.
- Arlt A, Sebens S, Krebs S, Geismann C, Grossmann M, Kruse ML, Schreiber S, Schafer H (2013) Inhibition of the Nrf2 transcription factor by the alkaloid trigonelline renders pancreatic cancer cells more susceptible to apoptosis through decreased proteasomal gene expression and proteasome activity. *Oncogene* 32:4825-4835.
- Asayama C (1916) Feeding Experiments with Kynurenic Acid. *The Biochemical journal* 10:466-472.
- Attwell D, Laughlin SB (2001) An energy budget for signaling in the grey matter of the brain. *Journal of cerebral blood flow and metabolism : official journal of the International Society of Cerebral Blood Flow and Metabolism* 21:1133-1145.
- Backhaus C, Rahman H, Scheffler S, Laatsch H, Hardeland R (2008) NO scavenging by 3-hydroxyanthranilic acid and 3-hydroxykynurenine: N-nitrosation leads via oxadiazoles to o-quinone diazides. *Nitric oxide : biology and chemistry / official journal of the Nitric Oxide Society* 19:237-244.
- Balaban-Malenbaum G, Gilbert F (1977) Double minute chromosomes and the homogeneously staining regions in chromosomes of a human neuroblastoma cell line. *Science* 198:739-741.
- Balaban RS, Nemoto S, Finkel T (2005) Mitochondria, oxidants, and aging. *Cell* 120:483-495.
- Balazs R (2006) Trophic effect of glutamate. *Current topics in medicinal chemistry* 6:961-968.
- Balazs R, Jorgensen OS, Hack N (1988) N-methyl-D-aspartate promotes the survival of cerebellar granule cells in culture. *Neuroscience* 27:437-451.
- Baran H, Schwarcz R (1990) Presence of 3-hydroxyanthranilic acid in rat tissues and evidence for its production from anthranilic acid in the brain. *J Neurochem* 55:738-744.
- Baran H, Cairns N, Lubec B, Lubec G (1996) Increased kynurenic acid levels and decreased brain kynurenine aminotransferase I in patients with Down syndrome. *Life Sci* 58:1891-1899.
- Baret A, Emerit I (1983) Variation of superoxide dismutase levels in fetal calf serum. *Mutat Res* 121:293-297.
- Bauer G (2014) Targeting extracellular ROS signaling of tumor cells. *Anticancer Res* 34:1467-1482.

- Beadle GW, Mitchell HK, Nyc JF (1947) Kynurenine as an Intermediate in the Formation of Nicotinic Acid from Tryptophane by *Neurospora*. *Proc Natl Acad Sci U S A* 33:155-158.
- Beal MF (2005) Mitochondria take center stage in aging and neurodegeneration. *Annals of neurology* 58:495-505.
- Beal MF, Shults CW (2003) Effects of Coenzyme Q10 in Huntington's disease and early Parkinson's disease. *BioFactors* 18:153-161.
- Beal MF, Swartz KJ, Isacson O (1992) Developmental changes in brain kynurenic acid concentrations. *Brain research Developmental brain research* 68:136-139.
- Beal MF, Kowall NW, Ellison DW, Mazurek MF, Swartz KJ, Martin JB (1986) Replication of the neurochemical characteristics of Huntington's disease by quinolinic acid. *Nature* 321:168-171.
- Beck B, Blanpain C (2013) Unravelling cancer stem cell potential. *Nature reviews Cancer* 13:727-738.
- Beckman JS, Koppenol WH (1996) Nitric oxide, superoxide, and peroxynitrite: the good, the bad, and ugly. *The American journal of physiology* 271:C1424-1437.
- Bedard K, Krause KH (2007) The NOX family of ROS-generating NADPH oxidases: physiology and pathophysiology. *Physiological reviews* 87:245-313.
- Behar TN, Scott CA, Greene CL, Wen X, Smith SV, Maric D, Liu QY, Colton CA, Barker JL (1999) Glutamate acting at NMDA receptors stimulates embryonic cortical neuronal migration. *The Journal of neuroscience : the official journal of the Society for Neuroscience* 19:4449-4461.
- Behe P, Stern P, Wyllie DJ, Nassar M, Schoepfer R, Colquhoun D (1995) Determination of NMDA NR1 subunit copy number in recombinant NMDA receptors. *Proceedings Biological sciences / The Royal Society* 262:205-213.
- Belenky P, Bogan KL, Brenner C (2007) NAD⁺ metabolism in health and disease. *Trends in biochemical sciences* 32:12-19.
- Bender DA, McCreanor GM (1982) The preferred route of kynurenine metabolism in the rat. *Biochimica et biophysica acta* 717:56-60.
- Berciano MT, Lafarga M (1988) Colony-forming ectopic granule cells in the cerebellar primary fissure of normal adult rats: a morphologic and morphometric study. *Brain research* 439:169-178.
- Berthold F, Simon T (2005) Clinical Presentation Neuroblastoma. In: (Cheung N-K, Cohn S, eds), pp 63-85: Springer Berlin Heidelberg.
- Bertolotti M, Yim SH, Garcia-Manteiga JM, Masciarelli S, Kim YJ, Kang MH, Iuchi Y, Fujii J, Vene R, Rubartelli A, Rhee SG, Sitia R (2010) B- to plasma-cell terminal differentiation entails oxidative stress and profound reshaping of the antioxidant responses. *Antioxidants & redox signaling* 13:1133-1144.

- Beske PH, Jackson DA (2012) NADPH oxidase mediates the oxygen-glucose deprivation/reperfusion-induced increase in the tyrosine phosphorylation of the N-methyl-D-aspartate receptor NR2A subunit in retinoic acid differentiated SH-SY5Y Cells. *Journal of molecular signaling* 7:15.
- Bi TQ, Che XM, Liao XH, Zhang DJ, Long HL, Li HJ, Zhao W (2011) Overexpression of Nampt in gastric cancer and chemopotentiating effects of the Nampt inhibitor FK866 in combination with fluorouracil. *Oncology reports* 26:1251-1257.
- Biedler JL, Spengler BA (1976) Metaphase chromosome anomaly: association with drug resistance and cell-specific products. *Science* 191:185-187.
- Biedler JL, Helson L, Spengler BA (1973) Morphology and growth, tumorigenicity, and cytogenetics of human neuroblastoma cells in continuous culture. *Cancer research* 33:2643-2652.
- Biedler JL, Roffler-Tarlov S, Schachner M, Freedman LS (1978) Multiple neurotransmitter synthesis by human neuroblastoma cell lines and clones. *Cancer research* 38:3751-3757.
- Birch PJ, Grossman CJ, Hayes AG (1988) Kynurenate and FG9041 have both competitive and non-competitive antagonist actions at excitatory amino acid receptors. *Eur J Pharmacol* 151:313-315.
- Bitton-Worms K, Pikarsky E, Aronheim A (2010) The AP-1 repressor protein, JDP2, potentiates hepatocellular carcinoma in mice. *Molecular cancer* 9:54.
- Blander G, de Oliveira RM, Conboy CM, Haigis M, Guarente L (2003) Superoxide dismutase 1 knock-down induces senescence in human fibroblasts. *J Biol Chem* 278:38966-38969.
- Blander G, Bhimavarapu A, Mammone T, Maes D, Elliston K, Reich C, Matsui MS, Guarente L, Loureiro JJ (2009) SIRT1 promotes differentiation of normal human keratinocytes. *The Journal of investigative dermatology* 129:41-49.
- Bobilev I, Novik V, Levi I, Shpilberg O, Levy J, Sharoni Y, Studzinski GP, Danilenko M (2011) The Nrf2 transcription factor is a positive regulator of myeloid differentiation of acute myeloid leukemia cells. *Cancer biology & therapy* 11:317-329.
- Bonina FP, Arenare L, Ippolito R, Boatto G, Battaglia G, Bruno V, de Caprariis P (2000) Synthesis, pharmacokinetics and anticonvulsant activity of 7-chlorokynurenic acid prodrugs. *International journal of pharmaceuticals* 202:79-88.
- Bough KJ, Wetherington J, Hassel B, Pare JF, Gawryluk JW, Greene JG, Shaw R, Smith Y, Geiger JD, Dingledine RJ (2006) Mitochondrial biogenesis in the anticonvulsant mechanism of the ketogenic diet. *Annals of neurology* 60:223-235.

- Bours V, Bentires-Alj M, Hellin AC, Viatour P, Robe P, Delhalle S, Benoit V, Merville MP (2000) Nuclear factor-kappa B, cancer, and apoptosis. *Biochemical pharmacology* 60:1085-1089.
- Braidy N, Grant R, Brew BJ, Adams S, Jayasena T, Guillemin GJ (2009) Effects of Kynurenine Pathway Metabolites on Intracellular NAD Synthesis and Cell Death in Human Primary Astrocytes and Neurons. *International journal of tryptophan research : IJTR* 2:61-69.
- Brigelius-Flohe R (1999) Tissue-specific functions of individual glutathione peroxidases. *Free radical biology & medicine* 27:951-965.
- Brocke KS, Staufner C, Luksch H, Geiger KD, Stepulak A, Marzahn J, Schackert G, Temme A, Ikonomidou C (2010) Glutamate receptors in pediatric tumors of the central nervous system. *Cancer biology & therapy* 9:455-468.
- Brodeur GM, Sekhon G, Goldstein MN (1977) Chromosomal aberrations in human neuroblastomas. *Cancer* 40:2256-2263.
- Brodeur GM, Green AA, Hayes FA, Williams KJ, Williams DL, Tsiatis AA (1981) Cytogenetic features of human neuroblastomas and cell lines. *Cancer research* 41:4678-4686.
- Brunet A, Sweeney LB, Sturgill JF, Chua KF, Greer PL, Lin Y, Tran H, Ross SE, Mostoslavsky R, Cohen HY, Hu LS, Cheng HL, Jedrychowski MP, Gygi SP, Sinclair DA, Alt FW, Greenberg ME (2004) Stress-dependent regulation of FOXO transcription factors by the SIRT1 deacetylase. *Science* 303:2111-2115.
- Bryan HK, Olayanju A, Goldring CE, Park BK (2013) The Nrf2 cell defence pathway: Keap1-dependent and -independent mechanisms of regulation. *Biochemical pharmacology* 85:705-717.
- Canals M, Angulo E, Casado V, Canela EI, Mallol J, Vinals F, Staines W, Tinner B, Hillion J, Agnati L, Fuxe K, Ferre S, Lluís C, Franco R (2005) Molecular mechanisms involved in the adenosine A and A receptor-induced neuronal differentiation in neuroblastoma cells and striatal primary cultures. *J Neurochem* 92:337-348.
- Cannazza G, Chiarugi A, Parenti C, Zanoli P, Baraldi M (2001) Changes in kynurenic, anthranilic, and quinolinic acid concentrations in rat brain tissue during development. *Neurochemical research* 26:511-514.
- Canto C, Sauve AA, Bai P (2013) Crosstalk between poly(ADP-ribose) polymerase and sirtuin enzymes. *Molecular aspects of medicine* 34:1168-1201.
- Cantor JR, Sabatini DM (2012) Cancer cell metabolism: one hallmark, many faces. *Cancer discovery* 2:881-898.
- Carlin JM, Ozaki Y, Byrne GI, Brown RR, Borden EC (1989) Interferons and indoleamine 2,3-dioxygenase: role in antimicrobial and antitumor effects. *Experientia* 45:535-541.

- Carpenedo R, Pittaluga A, Cozzi A, Attucci S, Galli A, Raiteri M, Moroni F (2001) Presynaptic kynurenate-sensitive receptors inhibit glutamate release. *Eur J Neurosci* 13:2141-2147.
- Cavalheiro EA, Olney JW (2001) Glutamate antagonists: deadly liaisons with cancer. *Proc Natl Acad Sci U S A* 98:5947-5948.
- Cecchi C, Pensalfini A, Liguri G, Baglioni S, Fiorillo C, Guadagna S, Zampagni M, Formigli L, Nosi D, Stefani M (2008) Differentiation increases the resistance of neuronal cells to amyloid toxicity. *Neurochemical research* 33:2516-2531.
- Chadha R, Mahal HS, Mukherjee T, Kapoor S (2009) Evidence for a possible role of 3-hydroxyanthranilic acid as an antioxidant. *Journal of Physical Organic Chemistry* 22:349-354.
- Chan EC, Jiang F, Peshavariya HM, Dusting GJ (2009) Regulation of cell proliferation by NADPH oxidase-mediated signaling: potential roles in tissue repair, regenerative medicine and tissue engineering. *Pharmacology & therapeutics* 122:97-108.
- Chance B, Sies H, Boveris A (1979) Hydroperoxide metabolism in mammalian organs. *Physiological reviews* 59:527-605.
- Chandra J, Samali A, Orrenius S (2000) Triggering and modulation of apoptosis by oxidative stress. *Free radical biology & medicine* 29:323-333.
- Chatterton JE, Awobuluyi M, Premkumar LS, Takahashi H, Talantova M, Shin Y, Cui J, Tu S, Sevarino KA, Nakanishi N, Tong G, Lipton SA, Zhang D (2002) Excitatory glycine receptors containing the NR3 family of NMDA receptor subunits. *Nature* 415:793-798.
- Chen J, Chattopadhyay B, Venkatakrishnan G, Ross AH (1990) Nerve growth factor-induced differentiation of human neuroblastoma and neuroepithelioma cell lines. *Cell growth & differentiation : the molecular biology journal of the American Association for Cancer Research* 1:79-85.
- Chen J, Jin K, Chen M, Pei W, Kawaguchi K, Greenberg DA, Simon RP (1997) Early detection of DNA strand breaks in the brain after transient focal ischemia: implications for the role of DNA damage in apoptosis and neuronal cell death. *J Neurochem* 69:232-245.
- Chen J, Zhou Y, Mueller-Steiner S, Chen LF, Kwon H, Yi S, Mucke L, Gan L (2005) SIRT1 protects against microglia-dependent amyloid-beta toxicity through inhibiting NF-kappaB signaling. *J Biol Chem* 280:40364-40374.
- Chen JH, Hales CN, Ozanne SE (2007) DNA damage, cellular senescence and organismal ageing: causal or correlative? *Nucleic Acids Res* 35:7417-7428.
- Chen JH, Stoeber K, Kingsbury S, Ozanne SE, Williams GH, Hales CN (2004) Loss of proliferative capacity and induction of senescence in oxidatively stressed human fibroblasts. *J Biol Chem* 279:49439-49446.

- Cheng X, Holenya P, Can S, Alborzinia H, Rubbiani R, Ott I, Wolf S (2014) A TrxR inhibiting gold(I) NHC complex induces apoptosis through ASK1-p38-MAPK signaling in pancreatic cancer cells. *Molecular cancer* 13:221.
- Cheung YT, Lau WK, Yu MS, Lai CS, Yeung SC, So KF, Chang RC (2009) Effects of all-trans-retinoic acid on human SH-SY5Y neuroblastoma as in vitro model in neurotoxicity research. *Neurotoxicology* 30:127-135.
- Chiarugi A, Carpenedo R, Moroni F (1996) Kynurenine disposition in blood and brain of mice: effects of selective inhibitors of kynurenine hydroxylase and of kynureninase. *J Neurochem* 67:692-698.
- Chiarugi A, Dolle C, Felici R, Ziegler M (2012) The NAD metabolome--a key determinant of cancer cell biology. *Nature reviews Cancer* 12:741-752.
- Chiarugi A, Carpenedo R, Molina MT, Mattoli L, Pellicciari R, Moroni F (1995) Comparison of the neurochemical and behavioral effects resulting from the inhibition of kynurenine hydroxylase and/or kynureninase. *J Neurochem* 65:1176-1183.
- Christen S, Southwell-Keely PT, Stocker R (1992) Oxidation of 3-hydroxyanthranilic acid to the phenoxazinone cinnabarinic acid by peroxy radicals and by compound I of peroxidases or catalase. *Biochemistry* 31:8090-8097.
- Christen S, Thomas SR, Garner B, Stocker R (1994) Inhibition by interferon-gamma of human mononuclear cell-mediated low density lipoprotein oxidation. Participation of tryptophan metabolism along the kynurenine pathway. *J Clin Invest* 93:2149-2158.
- Cimino F, Esposito F, Ammendola R, Russo T (1997) Gene regulation by reactive oxygen species. *Curr Top Cell Regul* 35:123-148.
- Cobbold SP, Adams E, Farquhar CA, Nolan KF, Howie D, Lui KO, Fairchild PJ, Mellor AL, Ron D, Waldmann H (2009) Infectious tolerance via the consumption of essential amino acids and mTOR signaling. *Proc Natl Acad Sci U S A* 106:12055-12060.
- Coggan SE, Smythe GA, Bilgin A, Grant RS (2009) Age and circadian influences on picolinic acid concentrations in human cerebrospinal fluid. *J Neurochem* 108:1220-1225.
- Cohen N, Betts DR, Rechavi G, Amariglio N, Trakhtenbrot L (2003) Clonal expansion and not cell interconversion is the basis for the neuroblast and nonneuronal types of the SK-N-SH neuroblastoma cell line. *Cancer genetics and cytogenetics* 143:80-84.
- Collingridge GL, Olsen RW, Peters J, Spedding M (2009) A nomenclature for ligand-gated ion channels. *Neuropharmacology* 56:2-5.
- Collins AR, Cadet J, Moller L, Poulsen HE, Vina J (2004) Are we sure we know how to measure 8-oxo-8-dihydroguanine in DNA from human cells? *Arch. Biochem. Biophys.*, 423. 7 SRC - GoogleScholar:57-65.

- Connick JH, Stone TW, Carla V, Moroni F (1988) Increased kynurenic acid levels in Huntington's disease. *Lancet* 2:1373.
- Connick JH, Carla V, Moroni F, Stone TW (1989) Increase in kynurenic acid in Huntington's disease motor cortex. *J Neurochem* 52:985-987.
- Connick JH, Heywood GC, Sills GJ, Thompson GG, Brodie MJ, Stone TW (1992) Nicotylalanine increases cerebral kynurenic acid content and has anticonvulsant activity. *General pharmacology* 23:235-239.
- Constantinescu R, Constantinescu AT, Reichmann H, Janetzky B (2007) Neuronal differentiation and long-term culture of the human neuroblastoma line SH-SY5Y. *Journal of neural transmission Supplementum*:17-28.
- Copeland CS, Neale SA, Salt TE (2013) Actions of Xanthurenic acid, a putative endogenous Group II metabotropic glutamate receptor agonist, on sensory transmission in the thalamus. *Neuropharmacology* 66:133-142.
- Cosi C, Mannaioni G, Cozzi A, Carla V, Sili M, Cavone L, Maratea D, Moroni F (2011) G-protein coupled receptor 35 (GPR35) activation and inflammatory pain: Studies on the antinociceptive effects of kynurenic acid and zaprinast. *Neuropharmacology* 60:1227-1231.
- Couillard-Despres S, Winner B, Schaubeck S, Aigner R, Vroemen M, Weidner N, Bogdahn U, Winkler J, Kuhn HG, Aigner L (2005) Doublecortin expression levels in adult brain reflect neurogenesis. *Eur J Neurosci* 21:1-14.
- Cui Y, Shen YT, Kalthof B, Iwase M, Sato N, Uechi M, Vatner SF, Vatner DE (1996) Identification and functional role of beta-adrenergic receptor subtypes in primate and rodent: in vivo versus isolated myocytes. *J Mol Cell Cardiol* 28:1307-1317.
- Cull-Candy SG, Leszkiewicz DN (2004) Role of distinct NMDA receptor subtypes at central synapses. *Science's STKE : signal transduction knowledge environment* 2004:re16.
- Cull-Candy SG, Howe JR, Ogden DC (1988) Noise and single channels activated by excitatory amino acids in rat cerebellar granule neurones. *J Physiol* 400:189-222.
- D'Mello S A, Flanagan JU, Green TN, Leung EY, Askarian-Amiri ME, Joseph WR, McCrystal MR, Isaacs RJ, Shaw JH, Furneaux CE, During MJ, Finlay GJ, Baguley BC, Kalev-Zylinska ML (2014) Evidence That GRIN2A Mutations in Melanoma Correlate with Decreased Survival. *Frontiers in oncology* 3:333.
- da Frota Junior ML, Pires AS, Zeidan-Chulia F, Bristot IJ, Lopes FM, de Bittencourt Pasquali MA, Zanotto-Filho A, Behr GA, Klamt F, Gelain DP, Moreira JC (2011) In vitro optimization of retinoic acid-induced neuritogenesis and TH endogenous expression in human SH-SY5Y neuroblastoma cells by the antioxidant Trolox. *Molecular and cellular biochemistry* 358:325-334.

- Danysz W, Parsons CG (1998) GlycineB recognition site of NMDA receptors and its antagonists. *Amino acids* 14:205-206.
- Danysz W, Fadda E, Wroblewski JT, Costa E (1989a) Different modes of action of 3-amino-1-hydroxy-2-pyrrolidone (HA-966) and 7-chlorokynurenic acid in the modulation of N-methyl-D-aspartate-sensitive glutamate receptors. *Molecular pharmacology* 36:912-916.
- Danysz W, Fadda E, Wroblewski JT, Costa E (1989b) Kynurenate and 2-amino-5-phosphonovalerate interact with multiple binding sites of the N-methyl-D-aspartate-sensitive glutamate receptor domain. *Neurosci Lett* 96:340-344.
- Datki Z, Juhasz A, Galfi M, Soos K, Papp R, Zadori D, Penke B (2003) Method for measuring neurotoxicity of aggregating polypeptides with the MTT assay on differentiated neuroblastoma cells. *Brain research bulletin* 62:223-229.
- Dayem AA, Choi HY, Kim JH, Cho SG (2010) Role of oxidative stress in stem, cancer, and cancer stem cells. *Cancers* 2:859-884.
- de Carvalho LP, Bochet P, Rossier J (1996) The endogenous agonist quinolinic acid and the non endogenous homoquinolinic acid discriminate between NMDAR2 receptor subunits. *Neurochemistry international* 28:445-452.
- de Rivero Vaccari JC, Casey GP, Aleem S, Park WM, Corriveau RA (2006) NMDA receptors promote survival in somatosensory relay nuclei by inhibiting Bax-dependent developmental cell death. *Proc Natl Acad Sci U S A* 103:16971-16976.
- Decker RH, Brown RR, Price JM (1963) Studies on the biological activity of nicotinylalanine, an analogue of kynurenine. *J Biol Chem* 238:1049-1053.
- DeNicola GM, Karreth FA, Humpton TJ, Gopinathan A, Wei C, Frese K, Mangal D, Yu KH, Yeo CJ, Calhoun ES, Scrimieri F, Winter JM, Hruban RH, Iacobuzio-Donahue C, Kern SE, Blair IA, Tuveson DA (2011) Oncogene-induced Nrf2 transcription promotes ROS detoxification and tumorigenesis. *Nature* 475:106-109.
- Dennis KL, Blatner NR, Gounari F, Khazaie K (2013) Current status of interleukin-10 and regulatory T-cells in cancer. *Curr Opin Oncol* 25:637-645.
- Deppert W (2008) SIRT1 protein levels in cancer: tuning SIRT1 to the needs of a cancer cell. *Cell cycle* 7:2947-2948.
- Desplat V, Faucher JL, Mahon FX, Dello Sbarba P, Praloran V, Ivanovic Z (2002) Hypoxia modifies proliferation and differentiation of CD34(+) CML cells. *Stem cells* 20:347-354.
- Diehn M *et al.* (2009) Association of reactive oxygen species levels and radioresistance in cancer stem cells. *Nature* 458:780-783.
- DiNatale BC, Murray IA, Schroeder JC, Flaveny CA, Lahoti TS, Laurenzana EM, Omiecinski CJ, Perdew GH (2010) Kynurenic acid is a potent endogenous aryl

- hydrocarbon receptor ligand that synergistically induces interleukin-6 in the presence of inflammatory signaling. *Toxicol Sci* 115:89-97.
- Dingledine R, Borges K, Bowie D, Traynelis SF (1999) The glutamate receptor ion channels. *Pharmacological reviews* 51:7-61.
- Do JH, Kim IS, Park TK, Choi DK (2007) Genome-wide examination of chromosomal aberrations in neuroblastoma SH-SY5Y cells by array-based comparative genomic hybridization. *Molecules and cells* 24:105-112.
- Do JH, Kim IS, Lee JD, Choi DK (2011) Comparison of genomic profiles in human neuroblastic SH-SY5Y and substrate-adherent SH-EP cells using array comparative genomic hybridization. *BioChip J* 5:165-174.
- Dobrachinski F, Bastos LL, Bridi JC, Corte CL, de Avila DS, da Rocha JB, Soares FA (2012) Cooperation of non-effective concentration of glutamatergic system modulators and antioxidant against oxidative stress induced by quinolinic acid. *Neurochemical research* 37:1993-2003.
- Dreves J, Loser R, Rattel B, Esser N (2003) Antiangiogenic potency of FK866/K22.175, a new inhibitor of intracellular NAD biosynthesis, in murine renal cell carcinoma. *Anticancer Res* 23:4853-4858.
- Du W, Hozumi N, Sakamoto M, Hata J, Yamada T (2008) Reconstitution of Schwannian stroma in neuroblastomas using human bone marrow stromal cells. *The American journal of pathology* 173:1153-1164.
- Dykens JA, Sullivan SG, Stern A (1987) Oxidative reactivity of the tryptophan metabolites 3-hydroxyanthranilate, cinnabarinic acid, quinolinic acid and picolinic acid. *Biochemical pharmacology* 36:211-217.
- Eastman CL, Urbanska E, Love A, Kristensson K, Schwarcz R (1994) Increased brain quinolinic acid production in mice infected with a hamster neurotropic measles virus. *Experimental neurology* 125:119-124.
- Echlin DR, Tae HJ, Mitin N, Taparowsky EJ (2000) B-ATF functions as a negative regulator of AP-1 mediated transcription and blocks cellular transformation by Ras and Fos. *Oncogene* 19:1752-1763.
- Edsjo A, Holmquist L, Pahlman S (2007) Neuroblastoma as an experimental model for neuronal differentiation and hypoxia-induced tumor cell dedifferentiation. *Seminars in cancer biology* 17:248-256.
- Egashira Y, Sato M, Tanabe A, Saito K, Fujigaki S, Sanada H (2003) Dietary linoleic acid suppresses gene expression of rat liver alpha-amino-beta-carboxymuconate-epsilon-semialdehyde decarboxylase (ACMSD) and increases quinolinic acid in serum. *Advances in experimental medicine and biology* 527:671-674.
- Ehlers MD, Zhang S, Bernhardt JP, Huganir RL (1996) Inactivation of NMDA receptors by direct interaction of calmodulin with the NR1 subunit. *Cell* 84:745-755.

- Encinas M, Iglesias M, Llecha N, Comella JX (1999) Extracellular-regulated kinases and phosphatidylinositol 3-kinase are involved in brain-derived neurotrophic factor-mediated survival and neuritogenesis of the neuroblastoma cell line SH-SY5Y. *J Neurochem* 73:1409-1421.
- Encinas M, Iglesias M, Liu Y, Wang H, Muhaisen A, Cena V, Gallego C, Comella JX (2000) Sequential treatment of SH-SY5Y cells with retinoic acid and brain-derived neurotrophic factor gives rise to fully differentiated, neurotrophic factor-dependent, human neuron-like cells. *J Neurochem* 75:991-1003.
- Erfani N, Mehrabadi SM, Ghayumi MA, Haghshenas MR, Mojtahedi Z, Ghaderi A, Amani D (2012) Increase of regulatory T cells in metastatic stage and CTLA-4 over expression in lymphocytes of patients with non-small cell lung cancer (NSCLC). *Lung Cancer* 77:306-311.
- Ezashi T, Das P, Roberts RM (2005) Low O₂ tensions and the prevention of differentiation of hES cells. *Proc Natl Acad Sci U S A* 102:4783-4788.
- Fallarino F, Grohmann U, Vacca C, Orabona C, Spreca A, Fioretti MC, Puccetti P (2003) T cell apoptosis by kynurenines. *Advances in experimental medicine and biology* 527:183-190.
- Fallarino F, Grohmann U, Vacca C, Bianchi R, Orabona C, Spreca A, Fioretti MC, Puccetti P (2002) T cell apoptosis by tryptophan catabolism. *Cell death and differentiation* 9:1069-1077.
- Fallarino F, Grohmann U, You S, McGrath BC, Cavener DR, Vacca C, Orabona C, Bianchi R, Belladonna ML, Volpi C, Santamaria P, Fioretti MC, Puccetti P (2006) The combined effects of tryptophan starvation and tryptophan catabolites down-regulate T cell receptor zeta-chain and induce a regulatory phenotype in naive T cells. *Journal of immunology* 176:6752-6761.
- Farooqui AA, Horrocks LA (1998) Lipid peroxides in the free radical pathophysiology of brain diseases. *Cell Mol Neurobiol* 18:599-608.
- Farooqui AA, Horrocks LA, Farooqui T (2007) Interactions between neural membrane glycerophospholipid and sphingolipid mediators: a recipe for neural cell survival or suicide. *Journal of neuroscience research* 85:1834-1850.
- Fatokun AA, Stone TW, Smith RA (2006) Hydrogen peroxide-induced oxidative stress in MC3T3-E1 cells: The effects of glutamate and protection by purines. *Bone* 39:542-551.
- Fatokun AA, Stone TW, Smith RA (2008a) Oxidative stress in neurodegeneration and available means of protection. *Frontiers in bioscience : a journal and virtual library* 13:3288-3311.
- Fatokun AA, Stone TW, Smith RA (2008b) Responses of differentiated MC3T3-E1 osteoblast-like cells to reactive oxygen species. *Eur J Pharmacol* 587:35-41.

- Favre D, Mold J, Hunt PW, Kanwar B, Loke P, Seu L, Barbour JD, Lowe MM, Jayawardene A, Aweeka F, Huang Y, Douek DC, Brenchley JM, Martin JN, Hecht FM, Deeks SG, McCune JM (2010) Tryptophan catabolism by indoleamine 2,3-dioxygenase 1 alters the balance of TH17 to regulatory T cells in HIV disease. *Science translational medicine* 2:32ra36.
- Fazio F, Lionetto L, Molinaro G, Bertrand HO, Acher F, Ngomba RT, Notartomaso S, Curini M, Rosati O, Scarselli P, Di Marco R, Battaglia G, Bruno V, Simmaco M, Pin JP, Nicoletti F, Goudet C (2012) Cinnabarinic acid, an endogenous metabolite of the kynurenine pathway, activates type 4 metabotropic glutamate receptors. *Molecular pharmacology* 81:643-656.
- Feng Z, Porter AG (1999) NF-kappaB/Rel proteins are required for neuronal differentiation of SH-SY5Y neuroblastoma cells. *J Biol Chem* 274:30341-30344.
- Fernandez-Pol JA, Johnson GS (1977) Selective toxicity induced by picolinic acid in simian virus 40-transformed cells in tissue culture. *Cancer research* 37:4276-4279.
- Ferrari-Toninelli G, Bonini SA, Uberti D, Buizza L, Bettinsoli P, Poliani PL, Facchetti F, Memo M (2010) Targeting Notch pathway induces growth inhibition and differentiation of neuroblastoma cells. *Neuro-oncology* 12:1231-1243.
- Filomeni G, De Zio D, Cecconi F (2014) Oxidative stress and autophagy: the clash between damage and metabolic needs. *Cell death and differentiation*.
- Fisher JP, Tweddle DA (2012) Neonatal neuroblastoma. *Seminars in fetal & neonatal medicine* 17:207-215.
- Ford J, Jiang M, Milner J (2005) Cancer-specific functions of SIRT1 enable human epithelial cancer cell growth and survival. *Cancer research* 65:10457-10463.
- Forrest CM, Mackay GM, Oxford L, Stoy N, Stone TW, Darlington LG (2006) Kynurenine pathway metabolism in patients with osteoporosis after 2 years of drug treatment. *Clin Exp Pharmacol Physiol* 33:1078-1087.
- Forrest CM, Mackay GM, Stoy N, Spiden SL, Taylor R, Stone TW, Darlington LG (2010) Blood levels of kynurenines, interleukin-23 and soluble human leucocyte antigen-G at different stages of Huntington's disease. *J Neurochem* 112:112-122.
- Foster AC, Kemp JA, Leeson PD, Grimwood S, Donald AE, Marshall GR, Priestley T, Smith JD, Carling RW (1992) Kynurenic acid analogues with improved affinity and selectivity for the glycine site on the N-methyl-D-aspartate receptor from rat brain. *Molecular pharmacology* 41:914-922.
- Fotopoulou C, Sehouli J, Pschowski R, S VONH, Domanska G, Braicu EI, Fusch G, Reinke P, Schefold JC (2011) Systemic changes of tryptophan catabolites via the indoleamine-2,3-dioxygenase pathway in primary cervical cancer. *Anticancer Res* 31:2629-2635.

- Francis KR, Wei L (2010) Human embryonic stem cell neural differentiation and enhanced cell survival promoted by hypoxic preconditioning. *Cell death & disease* 1:e22.
- Friberg M, Jennings R, Alsarraj M, Dessureault S, Cantor A, Extermann M, Mellor AL, Munn DH, Antonia SJ (2002) Indoleamine 2,3-dioxygenase contributes to tumor cell evasion of T cell-mediated rejection. *International journal of cancer Journal international du cancer* 101:151-155.
- Fridovich I (1989) Superoxide dismutases. An adaptation to a paramagnetic gas. *J Biol Chem* 264:7761-7764.
- Frumento G, Rotondo R, Tonetti M, Damonte G, Benatti U, Ferrara GB (2002) Tryptophan-derived catabolites are responsible for inhibition of T and natural killer cell proliferation induced by indoleamine 2,3-dioxygenase. *The Journal of experimental medicine* 196:459-468.
- Frye RA (1999) Characterization of five human cDNAs with homology to the yeast SIR2 gene: Sir2-like proteins (sirtuins) metabolize NAD and may have protein ADP-ribosyltransferase activity. *Biochemical and biophysical research communications* 260:273-279.
- Fuhrmann M, Bittner T, Jung CK, Burgold S, Page RM, Mitteregger G, Haass C, LaFerla FM, Kretschmar H, Herms J (2010) Microglial Cx3cr1 knockout prevents neuron loss in a mouse model of Alzheimer's disease. *Nature neuroscience* 13:411-413.
- Fujigaki S, Saito K, Fujii H, Wada H, Seishima M (1999) Quantification of anthranilic acid and its related enzyme activity in several different species. *Advances in experimental medicine and biology* 467:625-628.
- Fujigaki S, Saito K, Takemura M, Fujii H, Wada H, Noma A, Seishima M (1998) Species differences in L-tryptophan-kynurenine pathway metabolism: quantification of anthranilic acid and its related enzymes. *Archives of biochemistry and biophysics* 358:329-335.
- Fukui S, Schwarcz R, Rapoport SI, Takada Y, Smith QR (1991) Blood-brain barrier transport of kynurenines: implications for brain synthesis and metabolism. *J Neurochem* 56:2007-2017.
- Fulco M, Cen Y, Zhao P, Hoffman EP, McBurney MW, Sauve AA, Sartorelli V (2008) Glucose restriction inhibits skeletal myoblast differentiation by activating SIRT1 through AMPK-mediated regulation of Nampt. *Developmental cell* 14:661-673.
- Galderisi U, Jori FP, Giordano A (2003) Cell cycle regulation and neural differentiation. *Oncogene* 22:5208-5219.
- Ganesan AP, Johansson M, Ruffell B, Yagui-Beltran A, Lau J, Jablons DM, Coussens LM (2013) Tumor-infiltrating regulatory T cells inhibit endogenous cytotoxic T cell responses to lung adenocarcinoma. *Journal of immunology* 191:2009-2017.

- Gardner CR, Cheung BB, Koach J, Black DS, Marshall GM, Kumar N (2012) Synthesis of retinoid enhancers based on 2-aminobenzothiazoles for anti-cancer therapy. *Bioorganic & medicinal chemistry* 20:6877-6884.
- Garey L (1999) *Cortex: Statistics and Geometry of Neuronal Connectivity*, 2nd edn. By V. BRAITENBERG and A. SCHUZ. (Pp. xiii+249; 90 figures; ISBN 3 540 63816 4). Berlin: Springer. 1998. *Journal of Anatomy* 194:153-157.
- Gedik CM, Collins A, Escodd (2005) Establishing the background level of base oxidation in human lymphocyte DNA: results of an interlaboratory validation study. *FASEB journal : official publication of the Federation of American Societies for Experimental Biology* 19:82-84.
- George RE, Variend S, Cullinane C, Cotterill SJ, McGuckin AG, Ellershaw C, Lunec J, Pearson AD, United Kingdom Children Cancer Study G (2001) Relationship between histopathological features, MYCN amplification, and prognosis: a UKCCSG study. *United Kingdom Children Cancer Study Group. Medical and pediatric oncology* 36:169-176.
- Ghaffari S (2008) Oxidative stress in the regulation of normal and neoplastic hematopoiesis. *Antioxidants & redox signaling* 10:1923-1940.
- Gibney GT, Hamid O, Gangadhar TC, Lutzky J, Olszanski AJ, Gajewski T, Chmielowski B, Boasberg PD, Zhao Y, Newton RC, Scherle PA, Bowman J, Maleski J, Leopold L, Weber JS (2014) Preliminary results from a phase 1/2 study of INCB024360 combined with ipilimumab (ipi) in patients (pts) with melanoma. *ASCO Meeting Abstracts* 32:3010.
- Glantz SB, Cianci CD, Iyer R, Pradhan D, Wang KK, Morrow JS (2007) Sequential degradation of alphaII and betaII spectrin by calpain in glutamate or maitotoxin-stimulated cells. *Biochemistry* 46:502-513.
- Gleichman AJ, Spruce LA, Dalmau J, Seeholzer SH, Lynch DR (2012) Anti-NMDA receptor encephalitis antibody binding is dependent on amino acid identity of a small region within the GluN1 amino terminal domain. *The Journal of neuroscience : the official journal of the Society for Neuroscience* 32:11082-11094.
- Glick RD, Medary I, Aronson DC, Scotto KW, Swendeman SL, La Quaglia MP (2000) The effects of serum depletion and dexamethasone on growth and differentiation of human neuroblastoma cell lines. *Journal of pediatric surgery* 35:465-472.
- Gloire G, Legrand-Poels S, Piette J (2006) NF-kappaB activation by reactive oxygen species: fifteen years later. *Biochemical pharmacology* 72:1493-1505.
- Goldsmid Y, Erlich S, Pinkas-Kramarski R (2001) Neuregulin induces sustained reactive oxygen species generation to mediate neuronal differentiation. *Cell Mol Neurobiol* 21:753-769.

- Goldstein LE, Leopold MC, Huang X, Atwood CS, Saunders AJ, Hartshorn M, Lim JT, Faget KY, Muffat JA, Scarpa RC, Chylack LT, Jr., Bowden EF, Tanzi RE, Bush AI (2000) 3-Hydroxykynurenine and 3-hydroxyanthranilic acid generate hydrogen peroxide and promote alpha-crystallin cross-linking by metal ion reduction. *Biochemistry* 39:7266-7275.
- Goldstein MN (1968) Neuroblastoma cells in tissue culture. *Journal of pediatric surgery* 3:166-169.
- Goodman MT, Gurney JG, Smith MA, Olshan AF (1999) Sympathetic nervous system tumors. In: *Cancer Incidence and Survival among Children and Adolescents: United States SEER Program 1975-1995*, National Cancer Institute, SEER Program (Ries LA, Smith MA, Gurney JG, Linet M, Tamra T, Young JL, Bunin GR, eds), p 35. Bethesda, MD: National Cancer Institute.
- Gopalakrishna R, Gundimeda U, Schiffman JE, McNeill TH (2008) A direct redox regulation of protein kinase C isoenzymes mediates oxidant-induced neuritogenesis in PC12 cells. *J Biol Chem* 283:14430-14444.
- Gorrini C, Harris IS, Mak TW (2013) Modulation of oxidative stress as an anticancer strategy. *Nature reviews Drug discovery* 12:931-947.
- Gramsbergen JB, Schmidt W, Turski WA, Schwarcz R (1992) Age-related changes in kynurenic acid production in rat brain. *Brain research* 588:1-5.
- Grant RS, Coggan SE, Smythe GA (2009) The physiological action of picolinic Acid in the human brain. *International journal of tryptophan research : IJTR* 2:71-79.
- Green DR, Reed JC (1998) Mitochondria and apoptosis. *Science (New York, NY)* 281:1309-1312.
- Guidetti P, Amori L, Sapko MT, Okuno E, Schwarcz R (2007) Mitochondrial aspartate aminotransferase: a third kynurenate-producing enzyme in the mammalian brain. *J Neurochem* 102:103-111.
- Guillemin GJ, Cullen KM, Lim CK, Smythe GA, Garner B, Kapoor V, Takikawa O, Brew BJ (2007) Characterization of the kynurenine pathway in human neurons. *The Journal of neuroscience : the official journal of the Society for Neuroscience* 27:12884-12892.
- Gupta SC, Hevia D, Patchva S, Park B, Koh W, Aggarwal BB (2012) Upsides and downsides of reactive oxygen species for cancer: the roles of reactive oxygen species in tumorigenesis, prevention, and therapy. *Antioxidants & redox signaling* 16:1295-1322.
- Gupta SL, Carlin JM, Pyati P, Dai W, Pfefferkorn ER, Murphy MJ, Jr. (1994) Antiparasitic and antiproliferative effects of indoleamine 2,3-dioxygenase enzyme expression in human fibroblasts. *Infection and immunity* 62:2277-2284.

- Gutteridge JM, Halliwell B (2000) Free radicals and antioxidants in the year 2000. A historical look to the future. *Annals of the New York Academy of Sciences* 899:136-147.
- Haas HS, Pfragner R, Siegl V, Ingolic E, Heintz E, Schauenstein K (2005) Glutamate receptor-mediated effects on growth and morphology of human histiocytic lymphoma cells. *International journal of oncology* 27:867-874.
- Haas HS, Pfragner R, Siegl V, Ingolic E, Heintz E, Schraml E, Schauenstein K (2007) The non-competitive metabotropic glutamate receptor-1 antagonist CPCCOEt inhibits the in vitro growth of human melanoma. *Oncology reports* 17:1399-1404.
- Haas HS, Pfragner R, Tabrizi-Wizsy NG, Rohrer K, Lueftenegger I, Horwath C, Allard N, Rinner B, Sadjak A (2013) The influence of glutamate receptors on proliferation and metabolic cell activity of neuroendocrine tumors. *Anticancer Res* 33:1267-1272.
- Haigis MC, Sinclair DA (2010) Mammalian sirtuins: biological insights and disease relevance. *Annual review of pathology* 5:253-295.
- Halliwell B (2006) Oxidative stress and neurodegeneration: where are we now? *J Neurochem* 97:1634-1658.
- Halliwell B, Gutteridge JM (1992) Biologically relevant metal ion-dependent hydroxyl radical generation. An update. *FEBS letters* 307:108-112.
- Halliwell B, Gutteridge, J.M.C (1999) *Free radicals in biology and medicine*, 3rd edition Edition. Oxford, United Kingdom: Clarendon Press.
- Hamori J, Somogyi J (1983) Differentiation of cerebellar mossy fiber synapses in the rat: a quantitative electron microscope study. *The Journal of comparative neurology* 220:365-377.
- Han Q, Cai T, Tagle DA, Li J (2010) Structure, expression, and function of kynurenine aminotransferases in human and rodent brains. *Cellular and molecular life sciences : CMLS* 67:353-368.
- Han Q, Cai T, Tagle DA, Robinson H, Li J (2008) Substrate specificity and structure of human amino adipate aminotransferase/kynurenine aminotransferase II. *Bioscience reports* 28:205-215.
- Hanahan D, Weinberg RA (2000) The hallmarks of cancer. *Cell* 100:57-70.
- Hansford LM, McKee AE, Zhang L, George RE, Gerstle JT, Thorner PS, Smith KM, Look AT, Yeger H, Miller FD, Irwin MS, Thiele CJ, Kaplan DR (2007) Neuroblastoma cells isolated from bone marrow metastases contain a naturally enriched tumor-initiating cell. *Cancer research* 67:11234-11243.
- Harrison R (2002) Structure and function of xanthine oxidoreductase: where are we now? *Free radical biology & medicine* 33:774-797.

- Hart PE, Lodi R, Rajagopalan B, Bradley JL, Crilley JG, Turner C, Blamire AM, Manners D, Styles P, Schapira AH, Cooper JM (2005) Antioxidant treatment of patients with Friedreich ataxia: four-year follow-up. *Archives of neurology* 62:621-626.
- Hasmann M, Schemainda I (2003) FK866, a highly specific noncompetitive inhibitor of nicotinamide phosphoribosyltransferase, represents a novel mechanism for induction of tumor cell apoptosis. *Cancer research* 63:7436-7442.
- Hassel B, Dingledine R (2012) Chapter 17 - Glutamate and Glutamate Receptors. In: *Basic Neurochemistry (Eighth Edition)* (Scott TB, George JS, Albers RW, Donald L. Price A2 - Scott T, Brady GJSRWA, Donald LP, eds), pp 342-366. New York: Academic Press.
- Hayashi T, Rao SP, Takabayashi K, Van Uden JH, Kornbluth RS, Baird SM, Taylor MW, Carson DA, Catanzaro A, Raz E (2001) Enhancement of innate immunity against *Mycobacterium avium* infection by immunostimulatory DNA is mediated by indoleamine 2,3-dioxygenase. *Infection and immunity* 69:6156-6164.
- Hayes JD, McMahon M, Chowdhry S, Dinkova-Kostova AT (2010) Cancer chemoprevention mechanisms mediated through the Keap1-Nrf2 pathway. *Antioxidants & redox signaling* 13:1713-1748.
- Hayton SM, Muller DP (2004) Vitamin E in neural and visual function. *Annals of the New York Academy of Sciences* 1031:263-270.
- He Z, Simon HU (2013) A novel link between p53 and ROS. *Cell cycle* 12:201-202.
- Helferich WG, Denison MS (1991) Ultraviolet photoproducts of tryptophan can act as dioxin agonists. *Molecular pharmacology* 40:674-678.
- Heraud C, Hilairet S, Muller JM, Leterrier JF, Chadeneau C (2004) Neuritogenesis induced by vasoactive intestinal peptide, pituitary adenylate cyclase-activating polypeptide, and peptide histidine methionine in SH-SY5y cells is associated with regulated expression of cytoskeleton mRNAs and proteins. *Journal of neuroscience research* 75:320-329.
- Herner A, Sauliunaite D, Michalski CW, Erkan M, De Oliveira T, Abiatari I, Kong B, Esposito I, Friess H, Kleeff J (2011) Glutamate increases pancreatic cancer cell invasion and migration via AMPA receptor activation and Kras-MAPK signaling. *International journal of cancer Journal international du cancer* 129:2349-2359.
- Heyes MP, Lackner A (1990) Increased cerebrospinal fluid quinolinic acid, kynurenic acid, and L-kynurenine in acute septicemia. *J Neurochem* 55:338-341.
- Heyes MP, Chen CY, Major EO, Saito K (1997) Different kynurenine pathway enzymes limit quinolinic acid formation by various human cell types. *The Biochemical journal* 326 (Pt 2):351-356.
- Heyes MP, Mefford IN, Quearry BJ, Dedhia M, Lackner A (1990) Increased ratio of quinolinic acid to kynurenic acid in cerebrospinal fluid of D retrovirus-infected

- rhesus macaques: relationship to clinical and viral status. *Annals of neurology* 27:666-675.
- Heyes MP, Saito K, Crowley JS, Davis LE, Demitrack MA, Der M, Dilling LA, Elia J, Kruesi MJ, Lackner A, et al. (1992) Quinolinic acid and kynurenine pathway metabolism in inflammatory and non-inflammatory neurological disease. *Brain : a journal of neurology* 115 (Pt 5):1249-1273.
- Hille R, Nishino T (1995) Flavoprotein structure and mechanism. 4. Xanthine oxidase and xanthine dehydrogenase. *FASEB journal : official publication of the Federation of American Societies for Experimental Biology* 9:995-1003.
- Hilmas C, Pereira EF, Alkondon M, Rassoulpour A, Schwarcz R, Albuquerque EX (2001) The brain metabolite kynurenic acid inhibits alpha7 nicotinic receptor activity and increases non-alpha7 nicotinic receptor expression: physiopathological implications. *The Journal of neuroscience : the official journal of the Society for Neuroscience* 21:7463-7473.
- Hinoi E, Takarada T, Ueshima T, Tsuchihashi Y, Yoneda Y (2004) Glutamate signaling in peripheral tissues. *European journal of biochemistry / FEBS* 271:1-13.
- Hinsch N, Frank M, Doring C, Vorlander C, Hansmann ML (2009) QPRT: a potential marker for follicular thyroid carcinoma including minimal invasive variant; a gene expression, RNA and immunohistochemical study. *BMC cancer* 9:93.
- Hiramatsu R, Hara T, Akimoto H, Takikawa O, Kawabe T, Isobe K, Nagase F (2008) Cinnabarinic acid generated from 3-hydroxyanthranilic acid strongly induces apoptosis in thymocytes through the generation of reactive oxygen species and the induction of caspase. *Journal of cellular biochemistry* 103:42-53.
- Hirschmann-Jax C, Foster AE, Wulf GG, Nuchtern JG, Jax TW, Gobel U, Goodell MA, Brenner MK (2004) A distinct "side population" of cells with high drug efflux capacity in human tumor cells. *Proc Natl Acad Sci U S A* 101:14228-14233.
- Hokari M, Wu HQ, Schwarcz R, Smith QR (1996) Facilitated brain uptake of 4-chlorokynurenine and conversion to 7-chlorokynurenic acid. *Neuroreport* 8:15-18.
- Holen K, Saltz LB, Hollywood E, Burk K, Hanauske AR (2008) The pharmacokinetics, toxicities, and biologic effects of FK866, a nicotinamide adenine dinucleotide biosynthesis inhibitor. *Investigational new drugs* 26:45-51.
- Hollmann M, O'Shea-Greenfield A, Rogers SW, Heinemann S (1989) Cloning by functional expression of a member of the glutamate receptor family. *Nature* 342:643-648.
- Hu L, Magesh S, Chen L, Wang L, Lewis TA, Chen Y, Khodier C, Inoyama D, Beamer LJ, Emge TJ, Shen J, Kerrigan JE, Kong AN, Dandapani S, Palmer M, Schreiber SL, Munoz B (2013) Discovery of a small-molecule inhibitor and cellular probe of Keap1-Nrf2 protein-protein interaction. *Bioorganic & medicinal chemistry letters* 23:3039-3043.

- Huang K, Huang J, Xie X, Wang S, Chen C, Shen X, Liu P, Huang H (2013) Sirt1 resists advanced glycation end products-induced expressions of fibronectin and TGF-beta1 by activating the Nrf2/ARE pathway in glomerular mesangial cells. *Free radical biology & medicine* 65:528-540.
- Ichinose T, Yu S, Wang XQ, Yu SP (2003) Ca²⁺-independent, but voltage- and activity-dependent regulation of the NMDA receptor outward K⁺ current in mouse cortical neurons. *J Physiol* 551:403-417.
- Ikedo M, Tsuji H, Nakamura S, Ichiyama A, Nishizuka Y, Hayaishi O (1965) Studies on the Biosynthesis of Nicotinamide Adenine Dinucleotide. II. A Role of Picolinic Carboxylase in the Biosynthesis of Nicotinamide Adenine Dinucleotide from Tryptophan in Mammals. *J Biol Chem* 240:1395-1401.
- Ikonomidou C, Bosch F, Miksa M, Bittigau P, Vockler J, Dikranian K, Tenkova TI, Stefovskaja V, Turski L, Olney JW (1999) Blockade of NMDA receptors and apoptotic neurodegeneration in the developing brain. *Science* 283:70-74.
- Imahayashi S, So T, Sugaya M, Yasuda M, Eifuku R, Takenoyama M, Hanagiri T, Yoshimatsu T, Oyama T, Yasumoto K (2002) Establishment of an immortalized T-cell line from lung cancer tissue: phenotypic and functional analyses. *International journal of clinical oncology* 7:38-44.
- Ishii T, Iwahashi H, Sugata R, Kido R, Fridovich I (1990) Superoxide dismutases enhance the rate of autoxidation of 3-hydroxyanthranilic acid. *Archives of biochemistry and biophysics* 276:248-250.
- Ishiuchi S, Yoshida Y, Sugawara K, Aihara M, Ohtani T, Watanabe T, Saito N, Tsuzuki K, Okado H, Miwa A, Nakazato Y, Ozawa S (2007) Ca²⁺-permeable AMPA receptors regulate growth of human glioblastoma via Akt activation. *The Journal of neuroscience : the official journal of the Society for Neuroscience* 27:7987-8001.
- Iversen TZ, Engell-Noerregaard L, Ellebaek E, Andersen R, Larsen SK, Bjoern J, Zeyher C, Gouttefangeas C, Thomsen BM, Holm B, Thor Straten P, Mellemegaard A, Andersen MH, Svane IM (2014) Long-lasting disease stabilization in the absence of toxicity in metastatic lung cancer patients vaccinated with an epitope derived from indoleamine 2,3 dioxygenase. *Clinical cancer research : an official journal of the American Association for Cancer Research* 20:221-232.
- Jamsa A, Hasslund K, Cowburn RF, Backstrom A, Vasange M (2004) The retinoic acid and brain-derived neurotrophic factor differentiated SH-SY5Y cell line as a model for Alzheimer's disease-like tau phosphorylation. *Biochemical and biophysical research communications* 319:993-1000.
- Janardhanan R, Banik NL, Ray SK (2009) N-Myc down regulation induced differentiation, early cell cycle exit, and apoptosis in human malignant neuroblastoma cells having wild type or mutant p53. *Biochemical pharmacology* 78:1105-1114.

- Jansson LC, Akerman KE (2014) The role of glutamate and its receptors in the proliferation, migration, differentiation and survival of neural progenitor cells. *Journal of neural transmission* 121:819-836.
- Jantas D, Lason W (2009) Different mechanisms of NMDA-mediated protection against neuronal apoptosis: a stimuli-dependent effect. *Neurochemical research* 34:2040-2054.
- Jantas D, Pytel M, Mozrzymas JW, Leskiewicz M, Regulska M, Antkiewicz-Michaluk L, Lason W (2008) The attenuating effect of memantine on staurosporine-, salsolinol- and doxorubicin-induced apoptosis in human neuroblastoma SH-SY5Y cells. *Neurochemistry international* 52:864-877.
- Jiang Y, Xue ZH, Shen WZ, Du KM, Yan H, Yu Y, Peng ZG, Song MG, Tong JH, Chen Z, Huang Y, Lubbert M, Chen GQ (2005) Desferrioxamine induces leukemic cell differentiation potentially by hypoxia-inducible factor-1 alpha that augments transcriptional activity of CCAAT/enhancer-binding protein-alpha. *Leukemia* 19:1239-1247.
- Jin C, Li H, Murata T, Sun K, Horikoshi M, Chiu R, Yokoyama KK (2002) JDP2, a repressor of AP-1, recruits a histone deacetylase 3 complex to inhibit the retinoic acid-induced differentiation of F9 cells. *Molecular and cellular biology* 22:4815-4826.
- Kalariti N, Pissimissis N, Koutsilieris M (2005) The glutamatergic system outside the CNS and in cancer biology. *Expert opinion on investigational drugs* 14:1487-1496.
- Kamson DO, Mittal S, Buth A, Muzik O, Kupsky WJ, Robinette NL, Barger GR, Juhasz C (2013) Differentiation of glioblastomas from metastatic brain tumors by tryptophan uptake and kinetic analysis: a positron emission tomographic study with magnetic resonance imaging comparison. *Mol Imaging* 12:327-337.
- Kanai M, Funakoshi H, Takahashi H, Hayakawa T, Mizuno S, Matsumoto K, Nakamura T (2009) Tryptophan 2,3-dioxygenase is a key modulator of physiological neurogenesis and anxiety-related behavior in mice. *Molecular brain* 2:8.
- Kaneko Y, Kanda N, Maseki N, Sakurai M, Tsuchida Y, Takeda T, Okabe I, Sakurai M (1987) Different karyotypic patterns in early and advanced stage neuroblastomas. *Cancer research* 47:311-318.
- Kang HB, Kim YE, Kwon HJ, Sok DE, Lee Y (2007) Enhancement of NF-kappaB expression and activity upon differentiation of human embryonic stem cell line SNUhES3. *Stem cells and development* 16:615-623.
- Kania J, Baranska A, Guzdek A (2003) Cytokine action and oxidative stress response in differentiated neuroblastoma SH-SY5Y cells. *Acta Biochim Pol* 50:659-666.
- Kanzaki H, Shinohara F, Kajiya M, Kodama T (2013) The Keap1/Nrf2 protein axis plays a role in osteoclast differentiation by regulating intracellular reactive oxygen species signaling. *J Biol Chem* 288:23009-23020.

- Karakas E, Simorowski N, Furukawa H (2011) Subunit arrangement and phenylethanolamine binding in GluN1/GluN2B NMDA receptors. *Nature* 475:249-253.
- Katoh S, Mitsui Y, Kitani K, Suzuki T (1997) Hyperoxia induces the differentiated neuronal phenotype of PC12 cells by producing reactive oxygen species. *Biochemical and biophysical research communications* 241:347-351.
- Katoh S, Mitsui Y, Kitani K, Suzuki T (1999) Hyperoxia induces the neuronal differentiated phenotype of PC12 cells via a sustained activity of mitogen-activated protein kinase induced by Bcl-2. *The Biochemical journal* 338 (Pt 2):465-470.
- Kawai Y, Garduno L, Theodore M, Yang J, Arinze IJ (2011) Acetylation-deacetylation of the transcription factor Nrf2 (nuclear factor erythroid 2-related factor 2) regulates its transcriptional activity and nucleocytoplasmic localization. *J Biol Chem* 286:7629-7640.
- Kehrer JP, Biswal SS (2000) The molecular effects of acrolein. *Toxicol Sci* 57:6-15.
- Kemp JA, Foster AC, Leeson PD, Priestley T, Tridgett R, Iversen LL, Woodruff GN (1988) 7-Chlorokynurenic acid is a selective antagonist at the glycine modulatory site of the N-methyl-D-aspartate receptor complex. *Proc Natl Acad Sci U S A* 85:6547-6550.
- Kessler M, Baudry M, Lynch G (1989a) Quinoxaline derivatives are high-affinity antagonists of the NMDA receptor-associated glycine sites. *Brain research* 489:377-382.
- Kessler M, Terramani T, Lynch G, Baudry M (1989b) A glycine site associated with N-methyl-D-aspartic acid receptors: characterization and identification of a new class of antagonists. *J Neurochem* 52:1319-1328.
- Kew JN, Kemp JA (2005) Ionotropic and metabotropic glutamate receptor structure and pharmacology. *Psychopharmacology (Berl)* 179:4-29.
- Kikuchi H, Kuribayashi F, Kiwaki N, Nakayama T (2010) Curcumin dramatically enhances retinoic acid-induced superoxide generating activity via accumulation of p47-phox and p67-phox proteins in U937 cells. *Biochemical and biophysical research communications* 395:61-65.
- Kim B, Leventhal PS, Saltiel AR, Feldman EL (1997) Insulin-like growth factor-I-mediated neurite outgrowth in vitro requires mitogen-activated protein kinase activation. *J Biol Chem* 272:21268-21273.
- Kim CH, Lee J, Lee JY, Roche KW (2008) Metabotropic glutamate receptors: phosphorylation and receptor signaling. *Journal of neuroscience research* 86:1-10.

- Kim HM, Haraguchi N, Ishii H, Ohkuma M, Okano M, Mimori K, Eguchi H, Yamamoto H, Nagano H, Sekimoto M, Doki Y, Mori M (2012) Increased CD13 expression reduces reactive oxygen species, promoting survival of liver cancer stem cells via an epithelial-mesenchymal transition-like phenomenon. *Annals of surgical oncology* 19 Suppl 3:S539-548.
- Kim SR, Bae SK, Choi KS, Park SY, Jun HO, Lee JY, Jang HO, Yun I, Yoon KH, Kim YJ, Yoo MA, Kim KW, Bae MK (2007) Visfatin promotes angiogenesis by activation of extracellular signal-regulated kinase 1/2. *Biochemical and biophysical research communications* 357:150-156.
- Konopka R, Kubala L, Lojek A, Pachernik J (2008) Alternation of retinoic acid induced neural differentiation of P19 embryonal carcinoma cells by reduction of reactive oxygen species intracellular production. *Neuro endocrinology letters* 29:770-774.
- Koppenol WH (2001) The Haber-Weiss cycle--70 years later. *Redox report : communications in free radical research* 6:229-234.
- Korecka JA, van Kesteren RE, Blaas E, Spitzer SO, Kamstra JH, Smit AB, Swaab DF, Verhaagen J, Bossers K (2013) Phenotypic characterization of retinoic acid differentiated SH-SY5Y cells by transcriptional profiling. *PloS one* 8:e63862.
- Kovalevich J, Langford D (2013) Considerations for the use of SH-SY5Y neuroblastoma cells in neurobiology. *Methods in molecular biology* 1078:9-21.
- Krause D, Suh HS, Tarassishin L, Cui QL, Durafourt BA, Choi N, Bauman A, Cosenza-Nashat M, Antel JP, Zhao ML, Lee SC (2011) The tryptophan metabolite 3-hydroxyanthranilic acid plays anti-inflammatory and neuroprotective roles during inflammation: role of hemeoxygenase-1. *The American journal of pathology* 179:1360-1372.
- Kryh H, Caren H, Erichsen J, Sjoberg RM, Abrahamsson J, Kogner P, Martinsson T (2011) Comprehensive SNP array study of frequently used neuroblastoma cell lines; copy neutral loss of heterozygosity is common in the cell lines but uncommon in primary tumors. *BMC genomics* 12:443.
- Kudo Y, Boyd CA (2001) The physiology of immune evasion during pregnancy; the critical role of placental tryptophan metabolism and transport. *Pflugers Arch* 442:639-641.
- Kujoth GC, Bradshaw PC, Haroon S, Prolla TA (2007) The role of mitochondrial DNA mutations in mammalian aging. *PLoS Genet* 3:e24.
- Kulikov AV, Rzhabinova AA, Goldshtein DV, Boldyrev AA (2007) Expression of NMDA receptors in multipotent stromal cells of human adipose tissue under conditions of retinoic acid-induced differentiation. *Bulletin of experimental biology and medicine* 144:626-629.

- Kulkarni SR, Donepudi AC, Xu J, Wei W, Cheng QC, Driscoll MV, Johnson DA, Johnson JA, Li X, Slitt AL (2014) Fasting induces nuclear factor E2-related factor 2 and ATP-binding Cassette transporters via protein kinase A and Sirtuin-1 in mouse and human. *Antioxidants & redox signaling* 20:15-30.
- Kumar B, Koul S, Khandrika L, Meacham RB, Koul HK (2008) Oxidative stress is inherent in prostate cancer cells and is required for aggressive phenotype. *Cancer research* 68:1777-1785.
- Lapin IP (1973) Kynurenines as probable participants of depression. *Pharmakopsychiatrie, Neuro-Psychopharmakologie* 6:273-279.
- Lapin IP (1978) Stimulant and convulsive effects of kynurenines injected into brain ventricles in mice. *Journal of neural transmission* 42:37-43.
- Lapin IP, Mirzaev SM, Ryzov IV, Oxenkrug GF (1998) Anticonvulsant activity of melatonin against seizures induced by quinolinate, kainate, glutamate, NMDA, and pentylenetetrazole in mice. *J Pineal Res* 24:215-218.
- Lee SM, Lee YS, Choi JH, Park SG, Choi IW, Joo YD, Lee WS, Lee JN, Choi I, Seo SK (2010) Tryptophan metabolite 3-hydroxyanthranilic acid selectively induces activated T cell death via intracellular GSH depletion. *Immunology letters* 132:53-60.
- Leeson PD, Iversen LL (1994) The glycine site on the NMDA receptor: structure-activity relationships and therapeutic potential. *Journal of medicinal chemistry* 37:4053-4067.
- Leeson PD, Baker R, Carling RW, Curtis NR, Moore KW, Williams BJ, Foster AC, Donald AE, Kemp JA, Marshall GR (1991) Kynurenic acid derivatives. Structure-activity relationships for excitatory amino acid antagonism and identification of potent and selective antagonists at the glycine site on the N-methyl-D-aspartate receptor. *Journal of medicinal chemistry* 34:1243-1252.
- Lengauer C, Kinzler KW, Vogelstein B (1998) Genetic instabilities in human cancers. *Nature* 396:643-649.
- Leondaritis G, Petrikos L, Mangoura D (2009) Regulation of the Ras-GTPase activating protein neurofibromin by C-tail phosphorylation: implications for protein kinase C/Ras/extracellular signal-regulated kinase 1/2 pathway signaling and neuronal differentiation. *J Neurochem* 109:573-583.
- Leuthauser SW, Oberley LW, Oberley TD (1982) Antitumor activity of picolinic acid in CBA/J mice. *J Natl Cancer Inst* 68:123-126.
- Li A, Zhu X, Brown B, Craft CM (2003) Gene expression networks underlying retinoic acid-induced differentiation of human retinoblastoma cells. *Invest Ophthalmol Vis Sci* 44:996-1007.

- Li H, Sharp G, Pilkington C, Pifat D, Petteway S (2006) GLP-compliant assay validation studies: considerations for implementation of regulations and audit of studies. *The Quality Assurance Journal* 10:92-100.
- Li L, Hanahan D (2013) Hijacking the neuronal NMDAR signaling circuit to promote tumor growth and invasion. *Cell* 153:86-100.
- Li Y, Zhang H, Zhu X, Feng D, Gong J, Han T (2013) Interleukin-24 induces neuroblastoma SH-SY5Y cell differentiation, growth inhibition, and apoptosis by promoting ROS production. *Journal of interferon & cytokine research : the official journal of the International Society for Interferon and Cytokine Research* 33:709-714.
- Liebig J (1853) Ueber Kynurensäure. *Annalen der Chemie und Pharmacie* 86:125-126.
- Lima S, Kumar S, Gawandi V, Momany C, Phillips RS (2009) Crystal structure of the Homo sapiens kynureninase-3-hydroxyhippuric acid inhibitor complex: insights into the molecular basis of kynureninase substrate specificity. *Journal of medicinal chemistry* 52:389-396.
- Lin MT, Beal MF (2006) Mitochondrial dysfunction and oxidative stress in neurodegenerative diseases. *Nature* 443:787-795.
- Lin YC, Huang YC, Chen SC, Liaw CC, Kuo SC, Huang LJ, Gean PW (2009) Neuroprotective effects of ugonin K on hydrogen peroxide-induced cell death in human neuroblastoma SH-SY5Y cells. *Neurochemical research* 34:923-930.
- Lindskog M, Gleissman H, Ponthan F, Castro J, Kogner P, Johnsen JI (2006) Neuroblastoma cell death in response to docosahexaenoic acid: sensitization to chemotherapy and arsenic-induced oxidative stress. *International journal of cancer Journal international du cancer* 118:2584-2593.
- Liochev SI, Fridovich I (2001) The oxidation of 3-hydroxyanthranilic acid by Cu,Zn superoxide dismutase: mechanism and possible consequences. *Archives of biochemistry and biophysics* 388:281-284.
- Liu CY, Lee CF, Wei YH (2009) Role of reactive oxygen species-elicited apoptosis in the pathophysiology of mitochondrial and neurodegenerative diseases associated with mitochondrial DNA mutations. *J Formos Med Assoc* 108:599-611.
- Liu S, Wang F, Yan L, Zhang L, Song Y, Xi S, Jia J, Sun G (2013) Oxidative stress and MAPK involved into ATF2 expression in immortalized human urothelial cells treated by arsenic. *Archives of toxicology* 87:981-989.
- Liu W, Guo M, Xu YB, Li D, Zhou ZN, Wu YL, Chen Z, Kogan SC, Chen GQ (2006) Induction of tumor arrest and differentiation with prolonged survival by intermittent hypoxia in a mouse model of acute myeloid leukemia. *Blood* 107:698-707.

- Lodge D (1997) Subtypes of glutamate receptors: Historical perspectives on their pharmacological differentiation. Totowa. New Jersey. USA: Humana Press.
- Lodge D, Bond A, O'Neill MJ, Hicks CA, Jones MG (1996) Stereoselective effects-of 2,3-benzodiazepines in vivo: electrophysiology and neuroprotection studies. *Neuropharmacology* 35:1681-1688.
- Lohr SLW, Gerald G, Alyssa JM, Charles P, Elizabeth T, Nancy L, Linda JL, Jacqueline A, Sally CM, Timothy CC, Meera V, Kathleen N (2010) Comparative Effectiveness Review Methods: Clinical Heterogeneity.
- Lopes FM, Schroder R, da Frota ML, Jr., Zanutto-Filho A, Muller CB, Pires AS, Meurer RT, Colpo GD, Gelain DP, Kapczynski F, Moreira JC, Fernandes Mda C, Klamt F (2010) Comparison between proliferative and neuron-like SH-SY5Y cells as an in vitro model for Parkinson disease studies. *Brain research* 1337:85-94.
- LoPresti P, Poluha W, Poluha DK, Drinkwater E, Ross AH (1992) Neuronal differentiation triggered by blocking cell proliferation. *Cell growth & differentiation : the molecular biology journal of the American Association for Cancer Research* 3:627-635.
- Lujan R, Shigemoto R, Lopez-Bendito G (2005) Glutamate and GABA receptor signalling in the developing brain. *Neuroscience* 130:567-580.
- Luksch H, Uckermann O, Stepulak A, Hendruschk S, Marzahn J, Bastian S, Stauffer C, Temme A, Ikonomidou C (2011) Silencing of selected glutamate receptor subunits modulates cancer growth. *Anticancer Res* 31:3181-3192.
- Luo J, Nikolaev AY, Imai S, Chen D, Su F, Shiloh A, Guarente L, Gu W (2001) Negative control of p53 by Sir2alpha promotes cell survival under stress. *Cell* 107:137-148.
- Mackay GM (2007) Kynurenines in neurological disorders. In.
- Mackay GM, Forrest CM, Stoy N, Christofides J, Egerton M, Stone TW, Darlington LG (2006) Tryptophan metabolism and oxidative stress in patients with chronic brain injury. *European journal of neurology : the official journal of the European Federation of Neurological Societies* 13:30-42.
- MacKenzie CR, Hadding U, Daubener W (1998) Interferon-gamma-induced activation of indoleamine 2,3-dioxygenase in cord blood monocyte-derived macrophages inhibits the growth of group B streptococci. *The Journal of infectious diseases* 178:875-878.
- Maejima Y, Kuroda J, Matsushima S, Ago T, Sadoshima J (2011) Regulation of myocardial growth and death by NADPH oxidase. *J Mol Cell Cardiol* 50:408-416.
- Maillet A, Pervaiz S (2012) Redox regulation of p53, redox effectors regulated by p53: a subtle balance. *Antioxidants & redox signaling* 16:1285-1294.
- Maiorino M, Aumann KD, Brigelius-Flohe R, Doria D, van den Heuvel J, McCarthy J, Roveri A, Ursini F, Flohe L (1995) Probing the presumed catalytic triad of

- selenium-containing peroxidases by mutational analysis of phospholipid hydroperoxide glutathione peroxidase (PHGPx). *Biological chemistry Hoppe-Seyler* 376:651-660.
- Maki A, Berezesky IK, Fagnoli J, Holbrook NJ, Trump BF (1992) Role of $[Ca^{2+}]_i$ in induction of c-fos, c-jun, and c-myc mRNA in rat PTE after oxidative stress. *FASEB journal : official publication of the Federation of American Societies for Experimental Biology* 6:919-924.
- Maldonado PD, Molina-Jijon E, Villeda-Hernandez J, Galvan-Arzate S, Santamaria A, Pedraza-Chaverri J (2010) NAD(P)H oxidase contributes to neurotoxicity in an excitotoxic/prooxidant model of Huntington's disease in rats: protective role of apocynin. *Journal of neuroscience research* 88:620-629.
- Manthey MK, Pyne SG, Truscott RJ (1990) Mechanism of reaction of 3-hydroxyanthranilic acid with molecular oxygen. *Biochimica et biophysica acta* 1034:207-212.
- Manthey MK, Pyne SG, Truscott RJ (1992) Involvement of tyrosine residues in the tanning of proteins by 3-hydroxyanthranilic acid. *Proc Natl Acad Sci U S A* 89:1954-1957.
- Maris JM, Matthay KK (1999) Molecular biology of neuroblastoma. *Journal of clinical oncology : official journal of the American Society of Clinical Oncology* 17:2264-2279.
- Martindale JL, Holbrook NJ (2002) Cellular response to oxidative stress: signaling for suicide and survival. *J Cell Physiol* 192:1-15.
- Marzi I, D'Amico M, Biagiotti T, Giunti S, Carbone MV, Fredducci D, Wanke E, Olivetto M (2007) Purging of the neuroblastoma stem cell compartment and tumor regression on exposure to hypoxia or cytotoxic treatment. *Cancer research* 67:2402-2407.
- Masuko T, Suzuki T, Miyake M, Kusama-Eguchi K, Kizawa Y, Tomono K, Kashiwagi K, Igarashi K, Kusama T (2012) Antagonism of NMDA receptors by butanesulfonyl-homospermine guanidine and neuroprotective effects in in vitro and in vivo. *Neurosci Lett* 506:251-255.
- Mattson MP (2007) Calcium and neurodegeneration. *Aging cell* 6:337-350.
- McCord JM (1994) Mutant mice, Cu,Zn superoxide dismutase, and motor neuron degeneration. *Science* 266:1586-1587.
- Medan D, Wang L, Toledo D, Lu B, Stehlik C, Jiang BH, Shi X, Rojanasakul Y (2005) Regulation of Fas (CD95)-induced apoptotic and necrotic cell death by reactive oxygen species in macrophages. *J Cell Physiol* 203:78-84.
- Meghani MA, Martin DM, Singleton JR, Feldman EL (1993) Effects of serum and insulin-like growth factors on human neuroblastoma cell growth. *Regulatory peptides* 48:217-224.

- Meisel R, Zibert A, Laryea M, Gobel U, Daubener W, Dilloo D (2004) Human bone marrow stromal cells inhibit allogeneic T-cell responses by indoleamine 2,3-dioxygenase-mediated tryptophan degradation. *Blood* 103:4619-4621.
- Melillo G, Cox GW, Biragyn A, Sheffler LA, Varesio L (1994) Regulation of nitric-oxide synthase mRNA expression by interferon-gamma and picolinic acid. *J Biol Chem* 269:8128-8133.
- Mellor AL, Munn DH (2004) IDO expression by dendritic cells: tolerance and tryptophan catabolism. *Nature reviews Immunology* 4:762-774.
- Mellor AL, Baban B, Chandler PR, Manlapat A, Kahler DJ, Munn DH (2005) Cutting edge: CpG oligonucleotides induce splenic CD19+ dendritic cells to acquire potent indoleamine 2,3-dioxygenase-dependent T cell regulatory functions via IFN Type 1 signaling. *Journal of immunology* 175:5601-5605.
- Mellor AL, Chandler P, Baban B, Hansen AM, Marshall B, Pihkala J, Waldmann H, Cobbold S, Adams E, Munn DH (2004) Specific subsets of murine dendritic cells acquire potent T cell regulatory functions following CTLA4-mediated induction of indoleamine 2,3 dioxygenase. *Int Immunol* 16:1391-1401.
- Mezrich JD, Fechner JH, Zhang X, Johnson BP, Burlingham WJ, Bradfield CA (2010) An interaction between kynurenine and the aryl hydrocarbon receptor can generate regulatory T cells. *Journal of immunology* 185:3190-3198.
- Moffett JR, Namboodiri MA (2003) Tryptophan and the immune response. *Immunol Cell Biol* 81:247-265.
- Moffett JR, Els T, Espey MG, Walter SA, Streit WJ, Namboodiri MA (1997) Quinolinic immunoreactivity in experimental rat brain tumors is present in macrophages but not in astrocytes. *Experimental neurology* 144:287-301.
- Moncada S, Higgs EA (2006) The discovery of nitric oxide and its role in vascular biology. *Br J Pharmacol* 147 Suppl 1:S193-201.
- Morita T, Saito K, Takemura M, Maekawa N, Fujigaki S, Fujii H, Wada H, Takeuchi S, Noma A, Seishima M (2001) 3-Hydroxyanthranilic acid, an L-tryptophan metabolite, induces apoptosis in monocyte-derived cells stimulated by interferon-gamma. *Annals of clinical biochemistry* 38:242-251.
- Moriyoshi K, Masu M, Ishii T, Shigemoto R, Mizuno N, Nakanishi S (1991) Molecular cloning and characterization of the rat NMDA receptor. *Nature* 354:31-37.
- Moroni F, Cozzi A, Sili M, Mannaioni G (2012) Kynurenic acid: a metabolite with multiple actions and multiple targets in brain and periphery. *Journal of neural transmission* 119:133-139.
- Moroni F, Russi P, Lombardi G, Beni M, Carla V (1988) Presence of kynurenic acid in the mammalian brain. *J Neurochem* 51:177-180.

- Moroni F, Russi P, Gallo-Mezo MA, Moneti G, Pellicciari R (1991) Modulation of quinolinic and kynurenic acid content in the rat brain: effects of endotoxins and nicotinylalanine. *J Neurochem* 57:1630-1635.
- Muller AJ, Malachowski WP, Prendergast GC (2005) Indoleamine 2,3-dioxygenase in cancer: targeting pathological immune tolerance with small-molecule inhibitors. *Expert opinion on therapeutic targets* 9:831-849.
- Munn DH, Shafizadeh E, Attwood JT, Bondarev I, Pashine A, Mellor AL (1999) Inhibition of T cell proliferation by macrophage tryptophan catabolism. *The Journal of experimental medicine* 189:1363-1372.
- Munn DH, Sharma MD, Baban B, Harding HP, Zhang Y, Ron D, Mellor AL (2005) GCN2 kinase in T cells mediates proliferative arrest and anergy induction in response to indoleamine 2,3-dioxygenase. *Immunity* 22:633-642.
- Munn DH, Zhou M, Attwood JT, Bondarev I, Conway SJ, Marshall B, Brown C, Mellor AL (1998) Prevention of allogeneic fetal rejection by tryptophan catabolism. *Science* 281:1191-1193.
- Murray MR, Stout AP (1947) Distinctive Characteristics of the Sympathicoblastoma Cultivated in Vitro: A Method for Prompt Diagnosis. *The American journal of pathology* 23:429-441.
- Murray TV, Smyrniak I, Shah AM, Brewer AC (2013) NADPH oxidase 4 regulates cardiomyocyte differentiation via redox activation of c-Jun protein and the cis-regulation of GATA-4 gene transcription. *J Biol Chem* 288:15745-15759.
- Nagayama T, Lan J, Henshall DC, Chen D, O'Horo C, Simon RP, Chen J (2000) Induction of oxidative DNA damage in the peri-infarct region after permanent focal cerebral ischemia. *J Neurochem* 75:1716-1728.
- Nair VD, Niznik HB, Mishra RK (1996a) Interaction of NMDA and dopamine D2L receptors in human neuroblastoma SH-SY5Y cells. *J Neurochem* 66:2390-2393.
- Nair VD, Niznik HB, Mishra RK (1996b) NMDA and dopamine D2L receptor interaction in human neuroblastoma SH-SY5Y cells involves tyrosine kinase and phosphatase. *Neuroreport* 7:2937-2940.
- Naka K, Muraguchi T, Hoshii T, Hirao A (2008) Regulation of reactive oxygen species and genomic stability in hematopoietic stem cells. *Antioxidants & redox signaling* 10:1883-1894.
- Namba T, Morimoto K, Yamada N, Otsuki S (1993) Antiepileptogenic action of 7-chlorokynurenic acid on amygdala kindling of rats. *Pharmacology, biochemistry, and behavior* 46:275-281.
- Namkoong J, Shin SS, Lee HJ, Marin YE, Wall BA, Goydos JS, Chen S (2007) Metabotropic glutamate receptor 1 and glutamate signaling in human melanoma. *Cancer research* 67:2298-2305.

- Nelson DLLALCMM (2013) Lehninger principles of biochemistry. New York: W.H. Freeman.
- Nemeth H, Toldi J, Vecsei L (2005) Role of kynurenines in the central and peripheral nervous systems. *Curr Neurovasc Res* 2:249-260.
- Nicolini G, Miloso M, Zoia C, Di Silvestro A, Cavaletti G, Tredici G (1998) Retinoic acid differentiated SH-SY5Y human neuroblastoma cells: an in vitro model to assess drug neurotoxicity. *Anticancer Res* 18:2477-2481.
- Niecknig H, Tug S, Reyes BD, Kirsch M, Fandrey J, Berchner-Pfannschmidt U (2012) Role of reactive oxygen species in the regulation of HIF-1 by prolyl hydroxylase 2 under mild hypoxia. *Free radical research* 46:705-717.
- Nishida Y, Adati N, Ozawa R, Maeda A, Sakaki Y, Takeda T (2008) Identification and classification of genes regulated by phosphatidylinositol 3-kinase- and TRKB-mediated signalling pathways during neuronal differentiation in two subtypes of the human neuroblastoma cell line SH-SY5Y. *BMC Res Notes* 1:95.
- Nitti M, Furfaro AL, Cevasco C, Traverso N, Marinari UM, Pronzato MA, Domenicotti C (2010) PKC delta and NADPH oxidase in retinoic acid-induced neuroblastoma cell differentiation. *Cellular signalling* 22:828-835.
- Nitti M, Furfaro AL, Traverso N, Odetti P, Storace D, Cottalasso D, Pronzato MA, Marinari UM, Domenicotti C (2007) PKC delta and NADPH oxidase in AGE-induced neuronal death. *Neurosci Lett* 416:261-265.
- Nowak L, Bregestovski P, Ascher P, Herbet A, Prochiantz A (1984) Magnesium gates glutamate-activated channels in mouse central neurones. *Nature* 307:462-465.
- Oberley LW, Oberley TD, Buettner GR (1981) Cell division in normal and transformed cells: the possible role of superoxide and hydrogen peroxide. *Medical hypotheses* 7:21-42.
- Oe T, Sasayama T, Nagashima T, Muramoto M, Yamazaki T, Morikawa N, Okitsu O, Nishimura S, Aoki T, Katayama Y, Kita Y (2005) Differences in gene expression profile among SH-SY5Y neuroblastoma subclones with different neurite outgrowth responses to nerve growth factor. *J Neurochem* 94:1264-1276.
- Ogrunc M, Di Micco R, Lontos M, Bombardelli L, Mione M, Fumagalli M, Gorgoulis VG, d'Adda di Fagagna F (2014) Oncogene-induced reactive oxygen species fuel hyperproliferation and DNA damage response activation. *Cell death and differentiation* 21:998-1012.
- Oh GS, Pae HO, Choi BM, Chae SC, Lee HS, Ryu DG, Chung HT (2004) 3-Hydroxyanthranilic acid, one of metabolites of tryptophan via indoleamine 2,3-dioxygenase pathway, suppresses inducible nitric oxide synthase expression by enhancing heme oxygenase-1 expression. *Biochemical and biophysical research communications* 320:1156-1162.

- Oh MC, Kim JM, Safaee M, Kaur G, Sun MZ, Kaur R, Celli A, Mauro TM, Parsa AT (2012) Overexpression of calcium-permeable glutamate receptors in glioblastoma derived brain tumor initiating cells. *PloS one* 7:e47846.
- Okuda S, Nishiyama N, Saito H, Katsuki H (1998) 3-Hydroxykynurenine, an endogenous oxidative stress generator, causes neuronal cell death with apoptotic features and region selectivity. *J Neurochem* 70:299-307.
- Olesen UH, Christensen MK, Bjorkling F, Jaattela M, Jensen PB, Sehested M, Nielsen SJ (2008) Anticancer agent CHS-828 inhibits cellular synthesis of NAD. *Biochemical and biophysical research communications* 367:799-804.
- Oliveras-Ferraros C, Vazquez-Martin A, Cuyas E, Corominas-Faja B, Rodriguez-Gallego E, Fernandez-Arroyo S, Martin-Castillo B, Joven J, Menendez JA (2014) Acquired resistance to metformin in breast cancer cells triggers transcriptome reprogramming toward a degradome-related metastatic stem-like profile. *Cell cycle* 13:1132-1144.
- Olsson AK, Vadhammar K, Nanberg E (2000) Activation and protein kinase C-dependent nuclear accumulation of ERK in differentiating human neuroblastoma cells. *Experimental cell research* 256:454-467.
- Opitz CA, Litzenburger UM, Sahm F, Ott M, Tritschler I, Trump S, Schumacher T, Jestaedt L, Schrenk D, Weller M, Jugold M, Guillemin GJ, Miller CL, Lutz C, Radlwimmer B, Lehmann I, von Deimling A, Wick W, Platten M (2011) An endogenous tumour-promoting ligand of the human aryl hydrocarbon receptor. *Nature* 478:197-203.
- Ott M, Litzenburger UM, Rauschenbach KJ, Bunse L, Ochs K, Sahm F, Pusch S, Opitz CA, Blaes J, von Deimling A, Wick W, Platten M (2014) Suppression of TDO-mediated tryptophan catabolism in glioblastoma cells by a steroid-responsive FKBP52-dependent pathway. *Glia*.
- Ou X, Chae HD, Wang RH, Shelley WC, Cooper S, Taylor T, Kim YJ, Deng CX, Yoder MC, Broxmeyer HE (2011) SIRT1 deficiency compromises mouse embryonic stem cell hematopoietic differentiation, and embryonic and adult hematopoiesis in the mouse. *Blood* 117:440-450.
- Oxenkrug GF (2007) Tryptophan metabolism as a new target for the treatment of schizophrenia. *US Psychiatry Review*:38-39
- SRC - GoogleScholar.
- Pahlman S, Ruusala AI, Abrahamsson L, Mattsson ME, Esscher T (1984) Retinoic acid-induced differentiation of cultured human neuroblastoma cells: a comparison with phorbol ester-induced differentiation. *Cell differentiation* 14:135-144.
- Pahlman S, Hoehner JC, Nanberg E, Hedborg F, Fagerstrom S, Gestblom C, Johansson I, Larsson U, Lavenius E, Ortoft E, et al. (1995) Differentiation and survival

- influences of growth factors in human neuroblastoma. *European journal of cancer* 31A:453-458.
- Pantouris G, Mowat CG (2014) Antitumour agents as inhibitors of tryptophan 2,3-dioxygenase. *Biochemical and biophysical research communications* 443:28-31.
- Paoletti P (2011) Molecular basis of NMDA receptor functional diversity. *Eur J Neurosci* 33:1351-1365.
- Paoletti P, Bellone C, Zhou Q (2013) NMDA receptor subunit diversity: impact on receptor properties, synaptic plasticity and disease. *Nature reviews Neuroscience* 14:383-400.
- Park KW, Nozell SE, Benveniste EN (2012) Protective role of STAT3 in NMDA and glutamate-induced neuronal death: negative regulatory effect of SOCS3. *PloS one* 7:e50874.
- Park SY, Kwon HJ, Lee HE, Ryu HS, Kim SW, Kim JH, Kim IA, Jung N, Cho NY, Kang GH (2011) Promoter CpG island hypermethylation during breast cancer progression. *Virchows Archiv : an international journal of pathology* 458:73-84.
- Parks E, Traber MG (2000) Mechanisms of vitamin E regulation: research over the past decade and focus on the future. *Antioxidants & redox signaling* 2:405-412.
- Parsons CG, Quack G, Bresink I, Baran L, Przegalinski E, Kostowski W, Krzascik P, Hartmann S, Danysz W (1995) Comparison of the potency, kinetics and voltage-dependency of a series of uncompetitive NMDA receptor antagonists in vitro with anticonvulsive and motor impairment activity in vivo. *Neuropharmacology* 34:1239-1258.
- Parsons RB, Aravindan S, Kadampeswaran A, Evans EA, Sandhu KK, Levy ER, Thomas MG, Austen BM, Ramsden DB (2011) The expression of nicotinamide N-methyltransferase increases ATP synthesis and protects SH-SY5Y neuroblastoma cells against the toxicity of Complex I inhibitors. *The Biochemical journal* 436:145-155.
- Peck A, Mellins ED (2010) Plasticity of T-cell phenotype and function: the T helper type 17 example. *Immunology* 129:147-153.
- Perkins MN, Stone TW (1982) An iontophoretic investigation of the actions of convulsant kynurenines and their interaction with the endogenous excitant quinolinic acid. *Brain research* 247:184-187.
- Peter Guengerich F, Martin MV, McCormick WA, Nguyen LP, Glover E, Bradfield CA (2004) Aryl hydrocarbon receptor response to indigoids in vitro and in vivo. *Archives of biochemistry and biophysics* 423:309-316.
- Petros JA, Baumann AK, Ruiz-Pesini E, Amin MB, Sun CQ, Hall J, Lim S, Issa MM, Flanders WD, Hosseini SH, Marshall FF, Wallace DC (2005) mtDNA mutations increase tumorigenicity in prostate cancer. *Proc Natl Acad Sci U S A* 102:719-724.

- Phillips RS (2011) Structure, mechanism, and substrate specificity of kynureninase. *Biochimica et biophysica acta* 1814:1481-1488.
- Pilotte L, Larrieu P, Stroobant V, Colau D, Dolusic E, Frederick R, De Plaen E, Uyttenhove C, Wouters J, Masereel B, Van den Eynde BJ (2012) Reversal of tumoral immune resistance by inhibition of tryptophan 2,3-dioxygenase. *Proc Natl Acad Sci U S A* 109:2497-2502.
- Piscianz E, Cuzzoni E, De Iudicibus S, Valencic E, Decorti G, Tommasini A (2011) Differential action of 3-hydroxyanthranilic acid on viability and activation of stimulated lymphocytes. *International immunopharmacology* 11:2242-2245.
- Pizzi M, Boroni F, Bianchetti A, Moraitis C, Sarnico I, Benarese M, Goffi F, Valerio A, Spano P (2002) Expression of functional NR1/NR2B-type NMDA receptors in neuronally differentiated SK-N-SH human cell line. *Eur J Neurosci* 16:2342-2350.
- Platten M, Wick W, Van den Eynde BJ (2012) Tryptophan catabolism in cancer: beyond IDO and tryptophan depletion. *Cancer research* 72:5435-5440.
- Poderoso JJ, Carreras MC, Lisdero C, Riobo N, Schopfer F, Boveris A (1996) Nitric oxide inhibits electron transfer and increases superoxide radical production in rat heart mitochondria and submitochondrial particles. *Archives of biochemistry and biophysics* 328:85-92.
- Pollak N, Dolle C, Ziegler M (2007) The power to reduce: pyridine nucleotides--small molecules with a multitude of functions. *The Biochemical journal* 402:205-218.
- Poluha W, Poluha DK, Ross AH (1995) TrkA neurogenic receptor regulates differentiation of neuroblastoma cells. *Oncogene* 10:185-189.
- Potula R, Poluektova L, Knipe B, Chrastil J, Heilman D, Dou H, Takikawa O, Munn DH, Gendelman HE, Persidsky Y (2005) Inhibition of indoleamine 2,3-dioxygenase (IDO) enhances elimination of virus-infected macrophages in an animal model of HIV-1 encephalitis. *Blood* 106:2382-2390.
- Premkumar LS, Qin F, Auerbach A (1997) Subconductance states of a mutant NMDA receptor channel kinetics, calcium, and voltage dependence. *The Journal of general physiology* 109:181-189.
- Prendergast GC, Metz R, Muller AJ (2010) Towards a genetic definition of cancer-associated inflammation: role of the IDO pathway. *The American journal of pathology* 176:2082-2087.
- Prince JA, Orelan L (1997) Staurosporine differentiated human SH-SY5Y neuroblastoma cultures exhibit transient apoptosis and trophic factor independence. *Brain research bulletin* 43:515-523.
- Puccetti P, Grohmann U (2007) IDO and regulatory T cells: a role for reverse signalling and non-canonical NF-kappaB activation. *Nature reviews Immunology* 7:817-823.

- Rahman H, Qasim M, Schultze FC, Oellerich M, A RA (2011) Fetal calf serum heat inactivation and lipopolysaccharide contamination influence the human T lymphoblast proteome and phosphoproteome. *Proteome science* 9:71.
- Raj L, Ide T, Gurkar AU, Foley M, Schenone M, Li X, Tolliday NJ, Golub TR, Carr SA, Shamji AF, Stern AM, Mandinova A, Schreiber SL, Lee SW (2011) Selective killing of cancer cells by a small molecule targeting the stress response to ROS. *Nature* 475:231-234.
- Ralph SJ, Rodriguez-Enriquez S, Neuzil J, Saavedra E, Moreno-Sanchez R (2010) The causes of cancer revisited: "mitochondrial malignancy" and ROS-induced oncogenic transformation - why mitochondria are targets for cancer therapy. *Molecular aspects of medicine* 31:145-170.
- Ramaswamy P, Aditi Devi N, Hurmath Fathima K, Dalavaikodihalli Nanjaiah N (2014) Activation of NMDA receptor of glutamate influences MMP-2 activity and proliferation of glioma cells. *Neurological sciences : official journal of the Italian Neurological Society and of the Italian Society of Clinical Neurophysiology* 35:823-829.
- Ramsey MR, Sharpless NE (2006) ROS as a tumour suppressor? *Nature cell biology* 8:1213-1215.
- Ranjan P, Anathy V, Burch PM, Weirather K, Lambeth JD, Heintz NH (2006) Redox-dependent expression of cyclin D1 and cell proliferation by Nox1 in mouse lung epithelial cells. *Antioxidants & redox signaling* 8:1447-1459.
- Reddy NM, Kleeberger SR, Cho HY, Yamamoto M, Kensler TW, Biswal S, Reddy SP (2007) Deficiency in Nrf2-GSH signaling impairs type II cell growth and enhances sensitivity to oxidants. *American journal of respiratory cell and molecular biology* 37:3-8.
- Reddy PS, Umesh S, Thota B, Tandon A, Pandey P, Hegde AS, Balasubramaniam A, Chandramouli BA, Santosh V, Rao MR, Kondaiah P, Somasundaram K (2008) PBEF1/NAmPRTase/Visfatin: a potential malignant astrocytoma/glioblastoma serum marker with prognostic value. *Cancer biology & therapy* 7:663-668.
- Remacle J, Raes M, Toussaint O, Renard P, Rao G (1995) Low levels of reactive oxygen species as modulators of cell function. *Mutation research* 316:103-122.
- Reynolds CP, Matthay KK, Villablanca JG, Maurer BJ (2003a) Retinoid therapy of high-risk neuroblastoma. *Cancer letters* 197:185-192.
- Reynolds PR, Schaalje GB, Seegmiller RE (2003b) Combination therapy with folic acid and methionine in the prevention of retinoic acid-induced cleft palate in mice. *Birth defects research Part A, Clinical and molecular teratology* 67:168-173.

- Ribeiro CA, Grando V, Dutra Filho CS, Wannmacher CM, Wajner M (2006) Evidence that quinolinic acid severely impairs energy metabolism through activation of NMDA receptors in striatum from developing rats. *J Neurochem* 99:1531-1542.
- Robinson KM, Janes MS, Beckman JS (2008) The selective detection of mitochondrial superoxide by live cell imaging. *Nat Protoc* 3:941-947.
- Rodriguez-Martinez E, Camacho A, Maldonado PD, Pedraza-Chaverri J, Santamaria D, Galvan-Arzate S, Santamaria A (2000) Effect of quinolinic acid on endogenous antioxidants in rat corpus striatum. *Brain research* 858:436-439.
- Rogawski MA (1993) Therapeutic potential of excitatory amino acid antagonists: channel blockers and 2,3-benzodiazepines. *Trends in pharmacological sciences* 14:325-331.
- Rosen DR, Siddique T, Patterson D, Figlewicz DA, Sapp P, Hentati A, Donaldson D, Goto J, O'Regan JP, Deng HX, et al. (1993) Mutations in Cu/Zn superoxide dismutase gene are associated with familial amyotrophic lateral sclerosis. *Nature* 362:59-62.
- Ross RA, Spengler BA, Biedler JL (1983) Coordinate morphological and biochemical interconversion of human neuroblastoma cells. *J Natl Cancer Inst* 71:741-747.
- Ross RA, Spengler BA, Domenech C, Porubcin M, Rettig WJ, Biedler JL (1995) Human neuroblastoma I-type cells are malignant neural crest stem cells. *Cell growth & differentiation : the molecular biology journal of the American Association for Cancer Research* 6:449-456.
- Rothstein JD, Brem H (2001) Excitotoxic destruction facilitates brain tumor growth. *Nature medicine* 7:994-995.
- Rouleau M, Patel A, Hendzel MJ, Kaufmann SH, Poirier GG (2010) PARP inhibition: PARP1 and beyond. *Nature reviews Cancer* 10:293-301.
- Roy S, Venojarvi M, Khanna S, Sen CK (2002) Simultaneous detection of tocopherols and tocotrienols in biological samples using HPLC-coulometric electrode array. *Methods in enzymology* 352:326-332.
- Rycroft BK, Gibb AJ (2002) Direct effects of calmodulin on NMDA receptor single-channel gating in rat hippocampal granule cells. *The Journal of neuroscience : the official journal of the Society for Neuroscience* 22:8860-8868.
- Rycroft BK, Gibb AJ (2004) Inhibitory interactions of calcineurin (phosphatase 2B) and calmodulin on rat hippocampal NMDA receptors. *Neuropharmacology* 47:505-514.
- Rzeski W, Turski L, Ikonomidou C (2001) Glutamate antagonists limit tumor growth. *Proc Natl Acad Sci U S A* 98:6372-6377.
- Rzeski W, Turski L, Ikonomidou C (2005) Anticancer Effects of Glutamate Antagonists. In: *Glutamate Receptors in Peripheral Tissue: Excitatory Transmission Outside the CNS* (Gill S, Pulido O, eds), pp 77-85: Springer US.

- Saini A, Al-Shanti N, Sharples AP, Stewart CE (2012) Sirtuin 1 regulates skeletal myoblast survival and enhances differentiation in the presence of resveratrol. *Experimental physiology* 97:400-418.
- Saito K, Crowley JS, Markey SP, Heyes MP (1993a) A mechanism for increased quinolinic acid formation following acute systemic immune stimulation. *J Biol Chem* 268:15496-15503.
- Saito K, Chen CY, Masana M, Crowley JS, Markey SP, Heyes MP (1993b) 4-Chloro-3-hydroxyanthranilate, 6-chlorotryptophan and norharmaline attenuate quinolinic acid formation by interferon-gamma-stimulated monocytes (THP-1 cells). *The Biochemical journal* 291 (Pt 1):11-14.
- Salt TE, Herrling PL (1991) Excitatory amino acid transmitter function in mammalian central pathways. In: *Excitatory Amino Acids and Synaptic Function* (Wheal H, Thomson AM, eds), pp 155-170. London Academic Press.
- Salvati P, Ukmar G, Dho L, Rosa B, Cini M, Marconi M, Molinari A, Post C (1999) Brain concentrations of kynurenic acid after a systemic neuroprotective dose in the gerbil model of global ischemia. *Prog Neuropsychopharmacol Biol Psychiatry* 23:741-752.
- Santamaria A, Galvan-Arzate S, Lisy V, Ali SF, Duhart HM, Osorio-Rico L, Rios C, St'astny F (2001) Quinolinic acid induces oxidative stress in rat brain synaptosomes. *Neuroreport* 12:871-874.
- Santos DM, Santos MM, Moreira R, Sola S, Rodrigues CM (2013) Synthetic condensed 1,4-naphthoquinone derivative shifts neural stem cell differentiation by regulating redox state. *Molecular neurobiology* 47:313-324.
- Santos MA *et al.* (2014) DNA-damage-induced differentiation of leukaemic cells as an anti-cancer barrier. *Nature* 514:107-111.
- Sarkhosh K, Tredget EE, Li Y, Kilani RT, Uludag H, Ghahary A (2003a) Proliferation of peripheral blood mononuclear cells is suppressed by the indoleamine 2,3-dioxygenase expression of interferon-gamma-treated skin cells in a co-culture system. *Wound repair and regeneration : official publication of the Wound Healing Society [and] the European Tissue Repair Society* 11:337-345.
- Sarkhosh K, Tredget EE, Karami A, Uludag H, Iwashina T, Kilani RT, Ghahary A (2003b) Immune cell proliferation is suppressed by the interferon-gamma-induced indoleamine 2,3-dioxygenase expression of fibroblasts populated in collagen gel (FPCG). *Journal of cellular biochemistry* 90:206-217.
- Sastry PS, Rao KS (2000) Apoptosis and the nervous system. *J Neurochem* 74:1-20.
- Sauer H, Wartenberg M (2005) Reactive oxygen species as signaling molecules in cardiovascular differentiation of embryonic stem cells and tumor-induced angiogenesis. *Antioxidants & redox signaling* 7:1423-1434.

- Sawyer DT, Roberts JL, Jr., Calderwood TS, Sugimoto H, McDowell MS (1985) Reactivity and activation of dioxygen-derived species in aprotic media (a model matrix for biomembranes). *Philosophical transactions of the Royal Society of London Series B, Biological sciences* 311:483-503.
- Sayin VI, Ibrahim MX, Larsson E, Nilsson JA, Lindahl P, Bergo MO (2014) Antioxidants accelerate lung cancer progression in mice. *Science translational medicine* 6:221ra215.
- Schmidt SK, Muller A, Heseler K, Woite C, Spekker K, MacKenzie CR, Daubener W (2009) Antimicrobial and immunoregulatory properties of human tryptophan 2,3-dioxygenase. *European journal of immunology* 39:2755-2764.
- Schneider L, Giordano S, Zelickson BR, M SJ, G AB, Ouyang X, Fineberg N, Darley-Usmar VM, Zhang J (2011) Differentiation of SH-SY5Y cells to a neuronal phenotype changes cellular bioenergetics and the response to oxidative stress. *Free radical biology & medicine* 51:2007-2017.
- Schrocksnadel K, Widner B, Bergant A, Neurauter G, Schennach H, Schrocksnadel H, D. (2003) Fuchs study of tryptophan degradation during and after pregnancy. *Life Sci* 72 SRC - GoogleScholar:785-793.
- Schuck PF, Tonin A, da Costa Ferreira G, Viegas CM, Latini A, Duval Wannmacher CM, de Souza Wyse AT, Dutra-Filho CS, Wajner M (2007a) Kynurenines impair energy metabolism in rat cerebral cortex. *Cell Mol Neurobiol* 27:147-160.
- Schuck PF, Tonin A, da Costa Ferreira G, Rosa RB, Latini A, Balestro F, Perry ML, Wannmacher CM, de Souza Wyse AT, Wajner M (2007b) In vitro effect of quinolinic acid on energy metabolism in brain of young rats. *Neuroscience research* 57:277-288.
- Schwarcz R, Whetsell WO, Mangano RM (1983) Quinolinic acid: an endogenous metabolite that produces axon-sparing lesions in rat brain. *Science (New York, NY)* 219:316-318.
- Schwarcz R, Bruno JP, Muchowski PJ, Wu HQ (2012) Kynurenines in the mammalian brain: when physiology meets pathology. *Nature reviews Neuroscience* 13:465-477.
- Schwarz RF, Trinh A, Sipos B, Brenton JD, Goldman N, Markowitz F (2014) Phylogenetic quantification of intra-tumour heterogeneity. *PLoS computational biology* 10:e1003535.
- Seeger RC, Rayner SA, Banerjee A, Chung H, Laug WE, Neustein HB, Benedict WF (1977) Morphology, growth, chromosomal pattern and fibrinolytic activity of two new human neuroblastoma cell lines. *Cancer research* 37:1364-1371.

- Sekkai D, Guittet O, Lemaire G, Tenu JP, Lepoivre M (1997) Inhibition of nitric oxide synthase expression and activity in macrophages by 3-hydroxyanthranilic acid, a tryptophan metabolite. *Archives of biochemistry and biophysics* 340:117-123.
- Serrano-Castro PJ, Garcia-Torrecillas JM (2012) Cajal's first steps in scientific research. *Neuroscience* 217:1-5.
- Seyfried TN (2012) Nothing in Cancer Biology Makes Sense Except in the Light of Evolution. In: *Cancer as a Metabolic Disease*, pp 261-275: John Wiley & Sons, Inc.
- Shen Z (2011) Genomic instability and cancer: an introduction. *Journal of molecular cell biology* 3:1-3.
- Shi X, Zhang Y, Zheng J, Pan J (2012) Reactive oxygen species in cancer stem cells. *Antioxidants & redox signaling* 16:1215-1228.
- Shimada H, Umehara S, Monobe Y, Hachitanda Y, Nakagawa A, Goto S, Gerbing RB, Stram DO, Lukens JN, Matthay KK (2001) International neuroblastoma pathology classification for prognostic evaluation of patients with peripheral neuroblastic tumors: a report from the Children's Cancer Group. *Cancer* 92:2451-2461.
- Shin MK, Jung WR, Kim HG, Roh SE, Kwak CH, Kim CH, Kim SJ, Kim KL (2014) The ganglioside GQ1b regulates BDNF expression via the NMDA receptor signaling pathway. *Neuropharmacology* 77:414-421.
- Simpson PB, Bacha JI, Palfreyman EL, Woollacott AJ, McKernan RM, Kerby J (2001) Retinoic acid evoked-differentiation of neuroblastoma cells predominates over growth factor stimulation: an automated image capture and quantitation approach to neuritogenesis. *Analytical biochemistry* 298:163-169.
- Singh J, Kaur G (2005) Neuroprotection mediated by subtoxic dose of NMDA in SH-SY5Y neuroblastoma cultures: activity-dependent regulation of PSA-NCAM expression. *Brain research Molecular brain research* 137:223-234.
- Singh J, Kaur G (2007) Transcriptional regulation of polysialylated neural cell adhesion molecule expression by NMDA receptor activation in retinoic acid-differentiated SH-SY5Y neuroblastoma cultures. *Brain research* 1154:8-21.
- Singh L, Oles RJ, Tricklebank MD (1990) Modulation of seizure susceptibility in the mouse by the strychnine-insensitive glycine recognition site of the NMDA receptor/ion channel complex. *Br J Pharmacol* 99:285-288.
- Smith AJ, Stone TW, Smith RA (2007) Neurotoxicity of tryptophan metabolites. *Biochem Soc Trans* 35:1287-1289.
- Smothers CT, Woodward JJ (2007) Pharmacological characterization of glycine-activated currents in HEK 293 cells expressing N-methyl-D-aspartate NR1 and NR3 subunits. *The Journal of pharmacology and experimental therapeutics* 322:739-748.

- Song LP, Zhang J, Wu SF, Huang Y, Zhao Q, Cao JP, Wu YL, Wang LS, Chen GQ (2008) Hypoxia-inducible factor-1 α -induced differentiation of myeloid leukemic cells is its transcriptional activity independent. *Oncogene* 27:519-527.
- Sonntag Cv (1987) *The Chemical Basis of Radiation Biology*. London: Taylor & Francis.
- Sontheimer H (2008) A role for glutamate in growth and invasion of primary brain tumors. *J Neurochem* 105:287-295.
- Sousa FG, Matuo R, Soares DG, Escargueil AE, Henriques JA, Larsen AK, Saffi J (2012) PARPs and the DNA damage response. *Carcinogenesis* 33:1433-1440.
- Speciale C, Hares K, Schwarcz R, Brookes N (1989) High-affinity uptake of L-kynurenine by a Na⁺-independent transporter of neutral amino acids in astrocytes. *The Journal of neuroscience : the official journal of the Society for Neuroscience* 9:2066-2072.
- Speciale C, Wu HQ, Cini M, Marconi M, Varasi M, Schwarcz R (1996) (R,S)-3,4-dichlorobenzoylalanine (FCE 28833A) causes a large and persistent increase in brain kynurenic acid levels in rats. *Eur J Pharmacol* 315:263-267.
- Speleman F, De Preter K, Vandesompele J (2011) Neuroblastoma genetics and phenotype: a tale of heterogeneity. *Seminars in cancer biology* 21:238-244.
- Spencer JP, Jenner P, Daniel SE, Lees AJ, Marsden DC, Halliwell B (1998) Conjugates of catecholamines with cysteine and GSH in Parkinson's disease: possible mechanisms of formation involving reactive oxygen species. *J Neurochem* 71:2112-2122.
- Spengler BA, Biedler JL, Ross RA (2002) A corrected karyotype for the SH-SY5Y human neuroblastoma cell line. *Cancer genetics and cytogenetics* 138:177-178.
- Squadrito GL, Pryor WA (1995) The formation of peroxynitrite in vivo from nitric oxide and superoxide. *Chemico-biological interactions* 96:203-206.
- Stadtman ER (1992) Protein oxidation and aging. *Science* 257:1220-1224.
- Stadtman ER, Berlett BS (1997) Reactive oxygen-mediated protein oxidation in aging and disease. *Chem Res Toxicol* 10:485-494.
- Stamler JS (1994) Redox signaling: nitrosylation and related target interactions of nitric oxide. *Cell* 78:931-936.
- Stark G (2005) Functional consequences of oxidative membrane damage. *The Journal of membrane biology* 205:1-16.
- Stepulak A, Rola R, Polberg K, Ikonomidou C (2014) Glutamate and its receptors in cancer. *Journal of neural transmission* 121:933-944.
- Stepulak A, Sifringer M, Rzeski W, Endesfelder S, Gratopp A, Pohl EE, Bittigau P, Felderhoff-Mueser U, Kaindl AM, Buhner C, Hansen HH, Stryjecka-Zimmer M, Turski L, Ikonomidou C (2005) NMDA antagonist inhibits the extracellular signal-

- regulated kinase pathway and suppresses cancer growth. *Proc Natl Acad Sci U S A* 102:15605-15610.
- Stevens EA, Mezrich JD, Bradfield CA (2009) The aryl hydrocarbon receptor: a perspective on potential roles in the immune system. *Immunology* 127:299-311.
- Stiller CA, Parkin DM (1992) International variations in the incidence of neuroblastoma. *International journal of cancer Journal international du cancer* 52:538-543.
- Stone TW (1993) Neuropharmacology of quinolinic and kynurenic acids. *Pharmacological reviews* 45:309-379.
- Stone TW (2001) Endogenous neurotoxins from tryptophan. *Toxicol* 39:61-73.
- Stone TW (2007) Kynurenic acid blocks nicotinic synaptic transmission to hippocampal interneurons in young rats. *Eur J Neurosci* 25:2656-2665.
- Stone TW, Perkins MN (1981) Quinolinic acid: a potent endogenous excitant at amino acid receptors in CNS. *Eur J Pharmacol* 72:411-412.
- Stone TW, Darlington LG (2002) Endogenous kynurenines as targets for drug discovery and development. *Nature reviews Drug discovery* 1:609-620.
- Stoy N, Mackay GM, Forrest CM, Christofides J, Egerton M, Stone TW, Darlington LG (2005) Tryptophan metabolism and oxidative stress in patients with Huntington's disease. *J Neurochem* 93:611-623.
- Strehl R, Schumacher K, de Vries U, Minuth WW (2002) Proliferating cells versus differentiated cells in tissue engineering. *Tissue engineering* 8:37-42.
- Sun ZW, Zhang L, Zhu SJ, Chen WC, Mei B (2010) Excitotoxicity effects of glutamate on human neuroblastoma SH-SY5Y cells via oxidative damage. *Neuroscience bulletin* 26:8-16.
- Swanson KA, Zheng Y, Heidler KM, Mizobuchi T, Wilkes DS (2004) CD11c+ cells modulate pulmonary immune responses by production of indoleamine 2,3-dioxygenase. *American journal of respiratory cell and molecular biology* 30:311-318.
- Szatrowski TP, Nathan CF (1991) Production of large amounts of hydrogen peroxide by human tumor cells. *Cancer research* 51:794-798.
- Takahashi A, Ohtani N, Yamakoshi K, Iida S, Tahara H, Nakayama K, Nakayama KI, Ide T, Saya H, Hara E (2006) Mitogenic signalling and the p16INK4a-Rb pathway cooperate to enforce irreversible cellular senescence. *Nature cell biology* 8:1291-1297.
- Takano T, Lin JH, Arcuino G, Gao Q, Yang J, Nedergaard M (2001) Glutamate release promotes growth of malignant gliomas. *Nature medicine* 7:1010-1015.
- Tetich M, Kutner A, Leskiewicz M, Budziszewska B, Lason W (2004) Neuroprotective effects of (24R)-1,24-dihydroxycholecalciferol in human neuroblastoma SH-SY5Y cell line. *The Journal of steroid biochemistry and molecular biology* 89-90:365-370.

- Thaker AI, Rao MS, Bishnupuri KS, Kerr TA, Foster L, Marinshaw JM, Newberry RD, Stenson WF, Ciorba MA (2013) IDO1 metabolites activate beta-catenin signaling to promote cancer cell proliferation and colon tumorigenesis in mice. *Gastroenterology* 145:416-425 e411-414.
- Thomas MG, Saldanha M, Mistry RJ, Dexter DT, Ramsden DB, Parsons RB (2013) Nicotinamide N-methyltransferase expression in SH-SY5Y neuroblastoma and N27 mesencephalic neurones induces changes in cell morphology via ephrin-B2 and Akt signalling. *Cell death & disease* 4:e669.
- Thomas SR, Witting PK, Stocker R (1996) 3-Hydroxyanthranilic acid is an efficient, cell-derived co-antioxidant for alpha-tocopherol, inhibiting human low density lipoprotein and plasma lipid peroxidation. *J Biol Chem* 271:32714-32721.
- Tieu K, Zuo DM, Yu PH (1999) Differential effects of staurosporine and retinoic acid on the vulnerability of the SH-SY5Y neuroblastoma cells: involvement of bcl-2 and p53 proteins. *Journal of neuroscience research* 58:426-435.
- Tiligada E (2006) Chemotherapy: induction of stress responses. *Endocrine-related cancer* 13 Suppl 1:S115-124.
- Tohda C, Nakamura N, Komatsu K, Hattori M (1999) Trigonelline-induced neurite outgrowth in human neuroblastoma SK-N-SH cells. *Biological & pharmaceutical bulletin* 22:679-682.
- Toyokuni S (2006) Novel aspects of oxidative stress-associated carcinogenesis. *Antioxidants & redox signaling* 8:1373-1377.
- Trachootham D, Lu W, Ogasawara MA, Nilsa RD, Huang P (2008) Redox regulation of cell survival. *Antioxidants & redox signaling* 10:1343-1374.
- Travelli C, Drago V, Maldi E, Kaludercic N, Galli U, Boldorini R, Di Lisa F, Tron GC, Canonico PL, Genazzani AA (2011) Reciprocal potentiation of the antitumoral activities of FK866, an inhibitor of nicotinamide phosphoribosyltransferase, and etoposide or cisplatin in neuroblastoma cells. *The Journal of pharmacology and experimental therapeutics* 338:829-840.
- Traynelis SF, Hartley M, Heinemann SF (1995) Control of proton sensitivity of the NMDA receptor by RNA splicing and polyamines. *Science* 268:873-876.
- Turski WA, Gramsbergen JB, Traitler H, Schwarcz R (1989) Rat brain slices produce and liberate kynurenic acid upon exposure to L-kynurenine. *J Neurochem* 52:1629-1636.
- Turski WA, Nakamura M, Todd WP, Carpenter BK, Whetsell WO, Jr., Schwarcz R (1988) Identification and quantification of kynurenic acid in human brain tissue. *Brain research* 454:164-169.

- Uberti D, Rizzini C, Galli P, Pizzi M, Grilli M, Lesage A, Spano P, Memo M (1997) Priming of cultured neurons with sabeluzole results in long-lasting inhibition of neurotoxin-induced tau expression and cell death. *Synapse* 26:95-103.
- Uchida K (1999) Current status of acrolein as a lipid peroxidation product. *Trends in cardiovascular medicine* 9:109-113.
- Ueda T, Otsuka H, Goda K, Ishiguro I, Naito J, Kotake Y (1978) The metabolism of [carboxyl-¹⁴C]anthranilic acid. I. The incorporation of radioactivity into NAD⁺ and NADP⁺. *Journal of biochemistry* 84:687-696.
- Uhasz GJ, Barkoczi B, Vass G, Datki Z, Hunya A, Fulop L, Budai D, Penke B, Szegedi V (2010) Fibrillar Aβ₁₋₄₂ enhances NMDA receptor sensitivity via the integrin signaling pathway. *Journal of Alzheimer's disease : JAD* 19:1055-1067.
- Uyttenhove C, Pilotte L, Theate I, Stroobant V, Colau D, Parmentier N, Boon T, Van den Eynde BJ (2003) Evidence for a tumoral immune resistance mechanism based on tryptophan degradation by indoleamine 2,3-dioxygenase. *Nature medicine* 9:1269-1274.
- Valencia A, Moran J (2001) Role of oxidative stress in the apoptotic cell death of cultured cerebellar granule neurons. *Journal of neuroscience research* 64:284-297.
- Valentine JS, Miksztal AR, Sawyer DT (1984) Methods for the study of superoxide chemistry in nonaqueous solutions. *Methods in enzymology* 105:71-81.
- Vamos E, Pardutz A, Klivenyi P, Toldi J, Vecsei L (2009) The role of kynurenines in disorders of the central nervous system: possibilities for neuroprotection. *J Neurol Sci* 283:21-27.
- Van den Eynde B, Lethe B, Van Pel A, De Plaen E, Boon T (1991) The gene coding for a major tumor rejection antigen of tumor P815 is identical to the normal gene of syngeneic DBA/2 mice. *The Journal of experimental medicine* 173:1373-1384.
- Vangipuram SD, Wang ZJ, Lyman WD (2010) Resistance of stem-like cells from neuroblastoma cell lines to commonly used chemotherapeutic agents. *Pediatric blood & cancer* 54:361-368.
- Vargas MR, Burton NC, Kutzke J, Gan L, Johnson DA, Schafer M, Werner S, Johnson JA (2013) Absence of Nrf2 or its selective overexpression in neurons and muscle does not affect survival in ALS-linked mutant hSOD1 mouse models. *PLoS one* 8:e56625.
- Veal GJ, Errington J, Rowbotham SE, Illingworth NA, Malik G, Cole M, Daly AK, Pearson AD, Boddy AV (2013) Adaptive dosing approaches to the individualization of 13-*cis*-retinoic acid (isotretinoin) treatment for children with high-risk neuroblastoma. *Clinical cancer research : an official journal of the American Association for Cancer Research* 19:469-479.

- Velisek L, Roztocilova L, Kusa R, Mares P (1995) Excitatory amino acid antagonists and pentylenetetrazol-induced seizures during ontogenesis: III. The action of kynurenic acid and glutamic acid diethylester. *Brain research bulletin* 38:525-529.
- Vieira HL, Alves PM, Vercelli A (2011) Modulation of neuronal stem cell differentiation by hypoxia and reactive oxygen species. *Progress in neurobiology* 93:444-455.
- Virchow RLK (1863) *Die krankhaften Geschwülste: dressig Volesungen gehalten während des Wintersemesters 1862-1863 an der Universität zu Berlin*: A. Hirschwald.
- Vomhof-Dekrey EE, Picklo MJ, Sr. (2012) The Nrf2-antioxidant response element pathway: a target for regulating energy metabolism. *The Journal of nutritional biochemistry* 23:1201-1206.
- Vurusaner B, Poli G, Basaga H (2012) Tumor suppressor genes and ROS: complex networks of interactions. *Free radical biology & medicine* 52:7-18.
- Wada A, Takahashi H, Lipton SA, Chen HS (2006) NR3A modulates the outer vestibule of the "NMDA" receptor channel. *The Journal of neuroscience : the official journal of the Society for Neuroscience* 26:13156-13166.
- Wainwright DA, Dey M, Chang A, Lesniak MS (2013) Targeting Tregs in Malignant Brain Cancer: Overcoming IDO. *Front Immunol* 4:116.
- Wainwright DA, Balyasnikova IV, Chang AL, Ahmed AU, Moon KS, Auffinger B, Tobias AL, Han Y, Lesniak MS (2012) IDO expression in brain tumors increases the recruitment of regulatory T cells and negatively impacts survival. *Clinical cancer research : an official journal of the American Association for Cancer Research* 18:6110-6121.
- Walczak K, Dabrowski W, Langner E, Zgrajka W, Pilat J, Kocki T, Rzeski W, Turski WA (2011) Kynurenic acid synthesis and kynurenine aminotransferases expression in colon derived normal and cancer cells. *Scandinavian journal of gastroenterology* 46:903-912.
- Walczak K, Zurawska M, Kis J, Starownik R, Zgrajka W, Bar K, Turski WA, Rzeski W (2012) Kynurenic acid in human renal cell carcinoma: its antiproliferative and antimigrative action on Caki-2 cells. *Amino acids* 43:1663-1670.
- Walczak K, Deneka-Hannemann S, Jarosz B, Zgrajka W, Stoma F, Trojanowski T, Turski WA, Rzeski W (2014) Kynurenic acid inhibits proliferation and migration of human glioblastoma T98G cells. *Pharmacological reports : PR* 66:130-136.
- Wallace DC (1992) Mitochondrial genetics: a paradigm for aging and degenerative diseases? *Science* 256:628-632.
- Walton JD, Kattan DR, Thomas SK, Spengler BA, Guo HF, Biedler JL, Cheung NK, Ross RA (2004) Characteristics of stem cells from human neuroblastoma cell lines and in tumors. *Neoplasia* 6:838-845.

- Wang B, Hasan MK, Alvarado E, Yuan H, Wu H, Chen WY (2011) NAMPT overexpression in prostate cancer and its contribution to tumor cell survival and stress response. *Oncogene* 30:907-921.
- Wang J, Simonavicius N, Wu X, Swaminath G, Reagan J, Tian H, Ling L (2006) Kynurenic acid as a ligand for orphan G protein-coupled receptor GPR35. *J Biol Chem* 281:22021-22028.
- Wang RH, Sengupta K, Li C, Kim HS, Cao L, Xiao C, Kim S, Xu X, Zheng Y, Chilton B, Jia R, Zheng ZM, Appella E, Wang XW, Ried T, Deng CX (2008) Impaired DNA damage response, genome instability, and tumorigenesis in SIRT1 mutant mice. *Cancer cell* 14:312-323.
- Watanabe K, Kanno T, Oshima T, Miwa H, Tashiro C, Nishizaki T (2008) The NMDA receptor NR2A subunit regulates proliferation of MKN45 human gastric cancer cells. *Biochemical and biophysical research communications* 367:487-490.
- Watkins JC, Jane DE (2006) The glutamate story. *Br J Pharmacol* 147 Suppl 1:S100-108.
- Wei X, Walia V, Lin JC, Teer JK, Prickett TD, Gartner J, Davis S, Program NCS, Stemke-Hale K, Davies MA, Gershenwald JE, Robinson W, Robinson S, Rosenberg SA, Samuels Y (2011) Exome sequencing identifies GRIN2A as frequently mutated in melanoma. *Nature genetics* 43:442-446.
- Weinreb O, Bar-Am O, Amit T, Drigues N, Sagi Y, Youdim MB (2008) The neuroprotective effect of ladostigil against hydrogen peroxide-mediated cytotoxicity. *Chemico-biological interactions* 175:318-326.
- Werner-Felmayer G, Werner ER, Fuchs D, Hausen A, Reibnegger G, Wachter H (1989) Characteristics of interferon induced tryptophan metabolism in human cells in vitro. *Biochimica et biophysica acta* 1012:140-147.
- Whetsell WO, Jr., Schwarcz R (1989) Prolonged exposure to submicromolar concentrations of quinolinic acid causes excitotoxic damage in organotypic cultures of rat corticostriatal system. *Neurosci Lett* 97:271-275.
- White MJ, DiCaprio MJ, Greenberg DA (1996) Assessment of neuronal viability with Alamar blue in cortical and granule cell cultures. *Journal of neuroscience methods* 70:195-200.
- Wilson A, Laurenti E, Trumpp A (2009) Balancing dormant and self-renewing hematopoietic stem cells. *Current opinion in genetics & development* 19:461-468.
- Witsch E, Sela M, Yarden Y (2010) Roles for growth factors in cancer progression. *Physiology* 25:85-101.
- Woo EY, Yeh H, Chu CS, Schlienger K, Carroll RG, Riley JL, Kaiser LR, June CH (2002) Cutting edge: Regulatory T cells from lung cancer patients directly inhibit autologous T cell proliferation. *Journal of immunology* 168:4272-4276.

- Wright JH (1910) Neurocytoma or Neuroblastoma, a Kind of Tumor Not Generally Recognized. *The Journal of experimental medicine* 12:556-561.
- Wszelaki N, Melzig MF (2011) Research on an in vitro cell system for testing the neurotoxicity of kynurenine pathway metabolites. *Die Pharmazie* 66:899-903.
- Wu H, Ichikawa S, Tani C, Zhu B, Tada M, Shimoishi Y, Murata Y, Nakamura Y (2009) Docosahexaenoic acid induces ERK1/2 activation and neuritogenesis via intracellular reactive oxygen species production in human neuroblastoma SH-SY5Y cells. *Biochimica et biophysica acta* 1791:8-16.
- Wu HQ, Ungerstedt U, Schwarcz R (1992a) Regulation of kynurenic acid synthesis studied by microdialysis in the dorsal hippocampus of unanesthetized rats. *Eur J Pharmacol* 213:375-380.
- Wu HQ, Baran H, Ungerstedt U, Schwarcz R (1992b) Kynurenic Acid in the Quinolate-lesioned Rat Hippocampus: Studies In Vitro and In Vivo. *Eur J Neurosci* 4:1264-1270.
- Xie HR, Hu LS, Li GY (2010) SH-SY5Y human neuroblastoma cell line: in vitro cell model of dopaminergic neurons in Parkinson's disease. *Chinese medical journal* 123:1086-1092.
- Yamaguchi-Iwai Y, Satake M, Murakami Y, Sakai M, Muramatsu M, Ito Y (1990) Differentiation of F9 embryonal carcinoma cells induced by the c-jun and activated c-Ha-ras oncogenes. *Proc Natl Acad Sci U S A* 87:8670-8674.
- Yan GM, Ni B, Weller M, Wood KA, Paul SM (1994) Depolarization or glutamate receptor activation blocks apoptotic cell death of cultured cerebellar granule neurons. *Brain research* 656:43-51.
- Yang BX, Duan YJ, Dong CY, Zhang F, Gao WF, Cui XY, Lin YM, Ma XT (2011) Novel functions for mda-7/IL-24 and IL-24 delE5: regulation of differentiation of acute myeloid leukemic cells. *Molecular cancer therapeutics* 10:615-625.
- Yang H, Yang T, Baur JA, Perez E, Matsui T, Carmona JJ, Lamming DW, Souza-Pinto NC, Bohr VA, Rosenzweig A, de Cabo R, Sauve AA, Sinclair DA (2007) Nutrient-sensitive mitochondrial NAD⁺ levels dictate cell survival. *Cell* 130:1095-1107.
- Yang Y, Karakhanova S, Werner J, Bazhin AV (2013) Reactive oxygen species in cancer biology and anticancer therapy. *Current medicinal chemistry* 20:3677-3692.
- Ye ZC, Sontheimer H (1999) Glioma cells release excitotoxic concentrations of glutamate. *Cancer research* 59:4383-4391.
- Yen A, Albright KL (1984) Evidence for cell cycle phase-specific initiation of a program of HL-60 cell myeloid differentiation mediated by inducer uptake. *Cancer research* 44:2511-2515.

- Yin L, Wu Z, Avigan D, Rosenblatt J, Stone R, Kharbanda S, Kufe D (2011) MUC1-C oncoprotein suppresses reactive oxygen species-induced terminal differentiation of acute myelogenous leukemia cells. *Blood* 117:4863-4870.
- Ying W (2008) NAD⁺/NADH and NADP⁺/NADPH in cellular functions and cell death: regulation and biological consequences. *Antioxidants & redox signaling* 10:179-206.
- Young JL, Jr., Ries LG, Silverberg E, Horm JW, Miller RW (1986) Cancer incidence, survival, and mortality for children younger than age 15 years. *Cancer* 58:598-602.
- Yusuf N (2014) Toll-like receptor mediated regulation of breast cancer: a case of mixed blessings. *Front Immunol* 5:224.
- Zhang H, Trachootham D, Lu W, Carew J, Giles FJ, Keating MJ, Arlinghaus RB, Huang P (2008) Effective killing of Gleevec-resistant CML cells with T315I mutation by a natural compound PEITC through redox-mediated mechanism. *Leukemia* 22:1191-1199.
- Zhang J, Nuebel E, Daley GQ, Koehler CM, Teitell MA (2012a) Metabolic regulation in pluripotent stem cells during reprogramming and self-renewal. *Cell stem cell* 11:589-595.
- Zhang L, Ovchinnikova O, Jonsson A, Lundberg AM, Berg M, Hansson GK, Ketelhuth DF (2012b) The tryptophan metabolite 3-hydroxyanthranilic acid lowers plasma lipids and decreases atherosclerosis in hypercholesterolaemic mice. *European heart journal* 33:2025-2034.
- Zhao F, Wu T, Lau A, Jiang T, Huang Z, Wang XJ, Chen W, Wong PK, Zhang DD (2009) Nrf2 promotes neuronal cell differentiation. *Free radical biology & medicine* 47:867-879.
- Zhao T, Zhu Y, Morinibu A, Kobayashi M, Shinomiya K, Itasaka S, Yoshimura M, Guo G, Hiraoka M, Harada H (2014) HIF-1-mediated metabolic reprogramming reduces ROS levels and facilitates the metastatic colonization of cancers in lungs. *Scientific reports* 4:3793.
- Zheng F, Luo Y, Wang H (2009) Regulation of brain-derived neurotrophic factor-mediated transcription of the immediate early gene Arc by intracellular calcium and calmodulin. *Journal of neuroscience research* 87:380-392.
- Zheng X, Baker H, Hancock WS, Fawaz F, McCaman M, Pungor E, Jr. (2006) Proteomic analysis for the assessment of different lots of fetal bovine serum as a raw material for cell culture. Part IV. Application of proteomics to the manufacture of biological drugs. *Biotechnology progress* 22:1294-1300.

- Zhou F, Shen Q, Claret FX (2013) Novel roles of reactive oxygen species in the pathogenesis of acute myeloid leukemia. *Journal of leukocyte biology* 94:423-429.
- Zhou F, Xu Y, Hou XY (2014) MLK3-MKK3/6-P38MAPK cascades following N-methyl-D-aspartate receptor activation contributes to amyloid-beta peptide-induced apoptosis in SH-SY5Y cells. *Journal of neuroscience research* 92:808-817.